

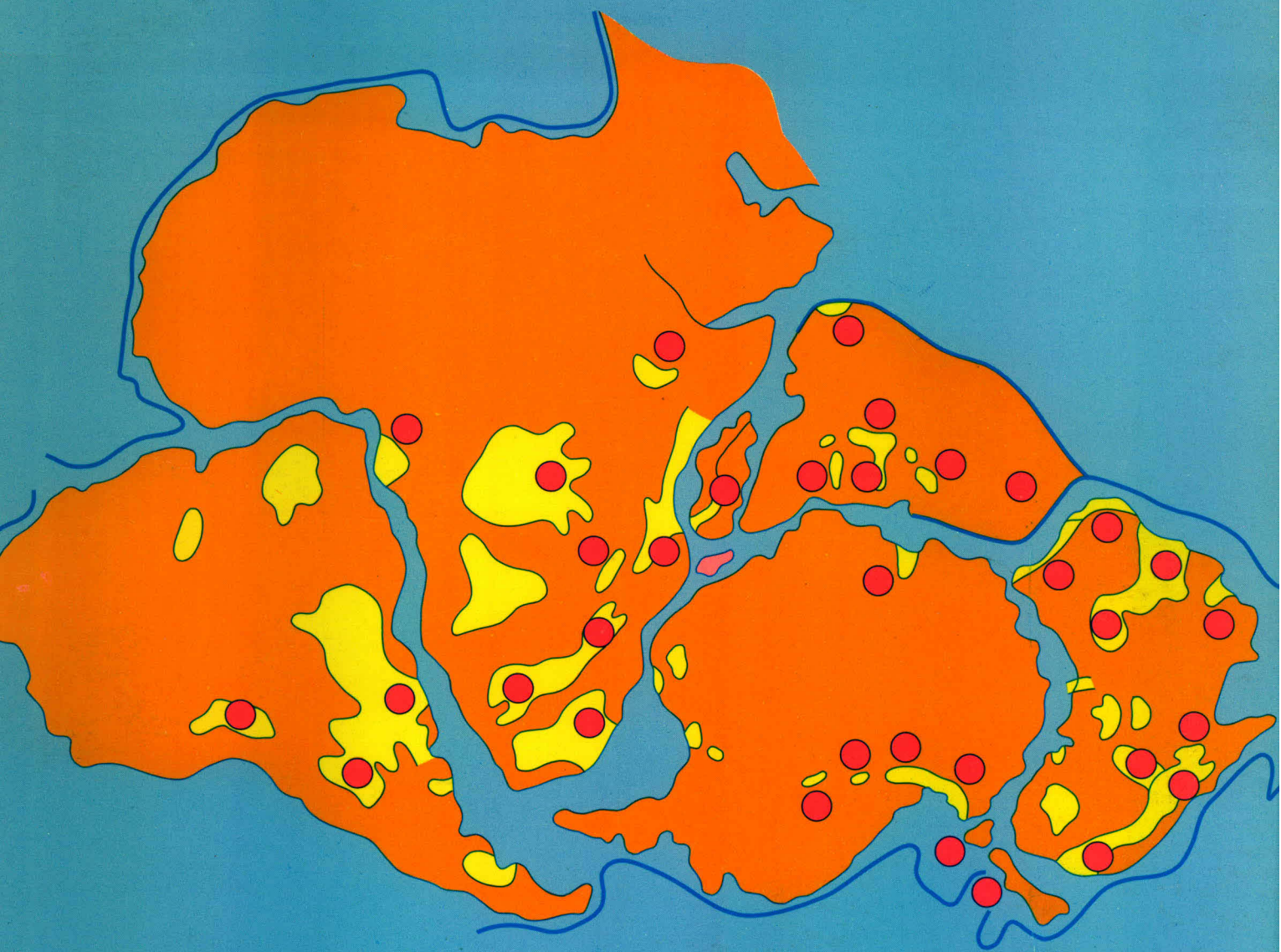
BMR CONTRACTS

071937

COPY 3



# BMR JOURNAL of Australian Geology & Geophysics



MR  
55(94)  
GS.6

C3

VOLUME 5, NUMBER 2 JUNE 1980



**Department of National Development and Energy, Australia**

Minister: Senator the Hon. J. L. Carrick

Secretary: A. J. Woods

**Bureau of Mineral Resources, Geology and Geophysics**

Acting Director: L. W. Williams

Editor, BMR Journal: J. F. Truswell

The BMR Journal of Australian Geology and Geophysics is a quarterly journal of research and related activities. Contributions are from officers of the BMR, from BMR officers working in collaboration with others, or requested work sponsored by the BMR. In addition to articles the Journal may include shorter notes and discussion of papers published in it. Discussion of papers is invited from anyone.

Annual subscription to the Journal is at the rate of \$10 (Australian). Individual numbers, if available, cost \$3. Subscriptions, etc., made payable to the Receiver of Public Moneys in Australian dollars, should be sent to the Director, Bureau of Mineral Resources, Geology & Geophysics, P.O. Box 378, Canberra, A.C.T. 2601, Australia. The Journal can also be obtained from the offices of the Department of National Development in Sydney and Melbourne.

Other matters concerning the Journal should be sent to the Director, marked for the attention of the Editor, BMR Journal.



071937



# BMR JOURNAL of Australian Geology & Geophysics

**BMR PUBLICATIONS COMPACTUS  
(LENDING SECTION)**

*Volume 5, No. 2*

*June 1980*

AUSTRALIAN GOVERNMENT PUBLISHING SERVICE  
CANBERRA 1980



**Front cover:**

The cover shows Late Palaeozoic sedimentary basins, and locations in them for which Permo-Carboniferous palynological data are available. These data are reviewed in an article in this issue. The Gondwana reconstruction is after Smith & Hallam (1970), Greater India after Veevers & others (1975).

Design assistance: R. Melsom, P. Corrigan, J. Mifsud.

The text figures in this issue were drawn by a cartographic team of J. Mifsud, R. Bates, I. Hartig, R. Anderson, and C. Fitzgerald.

ISSN 0312-9608



# TEM model studies of the Elura deposit, Cobar, New South Wales

B. R. Spies

A series of transient electromagnetic (TEM) scale-model studies of the Elura zinc-lead-silver deposit near Cobar, NSW, has been carried out. The results are generalised inasmuch as they are not restricted to the Elura deposit, but may be applied to other pipe-like bodies. A model of Elura was cast out of typemetal into a graphite mould, which simulated a conductive host rock. For both one-loop and two-loop geometries the response of the body at early times is masked by the host rock, and the response of the body at late times is two to three times background. By studying the fall-off of response with depth of burial, it was found that there is an optimum time range in which a conductive body can be detected. This time range depends on the conductivity and size of the body and the conductivity of the host rock. The optimum loop size for detecting a body in a resistive environment is slightly larger than the size of the body in plan. If the body is contained in a conductive host rock, then a smaller loop will minimise coupling with the host rock and will enable detection of the body over a wider time range. However the smaller loop also emphasises lateral inhomogeneities in the overburden. The response obtained with a two-loop system is more complex than for a coincident-loop geometry, and can be positive or negative in sign, depending on the sample time, loop separation, depth of burial of body, and host-rock conductivity. For loop separations less than the depth of the body, the two-loop response closely resembles the one-loop response.

## Introduction

The TEM scale-model studies described in this paper have been carried out by the Bureau of Mineral Resources, Geology and Geophysics (BMR) as a part of a continuing program of research into the geophysical applications of electrical and electromagnetic methods. The model studies were carried out using the TEM scale-model study facility at Macquarie University, North Ryde, NSW. This report describes the results of studies on models approximating the Elura zinc-lead-silver deposit. The results are generalised, inasmuch as they are not restricted to this deposit, but may be applied to other pipe-like bodies. The results can be used as a guide in the use of TEM methods to explore for targets having a wide range of size and conductivity.

## Geological description of deposit

The Elura zinc-lead-silver deposit is located 42 km north-northwest of Cobar, NSW, within the CSA Siltstone. It occurs at the northern end of the Cobar mineral field.

The deposit is oval-shaped in plan with a north-south length of 200 m, a width of up to 120 m, and a drilled depth below surface of over 500 m (Fig. 1). A central massive sulphide core composed of over 85 percent sulphide contains pyrite-sphalerite-galena mineralisation, with a discrete zone of pyrrhotite-bearing mineralisation within the core. The deposit is enveloped by semi-massive to disseminated mineralisation with siliceous gangue. The geological contact between the host rock and the mineralisation is sharp. Weathering has proceeded to a depth of 100 m; above this level the mineralisation is intensely oxidised (R. L. Adams, pers. comm.).

The resistivity of country rocks in the top 100 m varies from 1 to 20 ohm-m. Beneath this zone, the resistivity gradually increases from about 100 ohm-m at 110 m depth, to 2000 ohm-m at a depth of 200 m (Hone, in press).

## Results of TEM surveys

BMR has carried out ground geophysical surveys at Elura, including detailed TEM measurements, from 1974. A good response to single-loop TEM systems is obtained from conductive surface zones, which are in places up to 100 m thick, and have resistivities in the range 1 to 50 ohm-m. Using a one-loop TEM system a small but distinct anomaly is recorded over the deposit for sample times of greater than 2 ms (Hone, 1976). The results of a 100 m-loop TEM traverse at Elura are shown in Figure 2.

## Description of model setup

The TEM model study facility is described by Spies (1979). Briefly, a scale model will simulate a full-scale situation if the parameter  $\sigma L^2/t$  is the same for the model and field situations. This assumes that the magnetic permeability is that of free space, and displacement currents are neglected. Here  $\sigma$  and  $L$  are the conductivity and dimension of a typical parameter (e.g. orebody conductivity, and loop size) and  $t$  is sample time. The TEM responses  $e(t)$  of the model and full-scale situation are related by the expression

$$e(t)_m/e(t)_f = L_{mf}t_f/L_m t_m \quad \dots (1)$$

where the subscripts  $m$  and  $f$  refer to the model and full-scale cases respectively (Spies, 1976).

## Description of model

A simplified 1:2500 scale model of the Elura deposit was cast out of typemetal in a graphite mould. The model dimensions were: length 8 cm, width 4 cm, and depth extent 6 cm. In plan, the ends of the model are semi-circular, with a radius of 2 cm. The main differences between the geometry of the model and that of the deposit are in the limited depth extent and absence of the tapered twin cone-shaped top in the model.

TEM measurements were made of the response of single and two-loop traverses, using multiturn circular loops of diameter 6 cm and 2.7 cm. For some measurements the body was contained within a graphite host,



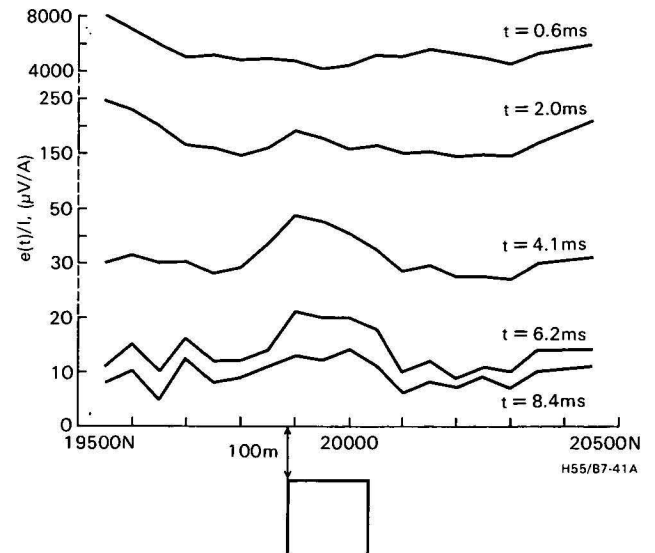
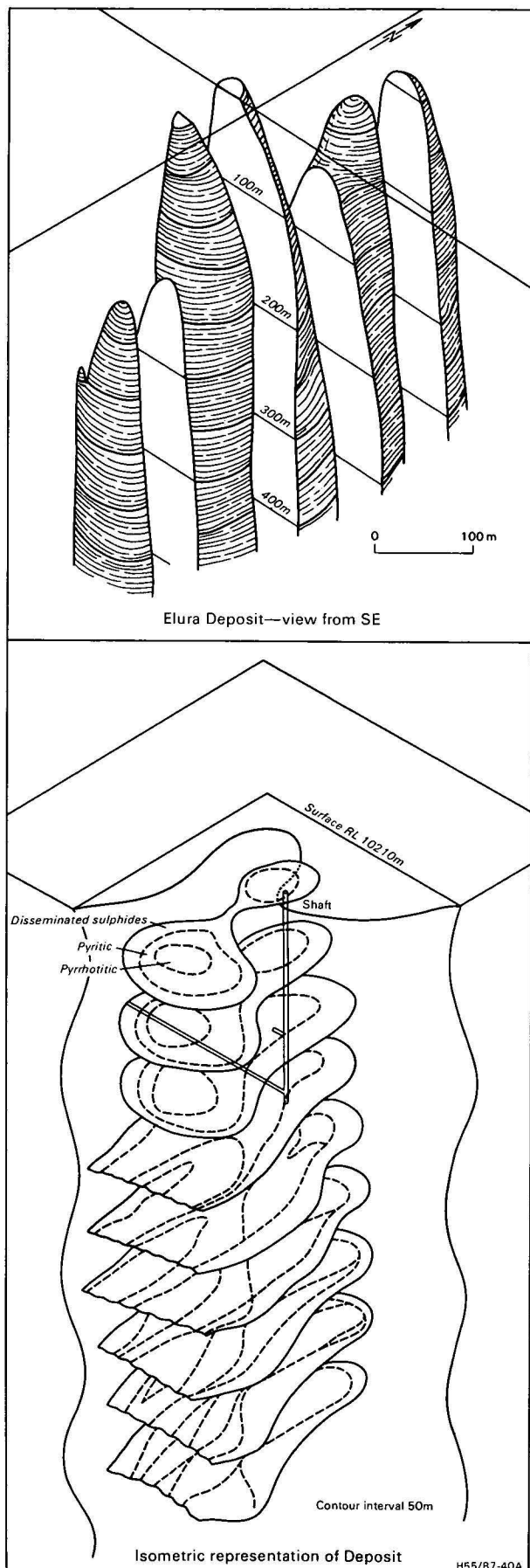


Figure 2. 100 m loop field results at Elura, measured with MPPO-1 equipment (from Hone, 1976). A large response owing to the conductive surface layers is seen. At late times the anomaly over the Elura body is evident.

of dimensions 40 cm x 25 cm x 10 cm deep. Good electrical contact between the typemetal and graphite was achieved using conductive epoxy resin, which has a similar conductivity to the graphite.

The modelling parameters, including conductivity, time, and scaling factors, are listed in Table 1. In the rest of this paper, modelling parameters are scaled to field values.

The main difference between the model and the field case is that the model is encased in an overburden and host of uniform conductivity, whereas the Elura deposit is surrounded by a relatively resistive host rock beneath the zone of intense oxidation (110 m). Thus a more valid model for overburden and host would be a two-layered ground. However, Hone (in press) has shown that the resistivity of the host rock surrounding the Elura deposit increases gradually with depth, and thus the deposit has electrical continuity with both the overburden and host.

The difference in response between a two-layered ground and a uniform ground (halfspace) can be calculated, using the two-layer TEM master curves of Raiche & Spies (in press). At times earlier than 3 ms the two responses are identical. At later times the layered ground response decreases with respect to the halfspace response. The decrease at 5 ms, 10 ms, and 20 ms is 25, 60, and 75 percent respectively.

However, the graphite block used in the model is of limited lateral and depth extent, and is not large enough to simulate a halfspace at late times. Although the model is simplified, it does provide an insight into the effects of electromagnetic screening.

Figure 1. Geometry of Elura deposit. The central core consists of massive pyrite-sphalerite-galena with sections of pyrrhotite; it is surrounded by a zone of disseminated mineralisation in a silicified gangue.



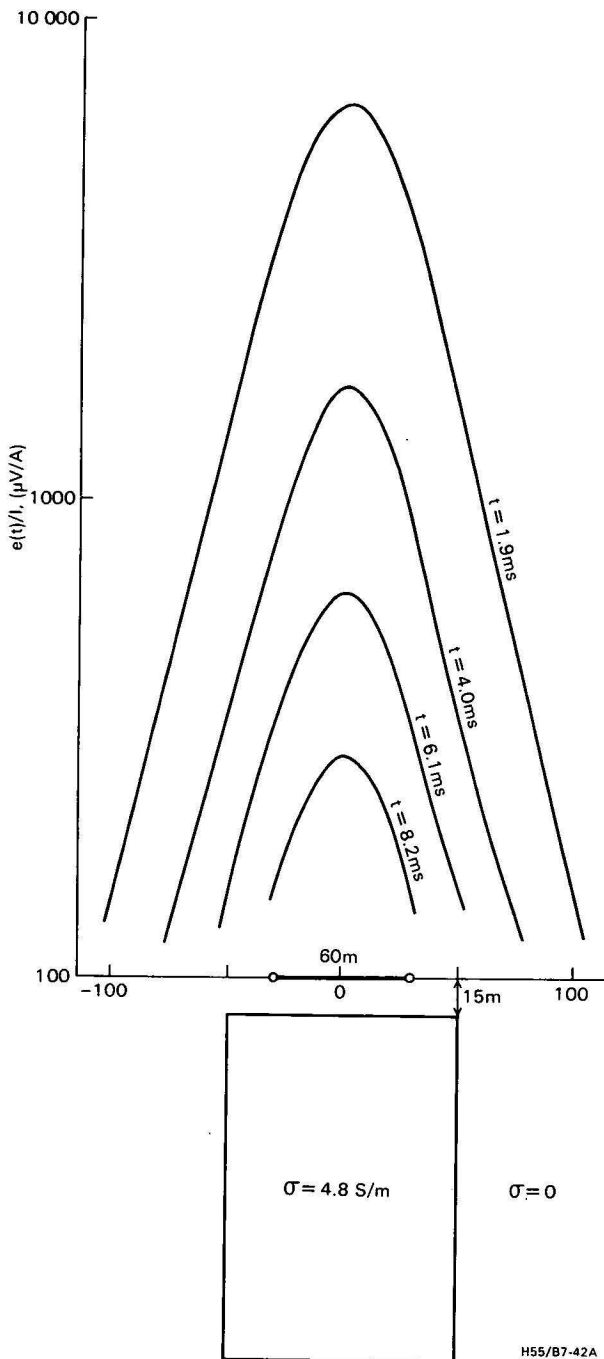


Figure 3. Profiles of coincident loop data; Elura in air at 15 m depth, 60 m loop.

### Response of model in air, with coincident loops

Profiles over the model alone at depths of 15 m and 125 m are shown in Figures 3 to 5. The most obvious relationship evident in Figures 3 and 4 is that the width of the anomaly is mainly controlled by the depth of the model. With the model at a depth of 125 m, the effect of increasing the loop size from 60 m to 130 m is to substantially increase the anomaly amplitude, but not the anomaly width. The increase in the amplitude is approximately equal to the ratio of the square of the loop areas (about 16). This suggests that loop sizes the same as, or smaller than the depth of the body can be thought of as dipoles.

### Response of model in conducting host with coincident loops

In this model, the Elura body (4.8 S/m) is enclosed in a 0.25 S/m host, which has dimensions 1000 m x 625 m x 250 m deep. The host is not large enough to represent a halfspace, and background readings are thus lower than the true halfspace response.

Parameter	Model	Field
Dimension scaling	1	2500
Time scaling	1	10
Conductivity scaling	1	$1.6 \times 10^{-6}$
Voltage scaling	1	250
Deposit —		
Length	8 cm	200 m
Width	4 cm	100 m
Depth below surface	5 cm	125 m
Depth extent	6 cm	150 m
Conductivity	$3 \times 10^6$ S/m	4.8 S/m
Host —		
Length	40 cm	1000 m
Width	25 cm	625 m
Depth extent	10 cm	250 m
Conductivity	$1.5 \times 10^5$ S/m	0.25 S/m
Loop sizes — Diameter		
	6 cm	158 m
	2.7 cm	68 m
Equivalent square loop		
	5.3 cm	130 m
	2.4 cm	60 m

Table 1. Modelling parameters — Elura deposit.

Profiles for 60 m and 130 m loops are presented in Figures 6 and 7. Both loop sizes indicate a small low over the body at early times, but later this changes to a conventional positive anomaly approximately 2 to 3 times background. At early times, the response is less

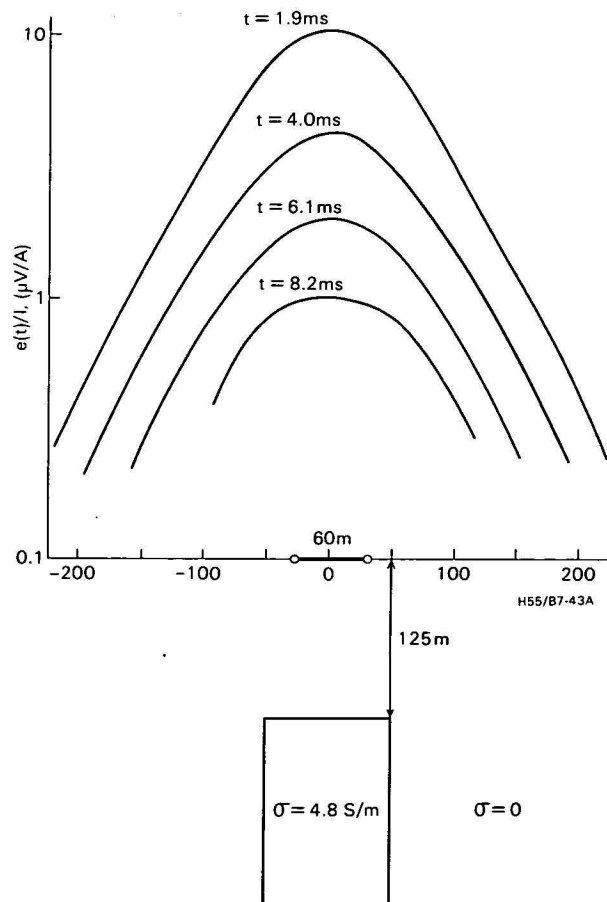


Figure 4. Profiles of coincident loop data; Elura in air at 125 m depth, 60 m loop.

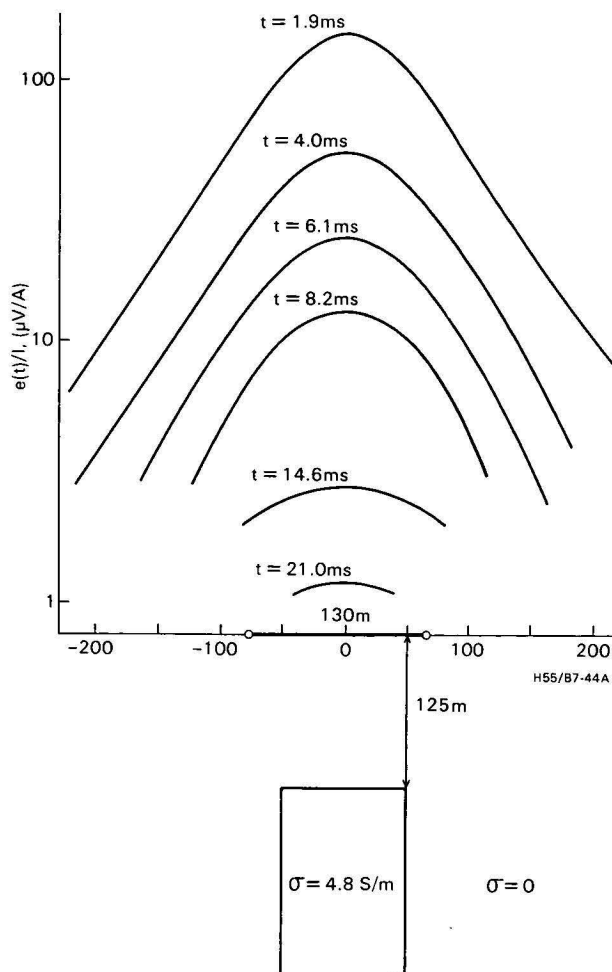


Figure 5. Profiles of coincident loop data; Elura in air at 125 m depth, 130 m loop.

than it would be without the body, since there is a relative low located directly over the body. The small low is similar to the theoretical response of layered structures (Raiche & Spies, in press) and is attributed to interference phenomena.

At later times (5 to 15 ms) the response of the combined model is greater than that of the host. To a first approximation, the total response can be considered to be the sum of the individual responses of the body and host. This approximation, known as superposition, appears to be valid to an accuracy of 50 percent for a coincident loop system for the time range in which the maximum anomaly is obtained (Spies, unpublished data). This assumption is made in the following section.

### Attenuation of peak response with depth of burial

The peak response of the Elura model in air at different depth is summarised in Figures 8 and 9. Results are shown for 130 m and 60 m loops at a number of sample times,  $t$ . The TEM response  $e(t)/I$  falls off rapidly with depth of burial at all sample times. As the depth increases from 25 m to 50 m, the curves show a three to four-fold reduction in  $e(t)/I$ , whereas from 50 m to 100 m the response falls off by a factor of between 7 and 10.

To gain an indication of the significance of these results, the TEM response of a loop on a homogeneous

halfspace with conductivities of 0.16, 0.1, 0.03 and 0.01 S/m, is shown in the figures as dashed lines. Where these lines cross the solid lines, the magnitude of the Elura anomaly equals the magnitude of the homogeneous halfspace response. To the right of the dashed lines the halfspace response is larger than the Elura response, and on the left it is smaller. As expected, as the depth of the body increases, the conductivity of the halfspace must decrease if the body is still to be detected. In an exploration environment where lateral variations are likely to be present it is reasonable to expect that a body will be detected if its response is approximately three times that of the background, or in this case, the halfspace response. The response of the host may be thought of as geological noise. Velikin (1971) uses a similar approach in assessing the detectability of bodies in a conducting host, but assumes

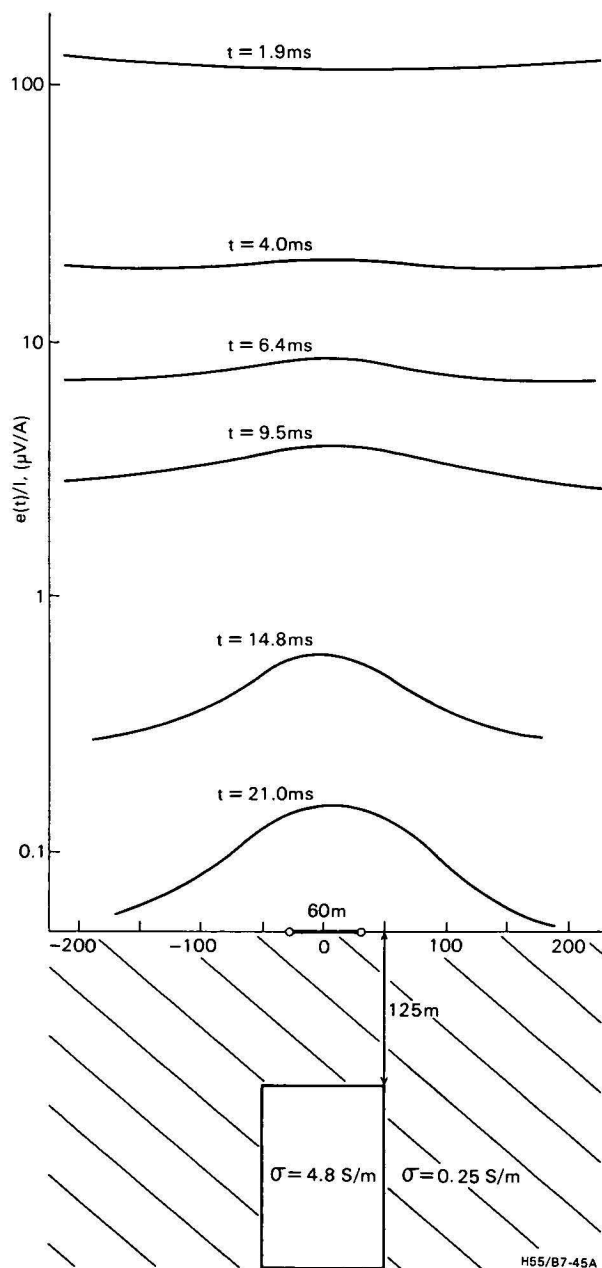


Figure 6. Profiles of coincident loop data, Elura in conducting host, 60 m loop. The response of the body is masked at early times.

that the response of the body must be ten times the response of the host.

The halfspace curves shown in Figures 8 and 9 are concave to the left; they imply that for a given depth of burial and loop size there is a certain time range over which the body will be detected (its response is greater than three times the host response). At earlier or later times the response will be less than the geological noise (halfspace response). For example, if the body were at a depth of 40 m, and contained in a halfspace of 0.16 S/m, the response of the body is greater than three times the halfspace response for times between approximately 4.0 ms and 13.0 ms for a 130 m loop, and approximately 1.9 to later than 20 ms for a 60 m loop. As the host becomes less conductive, a body at the same depth can be detected over a much wider time range.

When the depth of the body is increased to 50 m, it can be detected with a 60 m-loop between 4 ms and about 15 ms. However, it will be undetected with a 130 m loop at all sample times because of the over-

whelming response of the halfspace. If the depth of the body is 60 m, then it will not be detectable with either loop size if enclosed in a halfspace of conductivity 0.16 S/m.

If the conductivity of the halfspace is decreased, say to 0.03 S/m, then the body at a depth of 100 m can be detected between 6 ms to later than 10 ms with a 130 m loop, and from 0.19 ms to later than 10 ms with a 60 m loop.

This approach can also be applied to cases where the host can be regarded as a two-layered ground, by using the master curves of Raiche & Spies (in press). In general, the effect of limiting the depth of conductive overburden will be to increase the late-time limit. Usually, the early-time limit will remain unchanged.

### Choice of loop size

The results of modelling Elura with coincident loops show that a careful choice of loop size must be made when designing a TEM survey. The optimum size of the loop will depend on many factors. The model study in air shows that the 130 m loop gives a much greater response than the 60 m loop. With the Elura model at a depth of 125 m, the larger loop results in a factor of 13 increase in response. If we consider the ideal geological case where no other conductors are present in the

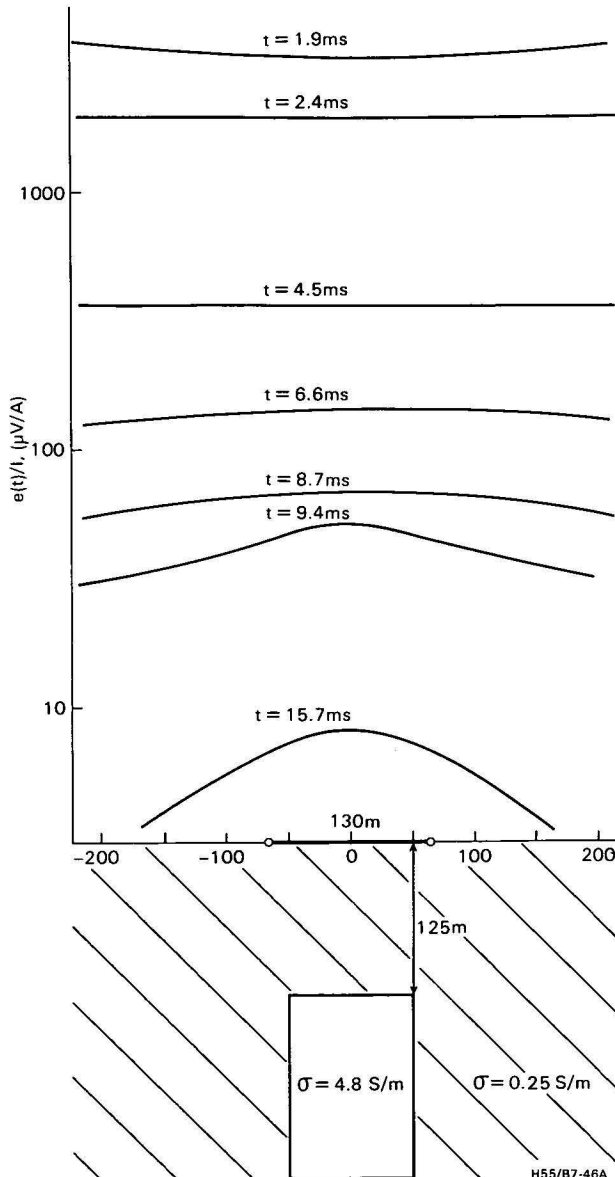


Figure 7. Profiles of coincident loop data; Elura in conducting host, 130 m loop.

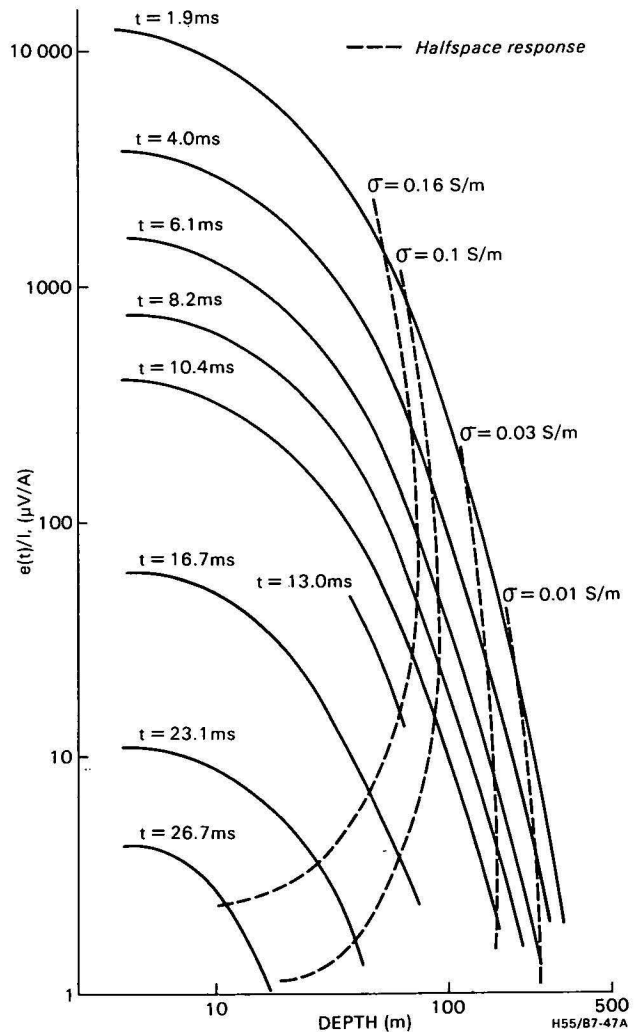


Figure 8. Response of Elura in air at different depths, 130 m coincident loop. The response of a homogeneous ground is shown by dashed lines.



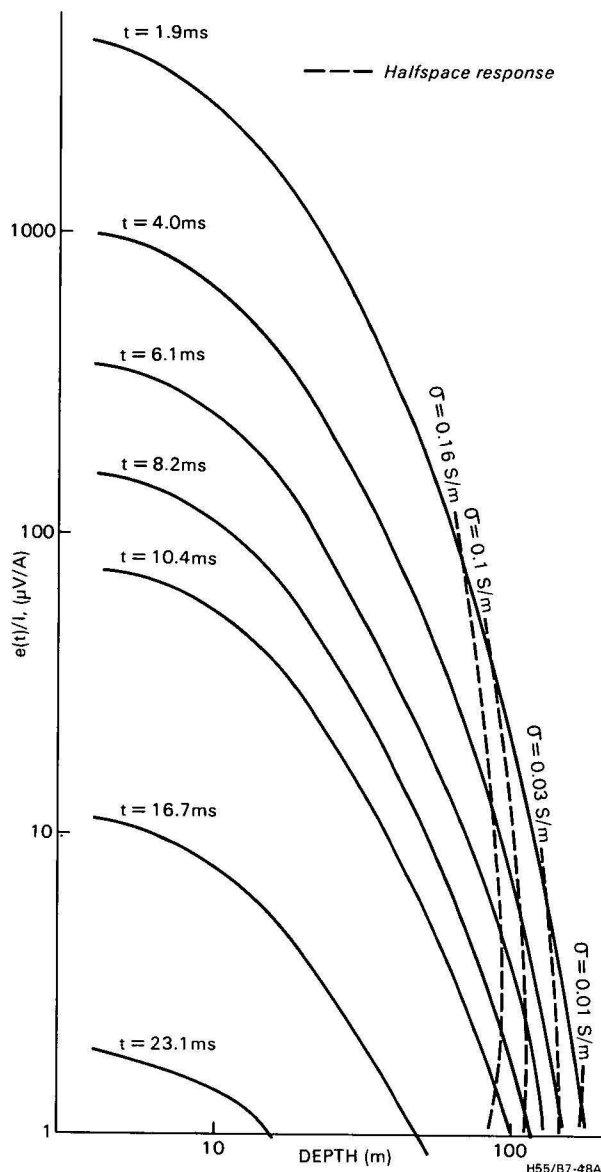


Figure 9. Response of Elura in air at different depths, 60 m coincident loop.

overburden or host (no geological noise), then the main noise source would be external electrical interference which would increase as the loop area. This temporal noise would be a factor of 4.8 greater for the 130 m loop than for the 60 m loop. The signal-to-noise ratio, then, would be 2.7 times larger for the 130 m loop.

Thus, in a resistive environment the larger loop is preferable to the smaller loop. The larger loop (130 m) is of comparable size to the Elura deposit. This result is consistent with the work of Lee (1975), who found that the optimum response of a sphere was obtained when the sizes of the loop and sphere were equal. In practice it may be desirable to use larger loops to increase areal coverage in the initial reconnaissance phase of exploration.

All loop sizes smaller than the depth of the target will give an identical response if normalised for loop moment, because they act as dipoles. For dipole loops, the normalised amplitude, and hence the width of the anomaly, is independent of loop size. For the Elura model, the anomaly half-width (the width of the anomaly at half its maximum amplitude), appears to pro-

vide an estimate of the depth of the body. For this model a 30 percent over-estimate of the depth results, partly because the width of the model contributes to the increased anomaly width. For cases where the loop size or depth to the body is much larger than the size of the body, the theoretical expressions of Kamenetskii (1976) can be used.

When the deposit is contained in a conductive host, the choice of loop size is more critical. For such cases, the dominant noise source will be geological, and temporal noise will be of lesser importance. The example earlier showed that the Elura model located in a 0.16 S/m host could be detected with a 60 m loop, but not with a 130 m loop; this is because the response of the host increases as the fourth power of the loop size over most of the time range. This increase is much faster than for a finite target. Thus in highly conductive terrains loop sizes smaller than the size of the target may be preferable. The optimum loop size will depend on the relative response expected from the host and the body, and thus is dependent on the depth and conductivity of the body, and the conductivity of the host rock.

Often the effect of lateral inhomogeneities in the overburden will offset the advantages of using a smaller loop, because these will be more sensitive to small-

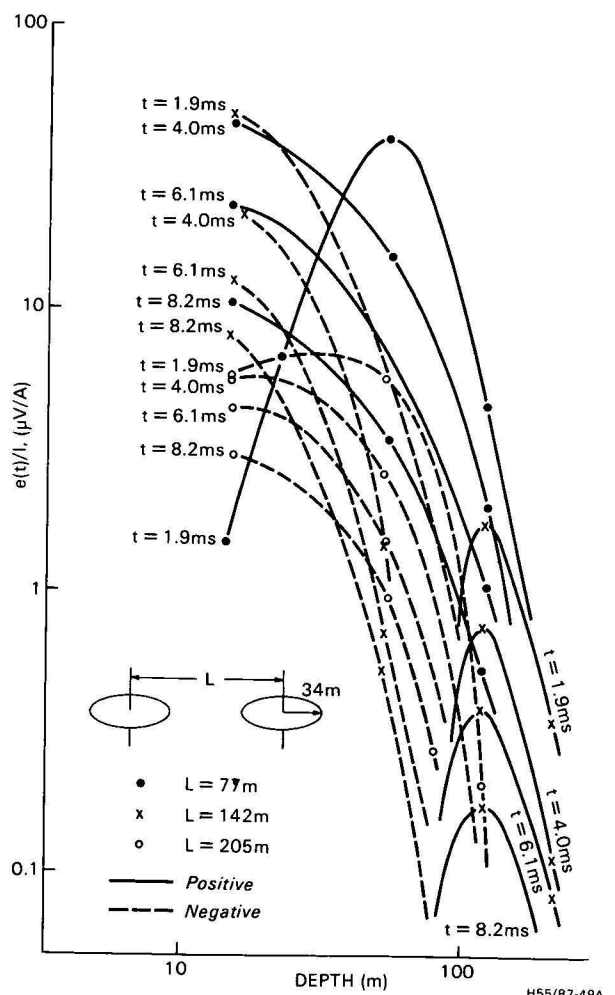


Figure 10. Response of Elura in air, at different depths, two-loop mode. The response can be positive or negative in sign depending on depth and loop separation.

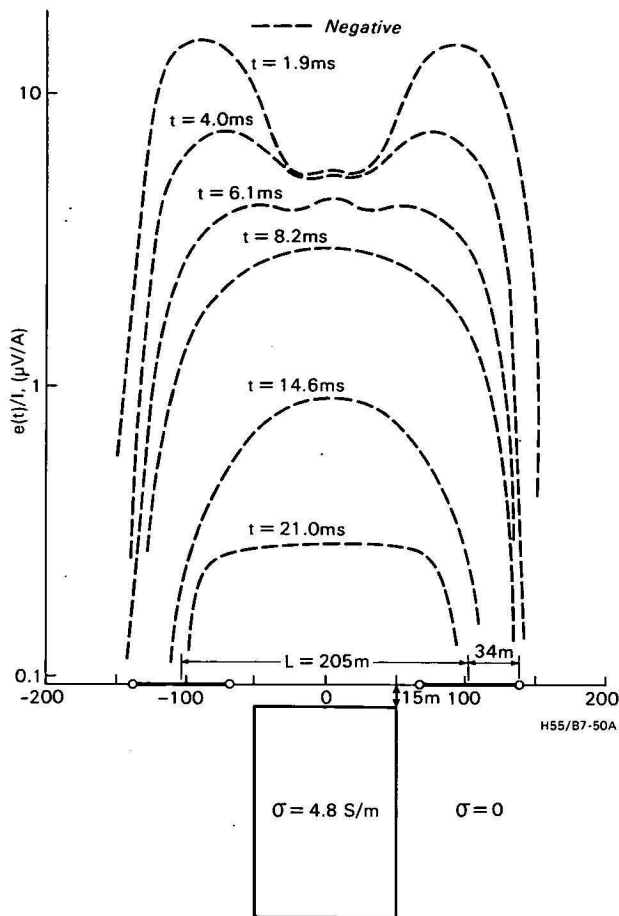


Figure 11. Profiles of two-loop data; Elura in air at 15 m depth,  $L = 205$  m. The response is negative for all times.

scale lateral changes than larger loops (see for example, field results in Spies, in press).

In exploring for an Elura-type target at a depth of 125 m, using a dipole loop and a station spacing of 200 m would ensure a minimum anomaly of one-third of the peak value.

### Response of the Elura model in air at different depths, with a two-loop mode

#### Response over centre of body

The two-loop response measured over the Elura model at various depths is presented in Figure 10, for loop separations,  $L$ , of 77, 142 and 205 m. The transmitter and receiver loop diameters are 68 m.

The curves are fairly complex, as values can be either positive or negative. The sign convention used in this paper is consistent with that adopted for coincident-loop data. That is, for very small loop separations, or for large times, the responses from the two-loop and coincident loop systems are identical and, for convenience, are regarded as being positive in sign.

Referring to the  $L = 142$  m data, the response is negative at small depths, and changes to positive with increasing depth. The only positive responses at all sample times were observed for the  $L = 77$  m data; all  $L = 205$  m data were negative. Changes in sign as the depth of the body or loop separation is changed could lead to interpretational difficulties, as sign changes

also occur in a two-loop system over a uniform ground (Spies, 1980).

#### Profiles

Profiles measured for a depth of burial of 15 m for  $L = 205$  m and 77 m are shown in Figures 11 and 12. The 205 m results are all negative, and exhibit a low over the centre of the body at early times. The width of the anomaly is approximately equal to the loop spacing.

For  $L = 77$  m (Fig. 12) results vary from positive to negative over much of the time range. The negative values generally occur over the edges of body, positive values over the centre and away from the edges of the body, at all times.

The anomaly shape is a complex function of the width, depth and conductivity of the body, and the loop spacing.

When the depth of burial is increased to 125 m, the profile shape is greatly simplified. Results for  $L = 77$  m and 142 m (Fig. 13) exhibit a simple positive anomaly over the body.

#### Discussion

The two-loop response is complicated by the fact that the response can be either positive or negative, depending on loop separation, sample time, and the depth and conductivity of the body. For loop separations less than the depth of the body, the response is similar to the one-loop response (e.g., compare Figs. 5 and 13). Thus for these cases it is advisable to use a one-loop

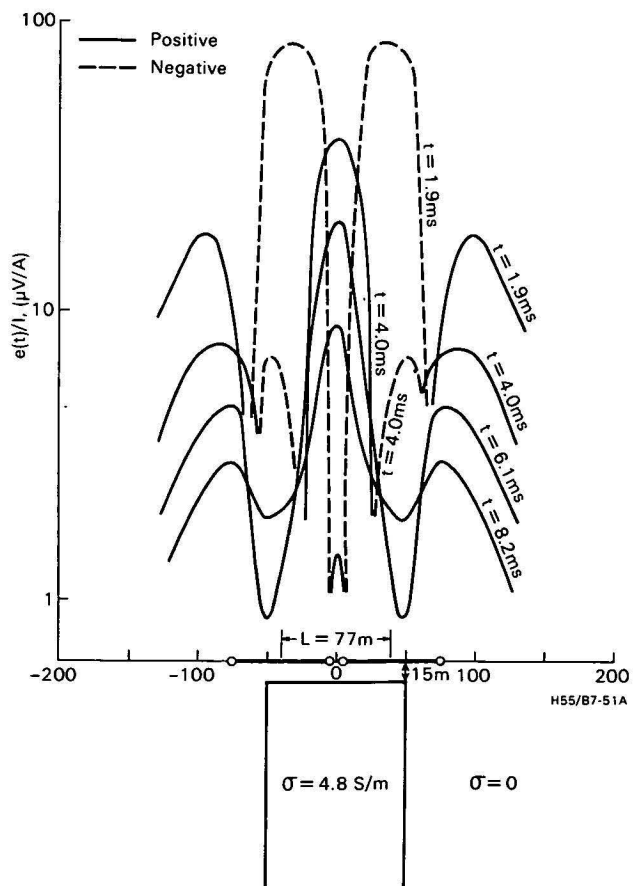


Figure 12. Profiles of two-loop data; Elura in air at 15 m depth,  $L = 77$  m. The response exhibits a complex shape along the profile.

instead of a two-loop configuration, because of the simpler field logistics and ease of interpretation.

### Response of the model in conductive host with two-loop mode

Profiles for the Elura model buried in a 0.25 S/m host measured with loop separations of 77 m and 142 m are shown in Figure 14. The profiles are again positive, and are simple in shape. A small anomaly, 20 to 30 percent above background values, is obtained over the body. The Elura anomaly is screened by the host for the first few milliseconds and is first evident at 6 ms with  $L = 77$  m. For  $L = 142$  m, this time is increased to 8 ms, and presumably reflects the variation of the transmitter-body-receiver distance for the two Rx-Tx spacings.

These results for the two-loop configuration are again similar to those obtained with the one-loop configuration, and there appear to be no inherent advantages in using the two-loop configuration. The difference in the amplitudes measured with the one-loop and two-loop configurations is probably because of the finite size of the block simulating the host rock.

### Conclusions

Use of scale model studies provides a valuable insight into the response of complex conductors, and different loop geometries can be obtained.

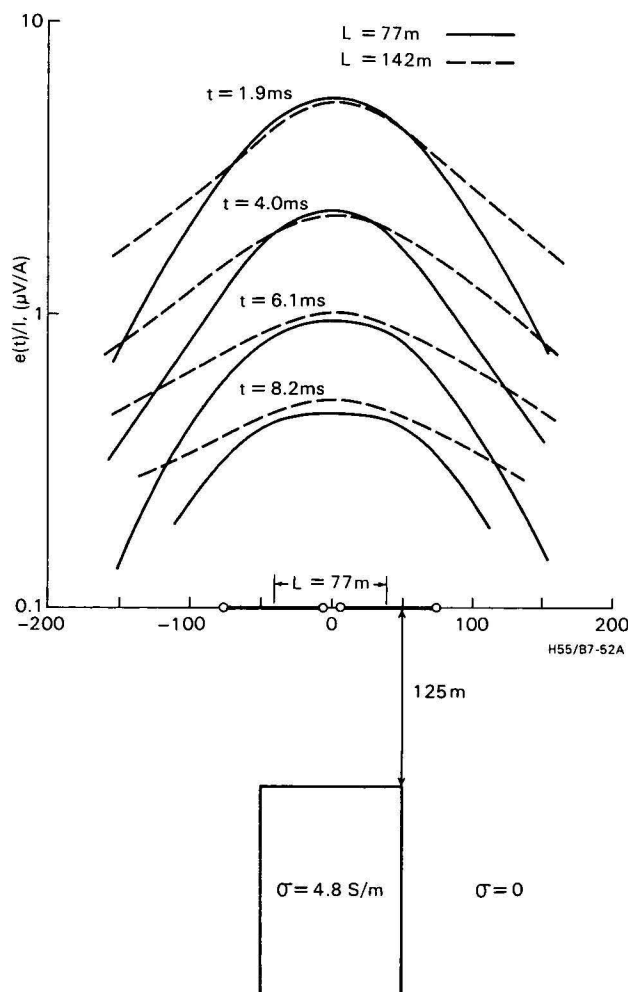


Figure 13. Profiles of two-loop data, Elura in air at 125 m depth,  $L = 77$  m and 142 m. The response for both loop separations is positive in sign.

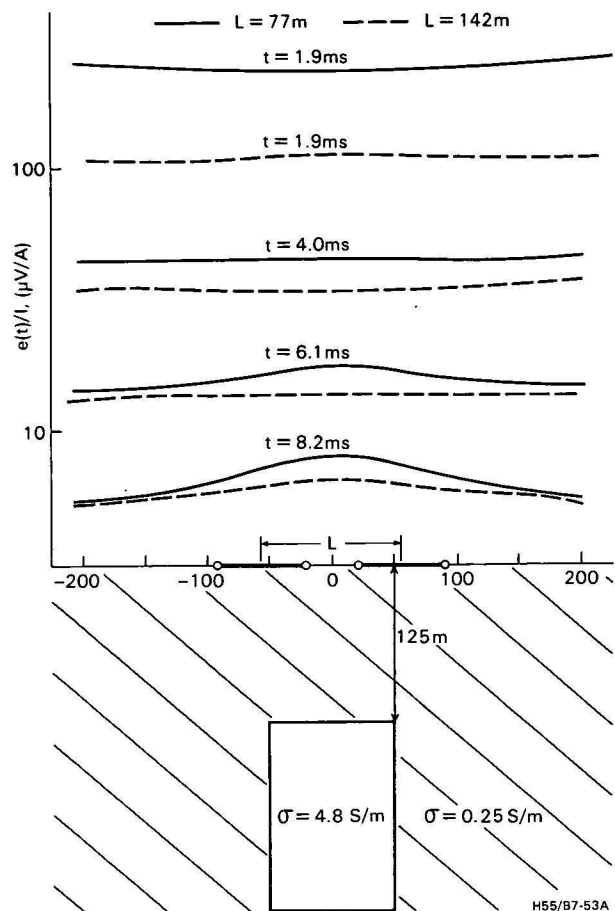


Figure 14. Profiles of two-loop data, Elura in conducting host,  $L = 77$  m and 142 m. The orebody response is masked at early times by the host.

For both one-loop and two-loop geometries, the response of the Elura model is masked at early times by the presence of a conductive host rock. The response of the model studied is first seen at a time,  $t_1$ , of about 4 ms, when the depth of burial,  $d$ , is 125 m and the conductivity of the overlying medium,  $\sigma$ , is 0.25 S/m. It is possible to relate  $t_1$  to the other parameters using modelling relationships, so that a general expression can be obtained for the time of departure:

$$t_1 \approx 10^{-6} \sigma d^2 \text{ seconds,} \quad (2)$$

as was done by Raiche & Spies (in press). Equation (2) gives the earliest time at which an Elura-type structure can be seen through overburden. However, to determine whether the body can be detected in practice it is necessary to use additional criteria, such as the relative signal strength from the body and host rock (geological noise). A good criterion for assessing the detection of a body is that its response in the absence of a conducting host is greater than three times the response of the host.

In a conducting environment in which lateral changes in conductivity are minor, the optimum loop size is smaller than the body in plan. Larger loops will be better coupled to the host rock, and the body will not be detected until later in time. For Elura-type models, the optimum times for measurement are in the range 2 to 30 ms. In practical situations lateral conductivity changes are often severe; this may offset the advantages of using smaller loops.

The two-loop response can be much more complicated than the one-loop response. The sign of the

response will depend on depth of burial, loop separation and the conductivity of the host and body. For loop separations less than the depth to the body, the two-loop response is simplified and resembles the one-loop response.

### References

- HONE, I. G., 1976—Transient electromagnetic survey, Elura deposit, Cobar, New South Wales, 1974. *Bureau of Mineral Resources, Australia, Record 1976/99* (unpublished).
- HONE, I. G., in press—Goelectric properties of the Elura prospect, Cobar, N.S.W. *Bulletin Australian Society of Exploration Geophysicists*.
- KAMENETSKII, F. M., 1976—Applications handbook for transient process methods in the geophysics of ore bodies. *Nedra, Leningrad* (in Russian).
- LEE, T., 1975—Transient electromagnetic response of a sphere in a layered medium. *Geophysical Prospecting*, **23**, 492-512.
- RAICHE, A. P., & SPIES, B. R., in press—Coincident loop TEM master curves for interpretation of two-layer earths. *Geophysics*.
- SPIES, B. R., 1976—The derivation of absolute units in electromagnetic scale modelling. *Geophysics*, **41**, 1042-7.
- SPIES, B. R., 1979—Scale model studies of a transient electromagnetic prospecting system using an interactive mini-computer. *IEEE Transactions on Geoscience Electronics*, GE-17, 25-33.
- SPIES, B. R., 1980—Interpretation and design of time domain electromagnetic surveys in areas of conductive overburden. *Bulletin of the Australian Society of Exploration Geophysicists*, **11**.
- SPIES, B. R., in press—One-loop and two-loop surveys, Elura deposit, Cobar, N.S.W. *Bulletin Australian Society of Exploration Geophysicists*.
- VELIKIN, A. B., 1971—The optimum conditions for field work with the transient process method; in Fokin, A.F. (Editor) *THE METHOD OF TRANSIENT PROCESSES IN THE SEARCH FOR SULPHIDE ORE DEPOSITS. Nedra, Leningrad* (in Russian).





# Shallow structure and Late Cainozoic geological history of western Bass Strait and the west Tasmanian Shelf

H. A. Jones & G. R. Holdgate<sup>1</sup>

Shallow seismic reflection profiles in western Bass Strait and on the west Tasmanian continental shelf have been used to interpret the late Cainozoic geological history of this area. Palaeozoic and Precambrian rocks with little or no sedimentary cover form the structural highs separating the Bass, Torquay, and Otway Basins, and the inner shelf off Tasmania. The Neogene and Quaternary sequences are undeformed and relatively complete in the Bass Basin and off southern Tasmania. Elsewhere, a Late Miocene unconformity separates flat-lying Pliocene-Holocene sediments from gently folded Miocene and older rocks. Subaerial erosion, initiated in the Late Miocene and continued during Pleistocene low sea-level periods, controls sea-floor topography over extensive areas of shelf south of King Island.

## Introduction

During a marine geological reconnaissance survey by BMR in 1973 some 2100 km of low-energy seismic reflection lines were run in western Bass Strait and over the west Tasmanian shelf (Fig. 1). These give some insight into the seismic character and structure of the top few hundred metres of section. Geophysical surveys and some drilling for petroleum exploration have established the geological framework of the region, and the broad stratigraphic succession in the basinal sequences is fairly well known (Robinson, 1974; Robertson & others, 1978). However, little information on the distribution and structure of the near-surface sequences has hitherto been recorded.

A summary of the results of the cruise during which these shallow seismic profiles were obtained has been given by Davies & Marshall (1973). The seismic system used consisted of a 3-electrode sparker sound source with an energy output of about 1000 watt seconds and a 30-element single-channel streamer. Only the shipboard analogue display record was preserved. Record quality is somewhat uneven, being affected by prevailing sea state and the degree to which multiple reflections obscure the deeper events. Useful data usually extend to a depth of about 0.3 seconds (two-way time), and on some profiles to over 0.5 seconds.

The area covers the offshore part of the Torquay Basin, the western part of the Bass Basin and the west Tasmanian shelf, with the adjoining shallow basement areas. Interpretation of the data over the Torquay and Bass Basins and the intervening basement highs was primarily the responsibility of GRH, who participated on the cruise while an officer of the Geological Survey of Victoria; the west Tasmanian profiles have been interpreted by HAJ. GRH publishes with the permission of the Director of the Geological Survey of Victoria. The assistance of the Petroleum Division of BHP in providing data from Bass Strait oil wells is gratefully acknowledged.

## Torquay Basin

The Torquay Basin is a graben extending south-westwards from Port Phillip under the continental shelf, where it is bounded by the King Island-Mornington Peninsula Ridge on the southeast, the King Island-Cape Otway High on the southwest, and the Otway

Ranges High on the northwest (Fig. 2). Over 3000 m of mainly Cretaceous sediments overlie Palaeozoic basement in the deepest part of the basin along the coastline near Anglesea; offshore the Tertiary section thickens considerably, although the total sedimentary sequence thins in this direction. Two petroleum exploration wells have been drilled in the offshore part of the basin (Shell Nerita No. 1 and Hematite Snail No. 1).

Parts of BMR's shallow seismic lines 38, 39 and 40 traverse the Torquay Basin. All show a prominent reflector marking a unconformity between an upper flat-lying sequence up to 0.1 seconds thick and a lower gently folded sequence extending below the limit of penetration at 0.6 seconds. The angular discordance

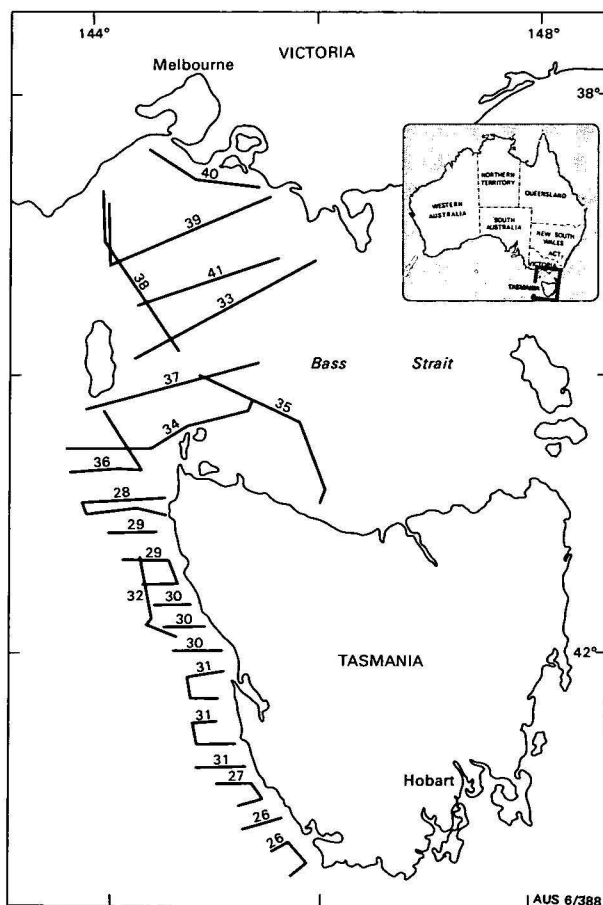


Figure 1. Location of seismic profiles.

<sup>1</sup>State Electricity Commission of Victoria, 15 William Street, Melbourne.

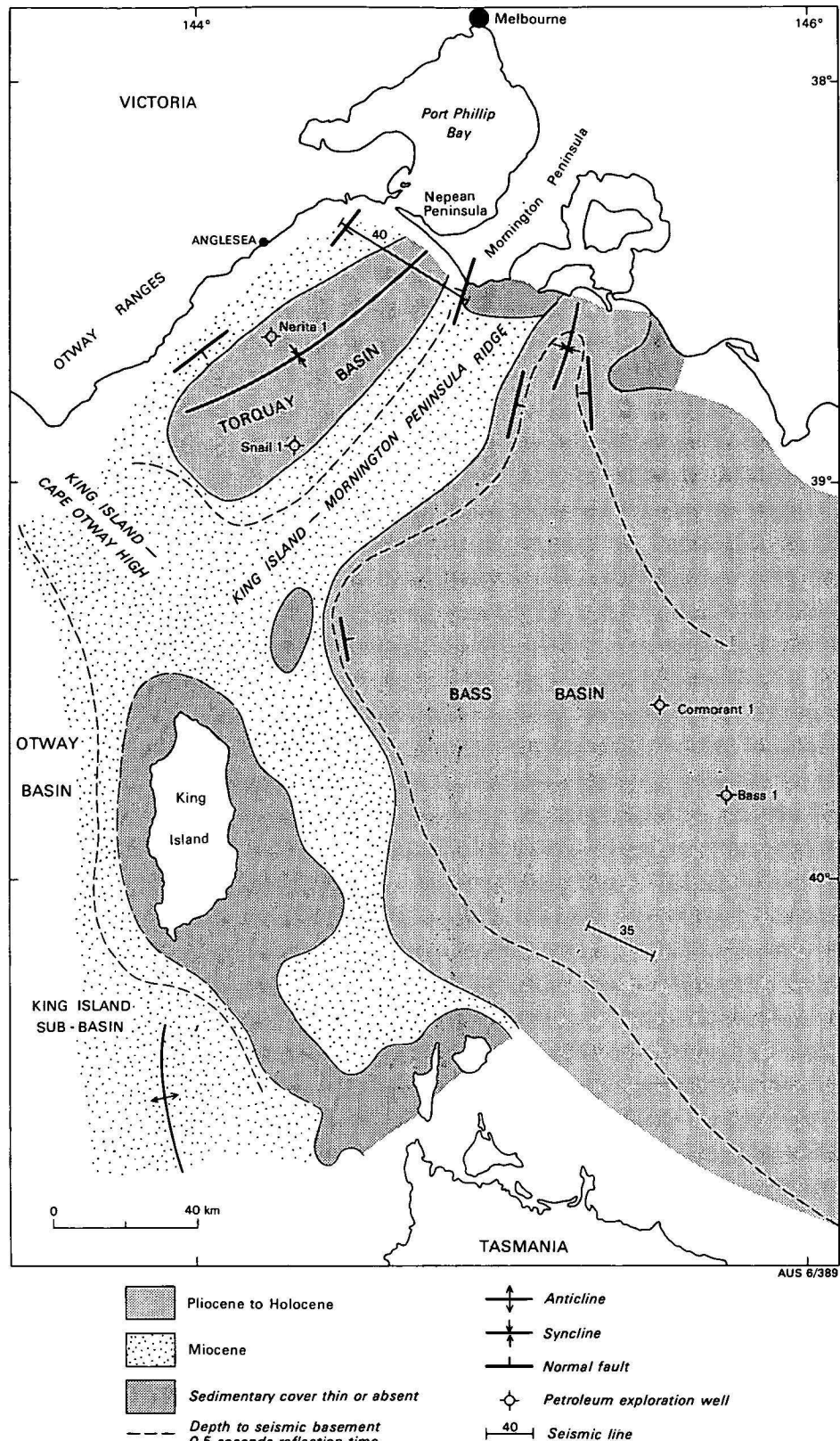


Figure 2. Geology and Cainozoic sediment thickness, western Bass Strait. Seismic sections are shown in Figure 4.

between the two sequences decreases towards the off-shore Tertiary depocentre, where they are almost conformable (Fig. 4). Onshore and offshore borehole data allow correlation with the seismic sections. Deep drilling by the Victorian Department of Minerals and Energy at Sorrento on the Nepean Peninsula showed

that a Pleistocene calcarenite sequence (Bridgewater Formation) overlies a Pliocene marine calcarenite sequence (Wannaeue Formation) (Holdgate, 1976). The Wannaeue Formation, when projected some 15 km southwest to seismic line 40, correlates in thickness and elevation with the upper flat-lying sequence. In the

Sorrento bores a thin parallel to non-marine sequence (Brighton Group) showing evidence of subaerial weathering underlies the Wannaeue Formation, and unconformably overlies the Miocene marine Torquay Group. The unconformity, dated by planktonic foraminifera, spans a time break between Blow's (1969) N.Zone 16 for the top of the Torquay Group, and N. Zone 19-20 for the base of the Wannaeue Formation (Mallet *in* Holdgate, 1976), with the Brighton Group remaining undated. The missing N. Zones 17, 18, and possibly part of 19, represent a time break of some 4 million years.

Data from the two offshore Torquay Basin oil wells confirm that the time break is considerably greater away from the synclinal axis. Thus at the Nerita No. 1 well site, on the western side of the basin, Zonule E marls (equivalent to N. Zone 8) occur at or very close to the surface (Shell Development (Australia), 1967); and at the Snail No. 1 well site on the eastern side of the basin probable Zonule D (N. Zone 9 to 12) marls and claystones commence near the sea floor (Taylor *in* Hodgson & Meblins, 1973). Therefore at the basin centre the top of the folded sequence ranges as high as N16 (Late Miocene), but towards the margins of the offshore basin it may only go as high as N8 (late Early Miocene) or earlier.

The upper flat-lying sequence consists mainly of Pliocene marine sediments but may include some Pleistocene in the upper part, and a thin superficial veneer of unconsolidated Holocene sand. Above the unconformity the Pliocene strata thicken towards the basin centre and are usually not faulted, whereas below the unconformity the Miocene and older sequences have undergone progressively greater deformation and faulting at depth (Fig. 4). The intensity of folding also increases towards the bounding faults along the basin margins.

### King Island — Mornington Peninsula Ridge

Direct evidence of the composition of basement forming the King Island-Mornington Peninsula Ridge is lacking, as no offshore drillholes have been sited along its length. On the Mornington Peninsula Ordovician and Silurian siltstones and mudstones intruded by Devonian granites are unconformably overlain by Mesozoic sandstone and arkose (Otway Group), or by thick sequences of early Tertiary basalt flows and interbedded tuffs (Older Volcanics). At the southern end of the ridge on King Island an older basement sequence of Upper Proterozoic sediments and metamorphics, overlain by Cambrian sediments intruded by Devonian granite, crops out. Offshore oil wells in the flanking Tertiary basins bottomed in possible Cambrian mudstones in Bass No. 2 well, and in Lower Palaeozoic black shale and quartzite in Bass No. 3 well (Brown, 1976).

Parts of seismic lines 38, 39 and 40 are located over the ridge. Line 40, which crosses the northern end of the ridge near Westernport, shows a flat, acoustically opaque surface which is almost certainly formed of Eocene basalt flows of the Older Volcanics. Bores at Cape Schanck nearby have proved over 259 m of basalt flows (Keble, 1950); these must certainly extend some distance offshore. Additional evidence supporting a southward extension of the Mornington Peninsula basalts is provided by aeromagnetic data; these show a confused pattern of strong anomalies, which was in-

terpreted as indicating shallow basaltic basement extending to 39°S, 90 km offshore (Haematite Explorations Pty Ltd, 1965). Our shallow seismic data, however, suggest that the near-surface basalts do not extend this far south; line 39, which crosses the ridge in a southwesterly direction between 38°50'S and 39°10'S, reveals a very irregular basement surface unconformably overlain by folded Tertiary strata. The contact between Tertiary sediments and Older Volcanics basalt is usually conformable, so the presence of this unconformity and the irregular nature of basement surface suggest that the basement here is of Palaeozoic age.

### Bass Basin

Some 13 petroleum exploration wells have been drilled in the western part of the Bass Basin and a mainly Tertiary sequence exceeding 3300 m in thickness has been proved. No sample recovery from the near-surface section was made at any of the wells; palaeontological examination of the first sample returns below 250 m indicate the presence of Zonule A (Pliocene to Holocene) foraminifera at about 330 m in the Cormorant No. 1 and Bass No. 1 wells, and Zonule C (late Middle Miocene) at about 460 m (Taylor *in* unpublished reports to Hematite Petroleum Pty Ltd). The Pliocene to Holocene sequence is therefore much thicker here than in the Torquay Basin, and occupies most, if not all, of the visible section in the shallow seismic profiles away from the basin margins. A similar contrast occurs on land between the incomplete Miocene-Pliocene sections of the Gippsland Basin to the west and east respectively of the Mornington Peninsula Ridge (Mallett, 1978).

Six of the shallow seismic lines cross parts of the western Bass Basin. On the two northern lines (Nos. 39 and 40) the unconformity separating the upper flat-lying Pliocene to Holocene sequence from the underlying, slightly disturbed Miocene sequence is visible at depths of up to 0.1 seconds. Farther south, towards the centre of the basin, the entire section visible on the profiles over wide areas consists of horizontal stratified sediments of Pliocene and post-Pliocene age.

Two broad subdivisions of the Pliocene to Holocene Bass Basin sequence seen on these profiles can be made, based upon the character of the seismic reflectors. An upper sequence of closely spaced reflectors with good lateral persistence thickens to the south from 0.16 seconds on line 41, to 0.26 seconds on line 35, and conformably overlies a lower sequence of sparsely occurring, less persistent reflectors which continue to the limit of penetration, or to acoustic basement. In both sequences the sediments probably mostly consist of marine calcarenites similar to those sampled at the seabed, and also below 250 m in the offshore wells, but the impersistent nature of the reflectors in the lower sequence is characteristic of fluvio-deltaic deposits and a non-marine influence may be indicated.

The northwestern embayment of the Bass Basin has different tectonic styles on its eastern and western margins. On the eastern side shallow acoustic basement with faulted margins forms a broad shelf out from the Victorian coastline, which is overlapped with the Pliocene to Holocene sequence. In contrast, the western margin against the shallow basement ridges between the Mornington Peninsula, King Island and northwest Tasmania appears to have acted as a hinge line with the Pliocene



to Holocene sequence thickening rapidly away from it eastwards into the basin. This hinge line appears to have acted as a 'pivot point' for the Pliocene to Holocene strata similar to that described by Van Siclen (1958). Faulting in the basement surface is not evident below the hinge line, except on line 41 east of the small basement high to the north of King Island.

Oil company data indicate that Tertiary volcanic activity occurred in this part of the Bass Basin throughout much of its history, but apparently the volcanics are too low in the section in most areas to appear on the shallow seismic lines. An exception occurs in the southwest of the basin near the intersection of lines 34 and 35, where reef-like structures occur at depth of 0.5 to 0.7 seconds (Fig. 4). Drilling by Esso-BHP on similar reef-like structures at the Bass No. 1 well has shown the volcanic material to consist of pyroclastics, tuffs and tuff breccias, although intrusive rocks have also been encountered in other wells. The volcanics shown on line 34 and 35 are of Late Miocene age as they are overlain by the characteristic Pliocene to Holocene sequence, and are part of the Miocene volcanics mapped in this area (Robinson, 1974).

### West Tasmanian shelf

The west Tasmanian shelf ranges in width from about 22 km near Port Davey to over 70 km off the northwest tip of Tasmania. Oil company data, particularly the seismic survey conducted by Esso in 1969, have shown that substantial sediment thicknesses occur in the north (the King Island Sub-basin) and also off Macquarie Harbour (Esso, 1969a). A single well (Clam No. 1) drilled in the King Island Sub-basin bottomed in Proterozoic metamorphics at 1622 m. As much as 4000 m of sediments may overlie basement in the complex graben west of Macquarie Harbour, but these sediments are untested by drilling.

Nineteen of BMR's shallow seismic lines (parts of lines 26-36) cross the shelf in an east-west direction; they run from close inshore to a little seaward of the shelf break, which lies at a depth of about 150 m. A number of short tie lines parallel to the coastline were also run. The line bounding the areas of shallow basement and basement outcrop shown in Figure 3 is necessarily generalised, particularly in the south, because of the very irregular nature of basement surface; sediment-filled pockets, some of considerable depth, may occur well inshore of the line marking the general seaward limit of basement outcrop (Fig. 4). The nature of basement is unknown. The broad area of shallow basement occupying nearly half the width of the shelf south of 43°S is likely to consist of Precambrian metamorphics that are continuous with those underlying southwestern Tasmania. The small basement high crossed by line 30 (Fig. 4) may be an offshoot of the extensive Late Devonian-Early Carboniferous granites exposed onshore in this region. It is possible that Tertiary basalts form acoustic basement locally, particularly in the far north.

Two sedimentary sequences, separated by a disconformity or low-angle unconformity, are present on the middle and outer shelf, except in the far north where the upper sequence is missing. Seabed sampling by BMR over the west Tasmanian shelf recovered only Holocene sands and reworked older material from a superficial veneer of sediment too thin to be resolved in the seismic sections. Thus the only stratigraphic control

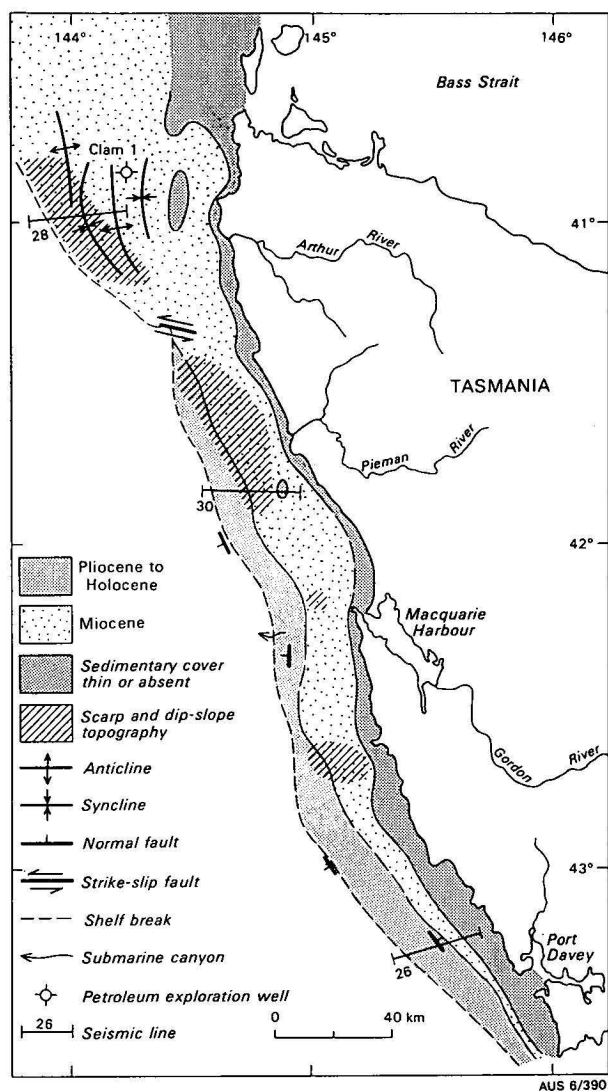


Figure 3. Geology and topography, west Tasmanian shelf. Seismic sections are shown in Figure 4.

is that provided by Esso's Clam No. 1 well; here the first samples recovered came from a depth of about 190 m below the sea bed, and consisted of hard brown limestone of Miocene age (Port Campbell Limestone equivalent) which was interpreted as comprising the interval from the sea bed to about 200 m depth (Esso, 1969b). Projecting this well section to our nearest seismic profile (line 28, 4 km to the south and line 36, 24 km north) shows that the gently folded strata underlying the sea bed in this area are likely to be Miocene limestone, with Oligocene and possibly Eocene rocks approaching the surface along the eroded axes of anticlines and near the inshore margin of the sedimentary wedge (Fig. 4).

Data coverage is inadequate to allow confident correlation of seismic reflectors southwards from the area of Clam No. 1 to the central and southern Tasmanian shelf. However, very little disturbance of the upper part of the section by faulting has occurred and seismic character does not alter southwards. It seems reasonable to assume that the near-surface Miocene section penetrated at Clam No. 1 extends southwards along the shelf, probably to the limit of the area studied.

The gently flexuring of the Miocene and older Tertiary strata evident off northwestern Tasmania dies out

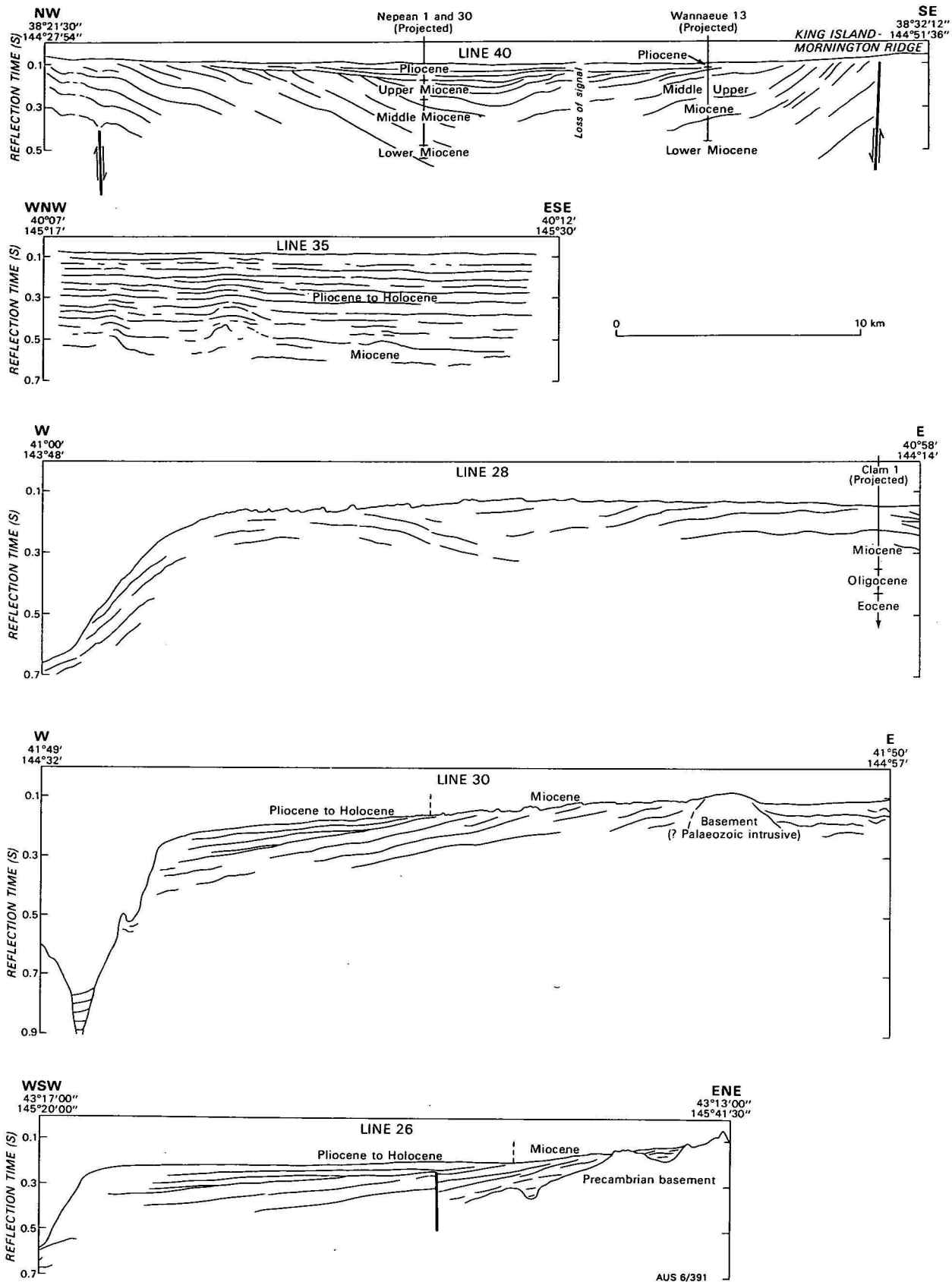


Figure 4. Interpretations of seismic profiles:

- (i) Part of Line 40, off Nepean Peninsula, Western Port.
- (ii) Part of Line 35, east of King Island.
- (iii) Part of Line 28, northwest Tasmanian continental shelf.
- (iv) Part of Line 30, central west Tasmanian continental shelf.
- (v) Part of Line 26, southwest Tasmanian continental shelf.

southwards and is replaced by a uniform westerly dip. Coincident with this change in structural style, a younger sedimentary sequence appears at the outer edge of the shelf at about 41°20'S and onlaps the older rocks to the west. The extent of onlap increases southwards and the younger sequence reaches half way across the shelf in the southern part of the area (Fig. 3).

There is no direct evidence on the age of the upper sequence. The seismic sections show that its base is diachronous and it is probably conformable with the underlying Miocene at the western extremity of the area in the deeper water beyond the shelf edge. The surface onlapped landwards by the upper sequence is an unconformity of regional extent, however it shows little evidence of subaerial erosion. From comparison with the Torquay Basin sections described above, the likelihood is that this unconformity is of Late Miocene age and that the bulk of the transgressive sequence overlying it is Pliocene. There is abundant Australian evidence of the drastic worldwide fall in sea level immediately preceding the Pliocene, which has been documented, for example, by Adams & others (1977) and Vale & others (1977); apart from the evidence from the Nepean Peninsula bores referred to previously Mallet (1978) cites supporting data from elsewhere in the southern Victorian basins, and a widespread unconformity of about this age has been recorded in continental shelf sequences off eastern Australia (Davies, 1979; Marshall, 1979) and northwestern Australia (Jones, 1973).

Erosion of the continental shelf sediments exposed during times of low sea level in the Pleistocene glacial stages must have occurred, but evidence of this is hard to detect in the shallow seismic profiles, except for the obvious and extensive dissection of the present-day sea floor. Areas where this dissection is particularly pronounced are shown on Figure 3; it is best developed over the Miocene limestones, where differential subaerial erosion of gently dipping strata has resulted in scarp and dip-slope topography, with a relief of 10 to 15 m (Fig. 4). This erosion took place mainly in the Late Miocene, but must have continued during Pleistocene glacial stages when some exhumation may have occurred.

The upper sequence is thickest under the shelf edge at the southern margin of the region, where it is of the order of 100 m thick, and thins steadily northwards, pinching out entirely at 41°20'S. This, with the extensive erosion of Miocene strata which has taken place in the north, indicates uplift of the northwest Tasmanian shelf. This uplift, which was accompanied by gentle folding, appears to have halted before the end of the Tertiary because the shelf break, sculptured during Pleistocene regressive cycles, lies at about 150 m, the usual depth for stable continental shelves, along all the west Tasmanian margin.

### Conclusions

Sedimentation in the central part of the Bass Basin has continued without major breaks throughout the late Cainozoic; here several hundred metres of flat-lying Pliocene to Holocene strata conformably overlie the Miocene. Thinner sequences laid down in this time span, again showing no evidence of major breaks, occur along the axis of the Torquay Basin and beneath the outer continental shelf off southwestern Tasmania.

Around the margins of the Torquay Basin, in the King Island Sub-basin, and along much of the west Tasmanian shelf gentle folding, faulting, uplift and erosion occurred during the late Miocene, and Pliocene to Quaternary sediments unconformably overlie Miocene and older rocks.

Cainozoic sediments are thin or absent where Palaeozoic and Precambrian rocks approach the surface over the basement highs separating the Bass, Torquay and Otway Basins and along the inner Tasmanian shelf.

Wide areas of the central and northern Tasmanian shelf and western Bass Strait south of King Island are also non-depositional, and a topography formed by differential subaerial erosion of gently dipping strata is preserved on the present-day sea floor. This erosion dates back to the Late Miocene, but must have also been active during Pleistocene glacial stages.

### References

- ADAMS, C. G., BENSON, R. H., KIDD, R. B., RYAN, W. B. F., & WRIGHT, R. C., 1977—The Messinian salinity crisis and evidence of late Miocene eustatic changes in the world ocean. *Nature*, 269, 383-6.
- BLOW, W. H., 1969—Late Middle Eocene to Recent planktonic foraminiferal biostratigraphy. *Proceedings of the International Conference on Planktonic Microfossils I*, 199-422.
- BROWN, B. R., 1976—Bass Basin—some aspects of the petroleum geology. In R. B. Leslie, H. J. Evans, & C. L. Knight (eds). *Economic Geology of Australia and Papua New Guinea, Part 3 Petroleum — Australasian Institute of Mining and Metallurgy, Monograph Series 7*, 67-82.
- DAVIES, P. J., 1979—Marine geology of the continental shelf off southeast Australia. *Bureau of Mineral Resources, Australia, Bulletin 195*.
- DAVIES, P. J., & MARSHALL, J. F., 1973—BMR marine geology cruise in Bass Strait and Tasmanian waters—February to May, 1973. *Bureau of Mineral Resources, Australia, Record 1973/134* (unpublished).
- ESSO, 1969a—West Tasmania T69A marine seismic and magnetic survey, final report. *Bureau of Mineral Resources, Australia, File 69/3000* (unpublished).
- ESSO, 1969b—Clam No. 1 well completion report. *Bureau of Mineral Resources Australia, File 69/2016* (unpublished).
- HAEMATITE EXPLORATIONS PROPRIETARY LTD, 1965—Bass Strait and Encounter Bay Aeromagnetic Surveys 1960-61. *Petroleum Search Subsidy Acts Publication 60*.
- HODGSON, E. A. & MELLINS, I., 1973—Snail No. 1 Well Completion Report. Unpublished report to Hematite Petroleum Pty Ltd 1973. *Bureau of Mineral Resources, Australia File 72/3159* (unpublished).
- HOLDGATE, G. R., 1976—Subsurface stratigraphy of the Nepean Peninsula. *Victorian Mines Dept* unpublished report 1976/34.
- JONES, H. A., 1973—Marine geology of the northwest Australian continental shelf. *Bureau of Mineral Resources, Australia, Bulletin 136*.
- KEBLE, R. A., 1950—The Mornington Peninsula. *Geological Survey of Victoria, Memoir, 17*.
- MALLETT, C. W., 1978—Sea level changes in the Neogene of Southern Victoria. *APEA Journal*, 18, 64-69.
- MARSHALL, J. F., 1979—The development of the continental shelf of northern New South Wales. *BMR Journal of Australian Geology & Geophysics 4*, 281-8.

- ROBERTSON, C. S., CRONK, D. K., MAYNE, S. J., & TOWNSEND, D. G., 1979—A review of petroleum exploration and prospects in the Otway Basin region. *Bureau of Mineral Resources, Australia, Record 1978/91* (unpublished).
- ROBINSON, V. A., 1974—Geological history of the Bass Basin. *APEA Journal* **14**, 45-9.
- SHELL DEVELOPMENT (AUSTRALIA) PTY LTD, 1967—Nerita No. 1, Offshore Victoria Well Completion Report. *Bureau of Mineral Resources, Australia, File 67/4258* (unpublished).
- VALE, P. R., MITCHUM, R. M., & THOMPSON, S., 1977—Seismic stratigraphy and global changes in sea level. Part 4: Global cycles of relative changes in sea level. In C. E. Payton (Editor) *Seismic stratigraphy—applications to hydrocarbon exploration. American Association of Petroleum Geologists Memoir* **26**, 83-97.
- VAN SICLEN, D. C., 1958—Depositional topography—examples and theory: *American Association of Petroleum Geologists Bulletin*, **42**, 1897-913.





## Permo-Carboniferous palynology of Gondwanaland: progress and problems in the decade to 1980

Elizabeth M. Truswell

The decade 1970-80 has seen the emergence of new regional, palynologically based biostratigraphic schemes, or the modification of existing ones, from late Carboniferous through Permian sequences on the major, now dispersed continents of Gondwanaland. Schemes comprising loosely defined assemblage zones and/or interval zones have been published for eastern and western Australia, Antarctica, India, south, east and west Africa, and South America. Inter-regional correlation based on these zones is for the most part of a broad kind, but the beginnings of a widely applicable chronostratigraphy are discernible, and relatively high-resolution correlation is possible between selected intervals in Australia, India and southern Africa.

During the decade there has been some emphasis on the palynology of late Palaeozoic glacial deposits, with data becoming available from all major continents. These data do not support the idea of a sequential migration of glacial centres across Gondwanaland. Information has also become available concerning the palynology of sediments transitional between the Permian intervals of coal measure sedimentation and the overlying red-bed sequences; palynological data suggest that the Permian-Triassic boundary lies well above the youngest coal measures, at least in India and eastern Australia. Palynological information accumulated during the decade points also to the existence of phytogeographic subprovinces within the *Glossopteris*-dominated Permian vegetation of Gondwanaland.

### Introduction

The last review of the Permo-Carboniferous palynology of Gondwanaland as a whole (Hart, 1971) contained very broad palynological biostratigraphic schemes from India, Australia and southern Africa, with a brief mention of a single Antarctic locality. In the ensuing years there has been a considerable extension of the geographic area within Gondwanaland from which palynological data are available; the present review takes into account information that has accrued from South America, from several regions of Antarctica, from west, east and south Africa, from Malagasy, from extra-peninsula India, and from many more Australian basins than were known a decade ago (Fig. 1). The geographic extension of available data has been accompanied by an intensification of stratigraphic effort, so that there now exists a plethora of reasonably detailed biostratigraphic schemes based on spore and pollen distribution.

In this overview I have briefly described the distinguishing features of the regional palynofloral successions and their distribution in local lithological units of the Lower Gondwana sequence. I have attempted too to assess progress and problems in inter-regional correlation based on them. Throughout, I have referred to the interval under discussion as 'Permo-Carboniferous', as the Carboniferous-Permian boundary remains difficult to identify within the region. On existing evidence, it seems likely that sediments bearing the imprint of glaciation either pre-date or straddle this boundary. The Permian-Triassic boundary is also difficult to fix, but, in the eastern Gondwanaland continents of India and Australia at least, it probably lies somewhat above the youngest coal measures, and within the basal formations of the red-bed sequences that succeed them. The time interval considered in this review corresponds then mainly to the Permian, but begins somewhere within the Late Carboniferous.

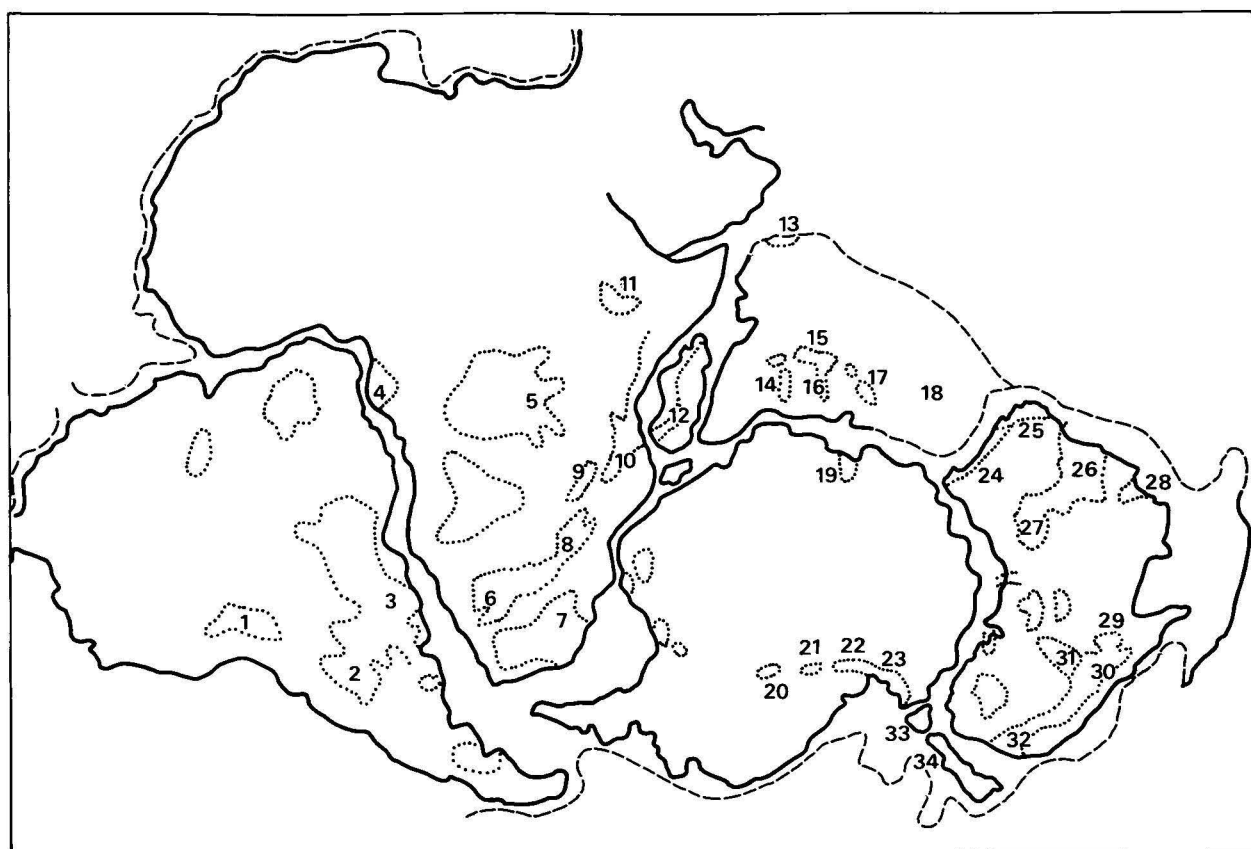
### Australia

Developments in Australian Permo-Carboniferous palynology are summarised only briefly here as they were discussed comprehensively in a relatively recent review (Kemp & others, 1977) in which the sequence beginning at the base of the Carboniferous was described. For the classic 'Lower Gondwana' sequence, which commences with glacial deposits of probable late Carboniferous age, palynostratigraphic schemes have arisen independently in Western and eastern Australia. For Western Australia, the sequence in the Canning Basin has provided a standard, and the presence there of marine intervals allows for some measure of correlation with internationally accepted standard scales. In the interval from the glacial deposits of the Grant Formation up to the top of the Liveringa Formation, Balme (*in* Kemp & others, 1977) defined eight informal palynological assemblages, designated Units I to VIII. The time span covered in this section is considered, on the basis of variable faunal evidence, to represent approximately a Stephanian to Chidruan interval.

In eastern Australian basins, the palynologically based zonal schemes that are currently applied are predominantly modifications of that synthesised by Evans in 1969. These units are a mixture of assemblage zones and interval zones. The modifications of Evan's scheme include a twofold subdivision of Stage 3, a threefold division of Stage 4, and a fivefold division of Stage 5. The subdivisions are based on the earliest appearance of individual miospore species; however, their identification is reinforced by quantitative data on the relative frequencies of selected species groups. They have been identified in the Bowen, Cooper, Galilee, Sydney and Tasmania Basins, and in a number of smaller basins; their relations to lithological units and to marine faunas was detailed in Kemp & others (1977). The correlation between palynostratigraphic units in eastern and Western Australia remains tentative (Fig. 2).

In Australian Lower Gondwana sequences, there is an upwards transition from assemblages dominated by

\* Paper presented at the 5th Gondwana Symposium, Wellington, New Zealand, February, 1980.



M(P) 861

Figure 1. Gondwanaland reconstruction (after Smith & Hallam, 1970; Greater India after Veevers & others, 1975) with outlines of Late Palaeozoic sedimentary basins shown by dotted lines.

Regions for which Permo-Carboniferous palynological data are available are numbered as follows: 1 — Bolivian or Tarija Basin; 2 — Paganzo Basin; 3 — Parana Basin; 4 — Gabon; 5 — Zaire; 6 — Namibia; 7 — Karoo Basin; 8 — Mid-Zambezi Basin, Zimbabwe-Rhodesia; 9 — North Luangwa Valley; 10 — Tanzania; 11 — Ethiopia; 12 — Sakoa-Sakamena Basin, Malagasy; 13 — Salt Range; 14 — Godavari Valley Coalfields; 15 — Son Valley Coalfields; 16 — Mahanadi Valley Coalfield; 17 — Damodar Valley Coalfield; 18 — Arunachal Pradesh; 19 — Prince Charles Mountains; 20 — Ohio Range; 21 — Wisconsin Range; 22 — Nilsen Plateau; 23 — South Victoria Land; 24 — Perth Basin; 25 — Carnarvon Basin; 26 — Canning Basin; 27 — Officer Basin; 28 — Bonaparte Gulf Basin; 29 — Galilee Basin; 30 — Bowen Basin; 31 — Cooper Basin; 32 — Sydney Basin; 33 — Tasmania; 34 — New Zealand.

radially symmetrical monosaccate pollens to suites in which disaccate forms, mainly taeniate, predominate — the same pattern of microfloral change is evident in other Gondwanaland continents. Over the same interval, however, the subdivisions Stages 3 to 5, and their western equivalents, are identified on the basis of initial appearances of distinctive pteridophyte spores. Of these, some index species, such as *Verrucosisporites pseudoreticulatus* Balme & Hennelly, *Granulatisporites trisinus* Balme & Hennelly, *Didecitriletes villosa* (Balme & Hennelly), and *Didecitriletes ericianus* (Balme & Hennelly) occur on other Gondwanaland continents; one important genus, *Dulhuntyispora*, which marks the base of Stage 5, is however confined to Australia and South Africa.

The youngest of the Australian palynological units, the *Protohaploxypinus microcorpus* Zone, has been extensively discussed in a recent paper by Foster (1979). This zone (the *P. reticulatus* Zone of Kemp & others, 1977) was identified in the uppermost Baralaba Coal Measures and the basal part of the overlying Rewan Formation on the eastern margin of the Bowen Basin of Queensland. The base of the *P. microcorpus* Zone is identified by the incoming of distinctive forms such as *Triplexisporites playfordii* (De Jersey & Hamilton), *Playfordiaspora crenulata* (Wilson), and *P. microcorpus* (Schaarschmidt) within the top part of the coal

measures in an interval wherein taeniate disaccate pollens continue to dominate. The microflora of this transitional interval is considered by Foster to correlate with microfloras from the uppermost Chhidru Formation of the Salt Range (Balme, 1970), and hence to be of Chhidruan age.

The basal Rewan Formation, which includes thick red-brown and green mudstones, yields palynological assemblages in which cavate and acavate trilete spores are dominant, and taeniate disaccate pollens a minor component. This assemblage forms the upper part of the *P. microcorpus* Zone which occurs also in post coal-measure sequences in the Sydney Basin and in the southern Perth Basin of Western Australia. From a comparison with the Salt Range sequence, Foster considered that the age of this part of the zone could lie in the interval late Chhidruan to early Griesbachian (the latter substage is deemed by Foster to be latest Permian). A tentative correlation between Salt Range, Indian and Australian assemblages is shown in Figure 3.

Other papers recently published in Australia include an account of the palynology of the complete Permian sequence on the Springsure Anticline, on the south-western margin of the Bowen Basin (Rigby & Hekel, 1977) and another of the Permo-Triassic transition in the same general area (de Jersey, 1979). The Spring-

sure Shelf sequence commences with the continental Reids Dome Beds, which contain Stage 3b microfloras, then passes upwards through a marine and non-marine sequence to the coal-bearing Bandanna Formation, which yields late Stage 5 microfloras. One point to emerge from this study concerns the use of *Praecolpatites sinuosus* (Balme & Hennelly) as an index species. This form is currently used to mark the upper division of Stage 4; Rigby & Hekel (1977), however, report its occurrence with Stage 3 assemblages in the Springsure area. In the study of de Jersey (1979), the *P. microcorpus* Zone was shown to be present in the western Bowen Basin, where *Triplexisporites playfordii* first appears in the top of the Bandanna Formation.

### Antarctica

Palynological work in the Permo-Carboniferous of Antarctica to 1977 was reviewed by Kyle (*in Kemp &*

others, 1977), so the present report is confined to material published since that date. Most data have come from the Transantarctic Mountains, where the late Palaeozoic sequence resembles that of eastern Australia, with the significant difference that marine intervals have not been found. The sequence in the Transantarctic Mountains is assigned to the Victoria Group, which forms the upper part of the Beacon Supergroup: it begins with glacial deposits, then passes upwards through lacustrine shales and feldspathic sandstones into *Glossopteris*-bearing coal measures. As in parts of the Karoo Basin of southern Africa, spore preservation has been adversely affected by thermal metamorphism associated with Jurassic tholeiitic basalts and dolerites.

Using material from several localities, Kyle (1977) and Kyle & Schopf (*in press*) managed to identify a sequence of palynological assemblages within the Victoria Group (Fig. 6). Shales and tillites of glacial se-

MAIN PALYNOLOGICAL CHARACTERISTICS	Palynological Units		International Stage / Substage	
	Eastern	Aust.		
1st appearance <i>Triplexisporites playfordii</i> Taeniate and non — taeniate disaccates dominant	P. microcorpus	P. microcorpus	Chhidruan	
	Upper stage 5	VIII		
1st appearance undescribed <i>Dulhuntyispora</i> sp.	Upper stage 5a	VII	Baigendzhinian	
1st appearance <i>Dulhuntyispora parvithola</i>	Lower stage 5c			
1st appearance <i>Dulhuntyispora dulhuntyi</i> variety 297	Lower stage 5b			
1st appearance <i>Didecitriletes ericianus</i>	Lower stage 5a			
1st appearance <i>Dulhuntyispora dulhuntyi</i>	Upper stage 4b	VI		
1st appearance <i>Didecitriletes villosa</i>	Upper stage 4a			
1st appearance <i>Praecolpatites sinuosus</i>	Lower stage 4	V		Early Baigendzhinian
1st appearance <i>Polypodioidites cicatricosus</i>	Stage 3b	IV		Aktastinian
1st appearance <i>Granulatisporites trisinus</i>	Stage 3a	III		Sterlitamakian Tastubian
1st appearance <i>Verrucosisporites pseudoreticulatus</i>	Stage 2	II		
1st taeniate disaccate pollens mostly monosaccate pollens. Taeniate disaccates, absent	Stage I	I		

M(P) 862

Figure 2. Characteristics of eastern Australian palynological stages, and their tentative correlation with Western Australian units; ages as suggested by marine faunas shown in column on right.



quences in the Darwin, Ohio and Wisconsin Ranges, and post-glacial shales of the Roaring Formation on the Nilsen Plateau yielded sparse assemblages referable to Kyle's (1977) informal *Parasaccites* Zone. They are dominated by monosaccate pollen, contain a low frequency of taeniate disaccate forms, and, locally, high frequencies of *Microbaculispora tentula* Tiwari and *Cycadopites cymbatus* (Balme & Henelly). They compare closely with microfloras assigned to the upper part of Stage 2 in Australia.

Assemblages from the lower part of the Mount Glossopteris Formation in the Ohio Range contain 18 percent of taeniate disaccate pollen, and may thus be as young as Stage 3 in Australia, although no species diagnostic of that stage have been identified in the poorly preserved material. Suites from the middle and upper Weller Coal Measures of South Victoria Land, assigned by Kyle (1977) to her informal *Protohaploxypinus* Zone, are distinguished by abundant disaccate pollen, much of its taeniate. In gross composition and species content they resemble Stage 4 assemblages from eastern Australia, especially those from the Blair Athol Coal Measures of Queensland (Foster, 1975), but as none of the index species of Stage 4 was identified, the correlation remains tentative.

Microfloras probably younger than these have been recovered from the Queen Maud Formation of the Nilsen Plateau, and the upper part of the Mount Glossopteris Formation of the Ohio Range. These assem-

blages contain up to 50 percent taeniate disaccate pollen, and infrequent *Praecolpites sinuosus* and *Bascanisporites undosus* Balme & Henelly suggesting correlation with upper Stage 4b through Stage 5 in eastern Australia. Nowhere in the Transantarctic Mountains have assemblages of Permian age younger than these been recovered; the oldest assemblages above the coal measures are probably early Triassic in age, equivalent to the *Triplexisporites playfordii* Zone (?Smithian to Anisian) of Western Australia.

Elsewhere in Antarctica, palynologically productive sequences have been found in the Prince Charles Mountains of East Antarctica. There, Late Palaeozoic sediments are assigned to the Amery Group, consisting of the Radok Conglomerate at the base, overlain by Bainmedart Coal Measures — a sequence of sandstones, shales and coals — which are succeeded upwards by a sandstone unit, the Flagstone Bench Formation. Palynological assemblages from the Radok Conglomerate and Bainmedart Coal Measures (Balme & Playford, 1967; Kemp, 1973) are similar in composition to those of Stage 5 of the Australian sequence, and contain the stratigraphically diagnostic species *Didecitriletes ericianus*, *Bascanisporites undosus*, *Microbaculispora villosa* and *Indospora clara* Bharadwaj. *Guttulapollenites hannonicus* Goubin, which is rare in Australia, is also present. A quantitative palynological analysis of all three formations of the Amery Group was recently published by Dibner (1978). She found species com-

Range of index species	PALYNOLOGICAL ZONES	BOWEN BASIN (QLD)	INDIA	SALT RANGE	Stage / Substage
<div style="display: flex; flex-direction: column; align-items: center;"> <div style="margin-bottom: 10px;">↓</div> <div style="margin-bottom: 10px;">↓</div> <div style="margin-bottom: 10px;">↓</div> <div style="writing-mode: vertical-rl; transform: rotate(180deg);"> <i>Triplexisporites playfordii</i>  <i>Playfordiaspora crenulata</i>  <i>Protohaploxypinus microcorpus</i> </div> </div>	LUNATISPORITES PELLUCIDUS ZONE = KRAEUSELISPORITES SAEPTATUS ZONE (in part)	Rewan Fm		Kathwai Fm	Griesbachian
	PROTOHAPLOXYPINUS MICROCORPUS		Maitur Fm		
	ZONE	Upper Lower			
		Baralaba Coal Measures	? ?	Chhidru Fm	Chhidruan
		Gyranda Fm			
		Flat Top Fm			
		Barfield Fm			
		Oxtrack Fm			
	UPPER STAGE 5				
	LOWER STAGE 5				
	UPPER STAGE 4				Baigendzhinian

M(P) 863

Figure 3. Suggested correlation of Indian and Salt Range formations with Australian units from the Bowen Basin, based on identification of Australian palynological zones. Modified from Foster (1979).

position to be constant throughout the sequence, but noted that there are changes in the abundance of miospore taxa. In the Flagstone Bench Formation, for instance, disaccate pollens do not dominate the assemblage as they do in the older formations; the dominant elements are instead smooth trilete spores. Changes in environment seem likely to be responsible for these differences.

None of the Stage 5 assemblages recovered to date from Antarctica contains the Australian guide genus *Dulhuntyispora*. Specimens referable to the genus have, however, been observed among recycled spores in bottom sediments of the Weddell Sea (Kemp, 1972). The source of this recycled material is unknown, but is possibly in Dronning Maud Land, or the Theron or Pensacola Mountains, all regions in which coal-bearing sequences with *Glossopteris* occur.

### India

Substantial description of the spore floras of peninsular India was carried out in the nineteen-sixties; the decade 1970-80 produced supplementary taxonomic studies, but the bulk of palynological research has been concerned with biostratigraphy directed especially towards coal-seam correlation. Much of the palynological biostratigraphy from the subcontinent has been based on relative frequencies of genera rather than the stratigraphic ranges of miospore species; this approach makes close comparison of Indian sequences with those from other parts of Gondwanaland difficult. There has been a tendency to describe each of the lithological subdivisions of the Gondwana sequence separately; thus we have accounts of the palynology of the Talchir, Karharbari, Barakar, Barren Measures and Raniganj Stages, but few papers that treat the stratigraphic ranges of species against a framework of the entire sequence. This has made for difficulties in intercontinental correlation.

The plethora of papers published makes it necessary to be selective in listing articles dealing with the palynology of the main stages. Fuller bibliographies are contained in the papers mentioned. The palynology of the glacial Talchir Stage (or Formation) has been described by Lele & Karim (1971), Lele & Chandra (1972, 1973), Lele & Makada (1972), Bharadwaj & Srivastava (1973), Lele (1975), and Tiwari (1975). The palynology of the overlying Karharbari Formation has been described from its type area in Giridih Coalfield by Srivastava (1973); a paper by Lele & Srivastava (1977) refers to the palynology of the formation from other areas. For the coal-bearing Barakar Stage, the account given by Lele & Chandra (1977) lists earlier contributions. The palynology of the Barren Measures has been described by Kar (1973), Srivastava & Maheshwari (1974) and Lele & Srivastava (1977). The coal seams of the Raniganj Stage have been individually analysed for the past two decades; recent contributions include studies by Tiwari (1976), and Bharadwaj & Tiwari (1977). The latter paper describes an interval extending from the uppermost coal seam in the Raniganj Coalfield, to the lowest formations of the overlying Panchet Group. The Panchet has traditionally been regarded as Triassic, but Banerji & Maheshwari (1974, 1975), Maheshwari & Banerji (1975) and Bharadwaj & Tiwari (1977), have presented data which suggest that a latest Permian age is more likely.

Bharadwaj (1970, 1975) summarised the palynological characteristics of each of the main lithological

units; Surange (1975) presented a similar summary in which microfloras were related to contemporary macrofossil floras. Both accounts list the characters of the main assemblages by generic, and sometimes supra-generic groups only — no species are mentioned. In these terms, the Talchir and Karharbari are distinguished by the epibole of the *Parasaccites* complex which declines in the upper part of the Karharbari, and is replaced in importance by non-taeniate disaccate pollen, notably *Scheuringipollenites*. This dominates the lower part of the Barakar also, in association with taeniate disaccates; the upper part of this unit is dominated exclusively by the latter group, as are the succeeding Barren Measures and Raniganj Stages, but in the former the monosaccate form *Densipollenites* is abundant, and the proportion of that genus within the stage has been used to effect a threefold subdivision within it (Bharadwaj, 1974a). In the Raniganj Stage, the presence of a distinctive suite of pteridophyte spores, including *Didecitriletes ericianus* is noteworthy; *Dulhuntyispora*, which characterises coeval Australian assemblages, has not been recorded.

From extra-peninsular India, the most important palynological work remains that of Balme (1970), who described Permian and Triassic sequences in the Salt Range of Pakistan. This detailed taxonomic study encompassed assemblages from the Amb Formation (Baigendzhinian) through the Wargal Limestone and Chhidru Formations of the Permian sequence, to the Mianwali and Tredian Formations of the Triassic, and furnished fundamental reference data for other parts of Gondwanaland. It has been particularly useful in enabling the recognition of the Chhidruan elsewhere, although the position of this sub-stage within a standard Permian sequence remains controversial.

Palynomorphs from the oldest part of the late Palaeozoic sequence in the Salt Range, the Boulder Beds which are the equivalent of the Talchir Formation of the peninsula, were briefly described by Kemp (1975) in a review of the palynology of glacial deposits. These assemblages are rich in monosaccate pollens, and clearly related to Stage 2 of the Australian sequence. The palynology of shales some 25 feet above the boulder beds at Kathwai, described by Virkki (1946), and by Venkatachala & Kar (1968), was reassessed by Tiwari (1975), who considered that abundant taeniate disaccate pollen at that horizon suggested correlation with the Barakar Stage of the peninsula. Foster (1979) considers that the presence in this assemblage of *Protohaploxypinus microcorpus* and possibly *Petricolpitenites bharadwajii* Balme suggests that it may be as young as Chhidruan.

A significant contribution to extra-peninsula palynology was made by Srivastava & Dutta (1977), who provided the first palynological evidence for Lower Gondwana rocks in the extreme northeast. In the Siang district of Arunachal Pradesh, shales and sandstones of the Garu Formation are apparently thrust over Tertiary sequences; they contain palynological assemblages suggesting correlation with the Talchir and Karharbari. Palynological studies suggesting a Carboniferous age for the conglomeratic Blaini Formation of Himachal Pradesh (Shrivastava & Venkataraman, 1975) are inconclusive.

In what is admittedly a subjective assessment, I consider that the most significant advances in the palynostratigraphy of the Indian region have been made in the Talchir Stage, and at the base of the Panchet

Group, immediately above the youngest Raniganj coal seams. Aspects of both are discussed below. In peninsular India, the Talchir Formation occurs in elongate Late Palaeozoic basins; the base is frequently marked by a boulder bed, which is succeeded by shales, siltstones and local turbidites. On faunal grounds it has long been considered that the base of the Talchir is not isochronous, but only recently has palynological information been advanced in support of that view with the identification of a sequence of palynological assemblages within the formation. An 'early Talchir' assemblage was identified from siltstones immediately above the basal boulder bed in the West Bokaro Coalfield (Lele, 1975) and a 'late Talchir' assemblage from siltstones below the contact with the overlying Barakar Stage and above the ubiquitous Talchir 'needle shales'. The latter assemblage is more diverse, and contains rare taeniate disaccate pollen, which are absent from the older suite. In his review of peninsula Talchir assemblages, Lele (1975) concluded that microfloras of early Talchir type were rare and typified by those from Manendragarh (Lele & Chandra, 1972). Late Talchir microfloras occur in the South Rewa, Johilla and Jayanti Coalfields (Potonié & Lele, 1961; Lele & Chandra, 1973; Lele & Makada, 1972).

Tiwari (1975) identified three palynological zones within the Talchir, based on overall diversity and the relative frequencies of certain monosaccate genera. In this, as in Lele's zonal scheme, there is some suggestion of facies control on the assemblages; there is usually an increase in diversity upwards from the base, suggesting ameliorating conditions after an initial glacial phase. Palynological data have been used to suggest a return to near-glacial conditions in the lower part of the Kaharbari Stage. Assemblages immediately above those of Zone T-III, the youngest of Tiwari's Talchir units, generally show first an increase in diversity, but are followed by a relatively non-diversified monosaccate-dominated suite, which Bharadwaj (1974b) had interpreted as reflecting a phase of renewed cooling, somewhat less intense than the first. The concept of a second glacial phase is not supported by lithological data; according to recent sedimentological studies (Geological Survey of India, 1977; Casshyap, 1977) the widespread conglomerate at the base of the Karharbari accumulated not from glacial deposits, but by rapid deposition of debris from denuded highland areas after deglaciation.

That part of the Indian sequence which can be broadly referred to as late Permian has also been the subject of considerable palynological study in the seventies. Recent comparative studies of coeval intervals in Australia (Foster, 1979) have provided a biostratigraphic framework within which the time relations of the Indian floras can be better understood. The Maitur Formation, a sequence dominantly of brown and khaki shales and mudstones at the base of the Panchet Group, and lying above the Raniganj Coal Measures, is one of the intervals that has recently been thus reinterpreted. Microfloras from basal Panchet strata in the Raniganj Coalfield have been described by Banerji & Maheshwari (1974, 1975), Maheshwari & Banerji (1975) and Bharadwaj & Tiwari (1977). Characteristically, taeniate disaccate pollen is dominant in beds immediately above the coal seams, but diminishes thereafter.

Raniganj Stage assemblages are closely comparable to spore and pollen floras of the Baralaba Coal Measures of the Bowen Basin, Queensland (Foster, 1979),

except for the absence of *Dulhuntyispora* species in India. The Baralaba Coal Measures assemblages belong almost entirely to Upper Stage 5. However, assemblages from the uppermost part of the Baralaba coals belong to the lower subdivision of the *Protohaploxy-pinus microcorpus* Zone; the overlying basal Rewan Formation belongs to its upper subdivision. On Foster's interpretation of the Indian assemblages, those from the Maitur Formation belong to the *P. microcorpus* Zone, and are thus equivalent to those from the basal Rewan (Fig. 3).

The nature of floral change through this late Permian interval seems to be gradational in both Australia and India. In Australia, forms characteristic of the *P. microcorpus* Zone appear in the upper part of the coal measures, and the same gradual incoming of these forms seems to be evident in the sequence in the Raniganj Coalfield (Bharadwaj & Tiwari, 1977). There, three zones occur in the interval; the basal one of these, from a coal seam, is dominated by taeniate disaccates, but also includes the species *Playfordiaspora crenulata*, a characteristic element of the *P. microcorpus* Zone. It is for this reason that in Figure 3, the uppermost part of the Raniganj is tentatively shown to correlate with the upper part of the Baralaba Coal Measures. *Triplexisporites playfordii*, which is used in the definition of the base of this unit in Australia, appears slightly later at this Indian locality.

A recent re-evaluation of the stratigraphic position of another Indian microfloral assemblage deserves mention. Microfloras described by Bharadwaj & Srivastava (1969) from alleged Panchet Series strata near Nidpur in Madhya Pradesh, and ascribed to the lower Triassic, contain dominant taeniate disaccate pollen, many *Weylandites* species, and the colpate species *Praecolpatites sinuosus*. Balme (1970) suggested that this assemblage might be Permian; Foster (1979) made a more detailed appraisal, and confirmed that a middle or late Permian age seems likely.

## Africa

Since 1970 palynological studies of African strata of 'Karoo' age equivalent have burgeoned; new data have emerged from a region extending from South Africa north to Ethiopia. Extensive and intensive palynostratigraphic studies have been made in the Karoo Basin in South Africa, the Mid-Zambezi Basin of Zimbabwe-Rhodesia, the Luangwa Valley of Zambia, the Ketewake Coalfield of Tanzania, the eastern sector of the Congo Basin, and in Gabon. In addition, palynological analyses have established the presence of Karoo equivalent strata in Ethiopia, and new information has been presented on the composition of spore assemblages from post-glacial shales in Namibia. Sequences of Karoo rocks in Angola remain the only major ones in southern Africa for which no palynological information is available.

The most detailed study has been that of Anderson (1977) in South Africa. It was based on material from 12 boreholes and from surface samples in the northern Karoo Basin; spore preservation is better there than it is in the south of the same basin, where folding associated with the Cape Orogeny has affected preservation. In the northern Karoo, a scheme of 7 palynological zones and 18 subzones was established in the section commencing with the glacial diamictites and shales of the Dwyka, and passing upwards through coal measure and delta-front deposits of the Ecca, to the



floodplain deposits of the Beaufort. The Beaufort sediments include those assigned to the *Tapinocephalus*, *Cistecephalus* and *Daptocephalus* Zones. The succeeding *Lystrosaurus* Zone sediments are mainly red beds and are palynologically barren. The palynostratigraphic units established are chiefly assemblage zones, but are also defined on first appearances of taxa, diversity, and frequency of selected supra-generic groups. In the southern part of the Karoo, some eight 'microfloral stages' were defined, but these are less well understood than the northern ones, and are poorly preserved, so that correlation with the north remains tentative. In his taxonomic descriptions, Anderson used a 'population' approach, with variations in the morphology of form species at a single horizon clearly and copiously illustrated. This approach is close to the 'biorecord' concept of Hughes (1975, and earlier), and allows comparisons with the South African material to be made with ease.

A number of interesting, though not closely related points arise from Anderson's South African data. The nature of assemblages from the lower part of the sequence, particularly from the Dwyka, is one such point. As is typical of assemblages from periglacial sediments elsewhere, the suites from the Dwyka diamictites are not very diverse. Microfloral Zone 1 occurs in the northern Karoo from the base of the Dwyka to the top of the highest diamictite or varved shale. In assemblages of this unit monosaccate pollen dominates and cavate, trilete forms are common; among trilete species, *Microbaculispora tentula* may reach abundances of 40 percent. In the southern Karoo, most of the Dwyka tillites are attributed to Anderson's microfloral zone 2, suggesting that they are equivalent in age to the basal Eccla of the north.

From the lower zones of the northern Karoo there is a point of conflict between microfloral and macrofloral data. Plumstead (1967) described lycopod remains from lower Eccla horizons in boreholes in the Welkom/Virginia area. These, by comparison with Australian and Cape Series fossils, were considered to be Devonian; microfloral assemblages from the same intervals favour instead an approximately early Permian age.

The Karoo assemblages show some similarity to Australian ones, particularly in the pteridophyte content. A number of pteridophyte species which are valuable stratigraphic markers in Australia occur in southern Africa, permitting tentative correlations between the two continents (Fig. 4). In the older part of the Karoo sequence, *Microbaculispora tentula*, *Verrucosisporites pseudoreticulatus* and *Granulatisporites trisinus* have been recorded; in Australia the sequential appearance of these species defines the boundaries of the palynological units 2, 3a and 3b. In the upper Karoo Permian, the presence of *Didictriletes villosa*, *D. ericianus* and *Dulhuntyispora dulhuntyi* Potonié establishes a close link with Australia. In eastern Australia *D. villosa* defines the upper part of Stage 4, *D. dulhuntyi* the base of Stage 5, and *D. ericianus* appears slightly later. The simultaneous appearance of all three species in the upper Eccla means either that the ranges are slightly different in South Africa, or that there is a time (or sampling?) break near the base of Subzone 4d in the Eccla sequence. The similarities between Australian and South African pteridophytic elements are not matched in the gymnosperm pollen suite. Disaccate pollens in particular differ: in South Africa *Guttulapollenites* and *Lueckisporites* are quantitatively important genera in

the upper part of the Karoo Permian, whereas in Australia they are rare.

A brief study of uppermost Beaufort Group sediments in the Karoo Basin was made by Stapleton (1978). Poorly preserved palynological suites from that interval contain *Protohaploxypinus microcorpus*, *Playfordiaspora crenulata*, and *Lunatisporites pellucidus* (Goubin); the last-named suggests that the interval is slightly younger than the *P. microcorpus* Zone of Australia. The admixture of species resembles Goubin's Zone I from the Lower Sakamena Group of Malagasy. Stapleton (1977) also described assemblages from probable Dwyka Shales penetrated in a borehole north of Etosha Pan in Namibia. These are rich in trilete spores, and can probably be assigned to Anderson's Microfloral Zone 2.

In the mid-Zambezi Basin of Zimbabwe-Rhodesia, Falcon (1973, 1975) made an intensive study of the Karoo sequence in the Matabola Flats borehole, where the Lower Karoo is apparently continuous. At the base the Dwyka section is exceptionally thick; above this are Lower Wankie Sandstones, black shales and coals, further sandstones, and, at the top, the Madumabisa Mudstone. Falcon identified four assemblage zones and eight subzones within the sequence (Fig. 6). Of the stratigraphically useful pteridophyte spores known from South Africa, only two were recorded in Rhodesia, both from the lower part of the sequence; *Microbaculispora tentula* is abundant in the lower Dwyka, and *Verrucosisporites pseudoreticulatus* is rare in the upper part of that formation. The higher units penetrated contain assemblages that might be regarded as typically 'African'. This distinctiveness is particularly notable in the disaccate pollen, which includes, as consistent elements, *Lueckisporites nyakapendensis* Hart and *Guttulapollenites hannonicus*. *Weylandites lucifer* (Bharadwaj & Salujha) is also well represented.

On the other side of the Zambezi River, in Zambia, Utting (1978) defined three concurrent range zones in the sequence in the Siankondobo Coalfield (Figure 6). The oldest of these, the *Plicatipollenites indicus*/*Cannoropollis obscurus* Zone (IO Zone) occurs in the Siankondobo Sandstone, and is broadly equivalent to the basal Zone I in Rhodesia. The lower part of the overlying Gwembe Coal Formation, a probable Eccla equivalent, is dominated by trilete spores, and referred to the *Apiculatisporis levis* (LP) Zone, equivalent to the Rhodesian Zone II, Carbonaceous mudstones above this yield assemblages referred to the *Vittatina africana*/*Gondisporites vrystaatensis* (AV) Zone, equated with Rhodesian Zone III. Within the sequence, *Verrucosisporites pseudoreticulatus* was identified sporadically, but the other 'index' trilete spores listed in Figure 4 are absent.

Utting correlated his units with assemblages that he had described earlier (Utting, 1976) from the north Luangwa Valley, northeastern Zambia. There, the two oldest lithological units of the Luwumbu Coal Formation contain an IO assemblage, and the overlying Mpwashii Carbonaceous Member an LP assemblage. Utting extended the correlation into the coal basins of Tanzania, whence assemblages were described earlier by Manum & Tien (1973). There, the entire coal-bearing sequence, comprising the lower, coal/sandstone beds (K2.1) and the overlying coal/shale beds (K2.2) belong to Utting's LP Zone, suggesting a very thick development of this interval in Tanzania.

Sequences referred to the late Permian have also been examined in the North Luangwa Valley (Utting,





in press). Assemblages from the Madumabisa Mudstone, at a level equivalent to the *Cistecephalus* Zone of South Africa, reflect a poorly diversified parent vegetation; this trait also distinguishes Anderson's (1977) equivalent Unit 6. They are dominated by taeniate disaccate pollens, and contain *Guttulapollenites hannonicus* and *Weylandites lucifer* in abundance. Utting noted similarities to the Chhidru Formation assemblages of the Salt Range but key species are missing, and it seems likely that they may be somewhat older. They differ distinctly from assemblages known from Gabon.

The recent discovery in Ethiopia of palynological assemblages similar to those of the Karoo (Davidson & McGregor, 1976) represents a considerable northern extension of known Lower Gondwana sequences in Africa. Suites of two ages were reported from isolated outcrops in the southwest; the older, from the Gilo Sandstone is poorly diversified and similar to those of the Dwyka or Lower Ecca. The younger, from the fluviatile Kari Sandstone, is possibly of late Permian age. Disaccate pollens dominate, and, like assemblages from Gabon, the suite seems to have a character transitional between European and typically Gondwanan microfloras. The presence of the characteristically European pollen *Klausipollenites schaubergeri* (Potonié & Klaus) reinforces this impression.

In the eastern part of the Congo Basin (Zaire) the youngest Palaeozoic rocks are represented by the Lukuga Series (Fig. 6). They begin with glacial deposits and pass upwards into dark post-glacial shales, which are succeeded by coal measures and then arkoses and sandstones of 'transition beds'. Comprehensive palynological studies of the entire sequence carried out in the nineteen-sixties were summarised by Bose (1971). Since then assemblages from the coal measures have been described by Kar & Bose (1976). A pan-African correlation attempted by Falcon (1975) suggests that the entire Congo Basin sequence is no younger than about middle Ecca, the coal measures being probably equivalent to the Barakar Stage of India. The fact that no assemblages dominated by disaccate pollens have been recorded supports the idea that no younger rocks are present.

In the coastal basin of Gabon, the late Palaeozoic commences with morainal deposits and varved clays, the n'Khom Series, then passes upwards into lacustrine sediments with anhydrites, then to red and green siltstones. These post-glacial sediments belong to the Agoula Series, and are believed to reflect increasing aridity and the eventual drying out of post-glacial lakes. Jardiné (1974) described the palynology of the post-glacial sequence in detail, identifying three microfloral associations (Fig. 6). Microflora PII, from the basal Bekang Member of the Agoula Series, he regarded as typically Gondwanan; in it both monosaccate and taeniate disaccate pollens are abundant. Microflora PIII, from the Koumiki Member, is characterised by abundant disaccates including, characteristically, species of *Lueckisporites* and *Corisaccites*. The north American form *Tornopollenites toreutos* Morgan is a notable component. This association has no clear links with either

northern or southern hemispheres; its age, calculated from known ranges of its component species, is estimated as Artinskian-Kungurian.

The youngest Gabonese microflora, PIV, from the Assango Member of the Agoula Series, is distinguished again by an abundance of disaccate pollen. Among this, *Lueckisporites virkkiae* Potonié & Klaus and *Klausipollenites schaubergeri* are prominent. Much in the assemblage is typical of the late Permian of Europe, and some elements occur in the Salt Range: some forms are characteristic of younger palynological zones of the South African Karoo, but much is different. The distinctive *Guttulapollenites hannonicus*, common also in east African sequences, is missing; absent also is the 'Australian' pteridophyte suite that distinguishes parts of the Beaufort of South Africa.

### Malagasy

No data have been published from Permian sequences in Malagasy since Rakotoarivelo (1970, 1972) described miospore assemblages from coal measures that directly overlie glacial deposits in the Sakoa Group of the Sakoa-Sakamena Basin, in the southwest (Fig. 6). A perusal of his illustrations (Rakotoarivelo, 1970) shows the probable presence of *Microbaculispora tentula*; *Granulatisporites trisinus* is common and *Verrucosisporites pseudoreticulatus* occurs sporadically. These species support the tentative correlation of Falcon (1975), who equated the Malagasy Coal Measures with Stages 3 and 4 of the Australian sequence, with the Kaharbari-Barakar Stages of India, and with the K<sub>1</sub> to K<sub>2-3</sub> intervals (Lower Wankie Sandstones, Black shales and coals) of the Zimbabwe-Rhodesian sequence.

Pollen assemblages described from the lower part of the Sakamena Group by Goubin (1965) were re-evaluated by Foster (1979), who noted that some species occur in common with the Australian *P. microcorpus* Zone assemblages. *Guttulapollenites hannonicus*, *Weylandites lucifer* and possibly *P. microcorpus* are examples of shared taxa; the first two are much more abundant in Malagasy than in Australia. The presence of *Lunatisporites pellucidus*, however, suggests that Goubin's Zone I is younger than the *P. microcorpus* Zone.

### South America

The palynology of Permo-Carboniferous sediments in South America has been reviewed recently by Azcuy (in press). The sequences for which published data are available are distributed in three sedimentary basins: the Paganzo Basin in the western part of Argentina, the Paraná Basin of Brazil and Uruguay, and the Tarija Basin of Bolivia. Sequences from the Chaco-Paraná Basin of Argentina are being described. A scheme of palynological zones erected in Lower Gondwana formations of the Paraná and Maranhão Basins by Bhara-dwaj & others (1976) was based on only 10 samples, so is less securely founded than the system erected by Azcuy.

Using information biased towards the sections in the Paganzo Basin, Azcuy defined five tentative palyno-

Figure 4. Correlation of palynological zones established in the northern Karoo Basin of South Africa with those from eastern Australia.

Ranges of selected species on which this correlation is based are shown for South Africa to the left of the centre line, ranges in Australia are to the right. Stage boundaries in Australia are shown by solid line only where the defining species occurs on both continents.

zones (Fig. 6). They are broad assemblage zones, defined by the appearance of key forms and by the relative frequencies of different morphological types, usually grouped at supra-generic level. The oldest palynological units were defined in the Paganzo Basin in a sequence of late Carboniferous age. The strata there are not typical of the Lower Gondwana sequence. Evidence of glaciation is confined to dubiously identified glacials of alpine origin on the western edge of the basin; most of the sequence consists of sandstones with thin carbonaceous clays and mudstones.

Palynozone I, which occurs in the oldest formations of the Paganzo Group, is dominated by trilete spores referable to genera such as *Raistrickia*, *Convolutispora*, *Retusotriletes* and *Verrucosisporites*; monosaccate pollen is represented by *Florinites* type grains. This assemblage, which was recently designated the *Ancistrospora* Palynozone (Azcuy & Jelin, in press), may be as old as Namurian, and possibly equates with microfloras identified, but not described, from the Machareti Group in the Tarija Basin of Bolivia (Reyes, 1972); diamictites possibly of glacial origin occur at the same level in that basin.

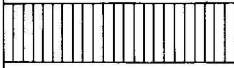
Palynozone II, (the *Potonieisporites* Palynozone of Azcuy & Jelin, in press), is characterised by the appearance of monosaccates such as *Parasaccites* and *Potonieisporites*; taeniate disaccate pollen is rare in this unit. The zone was defined from a few samples in the Paganzo Basin, but Azcuy considers that it correlates in part with the oldest of a suite of palynological assemblages delineated in the Brazilian part of the Paraná Basin by Daemon & Quadros (1970). These authors, and also Daemon (1974), consider that the units G-H, which are correlative with Palynozone II, occur in the basal formations of the glacially derived Itararé Group. Assemblages from varved shales at Itu, which were also examined by Kemp (1975) and referred to Stage 2 of the Australian sequence, fall into Daemon's palynological interval 'G'.

Palynozone III is characterised by a continuing high percentage of monosaccate pollens and a low frequency of taeniate disaccate types. *Vittatina* spp. are conspicuous. Characteristic spores are *Acanthotriletes filiformis*, (Balme & Hennelly) *Apiculatisporis cornutus* (Balme & Hennelly), *Polypodiisporites leopardus* (Balme & Hennelly) and *Horriditriletes ramosus* (Balme & Hennelly). In the Paganzo Basin the assemblage occurs in the Bajo de Velez Formation, in the middle Paganzo Group (Menendez, 1971); sequences at Bajo de Velez were attributed to deposition from glacial lakes, but evidence for glaciation remains equivocal (Frakes & Crowell, 1969). Azcuy correlated Palynozone III with interval H<sub>2</sub>-H<sub>3</sub> of the Paraná Basin (Daemon & Quadros, 1970). The coals of the Rio Bonito Formation, the basal unit of the Guatá Group that immediately overlies the glacial Itararé Group cannot be satisfactorily correlated with Azcuy's zones. The palynology of these coals has been described in detail (Ybert & others, 1971; Ybert, 1975), and it would appear that the assemblages are referable to Palynozone III. However Daemon (1974) related the Rio Bonito Formation in Santa Catarina and Paraná States to his interval I-J rather than to the older H<sub>2</sub>-H<sub>3</sub> interval. The significance of this apparent discrepancy is difficult to assess in view of the broad descriptions given of all palynological units.

In Palynozone IV of Azcuy monosaccate pollen declines, and taeniate disaccates correspondingly increase. Apiculate, monolet spores are locally important. As-

semblages from the coal-bearing Copacabana Group at Apillapampa in Bolivia (Cousminer, 1965) are assigned to this zone, which is not recognised in the Paganzo Basin. Problems continue to be apparent in the correlation of this unit with the Paraná Basin palynological intervals: Azcuy correlates Palynozone IV with the Paraná interval I-J, but, as noted above, Palynozone IV may correlate with older units.

Palynozone V shows a clear dominance of taeniate disaccate pollen. *Lueckisporites* is abundant. Azcuy has recognised this zone only in the San Gregorio Formation of Uruguay, on the evidence of assemblages described by Marques-Toigo (1972), in which disaccate pollen dominates and includes a high frequency of taeniate types. Marques-Toigo argued that the palynological evidence suggested a Permian age for the San Gregorio Formation, rather than the late Carboniferous age suggested by its contained ammonoids (Closs, 1969). The age of the unit in terms of an international standard remains unresolved, and problems remain too with its palynological correlation with other units in the Paraná Basin. The San Gregorio Formation contains a higher frequency of taeniate disaccate pollen than does the Rio Bonito coals, and Azcuy has implied that it is younger than these. Yet the San Gregorio is believed to be equivalent to the Itararé Group of Brazil, which underlies the Rio Bonito Formation. Questions of the facies control of microfloras may be involved; the high content of trilete miospores in the coals perhaps reflects a pteridophyte-rich swamp flora.

SOUTH AMERICA		EASTERN AUSTRALIA
Paganzo & Paraná Basins (Azcuy, in press; Azcuy & Jelin, in press)	Paraná Basin (Daemon & Quadros 1970)	(from Kemp and others, 1977)
		Stage 5
Palynozone V	Interval K-L	Stage 4
Palynozone IV	Interval I-J	Stage 3b ----- Stage 3a
Palynozone III	Interval H <sub>2</sub> -H <sub>3</sub>	Stage 2
Potonieisporites Palynozone	Interval G-H <sub>1</sub>	Stage 1 or Potonieisporites Assemblage
		----- ?
Ancistrospora Palynozone		Anabaculites yberti Assemblage

M(P) 865

Figure 5. Correlation between palynological units recognized in Paganzo and Paraná Basins, South America, with those from eastern Australia (from Azcuy, in press; Azcuy & Jelin, in press).

Azcuy compared his palynological units to those of Evans (1969) in eastern Australia, claiming that this region showed the closest correspondence with South America. His speculative correlations are reproduced in Figure 5. The species list presented by Azcuy does not, however, support the idea of a particularly close relationship to Australia: there is a similarity at the level of the broad abundance of different spore groups, but only a few species are common to the two continents. Of the index species used to define the Australian units, only *Verrucosiporites pseudoreticulatus* is present in the Rio Bonito coals, which show some similarity to Australian Stage 3: a tentatively identified *Granulatisporites trisinus* in Azcuy's palynozone IV reinforces this correlation.

For younger units there are clear differences. These are most manifest in the youngest units described from the Paraná Basin by Daemon & Quadros (1970) and Daemon (1974) which are characterised by common *Lueckisporites virkkiae* and *Vittatina* spp. and probably *Guttulapollenites hannonicus*. The presence of the last named as a significant component in associations of perhaps Kazanian age from Rio Claro has been stressed by Menendez (1977). There is no suggestion of equivalence to the *Dulhuntyispora* assemblage of Australia, and no floras younger than perhaps Kazanian have been described. The South American assemblages most closely resemble East African associations.

### Conclusions

From this broad appraisal it is possible to identify several discipline areas wherein advances have been made in understanding the Permo-Carboniferous palynology of Gondwanaland. Much of the information gathered in the last decade has served to identify problems rather than to offer solutions to them, but this must be considered forward progress. The most obvious development is the emergence of about a dozen regional, palynologically-based biostratigraphic schemes. Correlation between these is at present very tentative and permits only broad intervals to be recognised intercontinentally; only the very beginning of a pan-Gondwanaland chronostratigraphy can be discerned from these regional biostratigraphies. Some stratigraphic intervals have received more emphasis than others in recent years. There has been particular stress on the palynology of the Late Palaeozoic glacial deposits, and on the Late Permian interval transitional between coal measure and red-bed sedimentation. Finally, palynological data are now revealing distinct floral provinces within Gondwanaland during the Permian. These points are discussed separately below.

#### Regional biostratigraphic schemes

The schemes determined on different continents, with their distributions in local lithological units, are shown in Figure 6. They comprise mostly informal and loosely defined units. Many are a combination of assemblage zone and interval zone; the relative abundances of morphological types identified at a supra-generic level have been used in many cases to define 'zones'. In only a few instances have unit boundaries been clearly defined, and in even fewer have those boundaries been supported by designated reference sections. The usefulness of the biostratigraphic schemes in inter-regional correlation varies according to factors such as the thickness of the available (and palynologically productive) section, and on the quality of description and illustration of species present.

#### Inter-regional correlation

Broad correlations between lithological units on different Gondwana continents have been effected by palynological means for some time; in 1964, Balme pointed to similarities between his *Dulhuntyispora* Assemblage, from the Western Australian late Permian, and assemblages from the Raniganj Formation of India. Hart (1971) made broad comparisons between microfloras from Africa, Australia and India — these were based on gross quantitative changes within the microfloral successions, and the microfloral units that he identified mostly corresponded to lithological units. For instance, the Camerati Zone of southern Africa corresponded to the Dwyka, and the zone was correlated with Florizone I of the Indian sequence, which corresponded to the Talchir. More recently, Falcon (1975, fig. 10) attempted a pan-African correlation relating lithological units in Tanzania, Zambia, Malagasy and Zaïre to the Zimbabwe-Rhodesian sequence, and thence to the South African scheme as proposed by Hart (1967). She further correlated the African lithological units with palynological stages of Australia, India and Antarctica, equating upper Ecca and Lower Beaufort with Rhodesian subzones G and H, with Stage 5 of Australia, and with Barren Measures-Raniganj of India.

Increasing information on the detailed distribution of species, rather than higher taxa, in key sequences gives promise of finer resolution in inter-continental correlation, although the move away from correlation at the broadly based level of lithological 'stages' is in its early phases. The biostratigraphic scheme from the northern Karoo Basin of South Africa affords a particularly useful correlative standard for the western part of Gondwanaland, because the sequence is thick, the material well illustrated, and the ranges of species within it clearly shown. The proposed correlations of Australian sequences with those of the Karoo (Fig. 4) are an example of relatively high resolution correlation, wherein ranges of distinctive species have been used to relate 'horizons' or datum levels intercontinentally. Thus it is possible to suggest, for instance, that the South African Palynozone 4d correlates with the eastern Australian Lower Stage 5 boundary. In lithological terms this means that the microfloral changes occurring at an horizon within the Upper Ecca are roughly synchronous with those occurring within the Aldebaran Sandstone of the Bowen Basin in Queensland. There are weaknesses in the biostratigraphic philosophies underlying such correlations — the Australian scheme, for instance, is founded somewhat shakily on the sequential appearance of individual species, and inter-continental correlation is based on the assumption that species appeared simultaneously in widely separated areas.

Another example of a potentially high resolution intercontinental correlation is Foster's (1979) correlation of the Australian Baralaba-Rewan interval in the Bowen Basin with the Indian Raniganj-Maitur section, although the effectiveness of this is hampered somewhat by there being less detail available on species distribution for the Indian section than for the Australian.

#### Intervals of special emphasis

The past decade has seen the presentation from all continents of palynological data from the glacially deposited sediments at the base of the Gondwana sequence. From southern Africa, the composition of miospore suites from both diamictites and shales of the

## NORTHERN KAROO

Miospore zones	Lithological units
Anderson '77	
*	
7	Lystrosaurus
6	Daplocephalus
5	Cistecephalus
	Tapinocephalus Zone
4	Upper Eccia
3	Middle Eccia
2	Lower Eccia
1	Dwyka

\* Stapleton '78

ZIMBABWE  
RHODESIA

Miospore zones	Lithological units
Falcon '75	
H	M/K <sup>5</sup> Madumabisa
IV	Mudstones
G	L/K <sup>5</sup>
III	F K <sup>4</sup> Upper Wankie Sst
E	Black K <sup>2-3</sup> shales & coals
II	D
C	I K <sup>1</sup> Lower Wankie Sst
B	K <sup>0</sup> Dwyka
A	

SOUTHERN ZAMBIA  
NORTHEAST ZAMBIA

Miospore zones	Lithological units
Utting '78	Utting '76
	*
	Madumabisa Mudstone
	Madumabisa Mudstone
AV	Fimbria Grit Mbr
LP	Gwembe Coal Formation
	Mpwashii Carbonaceous Mbr
IO	Siankondobo Sst
	Mukumba Siltstone Mbr
	Musipizi Congl Mbr

\* Utting, in press

## TANZANIA

Miospore zones	Lithological units
Manum, Tien '73	
	K <sub>3</sub>
	K <sub>2</sub> <sup>e2</sup>
	Shale-coal measures
	Vesicaspora Zone
	K <sub>2</sub> <sup>e1</sup>
	Sandstone-coal measures
	Cordaitina Zone

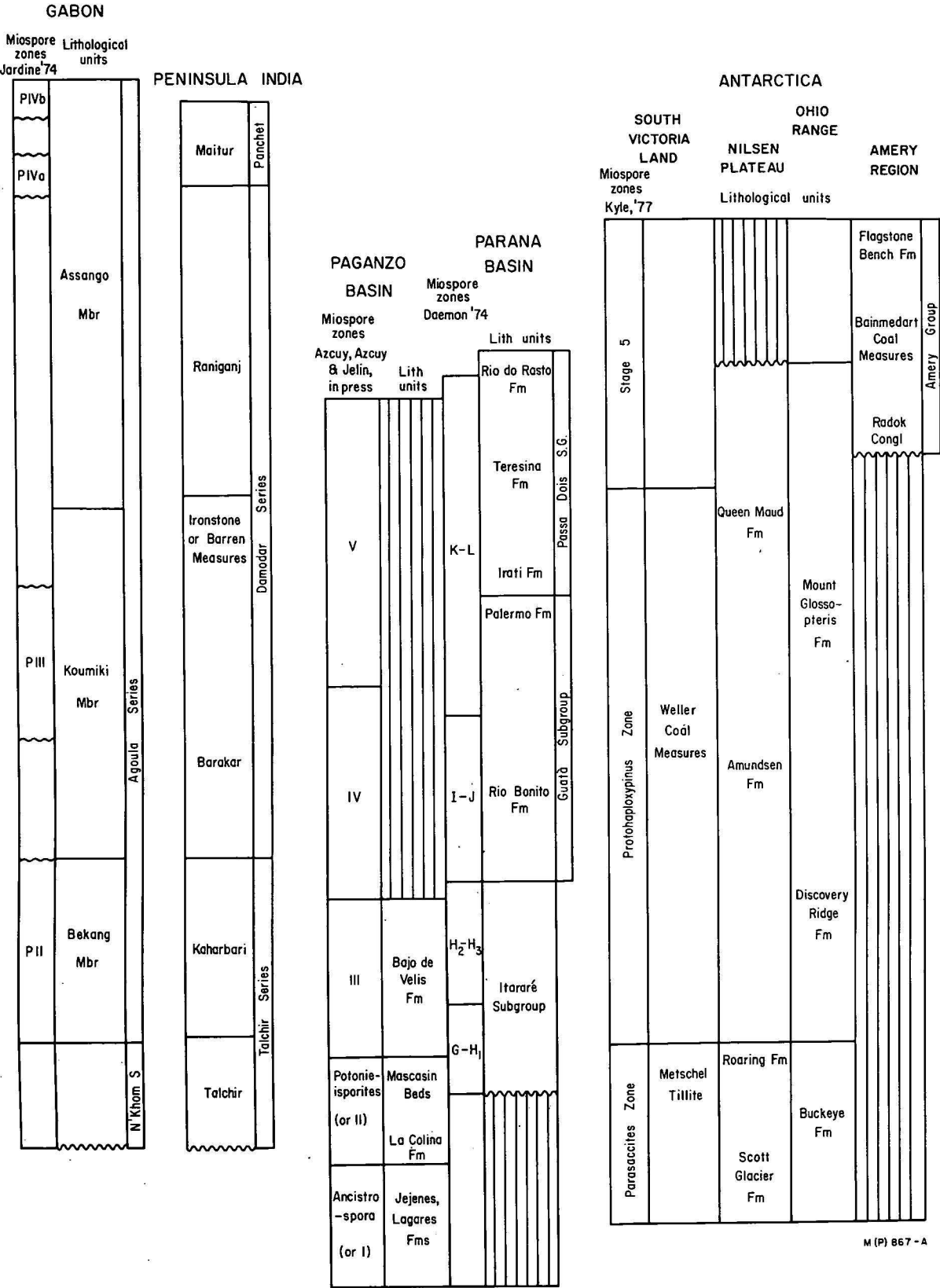
## MALAGASY

Miospore zones	Lithological units
Unit 1	Lower Sakamena
	Vohitolia Limestone
	Lower Red Beds
II	Couches a Houille
2	
I	Glacial unit

1 Goubin '65  
2 Rakotoarivelo '72ZAIRE  
Lithostratigraphy  
See Bose '71  
for  
palynology

Lithological units
Couches de houille
Schistes noirs de Lukuga
Schistes noirs de Walikale
Assises glaciares et periglaciares

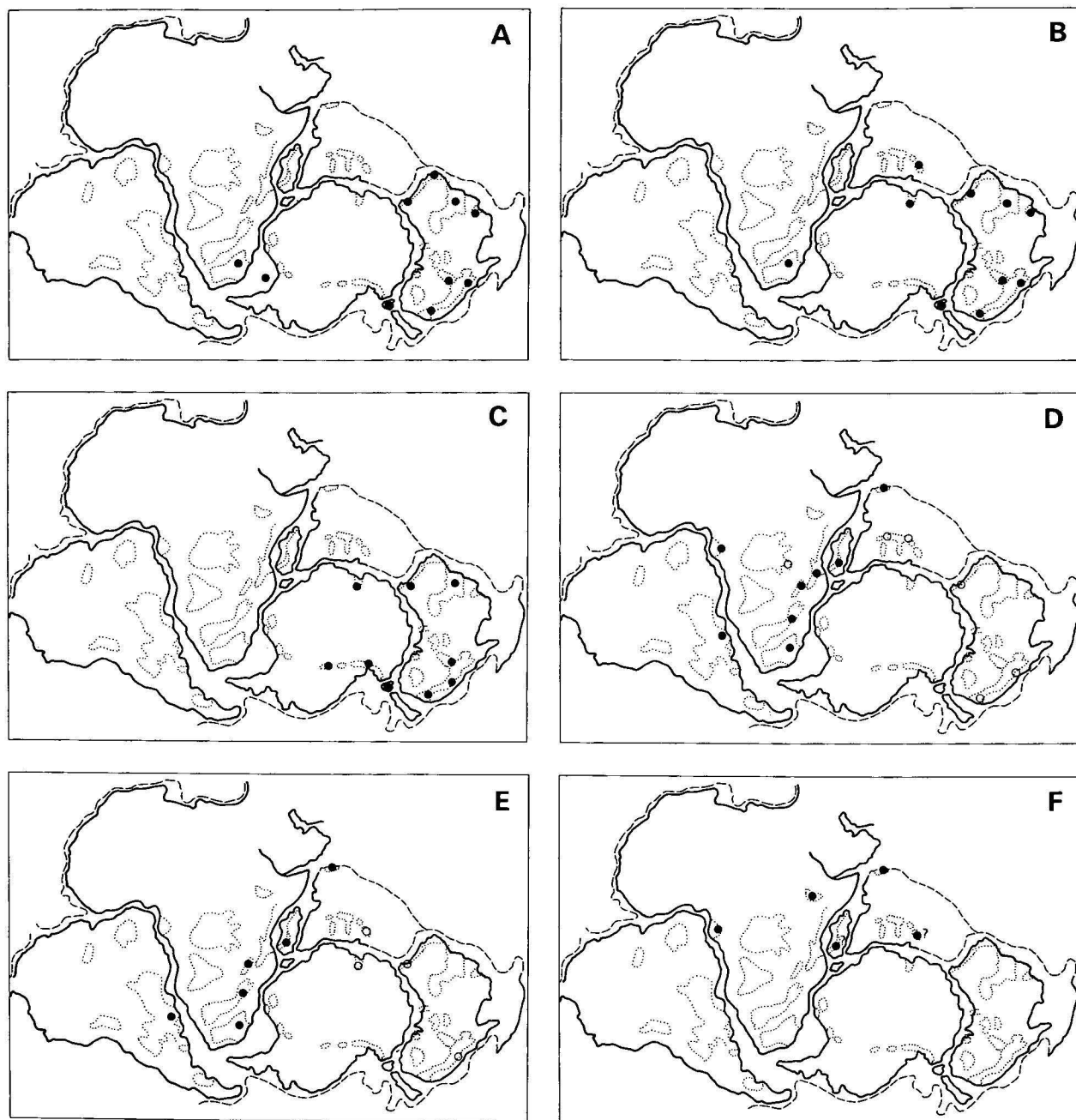
M (P) 867-B



M (P) 867 - A

Figure 6. Stratigraphic columns from Africa, Malagasy, India, South America and Antarctica, showing for most cases the relationship of palynostratigraphic units to local lithological units. In some instances, i.e. Zaire and peninsular India, no palynological units independent of lithology have been defined; the lithological sequences have been included here for clarity. The figure should not be interpreted as a correlation chart, although I have attempted to place lithological units that are probably correlative at approximately the same level. The correlation lines joining the Zambian and Tanzanian columns are from Utting (1978).





M(P) 866

**Figure 7. Gondwanaland reconstructions showing distribution of selected, geographically restricted form species.**  
**A** — *Dulhuntyispora dulhuntyi* Potonié; **B** — *Didecitriletes ericianus* (Balme & Hennelly); **C** — *Bascanisporites undosus* Balme & Hennelly; **D** — *Lueckisporites virkkiae* Potonié & Klaus/*L.nyakapendensis* Hart/*L.singhii* Balme. The three species are grouped together as they are morphologically closely related; *L.virkkiae* is typically European in distribution; *L.nyakapendensis* was described from east Africa but is regarded by some authors as a junior synonym of *L.virkkiae*; *L.singhii*, from the Salt Range, may be distinct, but was considered by Anderson (1977) to be a synonym of *L.nyakapendensis*. Solid circles depict areas where *Lueckisporites* spp. are quantitatively important; open circles where rare or dubiously identified. **E** — *Guttulapollenites hannonicus* Goubin; solid circles show regions where it is quantitatively important, open circles where rare. **F** — *Klausipollenites schaubergeri* (Potonié & Klaus); queries indicate dubious identifications.

Dwyka is now known; all assemblages are of low diversity, but contain rare taeniate disaccate pollens. They are assigned to Zones 1 and basal Zone 2 of Anderson's (1977) biostratigraphic scheme, and may be broadly correlated with Stage 2 of Australia. There are intrabasinal correlation problems within the Karoo and it is clear that much remains to be understood concerning time and facies relationships within this basin.

In India, a sequence of microfloral assemblages is now known within the glacials of the Talchir Stage.

The oldest microflora, from boulder beds, lacks taeniate disaccate pollens; it is not possible to assess how closely this unit compares with Stage 1 of the Australian sequence because the latter remains largely undescribed. In South America there are problems in interpreting the age of glacial deposits within the Paraná Basin. The San Gregorio Formation of Uruguay, believed to be equivalent to the glacial Itararé Group of Brazil, yields, from varved shales, spore assemblages which are assigned to the youngest of the palynozones erected

by Azcuy (in press) — equivalent to Stage 3-4 of Australia. Within the Paganzo Basin where Carboniferous spore assemblages are well known, glacial sediments are minor and of montane type. This recent wealth of palynological data from the Gondwanaland glacials has failed to produce any evidence supporting the idea that glaciation commenced in 'west Gondwanaland', or South America/southern Africa in the Carboniferous, and migrated across the supercontinent to India and Australia in the Permian (see also Kemp, 1975). It must be admitted, however, that the assemblages known are from post or periglacial sediments, and must represent specialised facies.

Within the latest Permian, understanding of time relationships has been made easier by the delineation of the *Protohaploxypinus microcorpus* Zone in Australia, and by assessment of the probable latest Permian age of this zone through its relationship to the Salt Range sequence. Identifying the zone beyond Australia and Pakistan remain problematical — it seems certain that no microfloras as young as this are known from South America, nor from southern Africa, where sediments of the probably correlative part of the Beaufort Group are not palynologically productive. Assemblages from the Sakamena Group of Malagasy are probably younger than *P. microcorpus*; the time relationships of Late Permian sequences in Gabon are difficult to assess, probably because of provincial differences between this region and Australia.

#### Phytogeographical provinces

The fossil macrofloras of Gondwanaland have long been considered to reflect a single phytogeographical province in the Permian, a province wherein *Glossopteris* was the most characteristic element. Details of microfloral composition throughout Gondwanaland suggest that this floristic unity was more apparent than real. From the foregoing review it is clear that differences in microfloras may be quite pronounced within the region; in some cases they are sufficient to make correlations between widely separated areas difficult. Data now available suggest that there was a differentiation into floras of 'African' or west Gondwanaland aspect, and those of 'Australian', or east Gondwanaland type. This distinction was most apparent in the later part of the Permian, when the influence of glaciation has waned.

As Balme (1970) pointed out, the most satisfactory units for examining past phytogeographic distribution patterns are well defined miospore species; form genera encompass too wide a range of parent taxa. In Figure 7, I have illustrated the distribution patterns for six spore species selected to show possible sub-provinces within the main Gondwanaland plant province. Figures 7A-C show stratigraphically useful species that are largely confined, on present records, to east Gondwanaland; Figures 7D-F show species that are confined to, or have their maximum development within, west Gondwanaland. As a generalisation, it appears that eastern Gondwanaland microfloras are distinguished by a greater diversity of pteridophyte spores; a greater morphological diversity of gymnosperm pollens is more characteristic of the western part of the supercontinent. As might be expected, the admixture of forms which are important elements of European Permian floras is more pronounced in the west.

#### Acknowledgement

I am indebted to Dr C. B. Foster, Geological Survey of Queensland, for his constructive criticism of a first draft of this paper.

#### References

- ANDERSON, J. M., 1977—The biostratigraphy of the Permian palynology with particular reference to the northern Permian and Triassic. Part 3. A review of Gondwana Per-Karoo Basin, South Africa. *Memoirs of the Botanical Survey of South Africa* 41.
- AZCUY, C. L., in press—A review of the Early Gondwana palynology of Argentina and South America. *Proceedings Fourth International Palynological Conference, Lucknow, India*, December 1976-January 1977.
- AZCUY, C. L. & JELIN, R., in press—Las palinozonas del limite Carbonico-Permico en la Cuenca Paganzo. *II Congreso Argentino de Paleontología y bioestratigrafía y I Congreso Latinoamericano de paleontología*, Buenos Aires, 1978.
- BALME, B. E., 1964—The palynological record of Australian pre-Tertiary floras: in Cranwell, L. M. (Editor), *ANCIENT PACIFIC FLORAS*, University of Hawaii Press, 49-80.
- BALME, B. E., 1970—Palynology of Permian and Triassic strata in the Salt Range and Surghar Range, West Pakistan: in Kummel, B., & Teichert, C. (Editors), *Stratigraphic boundary problems: Permian and Triassic of West Pakistan: University of Kansas, Special Publication* 4, 306-453.
- BALME, B. E., & PLAYFORD, G., 1967—Late Permian plant microfossils from the Prince Charles Mountains, Antarctica. *Révue de Micropaleontologie*, 10, 179-92.
- BANERJI, J., & MAHESHWARI, H. K., 1974—Palynology of the Panchet Group exposed in the Nonia Nala, near Asansol, West Bengal. *Palaeobotanist*, 21, 268-72.
- BANERJI, J., & MAHESHWARI, H. K., 1975—Palynomorphs from the Panchet Group exposed in Sukri River, Auranga Coalfield, Bihar. *Palaeobotanist*, 22, 158-70.
- BHARADWAJ, D. C., 1970—Palynological subdivision of the Gondwana sequence in India. *Proceedings and papers, 2nd Gondwana Symposium, South Africa*, 531-6.
- BHARADWAJ, D. C., 1947a—Palynological subdivision of Damuda Series; in Surange, K. R. (Editor), *ASPECTS AND APPRAISAL OF INDIAN PALAEOBOTANY*, Lucknow, 392-6.
- BHARADWAJ, D. C., 1947b—Palynology of Talchir and Karharbari Formations and Lower Gondwana glaciation; in Surange, K. R. (Editor), *ASPECTS AND APPRAISAL OF INDIAN PALAEOBOTANY*, Lucknow, 369-85.
- BHARADWAJ, D. C., 1975—Palynology in biostratigraphy and palaeoecology of Indian Lower Gondwana formations. *Palaeobotanist*, 22, 150-7.
- BHARADWAJ, D. C. & SRIVASTAVA, S. C., 1969—A Triassic mioflora from India: *Palaeontographica B*, 125, 119-49.
- BHARADWAJ, D. C., & SRIVASTAVA, S. C., 1973—Subsurface palynological succession in Korba Coalfield, M.P., India. *Palaeobotanist*, 20, 137-51.
- BHARADWAJ, D. C., KAR, R. K., & NAVALE, G. K. B., 1976—Palynostratigraphy of Lower Gondwana deposits in Paraná and Maranhão Basins, Brazil. *Biological Memoirs*, 1, 56-103.
- BHARADWAJ, D. C., & TIWARI, R. S., 1977—Permian-Triassic microfloras from the Raniganj Coalfield, India. *Palaeobotanist*, 24, 26-49.
- BOSE, M. N., 1971—Palynostratigraphy of the Lukuga Series in Congo. *Geophytology*, 1, 16-22.
- CASSHYAP, S. M., 1977—Patterns of sedimentation in Gondwana basins. Section 7, *Fourth International Gondwana Symposium*, Calcutta, 1-34.
- COUSMINER, H. L., 1965—Permian spores from Apillapampa, Bolivia. *Journal of Palaeontology*, 39, 1097-1111.

- DAEMON, R. F., 1974—Integracao dos resultados palinologicos aos de fauna e flora de camadas fossilíferas do Neopaleozoico da Bacia do Paraná — implicacoes estratigraficas e paleogeograficas. *Revista UNIMAR*, 4, 25-41.
- DAEMON, R. F., & QUADROS, L. P., 1970—Bioestratigrafia do Neopaleozoico da Bacia do Paraná. *Anais do XXIV Congresso Brasileira Geol.*, Brasilia, 1970, 359-412.
- DAVIDSON, A., & MCGREGOR, D. C., 1976—Palynomorphs indicating Permian rocks in Ethiopia. *Nature*, 262, 371-73.
- DE JERSEY, N. J., 1979—Palynology of the Permian-Triassic transition in the western Bowen Basin. *Geological Survey of Queensland Publication* 374. *Palaeontological Paper* 46, 1-39.
- DIBNER, A. F., 1978—Palynocomplexes and age of the Amery Formation deposits, East Antarctica. *Pollen et Spores*, 20, 405-22.
- EVANS, P. R., 1969—Upper Carboniferous and Permian palynological stages and their distribution in eastern Australia; in *Gondwana Stratigraphy*, IUGS, 1st *Gondwana Symposium*, Buenos Aires, 1967, UNESCO, 41-54.
- FALCON, R. M. S., 1973—Palynology of the Middle Zambezi Basin; in Bond, G. (Editor). *The Palaeontology of Rhodesia. Bulletin of the Rhodesian Geological Survey* 70, 43-70.
- FALCON, R. M. S., 1975—Palynostratigraphy of the Lower Karoo sequence in the central Sebungwe District, Mid-Zambezi Basin, Rhodesia. *Palaeontologia Africana*, 18, 1-29.
- FOSTER, C. B., 1975—Permian plant microfossils from the Blair Athol Coal Measures, central Queensland, Australia. *Palaeontographica B*, 154, 121-71.
- FOSTER, C. B., 1979—Permian plant microfossils of the Blair Athol Coal Measures, Baralaba Coal Measures, and basal Rewin Formation of Queensland. *Geological Survey of Queensland Publication* 372: *Palaeontological Paper* 45, 1-244.
- FRAKES, L. A., & CROWELL, J. C., 1969—Late Paleozoic glaciation: 1, South America. *Geological Society of America Bulletin*, 80, 1007-42.
- GEOLOGICAL SURVEY OF INDIA, 1977—Gondwana geology, —status, problems and possibilities. *Fourth International Gondwana Symposium*, Calcutta, 1977, 1-52.
- GOUBIN, N., 1965—Description et repartition des principaux pollenites Permiens, Triassiques et Jurassiques des sondages du Bassin de Morondava (Madagascar). *Révue de l'Institut Français du Pétrole et annales des combustibles liquides* 20, 1415-61.
- HART, G. F., 1967—Micropalaeontology of the Karoo deposits in South Africa and central Africa. *IUGS Reviews for 1st Symposium on Gondwana Stratigraphy*, Haarlem, Netherlands, 161-72.
- HART, G. F., 1971—The Gondwana Permian palynofloras. *Anais Academia brasileira de Ciencias*, 43, (Suplemento), 145-85.
- HUGHES, N. F., 1975—The challenge of abundance in palynomorphs. *Geoscience and Man*, 11, 141-4.
- JARDINÉ, S., 1974—Microflores des formations du Gabon attribuées au Karoo. *Review of Palaeobotany and Palynology*, 17, 75-112.
- KAR, R. K., 1973—Palynological delimitation of the Lower Gondwana in the North Karanpura Basin, India. *Palaeobotanist*, 20, 300-17.
- KAR, R. K., & BOSE, M. N., 1976—Palaeozoic spores dispersae from Zaïre (Congo). 12. Assise à couche des houilles from Greinerville region. *Annales de Musée Royal de l'Afrique Centrale, Sciences Géologiques*, Series 8, 77, 21-133.
- KEMP, E. M., 1972—Recycled palynomorphs in continental shelf sediments from Antarctica. *Antarctic Journal of the US*, 7, 190-91.
- KEMP, E. M., 1973—Permian flora from the Beaver Lake area. 1. Palynological examination of samples. *Bureau of Mineral Resources, Australia, Bulletin* 126, 7-12.
- KEMP, E. M., 1975—The palynology of Late Palaeozoic glacial deposits of Gondwanaland: in Campbell, K. S. W. (Editor) *GONDWANA GEOLOGY: PAPERS FROM THE 3RD GONDWANA SYMPOSIUM*, Canberra. *Australian National University Press*, 397-413.
- KEMP, E. M., BALME, B. E., HELBY, R. J., KYLE, R. A., PLAYFORD, G., & PRICE, P. L., 1977—Carboniferous and Permian palynostratigraphy in Australia and Antarctica: a review. *BMR Journal of Australian Geology & Geophysics*, 2, 177-208.
- KYLE, R. A., 1977—Palynostratigraphy of the Victoria Group of South Victoria Land, Antarctica. *New Zealand Journal of Geology & Geophysics*, 10, 1981-102.
- KYLE, R. A., & SCHOPF, J. M., in press—Permian and Triassic palynostratigraphy of the Victoria Group, Transantarctic Mountains. *Proceedings, 3rd Symposium on Antarctic Geology and Geophysics*, Madison, Wisconsin, 1977.
- LELE, K. M., 1975—Studies in the Talchir Flora of India—10. Early and late Talchir microfloras from the West Bokaro Coalfield, Bihar. *Palaeobotanist*, 22, 219-35.
- LELE, K. M., & CHANDRA, A., 1972—Palynology of the marine intercalations in the Lower Gondwana of Madhya Pradesh, India. *Palaeobotanist*, 19, 253-262.
- LELE, G. M., & CHANDRA, A., 1973—Studies in the Talchir Boulder Bed and overlying Needle Shales in the Johilla Coalfield (M.P., India). *Palaeobotanist*, 20, 39-47.
- LELE, K. M., & CHANDRA, S., 1977—Associations of mio and megaflores in the roof shale of some Barakar coal seams, South Karanpura Coalfield, Bihar. *Palaeobotanist*, 24, 254-60.
- LELE, K. M., & KARIM, R., 1971—Studies in the Talchir flora of India—6. Palynology of the Talchir Boulder Bed in Jayanti Coalfield, Bihar. *Palaeobotanist*, 19, 52-69.
- LELE, K. M. & MAKADA, R., 1972—Studies in the Talchir flora of India—7. Palynology of the Talchir Formation in the Jayanti Coalfield, Bihar. *Geophytology*, 2, 41-73.
- LELE, K. M., & SRIVASTAVA, A. K., 1977—A mioflora of Barren Measures age from the Auranga Coalfield, Bihar. *Palaeobotanist*, 24, 118-24.
- MAHESHWARI, H. K., & BANERJI, J., 1975—Lower Triassic palynomorphs from the Maitur Formation, West Bengal, India. *Palaeontographica B*, 152, 149-90.
- MANUM, S. B., & TIEN, N. D., 1973—Palynostratigraphy of the Ketewaka Coalfield (Lower Permian), Tanzania. *Review Palaeobotany and Palynology*, 16, 213-227.
- MARQUES-TOIGO, M., 1972—Ammonoids x pollen and the Carboniferous or Permian age of San Gregorio Formation of Uruguay, Paraná Basin. *Anais de Academia brasileira de Ciencias*, 44 (Supplement), 237-41.
- MENENDEZ, C. A., 1971—Estudio palinológico del Permico de Bajo de Velez, Pcia. de San Luis. *Revista Museo Argentina Ciencias Naturales. 'B. Rivadavia'*. *Palaeontologica*, 1, 263-306.
- MENENDEZ, C. A., 1977—Permian microfloras of Argentina and their relation with other Gondwanic microfloras. *Fourth International Gondwana Symposium*, Calcutta, 1977. Abstracts, 24.
- PLUMSTEAD, E. P., 1967—A general review of the Devonian fossil plants found in the Cape System of South Africa. *Palaeontologia africana*, 10, 1-83.
- POTONÍ, R., & LELE, K. M., 1961—Studies in the Talchir Flora of India—1. *Sporae dispersae* from the Talchir Beds of South Rewan Gondwana Basin. *Palaeobotanist*, 8, 22-37.
- RAKOTOARIVELO, H. J., 1970—Palynostratigraphic comparée du bassin houiller Gondwanien de la Sakoa-Sakamena, Madagascar. *Thesis, Faculty of Sciences, Paris*, volumes 1-3.
- RAKOTOARIVELO, H. J., 1972—Palynostratigraphic review of the coal basin of the Sakoa-Sakamena (Madagascar). *Proceedings and Papers, 2nd Gondwana Symposium, South Africa* 1970, 537-40.
- REYES, F. C., 1972—On the Carboniferous and Permian of Bolivia and north-western Argentina. *Anais da Academia brasileira de Ciencias*, 44, (Supplement), 261-77.

- RIGBY, J. F., & HEKEL, H., 1977—Palynology of the Permian sequence in the Springsure Anticline, central Queensland. *Geological Survey of Queensland Publication* 363, *Palaeontological Paper* 37, 1-76.
- SRIVASTAVA, R. N., & VENKATARAMAN, K., 1975—Palynostratigraphy of the Blaini Formation. *Bulletin Indian Geologists Association*, 8, 196-200.
- SMITH, A. G., & HALLAM, A., 1970—The fit of the southern continents. *Nature*, 225, 139-44.
- SRIVASTAVA, S. C., 1973—Palynostratigraphy of the Giridih Coalfield. *Geophytology*, 3, 184-94.
- SRIVASTAVA, S. C., & MAHESHWARI, H. K., 1974—Palynostratigraphy of the Damuda Group in the Brahmi Coalfield, Rajmahal Hills, Bihar. *Geophytology*, 4, 35-45.
- SRIVASTAVA, S. C., & DUTTA, S. K., 1977—A note on the palynology of the Gondwanas of Siang District, Arunachal Pradesh. *Geophytology*, 7, 281-3.
- STAPLETON, R. P., 1977—Early Permian miospores from a borehole in Southwest Africa. *Pollen et Spores*, 19, 143-162.
- STAPLETON, R. P., 1978—A microflora from a possible Permo-Triassic transition in South Africa. *Review of Palaeobotany & Palynology*, 25, 253-8.
- SURANGE, K. R., 1975—Indian Lower Gondwana floras: a review; in K. S. W. Campbell (Editor). *GONDWANA GEOLOGY: PAPERS FROM THE 3RD GONDWANA SYMPOSIUM*, Canberra, 1973.
- TIWARI, R. S., 1975—Palynological composition of the basal Gondwana in India. *Bulletin de la Société Belge de Géologie*, 84, 11-17.
- TIWARI, R. S., 1976—Palynological succession through Raniganj Formation (Upper Permian), Raniganj Coalfield, India. *Palaeobotanist*, 23, 16-24.
- UTTING, J., 1976—Pollen and spore assemblages in the Luwumbu Coal Formation (Lower Karoo) of the North Luangwa Valley, Zambia, and their biostratigraphic significance. *Review of Palaeobotany and Palynology*, 21, 295-315.
- UTTING, J., 1978—Lower Karoo pollen and spore assemblages from the coal measures and underlying sediments of the Siankondobo Coalfield, mid-Zambezi Valley, Zambia. *Palynology*, 2, 53-68.
- UTTING, J., in press—Pollen and spore assemblages from the Upper Permian of the North Luangwa Valley, Zambia. *Proceedings, 4th International Palynological Conference, Lucknow, India, December 1976-January 1977*.
- VEEVERS, J. J., POWELL, C., MCA., & JOHNSON, B. D., 1975—Greater India's place in Gondwanaland and in Asia. *Earth & Planetary Science Letters*, 27, 383-87.
- VENKATACHAL, B. S., & KAR, R. K., 1968—Palynology of the Kathwai Shales, Salt Range, West Pakistan. 1. Shales 25 ft above the Talchir Boulder Bed. *Palaeobotanist*, 16, 156-66.
- VIRKKI, C., 1946—Spores from the Lower Gondwanas of India and Australia. *Proceedings of the National Academy of Science, India*, 15, 93-176.
- YBERT, J. P., 1975—Étude des miospores du bassin houiller de Candiota-Hulha Negra, Rio Grande do Sul, Brésil. *Pesquisas, Porto Alegre*, 181-226.
- YBERT, J. P., NAHUY, J., & ALPERN, B., 1971—Étude palynologique et pétrographique de quelques charbon du sud du Brésil. *Compte Rendu, Sixième Congrès International de stratigraphie et de géologie du Carbonifère*, 1605-26.





## Geology of the Exmouth and Wallaby Plateaus off northwest Australia: sampling of seismic sequences

U. von Stackelberg<sup>1</sup>, N. F. Exon, U. von Rad<sup>1</sup>, P. Quilty<sup>2</sup>, S. Shafik,  
H. Beiersdorf<sup>1</sup>, E. Seibert<sup>1</sup>, & J. J. Veevers<sup>2</sup>

In this paper we present the first detailed geological information about the margins of the Exmouth and Wallaby Plateaus. New single-channel seismic profiles helped to select sampling targets, which were related to the established seismic stratigraphy. We obtained pre-Quaternary rocks, mainly by dredging, from 29 stations on the Exmouth Plateau, and from 12 stations on the Wallaby Plateau and the Cuvier Abyssal Plain. The results have led to major changes in our understanding of the northern margin of the Exmouth Plateau, which behaved more as part of the offshore Canning Basin than of the Carnarvon Basin. Middle and Late Triassic paralic, detrital sediments are generally overlain by an average of 2500 m of Early Jurassic shallow-water carbonates and mid-Jurassic 'coal measures' and ferruginous sediments. The coal-measure sequence (lithofacies association A) includes carbonaceous silty claystones with seams of an immature sub-bituminous vitreous coal and coaly mudstone, carbonaceous quartz siltstones and very fine sandstones, medium to coarse-grained quartz arenites, and pyrite concretions. The barren ferruginous sediments (B) consist of brown clayey ironstones, sandy ironstones, ferruginous concretions, and ironstones breccias. The Liassic transgressive shallow-water carbonates (C) are a heterogeneous group of micritic limestones, biocalcarenes, very coarse crinoidal biosparites, calcareous quartz arenites, recrystallised sparry limestones and dolosparites. On the northern margin of the Wombat Plateau (a sub-plateau of the Exmouth), at least 300 m of Late Triassic to earliest Jurassic flows of early-rift alkali rhyolite and undersaturated trachyte s.l. (213-192 m.y.) underlie the early Jurassic carbonate sequence. Above the main unconformity, which corresponds to the Callovian breakup of this margin, Early Cretaceous shallow-marine claystones (facies D) indicate the formation of a juvenile ocean. The mature ocean stage is indicated by a condensed sequence of pelagic foraminiferal nanno chalks of Aptian, Albian and Tertiary age (facies E). On the northwestern Exmouth Plateau we sampled Aptian and Miocene chalks. On the southern margin Mesozoic sandstone and shale, latest Jurassic or earliest Cretaceous marine shale, and Cainozoic chalks were recovered.

On the eastern and southern Wallaby Plateau, and on the Sonne Ridge which extends northward into the Cuvier Abyssal Plain, the layered sequence beneath the main Neocomian unconformity consists of interbedded weathered tholeiitic and differentiated alkali basalts, tuffs, basalt breccias and thick volcanoclastic sandstones and conglomerates. A minimum mid-Cretaceous age (K/Ar age: 89 m.y.) was determined for a somewhat altered basalt from the southern Wallaby Plateau. This suggests that intense volcanism and associated deposition of volcanoclastic debris flows formed the plateau, during or after the Neocomian breakup of this region. Therefore, the plateau appears to have no petroleum potential. Quaternary cores in the central Exmouth Plateau contain methane in very small amounts; the  $\delta^{13}\text{C}$  isotope results ( $-14$  to  $-40\%$ ) and the absence of higher hydrocarbons tend to downgrade the petroleum potential of this part of the plateau. Manganese nodules from the southern and eastern margins of the Wallaby Plateau have combined Cu + Ni + Co values of about 0.76%, and are of no commercial interest.

### Introduction

In January and February 1979, the West German research vessel *Sonne* was used to investigate the geological structure of the West Australian continental margin between  $16^\circ\text{S}$  and  $26^\circ\text{S}$  (Fig. 1). The cruise was designated SO-8, and was conducted under the auspices of the Australian-German Scientific Agreement; it continued a geoscientific investigation begun in 1977 with R.V. *Valdivia* in the Scott Plateau region (Hinz & others, 1978). The *Sonne* is a large, modern research vessel equipped with satellite navigation and stabilised narrow-beam echosounders. The work was divided into two 3-week cruises. It was planned by scientists from the Bundesanstalt für Geowissenschaften

und Rohstoffe (BGR), Hannover, and the Bureau of Mineral Resources (BMR), Canberra. German participants on the cruise came from BGR, the Geological-Palaeontological Institute of Kiel University, and from Preussag A.G., Hannover; Australian participants came from BMR, Macquarie University, Sydney, and Monash University, Melbourne.

The purpose of the investigation was to learn more about the structure and development of the Exmouth and Wallaby Plateaus and neighbouring deep-sea areas, especially by sampling older strata. This area of the western Australian continental margin is influenced by processes related to the separation of Greater India and Australia/Antarctica over the period 155 to 115 million years ago. Both plateaus are excellent examples of mature, starved passive margins, with low sedimentation rates after breakup. Thus seismic profiling can reveal the pre-drift history of the sequence, and very old rocks can be sampled along the steep flanks of the plateaus.

<sup>1</sup>Bundesanstalt für Geowissenschaften und Rohstoffe, Postfach 510153, 3000 Hannover 51, Federal Republic of Germany.

<sup>2</sup>School of Earth Sciences, Macquarie University, North Ryde, N.S.W. 2113.

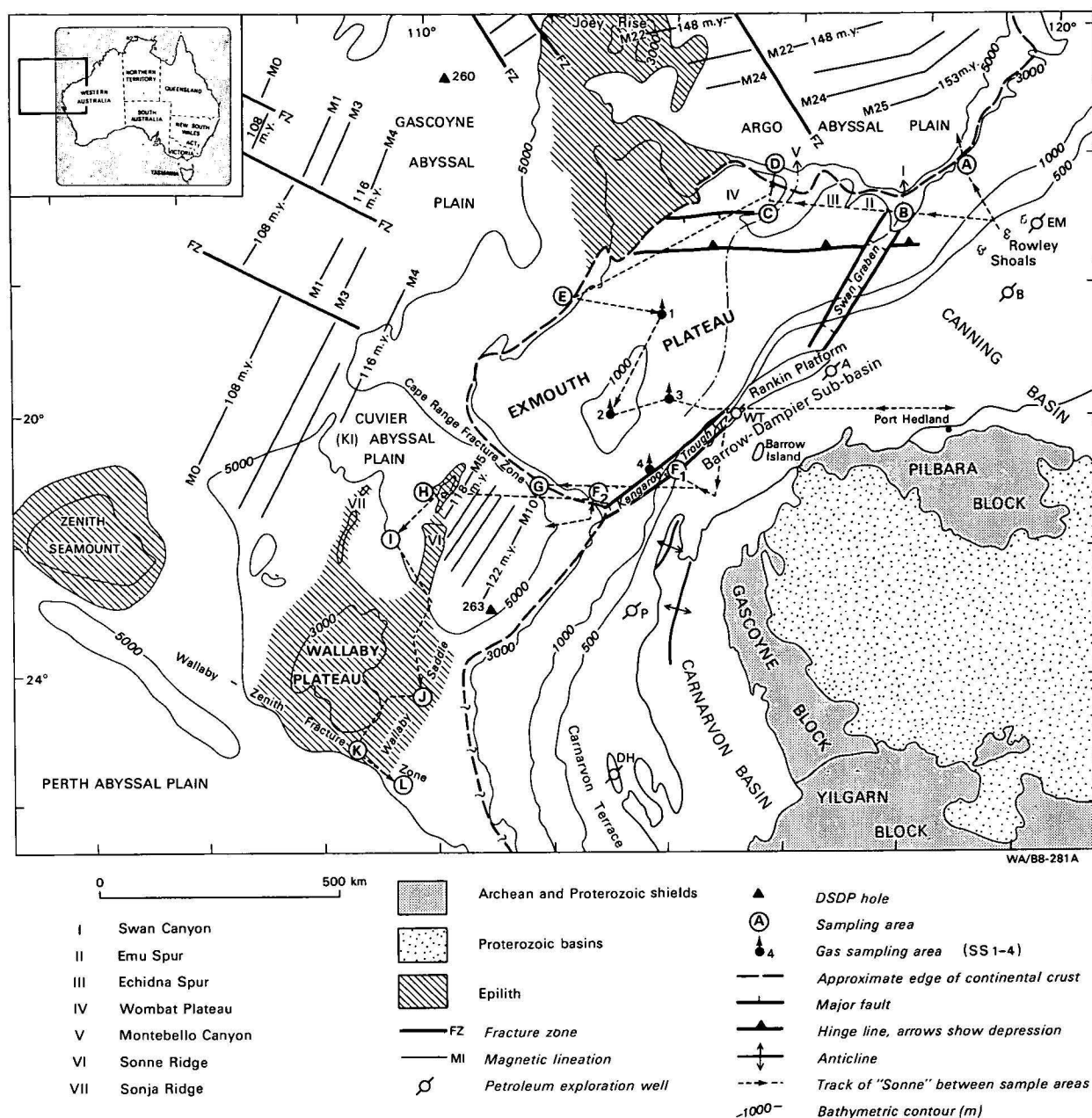


Figure 1. Regional setting, showing generalised ship's tracks for Sonne cruise SO-8.

Bathymetry after Veevers & Cotterill (1978); magnetic lineations after Larson & others (1979), and Heirtzler & others (1978).

The Exmouth Plateau, in particular, is covered by a relatively close network of bathymetric and seismic profiles recorded by petroleum exploration companies, BMR, and foreign research institutions. Publications dealing with the morphology and deep structure of the region are referred to by Symonds & Cameron (1977), and Exon & Willcox (1978). The seismic stratigraphy established by these authors depended mainly on long-distance correlation to petroleum exploration wells on the Northwest Shelf, and to Deep Sea Drilling Project (DSDP) holes on the abyssal plains. However, prior to the Sonne cruises, virtually no samples had been recovered that gave direct information about the stratigraphy of the plateaus, and so the seismic interpretation could not be verified.

Petroleum exploration drilling on the Exmouth Plateau commenced soon after the Sonne cruises and, following discussions with the exploration companies,

surface samples were taken in four areas for isotope analyses of gas traces to be undertaken at BGR.

During the SO-8 cruises a group from Kiel University undertook a program of sampling Quaternary sediments, to investigate the palaeoclimate and palaeo-oceanography of the west Australian continental margin. Samples were taken along two profiles from shallow water to the abyssal plains north and south of the Exmouth Plateau. The results of this program will be published elsewhere. J. B. Colwell and U. von Stackelberg are preparing a paper on the sedimentology of the Quaternary cores and B. Zobel a paper on their biostratigraphy. P. Quilty (1980) has written a paper on the Tertiary foraminiferal faunas and is preparing papers on the Cretaceous and Jurassic foraminiferal faunas. U. von Rad and N. F. Exon are preparing a paper on the Mesozoic and Cainozoic sediments and volcanics from the Exmouth, Scott and Wallaby

Plateaus. N. F. Exon, U. von Rad and U. von Stackelberg are preparing a paper outlining the development of the margins of the Exmouth Plateau.

The several tonnes of material recovered during the cruise is mostly stored at the BGR in Hannover, but a representative collection is held by BMR in Canberra.

#### Sampling procedures and equipment

Bathymetric and seismic data were used to select 16 areas (A-L and SS1-4) for detailed investigation (Fig. 1). Selection of sampling sites was made after running additional bathymetric and seismic lines in the likely areas. The seismic source was generally two airguns, each of 1.2 litre capacity, and penetration averaged one second of two-way travel time. Sampling points for the Kiel University program were chosen where the Quaternary sedimentary sequence appeared to be continuous. The sampling of pre-Quaternary rocks was carried out where the single-channel seismic records suggested that they cropped out on steep slopes.

Pre-Quaternary rocks were recovered in 31 dredge hauls, and 10 piston or gravity cores (Table 1). Dredging was carried out at 66 stations using a pipe dredge

fastened several metres in front of a chain-bag dredge. To allow better definition of the sequence sampled on steep slopes, only a limited range of water depths was sampled. Analogue records of the pull on the cable enabled us to infer the positions from which rocks were torn.

Other equipment used included a 5 or 10-m piston corer (outer diameter 80 or 105 mm), a 6 or 12 m Kastenlot (box corer with cross-section of 300 x 300 mm), a 6 m gravity corer (outer diameter 120 mm), free-fall grabs and corers (outer diameter 73 mm, length 1.2 m) and a Kastengreifer box corer. Altogether piston corers were used 18 times and recovered 81.94 m of sediment, the Kastenlot 3 times (13.88 m), the gravity corer 19 times (73.90 m), free-fall corers 31 times (18.70 m), and the Kastengreifer 29 times (5.22 m). Total recovery, including trigger cores from the piston corer (2.18 m), was 195.82 m.

#### Shore-based investigations of pre-Quaternary samples

At BGR thin sections were made from 79 selected dredge samples, and texture, composition and fabric

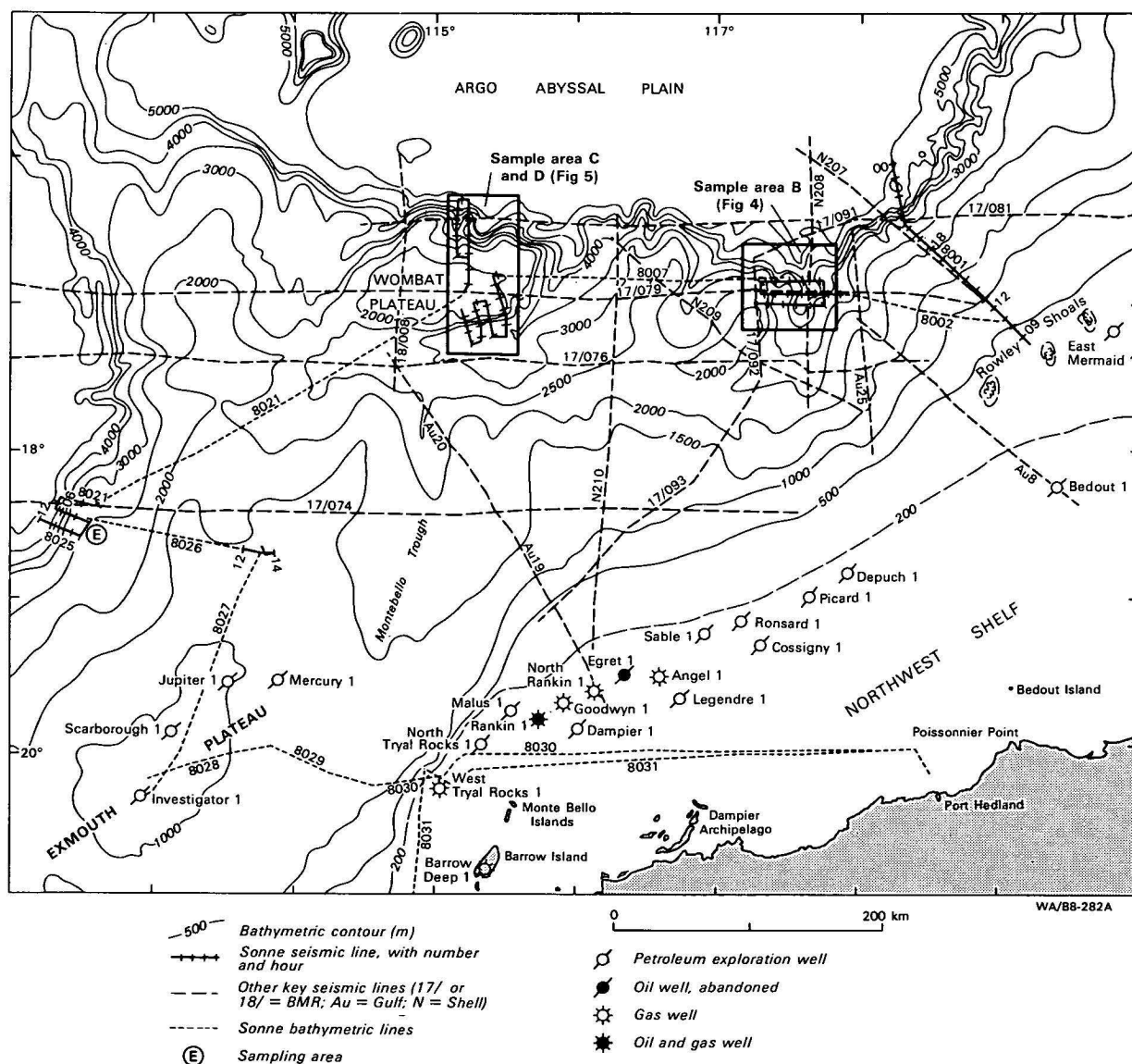


Figure 2. Bathymetry of northern and central Exmouth Plateau showing detailed ships' tracks for Cruise SO-8A. Contours from all available data.

Station number/ equipment (area)	Position		Corrected water depth (m)	Recovery	Seismic profile (reflectors)	Lithology	Age/ environment
28KD (B)	16°59.8' 16°59.2'	117°22.3' 117°21.4'	3035- 2300	10 kg	8006 (F-E)	(1) silty micac. qtzose carb. clayst. (A-2/+++); (2) carb. & qtzose micac. silty clayst. (A-2/+++); (3) semi-consol. mudst. ± ferrug. (A-2/+++); (4) micac. & qtzose silty clayst. with 0.3 — 1 mm thick silst. laminae (A-2/3/+); (5) qtz-rich clay (weathered 28/3) (A-2/+).	Jurassic paralic
29KD (B)	16°57.8' 16°57.4'	117°21.1' 117°20.2'	2530- 2310	30 kg	8006 (F-E)	(1) micac. silty clayst. with phosphorite concretions (A-2/+++); (2) v.f. qtz silst., alt. with lam. silty clayst. (A3/2/+++); (3) f. fspar-rich qtz sst. (?subarkose) (A-4/+++); (4) brown mudst. (A-2/+++); (5) White foram nanno chalk (E-1/+).	(?Jurassic) paralic  1. Miocene-e. Pliocene
32KD (B)	16°55.2' 16°55.2'	117°21.3' 117°20.3'	2950- 2470	100 kg	8002 (F-E)	(3) c qtzose biocalcarene with ooids, oncolites, microfoss., pelecypods, gasteropods, brachs. & echs. (C-2/+++). (2 A/B) silty v.f. qtz sst. (A-3/+++); (2c) foram. biomicrite (C-1/+++); (4) silty to sandy clayst. to clayey siltst. (A-2/+++); (5) silty v.f. sst. and siltst., micac. carbon. (A-2/+++); (6) well-sort. v.f.f. qtz sst. ± ferrug. (A-3/B-2/+); (7) purple silty clayst. (A-4/+); (9) clayey f.-m. qtz sst. (A-6/+).	(E. Jurassic) shallow marine  (? Jurassic) paralic-littoral
					(A-Sb)	(1) white foram nanno chalk.	m. Miocene (N12/13)
33KD (B)	16°49.4' 16°49.5'	117°35.2' 117°32.6'	5300- 3870	7 kg	8004 (F-E)	(1A) mudst. & brown siltst. (A-2/3/+); (1B) black carb. & micac. silty clayst. (A-2/+); (1c) black carb. silty shale with siltst. layers (A-2/+).	(?Early-) Middle Jurassic (J4) paralic
					(?)	(2A/B) weakly silicified (porcell.) rad. chalk (E-3/+); (2c) v. silicified rad. chalk (=porcellanite) (E-4/+)	e. Aptian pelagic
34KD (B)	16°49.6' 16°49.2'	117°33.8' 117°31.7'	5180- 3700	35 kg	8004 (F-E)	(1) m.-c. well-sort. porous qtz sst. (A-4/+++); (2) silty carb. shale; silty sst. layers (A-2/+++); (3) micac. muddy f. sst. to sandy mudst. with coal seams, plant roots (dull lam. coal) (A-1, 2, 3/+++); (4) vit. coal-(subbit) coal (im-mat., 60%C) (A-1/+); (5) Pyrite nodule (=pyritized f.-m. sst.) (A-5/+)	1. M. — e. L. Jurassic (J4) coal swamp-brackish
36KD (B)	16°50.2' 16°50.3'	117°33.2' 117°32.0'	4310- 3730	80 kg	8004 (F-E)	(1) m.-v.c. (± felds.) qtz sst., poorly sort. (A-4/+++) (5) Black carb. shale; some inter-bed. qtz sst., weakly gellified xylite frags. (A-2(1)/+); (4) br. ferrug. goethite-com. qtz sst., clayey ironst. (B-2, 1/+++).	(?Jurassic/paralic) M. Jurassic ? brackish
					(?) (A-Sb)	(2) silty qtzose clayst. (D-2/+++) (3) wh. siliceous foram nanno chalk with rads. & reworked <i>Inoceramus</i> prisms (E-2/+++)	1. Albian-e. Cen  1. Miocene-l. Pliocene (N14-19)
37SL (B)	16°55.00'	117°33.30'	3800	283 cm	8002	foraminiferal nanno chalk (E-1)	Quat.-l. Pliocene
39KD (B)	16°51.00' 16°49.7'	117°24.6' 117°26.7'	4010- 3850	200 kg	8004 (F-E)	1A Red-br. clayey ironst., (1B) ferrug. m.-c. qtz sst., (1C) ferrug. crusts and 'boxstones' (B-1, B-2/+++) (5) Massive ferrug. silty clayst. (?A-6/+++); (2) f.-c. qtz sst. with calcite cem. (C-5/+++); (3A) calc. qtz sst. with crinoids, corals, pelecypods & gasteropods (C-5/+++) 3B calcite — cemented cri-	(?Jurassic) terrestrial  Jurassic shallow marine

Station number/ equipment (area)	Position		Corrected water depth (m)	Recovery	Seismic profile (reflectors)	Lithology	Age/enviroment
	S	E					
39KD (B)	16°51.00' 16°49.7'	117°24.6' 117°26.7'	4010- 3850	200 kg	8004 (F-E)	noid breccia (crinoidal biosparite) (C-4/+); (4) f.-m. qtz sst., ferrug. & poorly sort. (B-2/+); (7A) slightly recrystall. biopel-microsparite (C-2/+); (7B) micritic 1st. (qtzose biomicrosparite) (C-1/+); (11) Brown oncolitic, well-sort. calcarenite (qtzose pel-sparite) (C-2/+); (12) Belemnites, solitary corals (C/+). (8) Br. ironst. breccia with clayey ironst. frags. and c. qtz sand (B-4/+); (9) pyritic concentrations (A-4/5/+).	Jurassic shallow marine
					(?)	(6) micac. qtzose sity clayst. with cac. tubes, agglutin. forams, <i>Inoceramus</i> , ± ferrug. (?A-6/+).	(?Jurassic) paralic
					(?)	(10) Phosphatized sandy & silty qtzose clayst. (D-1/+)	1. Alb.-earliest Cen. marine
43KD (C)	17°06.6' 17°05.7'	115°12.8' 115°13.7'	2600- 1800	4 kg	8014 (F-E)	(1) qtzose calcarenite with crinoids, mollusks & volc. rock frags. (C-3/+); (2) poorly sort. biocalcarenite with rounded fossil debris: colon. & sol. corals, crinoids, bryozoa, ech. spines, pelecypods, brachs., calc. algae (C-4/+); (3) semiconsol. silty clay (?A-4/+).	(?Jurassic) shallow marine
					(?)	(4) small piece rhyolitic pumice (bubble-wall shards) (H-6/+)	? Subrecent
46KD (C)	17°07.0' 17°06.3'	115°19.0' 115°19.0'	3140- 2710	1 kg	8012 (F-E)	(1) Grey v. poorly sorted f. sandy greywacke with mica & plant remains (A-3/+)	Triassic ? brackish
					(?)	(2) White foram nanno chalk (E-1/+)	1. Miocene (N17) eupel-bathyal
48KD (C)	17°06.5' 17°04.9'	115°19.2' 115°19.8'	2710- 1850	20 kg	8012 (G-E)	(1) Grey muddy siltst. to qtz-rich sandy shale with mica & plant remains (A-2/+)	mid-Triassic paralic
						(2) Pale grey to pink shale (A-2/+)	(?Jurassic/Triassic)
49KD (C)	17°07.9' 17°06.4'	115°21.7' 115°23.3'	3280- 2520	200 kg	8010 (F-E)	(1) dolom. biosparite with recrystall. pelecypods & echinoids, (3) porous biosparite with fossil remains (C-6/+); (4) (f.-m. calc. cemented qtz sst. (?C-5/+)	(?Jurassic) shallow marine
						(5) silty shale to muddy v.f. sandy siltst. (A-2/3/+); (2) clayey ironst. (B-1/+)	Triassic ? brackish
51KD (C)	17°05.8' 17°04.7'	115°23.3' 115°23.6'	2190- 1910	40 kg	8010 (?)	(1) grey-br. silty mudst. with plant frags., bivalve casts (A-2/D2/+); (3) Olive br. sl. calc. clayst. with forams	E. Cretaceous shallow marine
						(2) foram nanno chalk	L. Mioc.-l. PIOC. (N16-20)
57KD (C)	17°05.2' 16°02.7'	115°30.6' 115°31.9'	3200- 2800	40 g	8008 (F-E)	(1) Grey, pink friable shale (A6/3D/+); (2) br. flaggy micac. m. qtz sst. (A-4/+)	(?Jurassic) paralic
61KD (D)	16°28.7' 16°30.7'	115°14.4' 115°14.3'	4800- 4260	10 kg	8016 (G-F)	(4) Mn-coated intermed. volc. with pale phenocrysts (?trachyte' s.l.) (?H-4/+)	(? L. Triassic)
					(F-E)	(1) Interbed. pale grey micac. qtz sst. & calcisiltite, with <i>Inoceramus</i> , brachs., ostracods, echinoderms (C-3/C-7/+); (2) grey calc. v.f.-m. qtz sst. to sandy marlst., with pyrite, fish teeth, ostracods (C-2/+); (3) br. biocalcarenite to calcirudite, with <i>Lenticulina</i> , echinoids, crinoids, ostracods, pelecypods (C-2/+); br. calc. sandy mudst. with shell frags. (?C-1/+)	E. Jurassic (l. Sinemurian to Pliensbachian) Pockets m-l. Miocene (N14) shallow marine
62KD (D)	16°34.2' 16°35.2'	115°14.2' 115°15.0'	3110- 2580	2.5 kg	8016 (F-E)	White sparry biocalcarenite with benth. forams, echs., calc. algae, crinoids, <i>Inoceramus</i> (biopelmicrosparite) (C-2)	E. Jurassic shallow marine



Station number/ equipment (area)	Position		Corrected water depth (m)	Recovery	Seismic profile (reflectors)	Lithology	Age/ environment
S	E						
63KD (D)	16°35.2' 16°36.2'	115°15.4' 115°15.5'	2960- 2620	20 kg	8016 (G-F)	(1A) Red weathered amygd. fspar- rich volc. (SiO <sub>2</sub> undersat. 'trachyte' s.l. or mugearite) (H-4/+); (1B) weathered layered phenocryst-rich volc. (H-4/+); (1C) red plag- rich volcs. (H-4/+); (2B/1D) red-gray volc. breccia to alt. tuff/ lapillist. (H-4/+); (3) yellowish weathered silty clayst. (?altered tuff) (H-7/+)	(L. Triassic/earliest Jurassic)
					(F-E)	(2A) Olive, pink calc. m.-c. qtz sst. (C-3/+); (4) Red-br. clayey ironst. & f.-m. qtz sst. (B-1, 2/ +); (5A) grey muddy siltst. to v.f. qtz sst. (?A-3 ++); (5B) grey poorly sort. m.-c. qtz. sst. (A- 4/+); (6) grey silty mudst. with lenses qtz sst. (A-2/3/+).	(?Jurassic) paralic and shallow marine
64KL (D)	16°36.2'	115°14.0'	2600	408 cm	8016 (B-Sb)	Quat. foram sand to 320 cm; Plio- cene (+m.-e. Mioc.) grey-white chalk to 357 cm; buff late Oligo- cene (with m + e Eoc) chalk to base (E-1/).	Quat./Plioc./l. Oligoc. eupelagic/bafhyal (slumping)
65KD (D)	16°33.4' 16°34.4'	115°14.3' 115°14.7'	3510- 3040	400 g	8016 (?) (?)	(1) Black ang. felds.-rich volc. rock (?trachyte s.l.) (H-4/+) (2) white recryst. sparry lst. with byrozoans, crinoids (C-7?/+); (3) belemnites with thick-walled Ino- ceramus frags., not <i>in situ.</i> (C-7/ +)	Hettangian (192 ± 4 m.y.) (? Cretaceous)
66KD (D)	16°34.2' 16°35.7'	115°10.3' 115°10.2'	3120- 2490	50 kg	8016 (G-F)	Alk. rhyolite with large alk. feld- spar phenos in f. gndmass (H-5)	Carnian (L. Triassic) 213 ± 3 m.y.
72KD (E)	18°25.4' 18°26.3'	112°21.8' 112°23.6'	3920- 3450	500 g	8023 (?)	Foraminiferal nanno chalk (E-1/ 3/+)	l. Albian
73KD (E)	18°26.3' 18°27.3'	112°25.6' 112°27.3'	3050- 2690	100 g	8023 (?)	Recryst. carbonate rock with zeo- lit. tuff & Mn crust (C-7, H-7?/+)	(?Cretaceous) Mid-l. Plio. discoasters (? contam.)
76KL (E)	18°26.0'	112°25.8'	3100	traces	8023 (?)	Foraminiferal nanno ooze (E-1)	m. Miocene
78KL (E)	18°19.5'	112°26.0'	3860	344 cm	8021 (?)	Quat. foraminiferal sand & ooze above 60 cm; stiff br. foraminiferal nanno ooze & chalk below (E-1)	Quaternary/l. Oligo. -c. Miocene
131KD (G)	21°20.4' 21°18.3'	111°52.0' 111°54.3'	4415- 3770	200 g	8036 (?)	Dk grey v.f. carbonac. micac. qtz sst. (A-3)	(?Triassic or Jurassic)
132KL (F-2)	21°08.6'	112°18.0'	1715	340 cm	(?)	Pink foram sand to 60 cm; grey nanno ooze to 330 cm; white foram sand below 330 cm (E-1)	Quat. above 330 cm; m. Miocene below
138SL (F-2)	21°37.1'	112°31.9'	4017	429 cm	(?)	Reddish grading downward to grey ooze; grey micac. siltst. & shale frags. with glauc below 400 cm (D-2)	Quat./upper Late Jurassic ?, marine
142SL (F-2)	21°27.6'	112°30.5'	2798	121 cm	(?)	Reddish foram nanno ooze to 100 cm; white nanno chalk below 100 cm (E-1)	Quat./m. Oligo.
144SL (F-2)	21°21.8'	112°33.5'	2330	traces	(?)	White nanno chalk (E-1)	m. Miocene
148KD (H)	20°58.4' 20°57.8'	110°33.9' 110°33.3'	4875- 4540	80 kg	(?)	(1) Red highly alt. basaltic rock (?hawaiiite) (H-3/+); (2) phosph. replaced ± palygorskite- rich volc. sst. (H-9/+); (3) tuff, some brecciated (H-7/+); (4) highly alt. lithic-vitric tuff (H-7/ +++) (5/6) Mn nodules, poly- and mono-nodules, & crusts (G-1/2 /+)	(?M. Cretaceous)  subrecent
149KD (H)	21°24.9' 21°24.2'	110°18.5' 110°18.5'	4930- 4920	60 kg	(?)	(1) Multicol. smectite & zeolite- cemented volc. breccia with f. volc. frags. to 10 cm φ, in a yellow & grey clay matrix (H-8/+)	(?M. Cretaceous)

Station number/ equipment (area)	Position		Corrected water depth (m)	Recovery	Seismic profile (reflectors)	Lithology	Age/ environment
S	E						
155KD (J)	21°52.0' 21°52.7'	109°16.2' 109°15.2'	5060- 4830	25 kg	8048 (pre C)	(1) Dk. br. highly alt. differan. alk. basalt (?hawaiite) SiO <sub>2</sub> undersat (H-3/++); (2) pale grey phos. replaced volc. clay (H-7/+); (3) multicol. palagonite tuff/breccia H-8/+)	(?M. Cretaceous)
156KL (J)	21°53.3'	109°14.1'	4780	traces	8048 (post C)	White nanno marl and frags. of Mn crusts (E-1)	1. Palaeocene/Eocene
159KD (J)	24°23.5' 24°22.8'	109°43.1' 109°41.8'	4470- 4130	100 kg	8056 (pre C)	c. volc. sst. with clay matrix and volc. & rare glauc. phosph. clasts (H-8/+)	(?M. Cretaceous)
161KD (J)	24°24.0' 24°23.9'	109°45.0' 109°44.3'	4470- 4230	2 kg	8056 (pre C)	c. volc. sst. with clay matrix, weathered & Mn crusted (H-8/++)	(?M. Cretaceous)
162KL (J)	24°24.0'	109°41.3'	4060	88 cm	8056 (pre C)	Pebbly volc. sst. 50-92 cm (H-8/+)	(?M. Cretaceous)
165KD (J)	24°23.7' 24°23.7'	109°42.4' 109°44.0'	4415- 4240	5 kg	8056 (pre C)	(1) Pebbly volc. sst., clasts mainly alt. glass (H-8/++) (2) Mn polynodes, max. 7 cmφ (G-1/+)	(?M. Cretaceous) subrecent
167KD (K)	25°39.0' 25°35.4'	108°36.5' 108°35.1'	5340- 4750	2 kg		(1 + 2) Pink to grey br. ?volc. clayst. (H-7/+); (3A + B) grey f.-c. vitric-lithic volc. breccia & qtz-rich silty tuff with glassy matrix (H-7/+); (3C) silicified volc. breccia (H-8/+); (3D) pale br. v.f. basalt or tuff (H-1/7/+) (4) small Mn polynodes with volc. cores (G-1/+).	(M. Cretaceous) subrecent
168KD (K)	25°34.9' 25°33.4'	108°34.3' 108°35.0'	5100- 4050	200 kg		(1) alt. ± amygd. basalt (H-1/++); (2) volc. siltst. (H-7/+); (3) bl. fissile f. tuff (H-7/+); (4) ? volc. clayst. (H-7/+)	(M. Cretaceous)
170KD (K)	25°31.6' 25°31.0'	108°31.9' 108°32.4'	4620- 3970	120 kg	8063	(1) tholeiitic basalt (H-1/2/++); (2) basalt. breccia, clasts max. 20 cm φ, zeol. clay & cement (H-8/++); (3) volcanogenic mudst. (?tuff) with granules (H-7/+); (4) v.c. volc. sst., poorly sort. (H-8/+); (5) volc. breccia, clasts max 2 cm φ, ± amygd. (H-8/+) (7) One Mn polynodule (G-1/+)	> 89 m.y. (Coniacian) (M. Cretaceous) subrecent
173KD (L)	25°57.8' 25°55.3'	109°05.8' 109°04.4'	4980- 3885	200 g		(1) Reddish br. ferrug. (?radiol.) vitreous qtz chert (F /+); (2) highly alt. tuff-volc. clayst. (H-7/+)	(?M. Cretaceous)

**Table 1. Station data, seismic correlation, lithofacies type, age and tentative paleoenvironment of all *Sonne* 8 dredge and core stations containing pre-Quaternary rocks.**

For dredges two positions (start and end of bottom contact) are given. For stratigraphic range of reflectors A-G see Figure 7. Lithofacies: (1), (2), etc. refer to sub-sample numbers of each dredge haul; A-1, A-2, etc. to lithofacies types (see Table 2); (+) +, ++, +++ designate relative abundance of lithotype (very rare, rare, common, abundant). Ages in brackets are estimates. KD = dredge, SL = gravity corer, KL = Kastenlot box corer.

were analysed in order to understand the formation of the lithotypes. Samples were washed for biostratigraphic and sedimentological work, and others underwent XRD analysis. Two carbonaceous samples were investigated by coal petrography and organic geochemistry. The  $\delta^{13}\text{C}$  isotopic composition of adsorbed gases in 25 surface sediment samples was determined. Fifteen volcanic rocks were analysed petrographically and geochemically, and three were dated by the K/Ar method. Manganese nodules and crusts were analysed. Foraminifera from thin sections and washed material were studied.

In Australia the seismic stratigraphy was revised, following the sampling results and new seismic correlations. Biostratigraphic and environmental information came from palynological and foraminiferal investi-

gations. Twenty-one thin sections were prepared and briefly examined. Several manganese nodules and crusts were analysed for metal content.

#### Acknowledgements and responsibilities

The German Federal Ministry for Research and Technology (BMFT) sponsored and financed this cruise and chartered *R.V. Sonne*. BGR provided the bulk of the geological and geophysical equipment. Esso Exploration and Production, Australia, provided confidential seismic lines to aid in planning the sampling program.

Scientists who provided valuable assistance on board, but who have made no further major contribution to this paper, are E. Blümel, J. Colwell, K. Herbst, G. Hicks, G. Hildebrand, H. A. Jones, F.-C. Koegler, H.

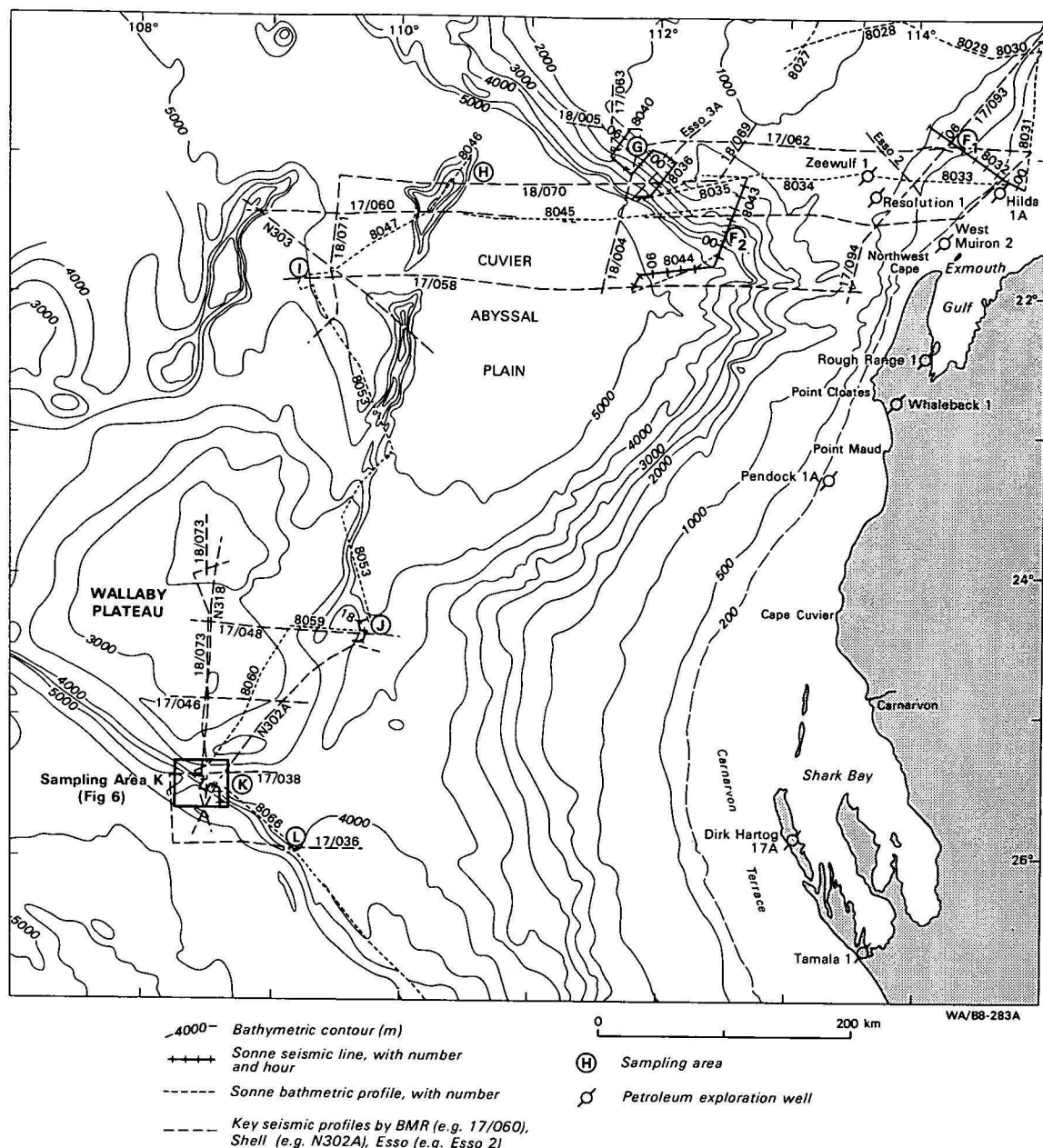


Figure 3. Bathymetry of southern Exmouth Plateau, Cuvier Abyssal Plain and Wallaby Plateau, showing detailed ships' tracks for Cruise SO-8B. Contours from all available data.

Lange, V. Reich, and E. Seibold. The main contributors to this paper, who were all on board, are U. von Stackelberg (chief scientist); N. F. Exon (bathymetry, seismic interpretation, hydrocarbons, geological evolution); U. von Rad (sedimentology, geological evolution); P. Quilty (foraminifera); S. Shafik (nannoplankton); H. Beiersdorf and E. Seibertz (manganese nodules and crusts).

Special thanks are due to shore-based scientists who contributed substantial data to the paper, but are not authors. These include E. Faber and W. Stahl, BGR (isotopic results of gas sampling), R. Emmermann, Karlsruhe Technical University (petrography of volcanic rocks), H. Kreuzer and H. Raschka, BGR (K/Ar dating of volcanic rocks), B. Zobel, BGR (foraminifera), P. Čeppek, BGR (nannoplankton), F. Gramann, BGR (ostracods), H. Röscher, BGR (x-ray diffraction results), and J. Koch and H. Wehner, BGR (coal petrography and organic geochemistry; see Appendix). BMR scientists who have made major contributions include

D. Burger (palynology) and G. Chaproniere (foraminifera). A. McMinn (Geological Survey of New South Wales) also helped with the palynology.

Thanks are also due to K. Hinz (BGR) for coordinating the *Sonne* cruises, to our marine technicians, and to Captain Ehle and his crew. We are indebted to F. Wilckens (BMFT), F. Bender (President, BGR) and L. C. Noakes (Director, BGR) for their support of this project.

### Bathymetry

Falvey & Veevers (1974) made the first detailed review of the physiography of the region; later studies include those of Symonds & Cameron (1977) for the Wallaby Plateau, and Exon & Willcox (1978) for the Exmouth Plateau. Within the area covered by the *Sonne* cruises (Fig. 1) a number of different physiographic elements can be recognised, ranging from the continental shelf to the abyssal plains.

Deep-sea dredging generally requires slopes of  $5^\circ$  or more, if pre-Quaternary samples are to be obtained, so the regional bathymetry helped define areas of interest, and the local bathymetry actual dredge sites.

The continental shelf varies greatly in width. Beyond the shelf break gradients suddenly increase to  $1^\circ$  or more, in water depths ranging from 100 to 600 m. The upper slope may have an even gradient, or be convex, stepped or contain scarps.

The Exmouth Plateau (Fig. 2) is separated from the upper slope by the broad Montebello Trough, whose minimum axial depth is 1050 m. A change of gradient, from generally  $1^\circ$  or less on the plateau to more than  $3^\circ$  on the lower slope, occurs between 2000 and 2500 m. The plateau is dominated by a gentle northeast-trending arch about 250 km offshore, whose minimum depth is about 800 m.

The Wallaby Plateau (Fig. 3) is separated from the Carnarvon Terrace by the Wallaby Saddle, whose minimum axial depth is about 3900 m, and by the lower and upper continental slopes. The plateau is broad and generally smooth, with culminations of 2200 m in the north and 2500 m in the south. The boundary between the plateau, on which the gradients are generally less than  $1^\circ$ , and the lower slope, which is steeper than  $3^\circ$ , lies between 3000 and 3500 m.

The lower, fault-controlled, slopes of the two plateaus have a certain similarity. The southwestern slopes are straight and trend at about  $220^\circ$ , the northwestern slopes trend generally northeast, and the northern slopes are very complex.

The southwestern slope of the Exmouth Plateau is controlled by the Cape Range Fracture Zone. The slope

is smooth, and its gradient lies between  $3^\circ$  and  $5^\circ$ . The northwestern slope consists of a number of terraces; gradients on it are very variable, but do not exceed  $10^\circ$ . The northern margin consists of a number of highs (Fig. 1: Rowley Terrace beneath Rowley Shoals, Emu Spur, Echidna Spur, Wombat Plateau) separated by large canyons. Slopes of  $10^\circ$  to  $20^\circ$  are quite common. Sampling on the Exmouth Plateau was most successful where the slopes were steepest, that is in the north.

The southwestern slope of the Wallaby Plateau is controlled by the Wallaby-Zenith Fracture Zone. The gradients of  $10^\circ$  to  $30^\circ$  far exceed those on the southwestern Exmouth Plateau, presenting a variety of excellent sampling locations. The northwestern slope of the plateau is poorly mapped, but gradients appear to be generally less than  $5^\circ$ . The northeastern slope of the plateau is dominated by the north-northeast trending Sonne and Sonja Ridges (new names Fig. 1), both of which rise more than 2000 m above the surrounding seabed; the gradients between these ridges seldom exceed  $1^\circ$ . Slopes of  $10^\circ$  to  $15^\circ$  characterise the flanks of both these volcanic ridges. The Sonne Ridge extends for almost 400 km, cutting the Cuvier Abyssal Plain in two, and forming the western flank of the Wallaby Saddle.

Four abyssal plains bound the Exmouth and Wallaby Plateaus. The Argo and Gascoyne Abyssal Plains lie at about 5700 m, and rise gently northward toward the Java Trench. The 5070 m deep Cuvier Abyssal Plain is shallower and flatter than the other plains. The Perth Abyssal Plain, about 5600 m deep, is cut by north-easterly-trending ridges, as is the Cuvier Abyssal Plain.

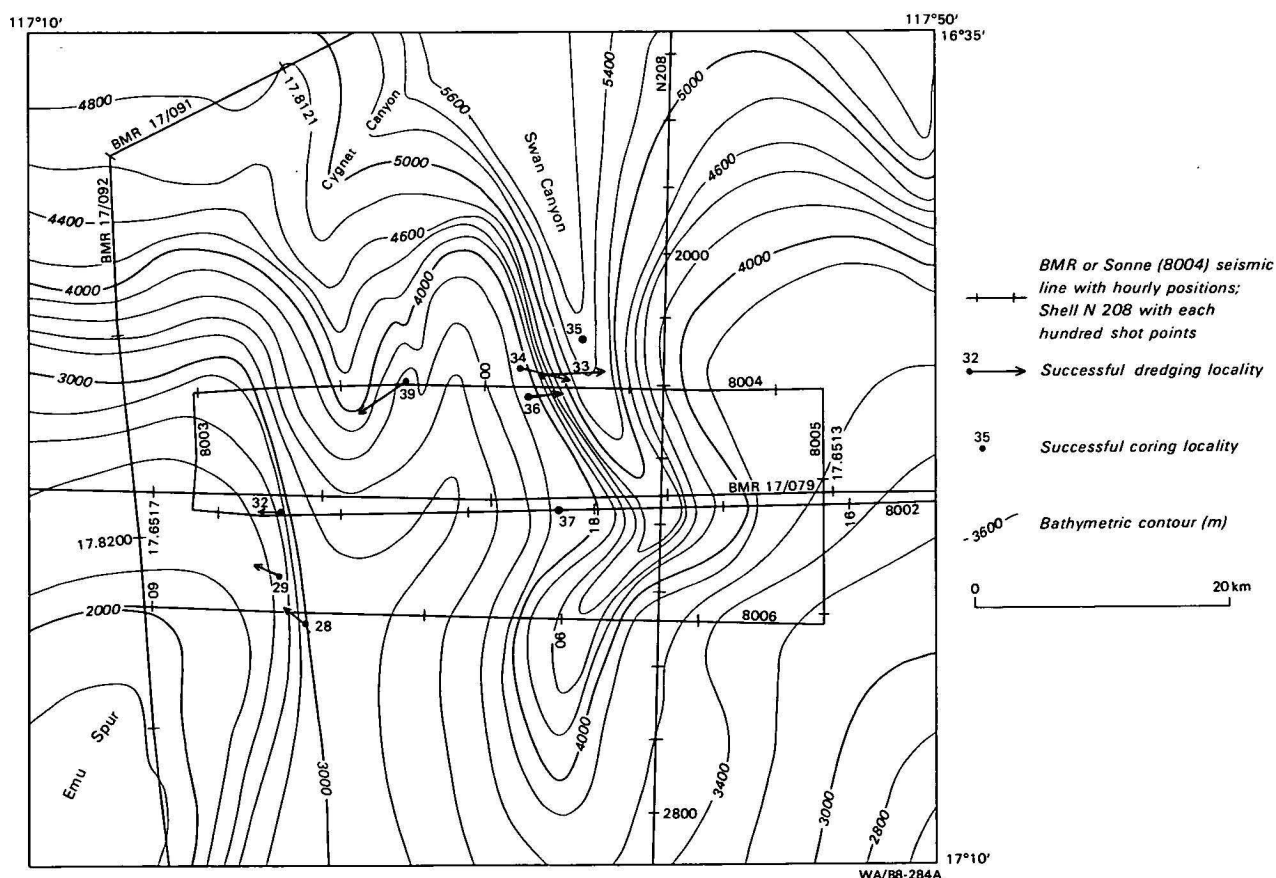
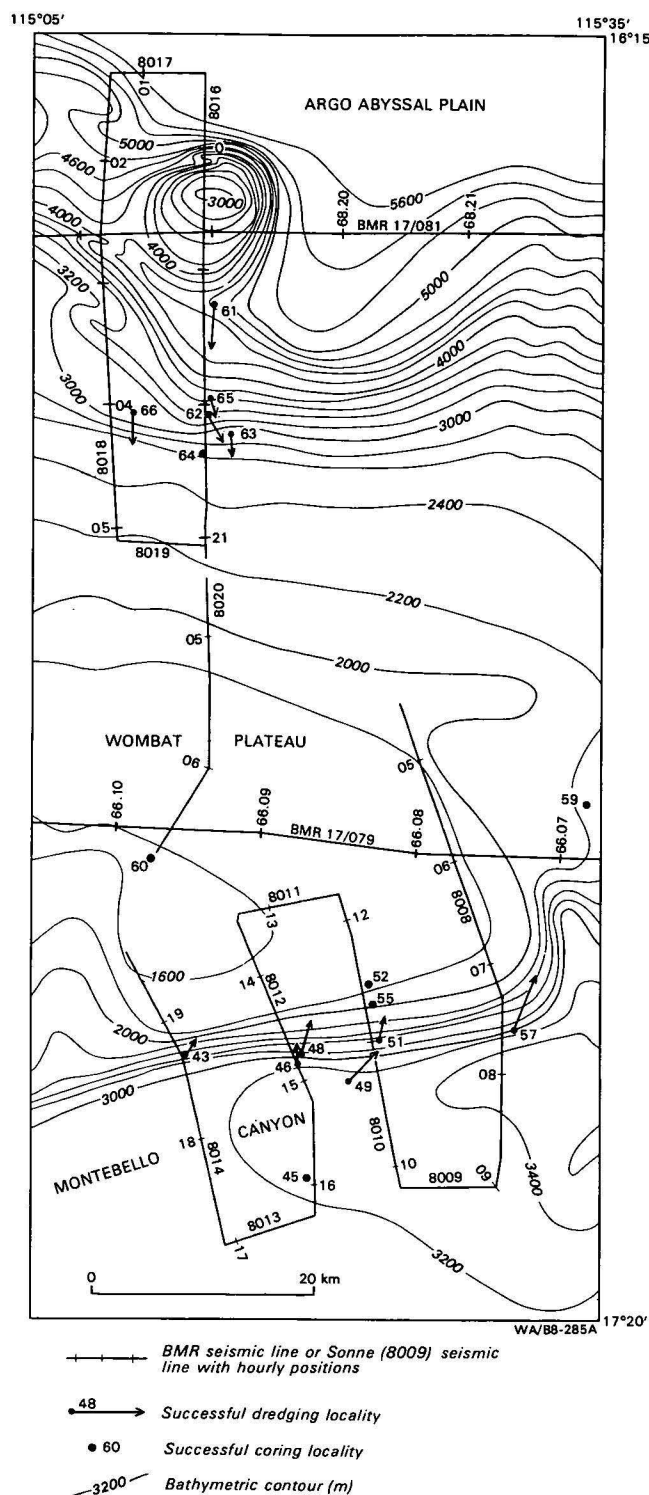


Figure 4. Detailed bathymetry, ships' tracks and sampling stations, for Area B. SO8-004 illustrated in Figure 9.



**Figure 5. Detailed bathymetry, ships' tracks and sampling stations, for Areas C and D.**  
SO8-008, 010 012, 014 illustrated in Figure 10; SO8-016, 018, 020 illustrated in Figure 11.

## Lithofacies and age of dredged and cored pre-Quaternary rocks

The general stratigraphy and seismic stratigraphy of the region is shown in Figure 7. Table 1 contains relevant data for the stations with dredged and cored pre-Quaternary *Sonne* samples, including seismic correlation, lithofacies type, age and depositional environment. Within most dredge hauls (e.g. SO8-28KD), several

lithologies were differentiated (e.g. 28KD/1, 28KD/2 etc.) and later assigned to one of the 35 lithofacies types (e.g. A2, B1), which are listed and explained in Table 2, and related to the regional stratigraphy in Figure 15. Detailed locations, for the more important sampling areas, are shown in Figures 4, 5 and 6. The relationship of many stations to bathymetry and seismic stratigraphy is shown in Figures 9-13.

The lithology and age of the observed 26 sedimentary and 9 volcanic/volcaniclastic lithofacies types will be described in more detail in a forthcoming paper. An interpretation of these lithofacies and their paleoenvironmental significance is given later in the present paper.

*Coal measure sequence (lithofacies A; mainly Middle Jurassic, partly Triassic)*

Lithofacies A is a heterogeneous group of carbonaceous, clayey to sandy sediments, which were dredged from seismic sequences F-E and G-F. Black vitreous coal seams (A-1) alternate with carbonaceous carbonate-free silty claystone (A-2). Also common are carbonaceous quartz siltstones and very fine sandstones (A-3), medium to coarse-grained arenites (A-4), pyrite concretions (A-5) and grey to pink claystones (A-6).

All these lithotypes are carbonate-free and palaeontologically barren, except for pollen and spores in A1 and A2/3, which generally indicate a Middle Jurassic (pre-Callovian, J4-5) age and a non-marine to brackish environment (D. Burger, personal communication). Reworked Permian pollen and Mesozoic acritarchs are common. Samples 46KD/1 (MFP7233) and 49KD/5 (MFP7409) in area D are dated Triassic on the presence of *Osmundacidites senectus* Balme, *Polypodisporites ipsiviciensis* (De Jersey), *Dictyophyllidites mortonii* (De Jersey), *Punctatisporites walkomii* De Jersey, *Enzonalasporites* sp., and *Lunatisporites* sp.

Several samples are dated Middle to Late Jurassic on the restricted stratigraphic ranges of *Contignisporites fornicatus* Dettmann, *Murospora florida* (Balme), *Klukisporites scaberis* (Cookson & Dettmann), *Calliasporites dampieri* (Balme), *Dictyophyllidites equiinus*

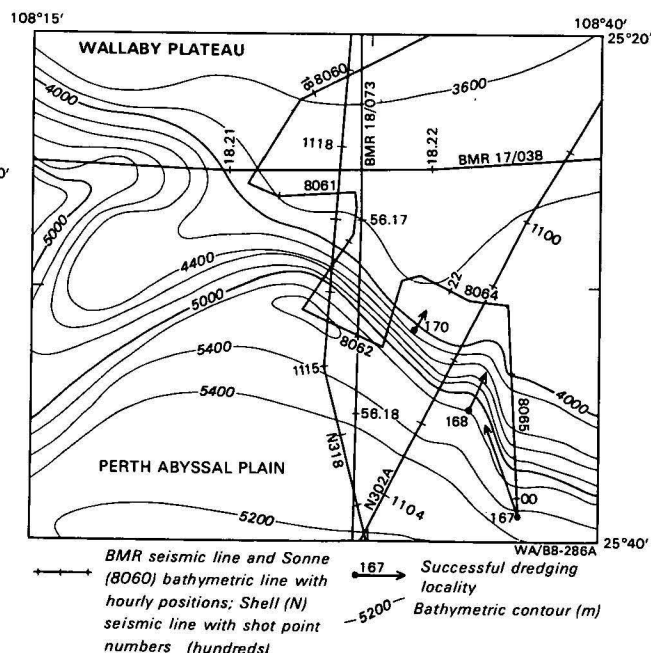


**Figure 6. Detailed bathymetry, ships' tracks and sampling stations, for Area K, BMR 18/073 illustrated in Figure 13.**



Lithofacies type	Colour and generalised lithology of facies type	Tentative facies interpretation (palaeoenvironment)	Age	Occurrence (areas)
Coal measure association	A-1 black vitreous subbituminous coal including vitrinitised wood fragm. from gymnosperms (xylite) (see Appendix)	coal swamp ? paralic	Middle to early Late Jurassic (c) In part: (mid-) Triassic (c)	B
	A-2 brown/gray carbonaceous, quartzose & micaceous silty claystone	paralic (fluvialite flood plain, swamp, lagoonal?) brackish to nonmarine palynomorphs		B, C, D
	A-3 gray/brown $\pm$ carbonaceous quartz siltstone to very fine sandstone		(?Jurassic)	B, C, D, G
	A-4 gray/brown fine to medium (coarse) quartz sandstone (qtz arenite)	paralic (fluvialite, flood plain, delta)	(?Jurassic)	B, C, D
	A-5 dark-gray pyrite-cemented medium quartz sandstone ('pyrite concretion')	paralic	(?Jurassic)	B
	A-6 pink to dusky red/purple siltstone/claystone (?transition to A-2)	flood plain (oxidising non-marine conditions)	(Mesozoic)	B, C
Ferruginous Association	B-1 reddish-brown clayey ironstone ('Toneisenstein'), in part transition to A-6/A-2/3	?terrestrial (quiet water)	later subaerially exposed to arid conditions (?Jurassic) ?coeval with A-facies	B, C, D
	B-2 reddish-brown ferruginous quartz sandstone (sandy ironstone)	fluvialite to littoral		B
	B-3 brown ferruginous concretions and 'boxstones' (goethite cement)	terrestrial		B
	B-4 dark brown ironstone breccia ('Trümmereisenerz')	reworking of B-1 (littoral?)		B
Pre-Tertiary shallow-water carbonates	C-1 Micritic limestone (calcilutite to siltite), slightly quartzose & foraminiferal	(intermediate) shelf open-marine	?Jurassic	B, D
	C-2 (a) white/gray foraminiferal-mollusk-echinoderm biocalcarenite (b) bio-pel-microsparite with peloids/pellets, calc. algae and volc. rock fragments	quiet-water (subtidal) open-marine shelf	Early Jurassic (Late Sinemurian-Pliensbachian) (b) (d)	D
	C-3 yellowish quartzose biocalcarenite, transitions to C-5 & C-2	(?inner) shelf		C
	C-4 (a) gray very coarse crinoid biosparite (grain-to rudstone) (b) poorly sorted algal-mollusk-echinoderm biocalcarenite	bank tops, forereef? high energy ('peri-reefal')	?Jurassic (d)	B
	C-5 calcite-cemented quartz arenite (to highly quartzose biocalcarenite)	littoral (high-energy) (transgression?)	(?Jurassic)	B, D
	C-6 recrystallised sparry limestone (micro-to macro-sparite, $\pm$ dolomitised)	intermediate shelf beyond wave base	?Early Jurassic (b) (d)	D
	C-7 yellowish-brown dolomicrite to dolosparite	shelf	?Jurassic-Cretac.	C, D
Marine Clay/siltst.	D-1 phosphatised claystone	?outer shelf/upper slope	(?Cretaceous/Tertiary)	B
	D-2 micaceous clayey siltstone w. some glauconite and dinoflagellates	fully marine	latest Jurassic (c) Early Cretaceous	B, C F-2, G
Pelagic (± siliceous) chalks	E-1 white semiconsolidated foraminiferal nanno chalk	eupelagic-bathyal	Paleocene to Pliocene (late Albian) (a) (b)	B, C D, E, F-2, I
	E-2 white quartzose and radiolarian chalk	?hemipelagic-bathyal	late Miocene-early Plioc. (a) (b)	B
	E-3 gray, weakly silicified radiolarian chalk (20% radiolarians, no terrigen. influx)	(?epicontinental Tethys)	Aptian (-? earliest Albian) (a)	B
	E-4 gray radiolarian porcellanite (20% calcite, 40% opal-CT cement)	(?upwelling)		
Ferrug. qtz chert	F reddish-brown ferruginous quartz chert with ghosts of ?radiolarians	?pelagic	?Mesozoic (?mid-Cretaceous)	L
Fe/Mn nodules & crusts	G-1 black manganese nodules, mono- & polynodules, up to 6 cm $\phi$	slow <i>in situ</i> growth on hard-grounds in bathyal/abyssal environment	subrecent-Neogene	H, J, K
	G-2 black manganese crusts encrusting sandstones, tuffs, volcanoclastic sandstones, basalts			B, H etc.
Volcanic and volcanoclastic rocks	H-1 $\pm$ altered tholeiitic basalt, $\pm$ vesicular, inter-sertal to intergranular	shallow water extrusion	pre-Turonian (89 m.y.) (e)	J, K
	H-2 $\pm$ altered (?tholeiitic) basalt breccia		?late Early Cretaceous	K
	H-3 $\pm$ altered differentiated alkali basalt (?hawaiite), transition to H-1			H, J
	H-4 SiO <sub>2</sub> -undersaturated 'trachyte' (s.l.) or mugearite (feldspar-rich)	?subaerial or shallow-water	earliest Liassic = 192 $\pm$ 4 m.y. (e)	D
	H-5 alkali rhyolite with porphyritic texture and large sanidine phenocrysts		Late Triassic = 213 $\pm$ 3 m.y. (e)	D
	H-6 light-colored rhyolitic pumice (highly vesicular)	subaerial, redeposited	? subrecent	C
	H-7 $\pm$ altered tuff to lapillistone (tuffaceous sand- and siltstone)	reworking of tuffs	? (Pliocene contam.?)	D, E, H, J, K, L
	H-8 volcanoclastic sandstone/breccia, incl. silicified tuff breccia	shallow-water, reworking, high-energy	?M. Cretaceous: post-Hauterivian, pre-Turonian)	H, F, K
	H-9 phosphatised white pyroclastic claystone (w. colophane cement)	shallow-water, later diagenesis		H, J

Table 2. Lithofacies type of pre-Quaternary SO-8 dredge and core samples.

These lithofacies type designations are used also in Table 1 and throughout the text. Age based on (a) calcareous nannoplankton, (b) foraminifera, (c) palynomorphs, (d) macrofossils, (e) K/Ar dating; ages in brackets estimated from seismic/magnetic evidence, or comparative facies. For sampling areas B-L see Figure 1.

Age		Reflect/ Symbol	NTH EXMOUTH PLATEAU		EXMOUTH PLATEAU		WALLABY PLATEAU		
			Sequence	Thick (m)	Sequence	Thick(m)	Sequence	Thick(m)	
CRETACEOUS	Late	Pleistocene	Miocene to Recent pelagic ooze and chalk	200-400	Miocene to Recent pelagic ooze and chalk	200-400	Miocene to Recent pelagic ooze and chalk	? 100-200	
		Pliocene							
		late							
		middle							
		early							
	Oligo	late	A						
		early							
	Eoc	late	Eoc	Eocene chalk	100-200	Eocene chalk	200-600	Eocene chalk	? 100-200
		middle							
		early							
Pal	late	B							
	early								
JURASSIC	Late	Kl	Late Cretaceous carbonates and marls	50-100	Late Cretaceous shelf carbonates and marls	50-400	Late Cretaceous carbonates	? 50-100	
									Senonian
									Campanian
									Santonian
									Coniacian
	Early	Km	Mid Cretaceous shallow marine shale	100-200	Mid Cretaceous shallow marine shale	200-400	Mid Cretaceous shallow marine shale	100-200	
							Cenomanian		
							Albian		
							Aptian		
							Barremian		
TRIASSIC	Late	Ke	Middle Jurassic coal measures	2000-3000	Tithonian — Neocomian deltaic sediments	500-2000	Neocomian to Mid Cretaceous volcanics and volcanogenic sediments	2000 +	
									Kimmeridgian
									Oxfordian
									Callovian
									Bathonian
	Early	Je-m	Early Jurassic shelf carbonates						
									Bajocian
									Toarcian
									Pliensbachian
									Sinemurian
Late	R	Middle and Late Triassic paralic detrital sediments	1000 +	Middle and Late Triassic fluvio-deltaic sediments	1500-2500				
								Hettangian	
								Rhaetian	
								Norian	
								Carnian	
Early	Ladinian								
	Anisian								
Early	Scythian			Early Triassic shallow marine shale					

WA/BB-287A

Figure 7. Simplified stratigraphy of Exmouth and Wallaby Plateaus, based on seismic and geological evidence.

(Couper), *Staplinisporites caminus* (Balme), *Matonisporites crassiangulatus* (Balme), *Lycopodiumsporites circolumenus* Cookson & Dettman, and *Lycopodiadites asperatus* Dettman. They correspond to Evans' (1966) spore units J4-5, and to Filatoff's (1975) *Callialasporites dampieri* Assemblage-zone.

One sample (48KD/1) from area C has a mid-Triassic age (McMinn, personal communication; based on 15 species). Lithofacies A is restricted to the Exmouth Plateau, and especially to its northern margin areas B, C, and D).

#### *Ferruginous lithofacies (Lithofacies B; probably mostly Jurassic)*

This association consists of reddish-brown, unfossiliferous ferruginous sediments, many of which are probably subaerially weathered representatives of the coal measure sequence, and hence of Jurassic age. They come from seismic sequence F-E, and possibly G-F. Texture and structure allow differentiation of clayey ironstones (B-1), sandy ironstones (B-2), ferruginous concretions (B-3) and ironstone breccia (B-4). These rocks are restricted to the northern Exmouth Plateau (mainly area B, rarely C and D).

#### *Shallow-water carbonates (lithofacies C; Early Jurassic)*

This is a heterogeneous group of shallow-water marine carbonate lithologies, which is restricted to the northern margin of the Exmouth Plateau (areas B, C, D). Because of incomplete cementation or secondary

solution of biogenic components, the biocalcarenes have very high porosities. These carbonates come from seismic sequence F-E.

Although many limestones were too recrystallised for biostratigraphic determination, a few biocalcarenes (especially 61KD 1-3, facies C-2/3) contained a fully marine fauna of benthic foraminifera, indicating shallow-water deposition near the coast. Quilty (unpublished data) notes a foraminiferal fauna of Late Sinemurian age, based on ranges of species of *Fronidularia* and *Lingulina* and by comparing this fauna with a similar one from New Guinea (Haig, 1979). Zobel (personal communication) found a similar age (Pliensbachian) by comparison with Liassic faunas from NW Europe (Nørvang, 1957; Zobel, 1960). F. Gramann (personal communication) has identified several ostracod species, including the Pliensbachian *Ogmochonchella* c.f. *aequalis*. This first record of Liassic marine rocks from Australia is a very important discovery of the *Sonne* cruise. Macrofossils in lithofacies C-2/3 include abundant crinoids (*Isocrinus* and *Pentacrinites*), and some thin-shelled *Inoceramus* fragments, belemnites (?*Belemnopsis* sp), brachiopods, ostracods and calcareous algae. Sample 61KD2 contains, in addition to its middle Liassic fauna, planktonic foraminifera of late middle Miocene (N14) age (B. Zobel, personal communication); they can only be explained by later contamination (e.g. as a lag deposit in a pocket formed during Miocene time).

The C facies association (see also Table 2) includes micritic limestone (C-1), foraminiferal-mollusc-echino-

derm biocalcarene (C-2), quartzose biocalcarene (C-3), very coarse crinoid biosparite (C-4), calcite-cemented quartz arenite (C-5), recrystallised sparry limestone (C-6), and dolosparite (C-7).

*Marine claystones and siltstones (lithofacies D; ? Late Mesozoic)*

In contrast to the terrestrial or paralic carbonaceous silty claystones of facies A-2, the D-facies consists of two types of fully marine noncalcareous or slightly calcareous clastic shallow-marine sediments.

The first type (D1) is a phosphatised clayey quartz sandstone to silty claystone (39KD/10; northern Exmouth Plateau) of unknown age (possibly Cretaceous to Paleogene?). The second type (D2) is a micaceous clayey siltstone (131KD, 138SL; southwest and south Exmouth Plateau) with some glauconite (area F-2). Sample 138SL (MPF7351) includes several marine (dinoflagellate) species, such as *Chlamydothorella nyei* Cookson & Eisenack, *Cleistosphaeridium aciculare* Davey, *Gardodinium trabeculosum* (Gocht), and *Spiniferites cingulatus* (O. Wetzel). This assemblage lies close to the Jurassic-Cretaceous boundary, and is tentatively dated as latest Jurassic (D. Burger, personal communication).

A slightly calcareous (?deltaic) claystone (51KD/3) contains Early Cretaceous radiolarians. A fissile shale (39KD/6; area B, lithofacies D-2) could be dated by McMinn (personal communication) as late Albian to earliest Cenomanian, an age which is consistent with the occurrence of thick-shelled *Inoceramus* prisms.

*Pelagic (more or less siliceous) chalks (lithofacies E; mid-Cretaceous to Tertiary)*

This lithofacies association consists of yellowish-brown to white pelagic foraminiferal nanno chalks, with various proportions of quartz and radiolarians. The siliceous chalks are often more or less silicified to porcellaneous chalk or diagenetically immature porcellanite. The age of these eupelagic sediments, which occur all along the Exmouth and Wallaby Plateaus, ranges from Middle Cretaceous to Tertiary.

White, semi-consolidated foraminiferal nanno chalk (E-1) consists of about 90 percent calcareous nannoplankton and undifferentiated calcite, and 10 percent planktonic foraminifera (see Table 1). This facies type includes a late Albian chalk with foraminifera of the *Ticinella roberti* zone and nannoplankton of the *Eiffellithus turriseiffeli* zone (sample 72KD); a late Paleocene to early Eocene chalk (156KL) (*Discoaster multiradiatus* nannoplankton zone); mid Oligocene chalk (*Sphenolithus distentus* nannoplankton zone) in 142SL, base of 64KL (which also contains foraminifera of the *Globigerina angulituralis*/*Globorotalia opima opima* zone); late Oligocene to early Miocene chalk (N5/6 foraminiferal zones) in 64KL and 78KL; middle to late Miocene chalk (N12-13) and late Miocene to Pliocene chalk (N14-19) in many samples. More detailed information on the foraminiferal assemblages is given in Quilty (1980).

A white quartzose and radiolarian chalk (E-2: 36KD/3) is of late Miocene to early Pliocene age. Sub-

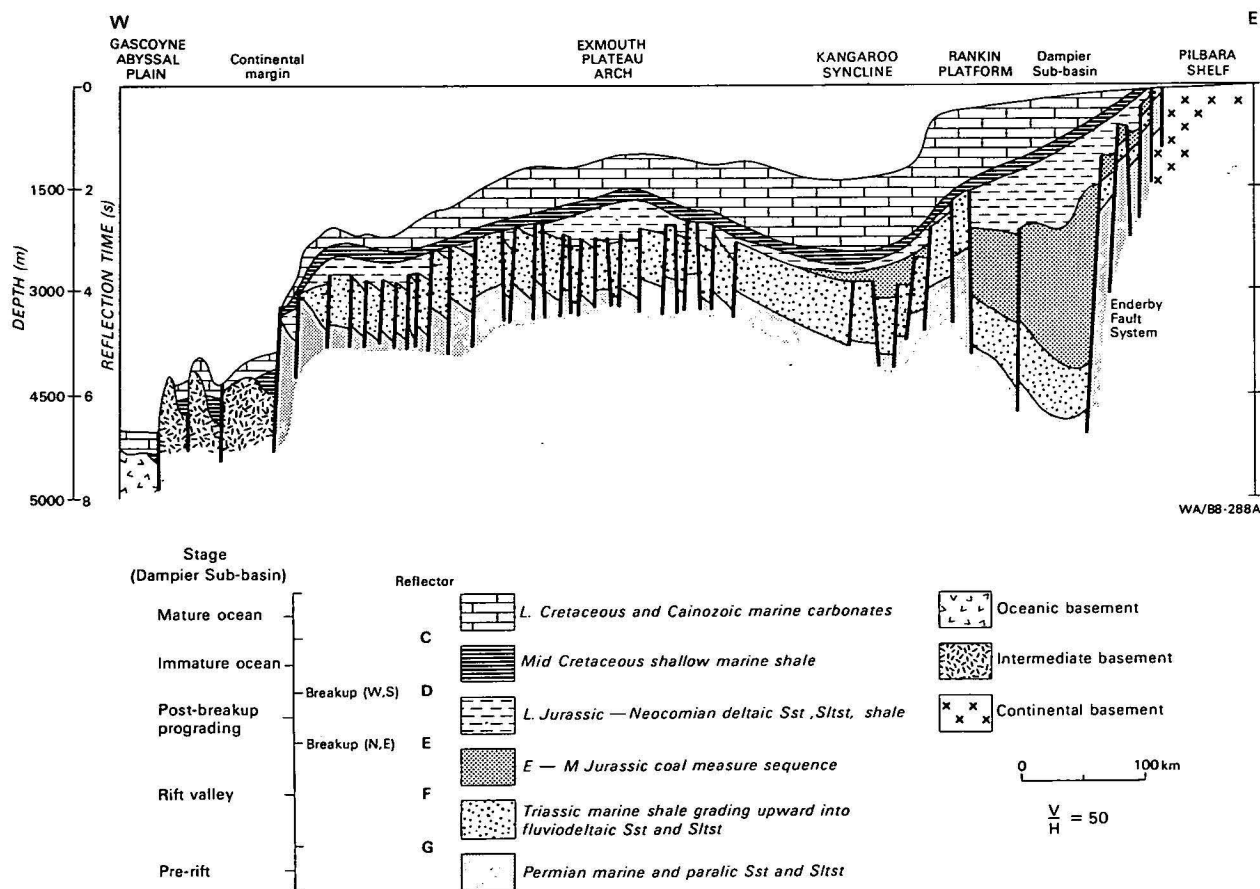


**Figure 8.** Schematic cross-section westward from Pilbara Shelf, through Exmouth Plateau Arch, to Gascoyne Abyssal Plain.

Compiled from Bureau of Mineral Resources data, and exploration company publications.

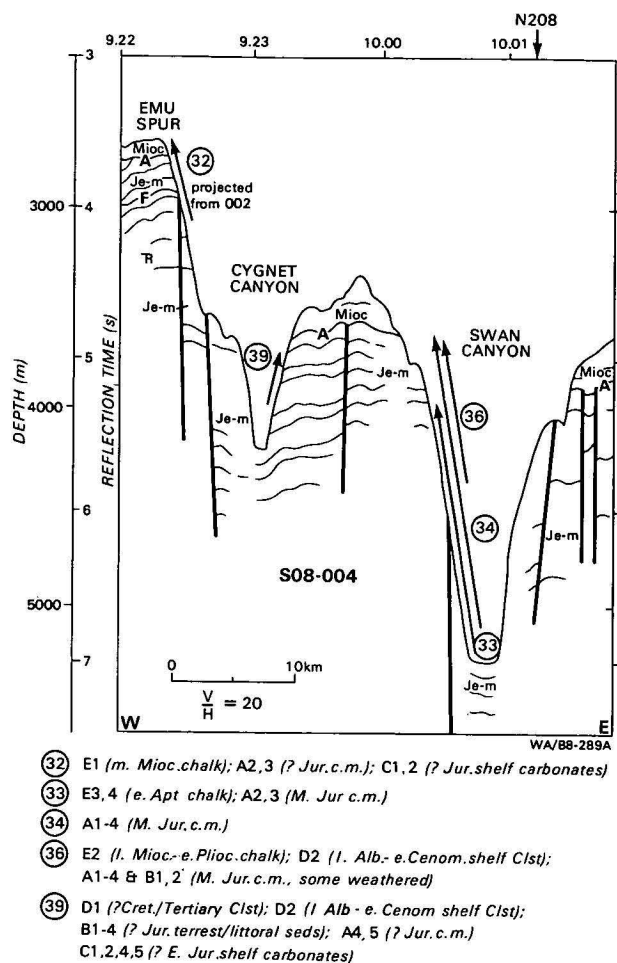


Figure 9. Line drawing of seismic profile S08-004, across Swan and Cygnet Canyons and Emu Spur, with seismic stratigraphy and dredge results. Profile located in Figure 4. Reflector and sequence nomenclature after Figure 7.

stantial amounts of well sorted, subangular to sub-rounded quartz of medium sand size (25% in coarse fraction) and traces of reworked *Inoceramus* prisms indicate a hemipelagic origin for these sediments.

A radiolarian chalk (33KD/2) contains up to 30% radiolarians, traces of sponge spicules and fish debris, but no terrigenous debris (E-3; northern margin of Exmouth Plateau). Further diagenesis and silica mobilisation has produced radiolarian porcellanite (E-4). The chalk contains early Aptian nannoplankton of the *Chiastozygus litterarius* zone (33KD/2C, P. Čepek, personal communication). The high percentage of radiolarians suggests a correlation with the Windalia Radiolarite of Aptian age.

#### Ferruginous quartz chert (lithofacies F; ? Late Mesozoic)

This vitreous chert, which was dredged only from the slope west of the Carnarvon Terrace (area L), has a different composition and genesis from the radiolarian porcellanite of facies E-4. Although circular fossil remains suggest the original presence of radiolarians, this completely recrystallised rock now contains 95 percent micro to macrocrystalline quartz cement and 5 percent iron oxides. Since pre-Cretaceous radiolarian-rich sediments are known from only one locality in the Carnarvon Basin, where they are Late Jurassic in age, the quartz chert may well be of mid Cretaceous age,

similar to the E-4 porcellanites. However, much deeper burial depths and/or higher *in situ* temperatures — possibly caused by heating by volcanic bodies — must be inferred to account for the much higher diagenetic maturity (i.e., the complete conversion of all opal-A via opal-CT into quartz).

#### Manganese crusts and nodules (lithofacies G)

Almost all the dredged rocks have blackish brown coatings of iron-manganese-oxides (G-2) of relatively recent (?Neogene) age; they were found in most areas, along the plateau margins and in the deep-sea. Manganese nodules (G-1), however, were found only at four stations, on the margin of the Sonne Ridge and the margins of the Wallaby Plateau. Thirty-nine samples were examined from thirty stations: thirty-two crusts and seven nodules. The thickness of the crusts ranges from fractions of a millimetre to about one centimetre. Their occurrence is generally independent of rock type, whether sediments or volcanics. Nodules, however, have always formed about a volcanic core. Both nodules and crusts have a rough surface, and a botryoidal, irregularly knotty form. In many crusts rock fragments have been included in the layers, which give the crusts a similar appearance to polynodules. The nodules display an internal structure consisting of more or less concentric shells, with the cores normally consisting of several volcanic rock fragments, and in one case of a single basalt fragment.

Table 3 compares atomic-absorption analyses of crusts and nodules obtained on this cruise with those of samples from Scott Plateau (Hinz & others, 1978; von Stackelberg, 1978) and off Cape Leeuwin (Noakes & Jones, 1976; Frakes & others, 1977). The metal values in the crusts are very variable, depending on the degree of impregnation by metal oxides. From north to south across the region (Scott Plateau/SO-8 samples/Cape Leeuwin) the contents of iron and cobalt fall and those of copper rise. No such trends are apparent for nickel and manganese — the SO-8 values are equal to or lower than those in the other two areas. The combined Ni + Cu + Co values in nodules for the SO-8 cruise average 0.76 percent with a maximum of 1.02 percent, indicating that the nodules are of no commercial interest.

The graphical comparison of the Fe/Mn ratio to manganese content (Fig. 14) allows several sampling areas to be separated from one another, essentially from changes in Mn content. Lower Mn contents are confined to crusts on sedimentary rocks (Areas B to G), but moderate Mn contents overlap with the areas (H to L) where crusts and nodules generally involve volcanic rocks.

#### Volcanic and volcanoclastic rocks (lithofacies H)

A heterogeneous suite of more or less altered volcanic rocks and volcanoclastic sediments was recovered during the SO-8 cruise (see Table 1): along the northern margin of the Wombat Plateau (area D); on the Sonne Ridge in the Cuvier Abyssal Plain (area H); along the northern, eastern and southern margins of the Wallaby Plateau (areas I, J, K); and at the westernmost extremity of the Carnarvon Terrace (area L). Areas H-K yielded only volcanic or volcanoclastic rocks, apart from Cainozoic pelagic chalks and oozes (facies E). The following brief description of the tentative lithofacies classification of these rocks is based on petrographic and geochemical analyses by R. Emmermann (Karlsruhe). A few volcanic rocks which



SO-8 area Nodules	Water depth (m)	Average values for major metals (%)						Analyst (No. of analyses)
		Fe	Mn	Ni	Cu	Co	Ni + Cu + Co	
Sonne Ridge (St. 148)	4800	12.00	15.63	0.39	0.28	0.19	0.86	BGR (1)
		13.40	18.40	0.54	0.28	0.20	1.02	BMR (1)
Wallaby Plateau	4400-4600	13.82	15.63	0.33	0.19	0.28	0.80	BGR (2)
East & South (Sts. 165, 170)		13.70	11.30	0.24	0.16	0.20	0.60	BMR (1)
Wallaby Plateau	5300	13.45	15.38	0.25	0.13	0.22	0.60	BGR (1)
East & South (St. 167)		13.60	16.70	0.31	0.15	0.23	0.69	BMR (1)
Average all nodules	4400-5300	13.09	15.55	0.32	0.20	0.23	0.75	BGR (4)
		13.57	15.47	0.36	0.20	0.21	0.77	BMR (3)
Average all crusts	2500-5300	12.71	12.23	0.28	0.09	0.16	0.53	BGR (26)
		18.15	15.93	0.32	0.14	0.20	0.66	BMR (6)
Scott Plateau								
Nodules	2050-2100	18.30	17.47	0.39	0.06	0.34	0.79	BMR (3)
Crusts	1900-2500	16.99	15.87	0.33	0.05	0.26	0.64	BGR (4)
								BMR (2)
Cape Leeuwin								
Nodules	4300-5000	9.42	17.09	0.62	0.34	0.12	1.08	BMR (10)

Table 3. Comparison of average metal values in ferromanganese crusts and nodules from the SO-8 cruise, Scott Plateau, and off Cape Leeuwin.

BGR and BMR analyses by atomic absorption method from same dredge, but different samples. Analyses from Scott Plateau by Hinz & others (1978) and von Stackelberg (1978); from Cape Leeuwin by Frakes & others (1977).

were not too weathered were dated using the K/Ar dating method (H. Kreuzer & H. Raschka, Hannover).

Variably altered tholeiitic basalts (H-1) were recovered from the Sonne Ridge (area H) and the Wallaby Plateau (area K). They have an intersertal to intergranular texture and are often amygdaloidal. For the Sonne Ridge (and possibly also for much of the Wallaby Plateau) a late Neocomian age is assumed from the magnetic anomalies. Only one somewhat questionable K/Ar age was obtained from 170KD/1 (area K, southern Wallaby Plateau): the apparent age is 89 m.y. (Turonian/Coniacian) but, because of the degree of alteration (loss on ignition = 3.4-3.7%), this is a minimum age. Thus the Valanginian/Hauterivian (125 m.y.) age of the onset of spreading in the Cuvier Abyssal Plain and of volcanism of the Wallaby Plateau, assumed by Larson & others (1979) and Johnson & others (in press) from magnetic anomalies, is not contradicted by our data.

H-2 is a volcanic breccia, probably of tholeiitic composition, which occurs along the southern margin of the Wallaby Plateau (area K). Altered basalt fragments (diameter 2 to more than 30 mm) are cemented by secondary smectite and phillipsite. H-3 designates altered, slightly differentiated alkali basalts (possibly hawaiites), which were recovered from Sonne Ridge (area H) and the northern margin of the Wallaby Plateau (area I).

A suite of rocks which only occurs along the northern flank of the Wombat Plateau (H-4, 5, 6: area D), is very different from the above-mentioned basaltic rocks, since it contains mainly silica-rich, intermediate to acid volcanics. H-4 is a fine-grained amygdaloidal mugearite to silica-undersaturated trachyte (*sensu lato*). The K/Ar age is  $192 \pm 4$  m.y. (at least early Liassic), which correlates well with the occurrence of these rocks below the Late Jurassic reflector E. H-5 is an alkali-rhyolite with porphyritic texture and large sanidine phenocrysts. The sanidines gave a K/Ar age of  $213 \pm 3$  m.y. (Middle/Late Triassic boundary), and the whole rock a K/Ar age of  $206 \pm 3$  m.y. H-6 is a light-coloured rhyolitic pumice (area C), and might be of

relatively recent age, derived from Indonesian volcanic eruptions.

H-7 facies rocks include more or less altered tuff to lapillistone, and poorly sorted tuffaceous sandstone to siltstone, with various admixtures of non-volcanic (epi-clastic) components. H-8 is a multicoloured, poorly sorted volcanoclastic sandstone or breccia occurring on Sonne Ridge (area H) and on the Wallaby Plateau, and H-9 is a white, phosphatised pyroclastic claystone, common along Sonne Ridge (area H) and the northern margin of Wallaby Plateau (area I).

### Revised seismic stratigraphy and marginal structure

During the Sonne cruise we tested interpretations of existing reflection seismic data across the Rowley Terrace (Stagg, 1978), the Exmouth Plateau (Exon & Willcox, 1978) and the Wallaby Plateau (Symonds & Cameron, 1977).

Altogether 1310 km of seismic data were recorded during the cruises (Fig. 12 shows the quality of the data); the general locations of the seismic profiles, including selected pre-existing seismic tie-lines, are shown in Figures 2 and 3; detailed locations of the more important sampling areas are shown in Figures 4, 5 and 6.

We discuss below the revised seismic stratigraphy of various areas (see Fig. 7). The reflectors A to F of Exon & Willcox (1978) can be identified in most of the region (e.g. Fig. 8). Figure 15 correlates the seismic stratigraphy with the lithostratigraphy of the Sonne samples and with the facies of the Northwest Shelf (Bedout No. 1 well).

#### Northern Exmouth Plateau

The Sonne cruises show that the geology of the northern Exmouth Plateau differs from that of the remainder of the plateau, and that the seismic stratigraphy (Exon & Willcox, 1978; Exon & Willcox, in press) requires revision in this area. The earlier work had indicated that on high blocks such as the Wombat



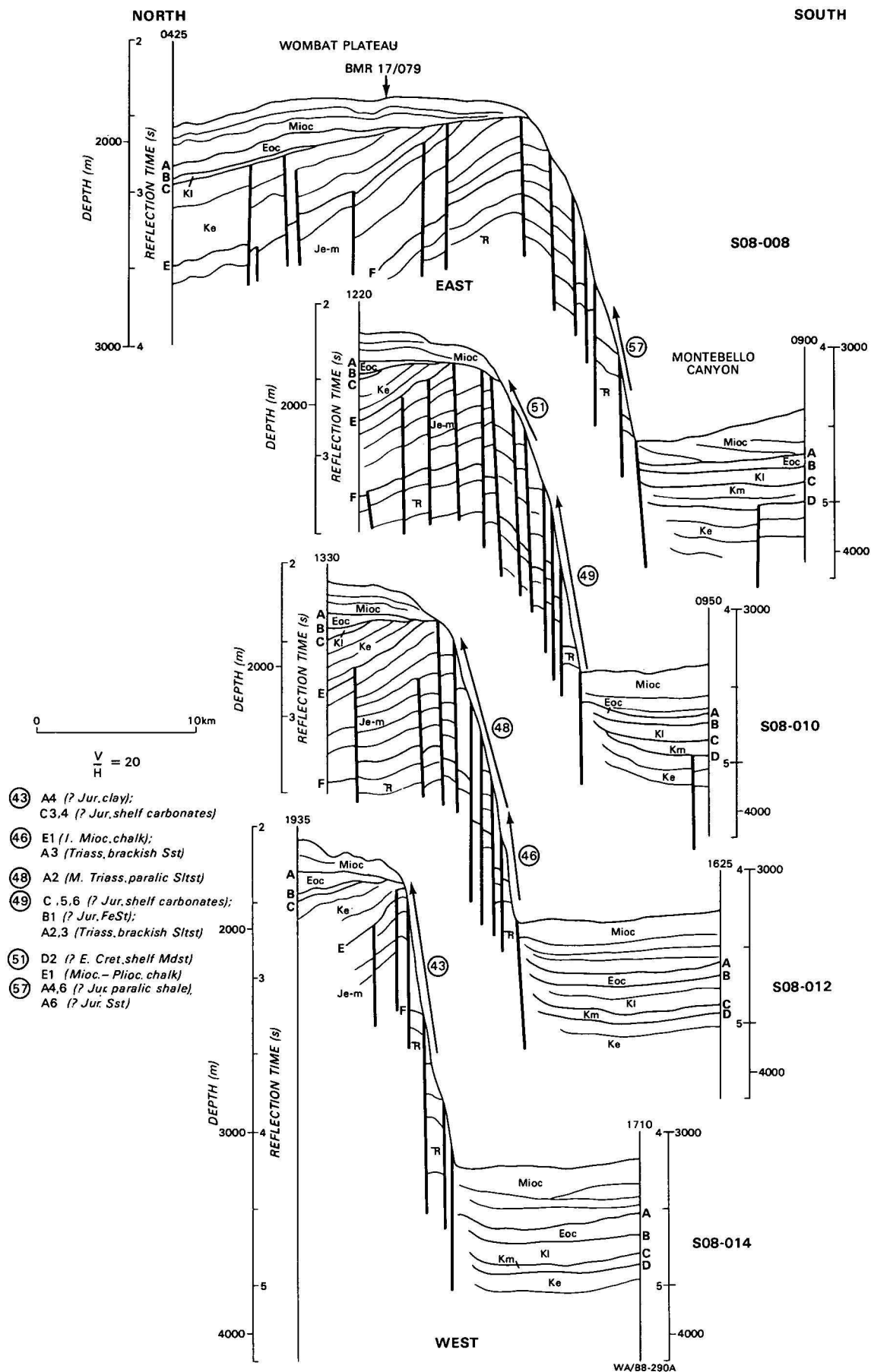


Figure 10. Line drawing of seismic profiles SO8-008, 010, 012, 014, across southeast flank of Wombat Plateau, with seismic stratigraphy and dredge results. Profiles located in Figure 5. Reflector and sequence nomenclature after Figure 7.

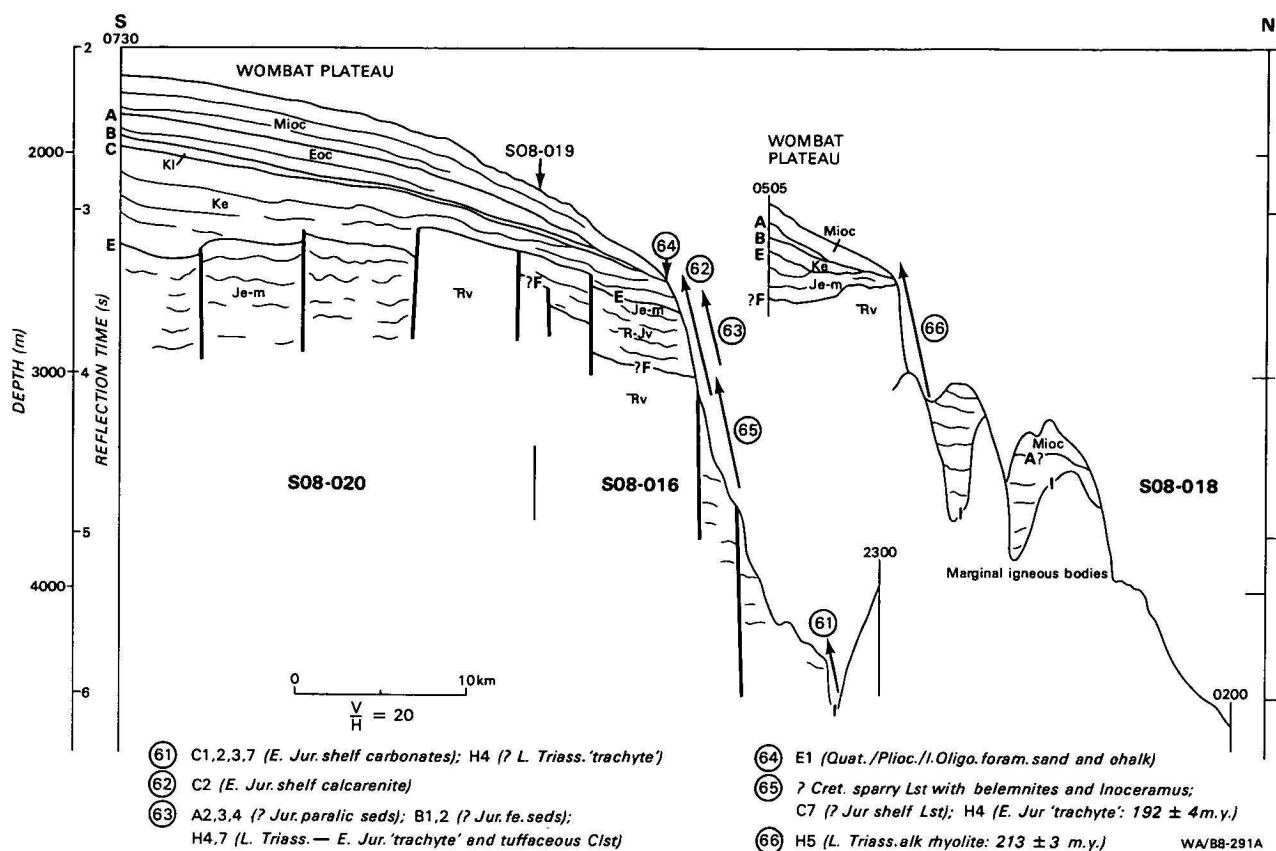


Figure 11. Line drawing of seismic profiles SO8-016, 018, 020, across northern flank of Wombat Plateau, with seismic stratigraphy and sampling results.

Profiles located in Figure 5. Reflector and sequence nomenclature after Figure 7. I is top of igneous basement.

Plateau and Emu Spur (Fig. 1) a Triassic sequence, underlying Horizon F, lay immediately beneath a condensed late Mesozoic and Cainozoic sequence, within which Horizons A, C and D were generally present. In downthrown blocks a thick Late Jurassic-Early Cretaceous sequence was believed to separate Horizons D and F.

The sampling results showed (Figs. 9, 10, 11) that in the north a condensed late Mesozoic and Cainozoic sequence generally overlies Horizon E, which is underlain by a thick Early and Middle Jurassic sequence; Horizon F, in turn, is underlain by a thick Triassic sequence. The latter sequence generally consists of fluviodeltaic sediments, which are overlain by well-bedded trachytes and rhyolites on the northern margin of the Wombat Plateau. From seismic evidence a thick Late Jurassic-Early Cretaceous sequence is present only on the southern Wombat Plateau and in the Montebello Trough; it is also present below the Rowley Terrace to the east. It appears that the northern Exmouth Plateau has a history more akin to that of the Rowley Sub-basin of the Canning Basin than to that of the Carnarvon Basin or the central and southern parts of the plateau.

The northern margin is controlled by an east-west hinge-line, which corresponds roughly to the 2000 m isobath. To the north the F-E sequence progrades northwestward and thickens. Normal faults form the southern margin of the Wombat Plateau, and give the Montebello Canyon the appearance of a half-graben in that region. Other prominent features are northeast-trending faults (Figs. 8, 16) which contribute to the rugged topography of the margin; horsts underlying the

Wombat Plateau, Echidna Spur and the Emu Spur are separated by grabens. The horsts have been bevelled by erosion, leading to a marked angular unconformity below the post-C sequence (Fig. 10).

The edge of the continental crust (Fig. 1) probably coincides roughly with the inner edge of the marginal igneous bodies (mostly intrusions) which are apparent in some seismic profiles. The bodies generally parallel the Callovian magnetic anomalies on the Argo Abyssal Plain, suggesting that the margin formed by rifting. At least one offset in the edge of continental crust (that northeast of the Echidna and Emu Spurs) appears to correspond with a fracture zone (probably a transform fault) on the abyssal plain.

#### Western and southern Exmouth Plateau

The geological results from the western (area E) and southern (areas F and G) margins of the Exmouth Plateau agree (Fig. 8) with the seismic interpretation of Exon & Willcox (1978). A major rift-onset unconformity (F) overlies a thick Triassic fluviodeltaic sequence, and is overlain by a thick Late Jurassic and Early Cretaceous deltaic sequence which built northward across the plateau. The Neocomian breakup unconformity (D) shows little angularity on the seismic profiles, and is overlain by acoustically transparent mid-Cretaceous marine shales. After breakup only thin Cretaceous and Cainozoic sequences were deposited. The change to carbonate sedimentation in the Turonian or Coniacian is marked by a major change of seismic character at Horizon C; the overlying Late Cretaceous carbonates are well-bedded. Two periods of erosion or non-deposition, marked by unconformities (B and

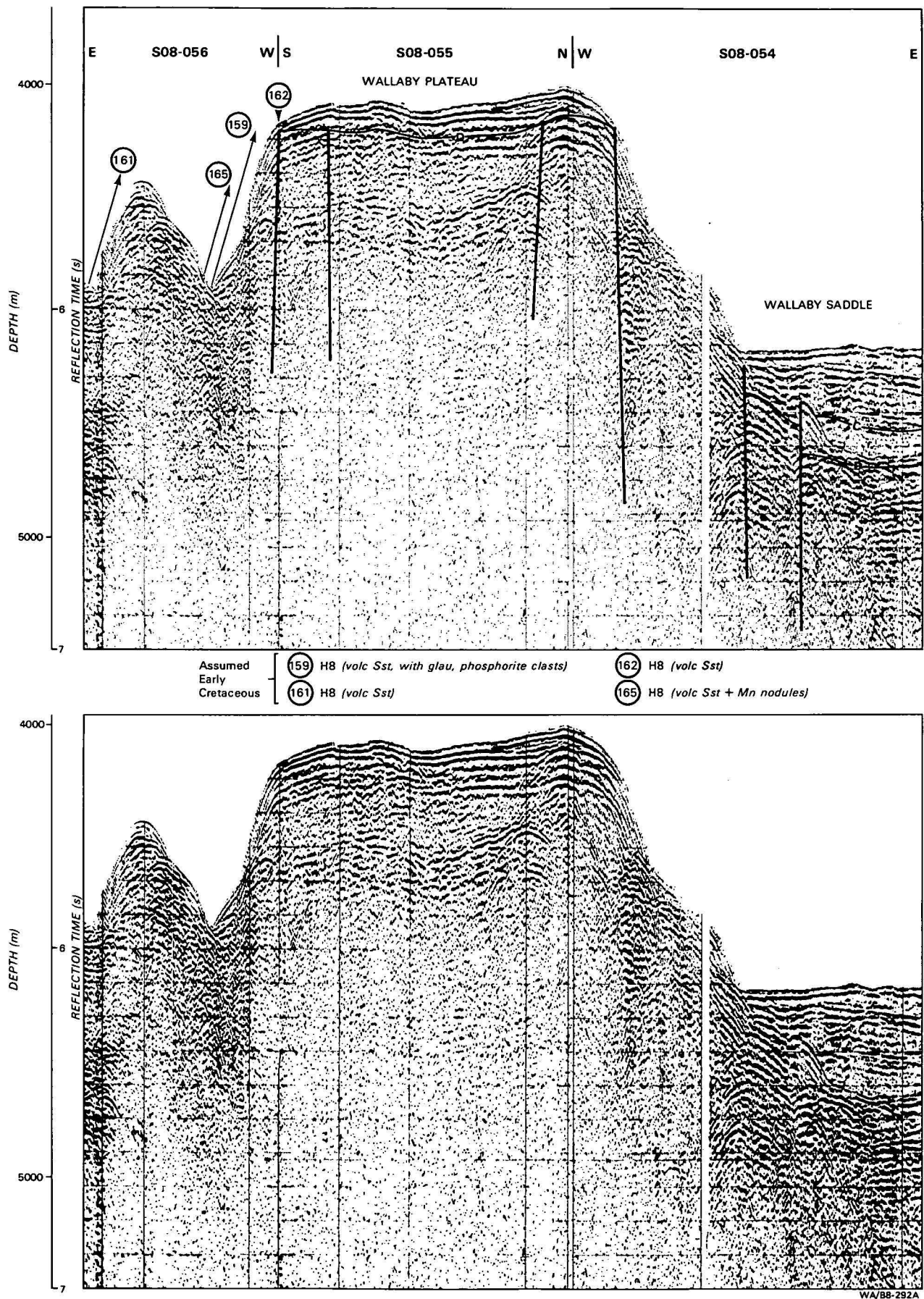
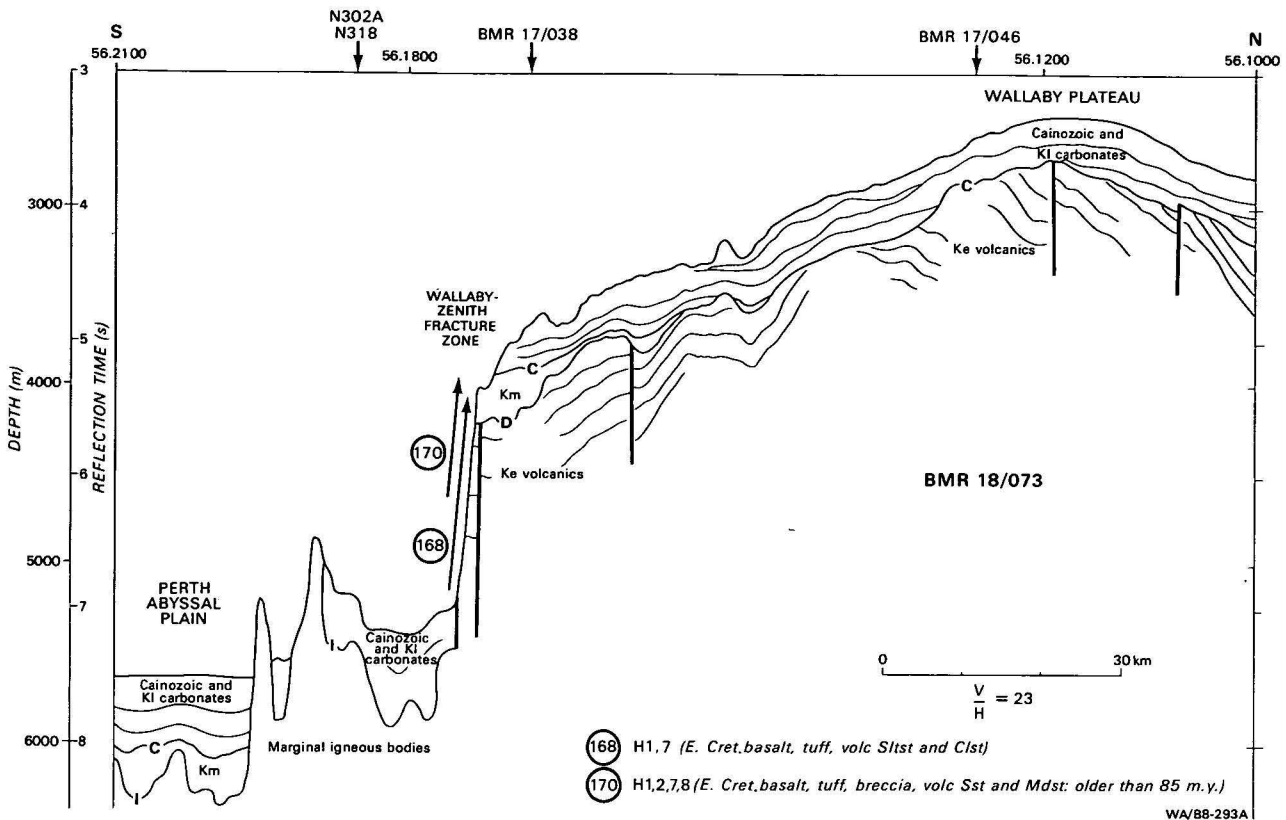


Figure 12. Seismic profiles SO8-054, 055, 056, across eastern margin of Wallaby Plateau, with interpretation and sampling results. Profiles located in Figure 3. Reflector and sequence nomenclature after Figure 7.



**Figure 13.** Line drawing of seismic profile BMR 18/073, across southern margin of Wallaby Plateau, with seismic stratigraphy and dredge results.

Profile located in Figures 3 and 6. Reflector and sequence nomenclature after Figure 7. I is top of igneous basement.

A), interrupted the pelagic carbonate sedimentation in the Cainozoic.

The western margin of the plateau consists of north-east-trending fault-blocks, which step down toward the Gascoyne Abyssal Plain (Fig. 8). This margin formed as the flank of a rift-valley. The southern margin of the plateau is bounded by the Cape Range Fracture Zone, which apparently lines up with a fracture zone on the Gascoyne Abyssal Plain (Fig. 1), and also with the structural trends of the Proterozoic basins south of the Pilbara Block. Northwest-trending normal faults parallel to the fracture zone presumably formed while oceanic crust below the Argo Abyssal Plain subsided. The magnetic lineations on the abyssal plain indicate that the fracture zone first formed in the Neocomian (Larson & others, 1979). This accords with the seismic evidence from the plateau that a southerly sediment source, which formed a major delta in the Late Jurassic and earliest Cretaceous, was cut off at that time. Veevers & Powell (1979) recently suggested that the southwestern part of the delta was derived from the uplifted southern (transform) rim of the Exmouth Plateau, and that it was deposited during the first 5 million years after breakup.

#### Wallaby Plateau and Sonne Ridge

The Wallaby Plateau has very steep margins on the west and south and, in places, on the east. Figures 12 and 13 show seismic profiles along which the slope appears to truncate the main unconformity (D). Beneath the unconformity is a dipping, layered sequence, which in some processed profiles is at least 2 seconds (ca. 3000 m) thick. The Sonne sampling suggests that this sequence consists of oceanic volcanics and volcanogenic sediments (area I, J, K).

Overlying the D unconformity is a thin, patchy, acoustically transparent unsampled sequence (Km in Figs. 7, 13) which may be equivalent to the mid-Cretaceous shales penetrated in DSDP hole 263 (Veevers & Johnstone, 1974). The overlying sequence, which rests on reflector C, contains several unconformities, is seldom more than 400 m thick, and consists of both well-bedded and transparent strata. It probably consists of Late Cretaceous and Cainozoic pelagic carbonates, equivalent to those on the Exmouth Plateau. Such carbonates, of Paleocene to Eocene age, have been sampled in Area J.

The seismic data indicate that the northern part of the Wallaby Plateau, below a water depth of 4 km, is underlain by oceanic basement, which is assumed to be of similar age to that beneath the Cuvier Abyssal Plain. The seismic stratigraphy changes between the Wallaby Saddle and the Carnarvon Terrace, where oceanic crust appears to give way to continental crust (Fig. 1); the layered volcanigenic rocks are probably not present east of the 3000 m isobath. The southern margin, the Wallaby-Zenith Fracture Zone, is believed to be a transform fault, whose formation is related to the Neocomian formation of the oceanic crust beneath the Perth Abyssal Plain (Markl, 1974). The formation of the complex western margin of the plateau remains little investigated, but it was probably influenced by rifting.

Sonne sampled the slope west of the Carnarvon Terrace in area L, on the Wallaby-Zenith Fracture Zone. BMR seismic profile 17/036 indicates that there is a structureless marginal body here, which is apparently different to the sequence beneath the D unconformity on the Carnarvon Terrace. It is possible that the re-

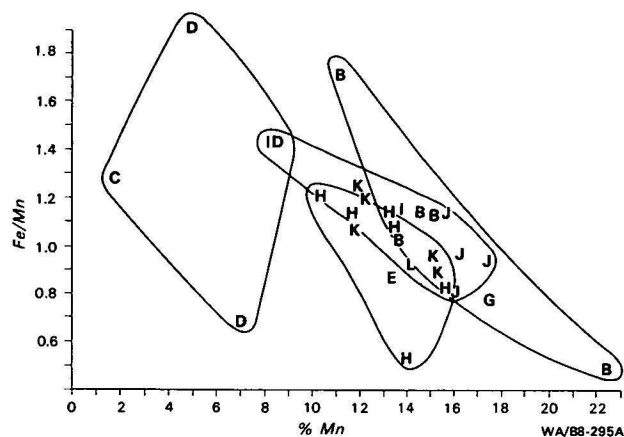


Figure 14. Plot of Fe/Mn ratio against Mn percentage for ferromanganese nodules and crusts dredged on Cruise SO-8, showing relationship of sampling areas to chemistry.

Analyses by atomic absorption; analysts G. Proschka and V. Marchig, BGR, Hannover, and B. I. Cruikshank, BMR, Canberra.

crystallised chert recovered by *Sonne* represents a Mesozoic radiolarite, which was baked by an intrusion — the structureless marginal body — along the fracture zone.

### Hydrocarbon potential

Sedimentary sequences beneath the Exmouth and Wallaby Plateaus have been regarded as having potential for hydrocarbon accumulations. The *Sonne* cruise has provided information about the rock-types cropping out there, and has also provided some direct evidence, from isotope analyses of gases adsorbed to the surface sediments, about the types of hydrocarbons which might be expected beneath the central Exmouth Plateau.

#### Exmouth Plateau

Exon & Willcox (1978) indicated that the plateau contained as much as 10 km of Phanerozoic strata, and that suitable source rocks, reservoir rocks and structures for the generation and trapping of hydrocarbons appeared to exist, making the plateau an attractive exploration target. Major unknowns were the thermal history, the details of rock types, and the timing of structural events. Numerous Triassic-Jurassic fault blocks, and a large Neocomian delta in the south, were obvious exploration targets.

Wright & Wheatley (1979) assessed about 5000 km of multichannel seismic data accumulated across the central and southern part of the plateau in 1976, and concluded that the fault blocks probably consisted of Middle to Upper Triassic sediments, probably sandstone and shale. They pointed out that seismic evidence of hydrocarbon generation includes a probable gas chimney associated with the western bounding fault of the highest fault block. They considered that the fault blocks had a higher potential for oil than the Neocomian delta, but estimated that recoverable volumes were unlikely to be in the 'giant' category.

Our sampling, while confirming the previous picture for the central and southern parts of the plateau, showed that a sequence equivalent to the Early and Middle Jurassic coal measures of the offshore Canning Basin, rather than to the Triassic fluviodeltaic sandstones and siltstones of the Carnarvon Basin, underlies the breakup unconformity in the northern part of the

plateau. The sequence appears to consist of about 500 m of Late Cretaceous and Cainozoic pelagic carbonates, angularly overlying 2500 m of Early Jurassic shelf carbonates and Middle Jurassic coal measures, and 1000 m or more of Triassic paralic sandstone and shale. Coal in the Middle Jurassic sequence showed vitrinite reflectances of less than 0.4 percent (Appendix), indicating that the exposed sequence is immature as a petroleum source rock. However, it could be an adequate source for gas if it was more deeply buried. The presence of marine Jurassic rocks upgrades the chance of source-rocks for oil being present. The Early Jurassic carbonates include many highly porous and permeable calcarenites which, given the right diagenetic history, could make excellent petroleum reservoir rocks. Quartzose sandstones in the coal measure sequence also have considerable potential as reservoir rocks.

A series of 25 boomerang cores and box cores was collected from four areas high on the Exmouth Plateau (Fig. 1; SS1-4) for isotopic analyses of gaseous hydrocarbons adsorbed to surface sediments.  $\delta^{13}\text{C}_1$  determinations were subsequently carried out by E. Faber and W. Stahl in the BGR laboratories. A special blender technique was applied to liberate the hydrocarbons adsorbed in the sediments, methane yield was determined by FID capillary chromatography, and carbon isotopes were investigated using a mass spectrograph (Faber & Stahl, in prep.). Area SS1 was at the intersection of two seismic lines which suggested that gas was reaching the surface, SS2 on the planned location of Investigator No. 1 well, SS3 in another area where seismic data suggested that gas was escaping (pictured in figure 4 of Wright & Wheatley, 1979), and SS4 at the planned location of Zeewulf No. 1 well.

Except for material from Station 97KA, all stations yielded too little methane for reliable isotope determinations. The sample from Station 97 (Fig. 1; area SS3) yielded approximately 18 ppb methane with a  $\delta^{13}\text{C}_1 = -40\text{‰}$ . This methane was probably generated by a sapropelic marine source material within the oil window. The  $\delta^{13}\text{C}$  determinations of all the other samples are less negative ( $-14\text{‰}$  to  $-39\text{‰}$ ), i.e. the methane is  $^{13}\text{C}$  enriched. This enrichment, and the tiny methane yields ( $<10$  ppb in all stations except Station 97) and the absence of higher hydrocarbons in the sediment samples, indicates a poor oil potential at the sampling locations. This assessment of potential is based on a limited number of samples, and on a method which is still under development, and could be modified by special geologic conditions. For example, thick, consolidated, but undisturbed, tight sediment layers could seal the source rocks, reducing migration to the surface.

By early 1980, six petroleum exploration wells had been drilled on the Exmouth Plateau (Figs. 2 & 3). Publicly available information indicates that no significant oil shows were found in the wells, but that gas shows were fairly common. The largest gas accumulation found in these six wells appears to be that of Scarborough No. 1.

Gas is not at present a commercial proposition in the water depths prevailing on the plateau, and so these results are not promising. However the plateau is large, containing various possible exploration plays, and cannot yet be regarded as adequately tested.

#### Wallaby Plateau

The petroleum potential of the Wallaby Plateau depends on whether it is a continental block (Symonds &



Cameron, 1977), or an accumulation of oceanic volcanics, an epilit (Veevers & Cotterill, 1978).

The evidence gathered on the *Sonne* cruise (discussed later) suggests an oceanic origin for the plateau. The plateau appears to consist of a very thick pile of volcanic and volcanoclastic rocks, laid down very rapidly during late Early Cretaceous times, and overlain by a veneer of mid-Cretaceous shale and Late Cretaceous and Cainozoic carbonates. If this is correct the plateau has negligible petroleum potential.

### Geological evolution

A revised geological history of the Exmouth and Wallaby Plateau is outlined below.

#### *Early rift history (Middle Triassic to Middle Jurassic)*

From Late Triassic to Middle Jurassic times the Exmouth Plateau region was part of a southerly embayment of Tethys, the Westralian Trough of Teichert (1939), with Gondwanaland to the east, south and west (Fig. 16). Tensional rifting, which later led to the breakup of the region, caused some extension and the development of northeast-trending normal faults.

Up to 3000 m of fluviodeltaic sands and muds (Mungaroo Formation and equivalents) accumulated in the embayment in Middle and Late Triassic times, over the Canning and Carnarvon Basins, and the Exmouth Plateau (Fig. 16A). *Sonne* recovered paralic Triassic sediments (A2 & A3 facies) including poorly sorted, fine-grained carbonaceous micaceous sandstone, siltstone and shale, from 3 stations in the north.

Late Triassic to earliest Jurassic eruption of trachytic and rhyolitic lavas (H4 & H5 facies) then occurred in the area of the northern flank of the Wombat Plateau (Figs. 1, 16). These flows extend for more than 10 km along the northern flank and at least 15 km into the plateau. A trachyte has been dated (K/Ar) as early Liassic at the youngest ( $192 \pm 4$  m.y.), and an alkali rhyolite as Carnian ( $213 \pm 3$  m.y.). These flows are similar to Late Cretaceous rhyolites from the Lord Howe Rise off southeast Australia, where spreading started about 15 m.y. after their extrusion (van der Lingen, 1973). The Wombat Plateau flows were apparently extruded subaerially, or under very shallow water, during the phase of rifting preceding the Callovian breakup which formed the northern part of the Exmouth Plateau.

In the Early and Middle Jurassic (Fig. 16B, C) rifting continued; thick sedimentary sequences of this age are preserved east of the Rankin Platform in the Carnarvon Basin, in the Canning Basin, and on the northern Exmouth Plateau. In the first two areas about 1000 m of predominantly non-marine clastic sediments including coal measures were laid down; thin shallow-marine carbonate beds were deposited in parts of the Canning Basin.

In the Early Jurassic the margin of the Exmouth Plateau sank northward of an east-west hinge line (Fig. 16B), and a northwesterly prograding and thickening wedge of Early Jurassic shelf carbonates (facies C) and Middle Jurassic coal measures (facies A), up to 2500 m thick, was deposited. The discovery of the shelf carbonates, largely calcarenites and calcilutites, is the first documentation of a Late Sinemurian-Pliensbachian marine transgression in the Westralian Trough (Quilty, 1980). Freshwater deposits, including coal measures, were deposited at this time in most of the Canning and Carnarvon Basins (Fig. 16B); the central Exmouth

Plateau was a high area, undergoing intermittent erosion.

The calcarenites consist largely of the skeletons of shelf organisms, and were laid down in environments ranging from lagoonal to subtidal, bank, and mid-shelf. A biocalcarenite (43) contains reworked fragments of trachyte with algal coating, suggesting reworking of volcanic fragments on an extremely shallow carbonate platform. Crinoidal biocalcarenite (C4) was probably reworked from very shallow water depths, and possibly deposited along an outer reef or carbonate bank flank (fore-reef?). The calcilutites (C1) probably originated below wave base, possibly on the middle shelf.

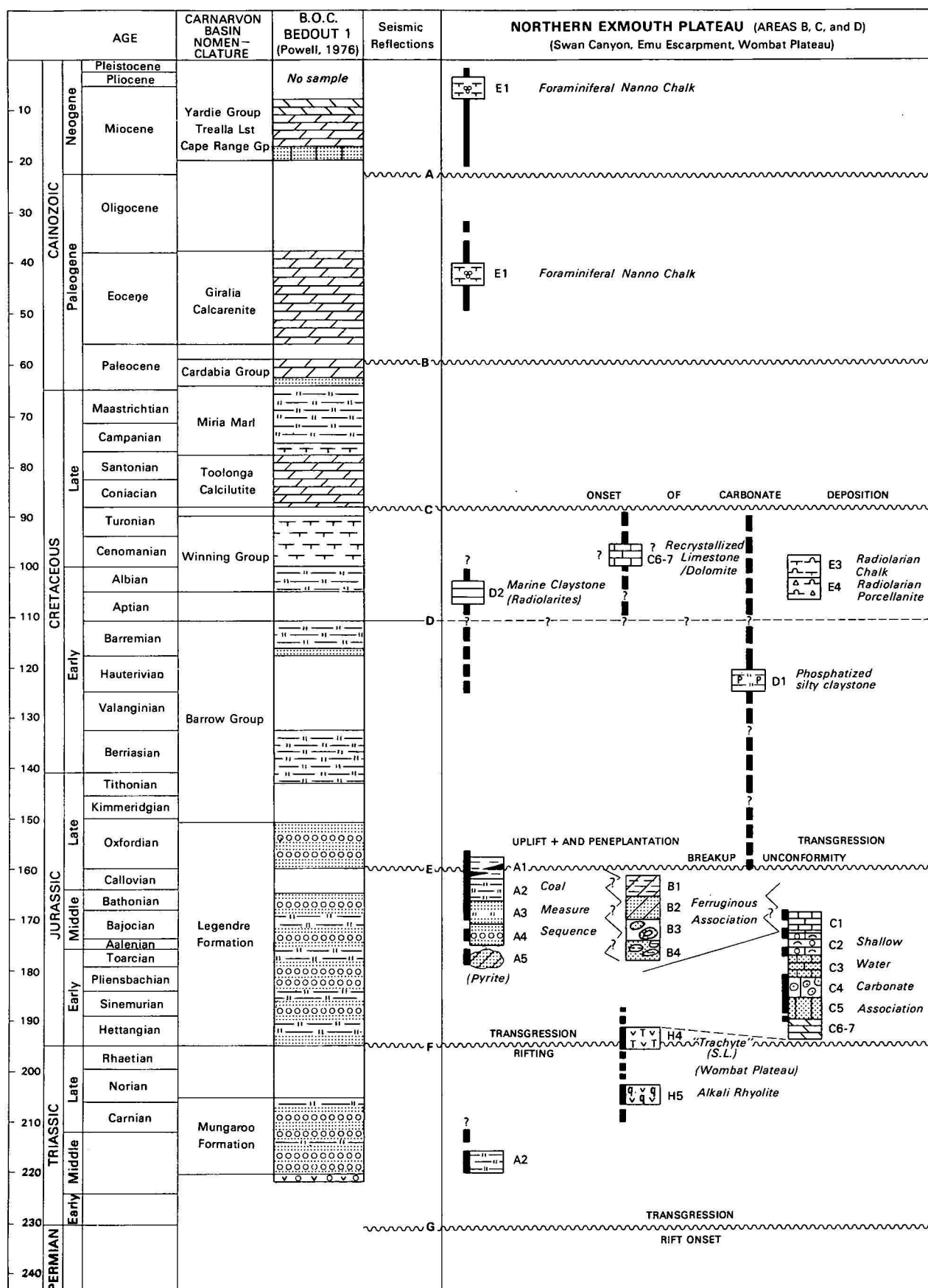
A thick sequence of coal measures (facies A) was deposited on the shelf carbonates on the northern Exmouth Plateau. We recovered coal measures from 11 stations; palynomorphs from several samples suggest that most of the coal measure sequences are of Middle Jurassic age. They consist mainly of carbonaceous, micaceous silty claystone (A2), grading to siltstone (A3) and sandstone (A4); they contain thin stringers of an immature sub-bituminous coal (A1; see Appendix). They were accumulating in a variety of paralic environments during a mid-Jurassic regressive period — dominantly in fresh water (landward part of delta, flood plain, coal swamp), but with brief marine to brackish incursions. Well evidence suggests that such coal measures were deposited over large areas of the Canning and Carnarvon Basins (Fig. 16C). Seismic evidence indicates that the central Exmouth Plateau was still high, undergoing little sedimentation, in the Middle Jurassic.

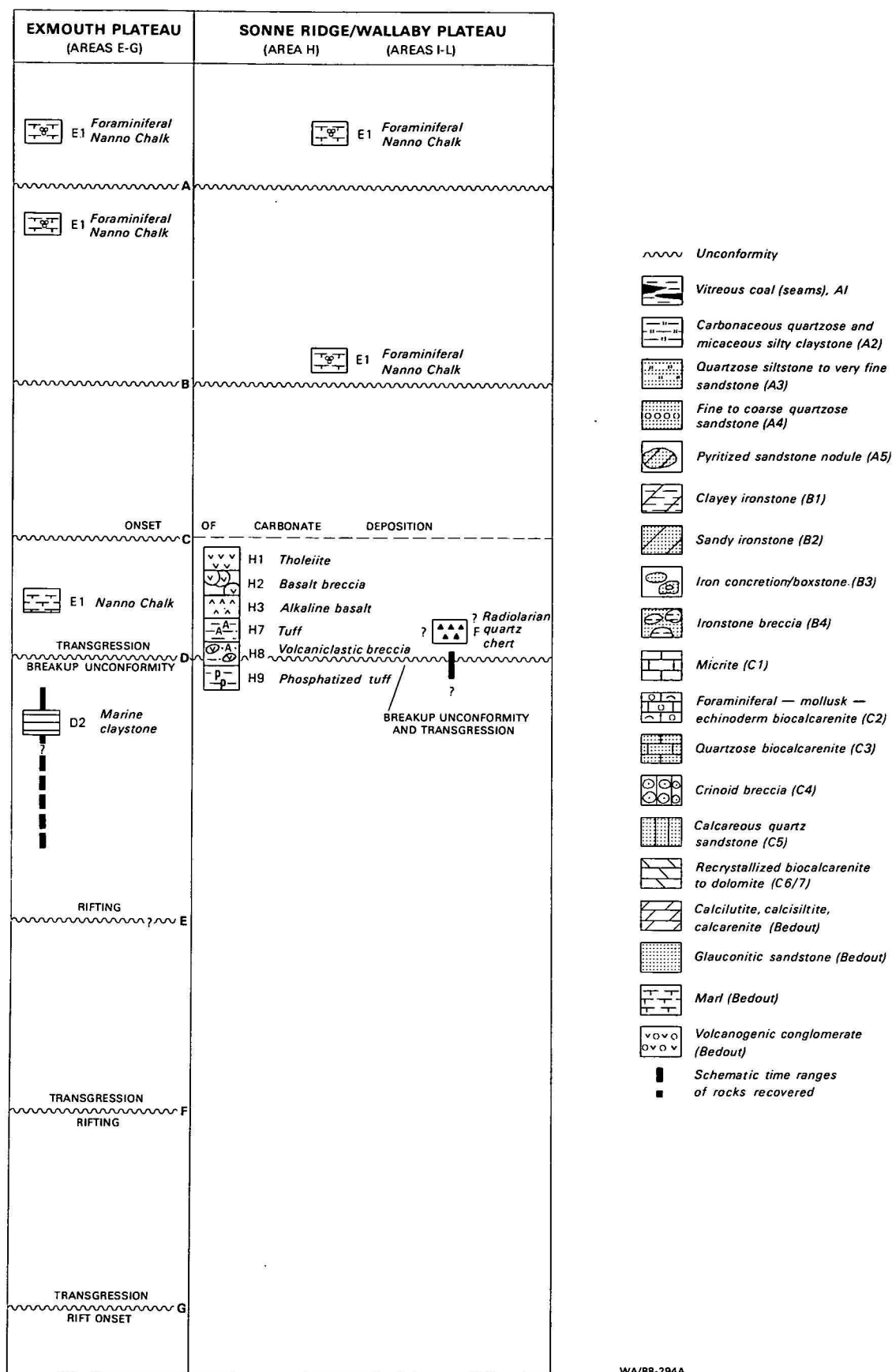
A period of emergence and penecontemporaneous erosion on the northern Exmouth Plateau is indicated by ferruginised sediments, such as clayey and sandy ironstones (B1, 2), concretions and boxstones (B3), recovered from 5 stations. An ironstone breccia (B4) from the Swan Canyon area (39) may represent littoral reworking of the ironstones during a marine transgression. As the coal measure lithologies (A2-6) are similar, and commonly somewhat oxidised, we suspect that the unfossiliferous ferruginised sediments are probably mostly altered coal measures. The period of uplift probably coincided with the onset of seafloor-spreading in the north, i.e. late Middle to early Late Jurassic.

Throughout the rifting phase (Early Triassic-Middle Jurassic) the region remained near sea level. In the Triassic, sedimentation and subsidence rates were about 50-100 m per million years. In the Early and Middle Jurassic sedimentation and subsidence rates were very low on the Exmouth Plateau proper and the Rankin Platform, but about 50-100 m per million years in the Dampier Sub-basin, the Canning Basin and along the northern margin of the Exmouth Plateau. The tectonic component of subsidence was probably related to crustal thinning due to extension caused by rifting, rather than to simple cooling of the aging crust. Sediment loading was only important where thick Late Jurassic to Early Cretaceous sedimentary wedges formed.

#### *Breakup of Gondwanaland and immature ocean stage (Late Jurassic and Early Cretaceous)*

The breakup of this part of Gondwanaland took place in two phases: an initial Callovian phase, when the northern margin of the Exmouth Plateau, and the northwestern margin of the Canning Basin, formed (Fig. 16D); and a Neocomian phase, in which drifting started along the northwestern and southwestern margins of the Exmouth Plateau, and the Wallaby Plateau





WA/B8-294A

**Figure 15. Stratigraphic distribution of pre-Quaternary lithotypes dredged and cored on the Exmouth Plateau, Sonne Ridge and Wallaby Plateau.**

Correlated with seismic reflectors and the stratigraphy and facies of the adjacent offshore Carnarvon and Canning Basins (BOC Bedout No. 1 well).

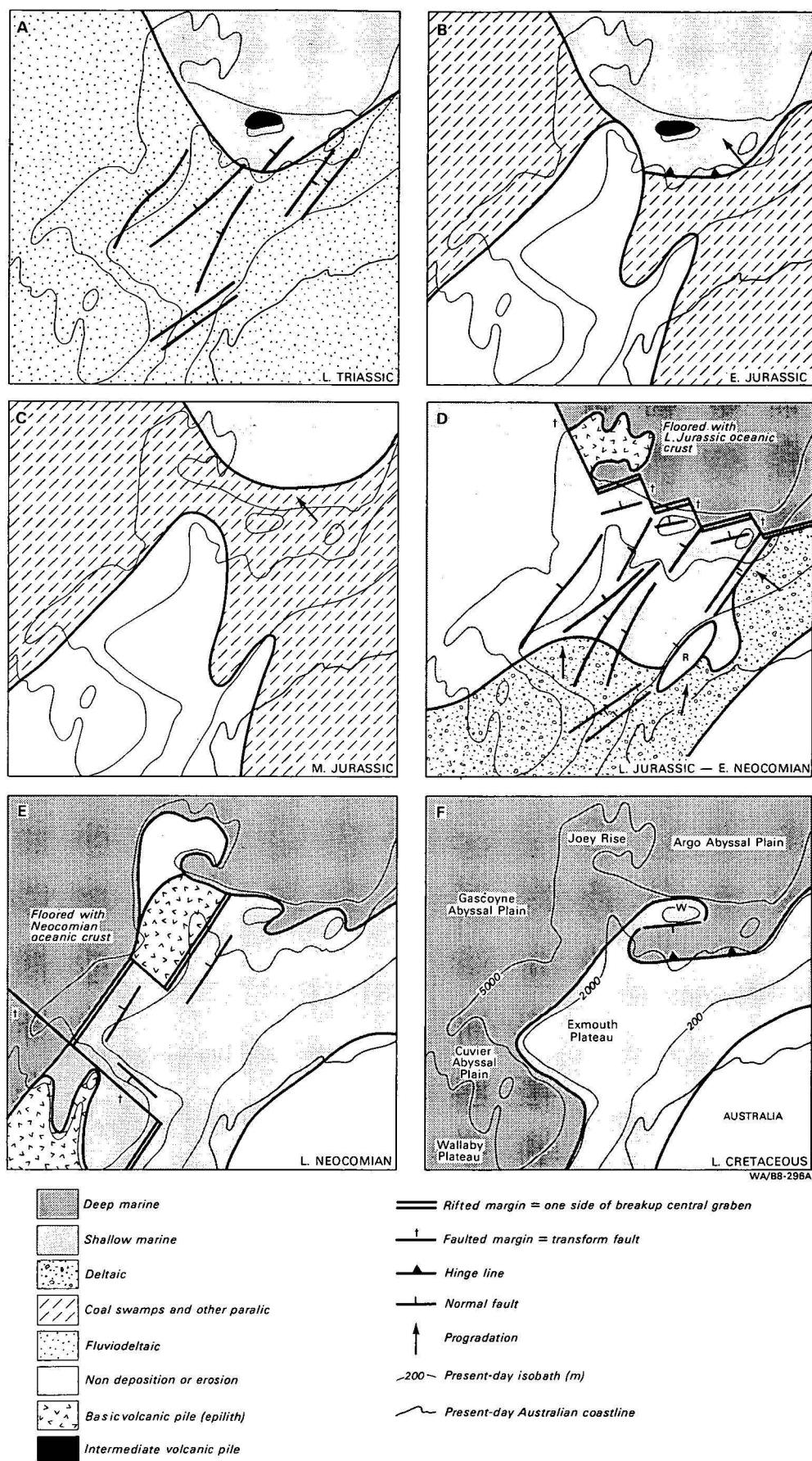


**Figure 16.** Palaeogeographic sketches of the Exmouth Plateau and its vicinity, related to present-day bathymetry. Based on seismic evidence, well control, and *Sonne* samples. R = Rankin Platform, W = Wombat Plateau.

formed as an epilith (Fig. 16E). There were extensive movements on the northeast-trending normal faults of the Exmouth Plateau, especially in the Callovian.

The Callovian breakup, and the preceding rifting phases, led to major changes in the region, with the separation of the previously essentially continuous depositional basin of the Westralian Trough into a number of structural elements. The northeast-trending Rankin Platform became a major high, with complementary depressions forming on either side of it: the Barrow and Dampier Sub-basins to the east, and a depression to the west extending from the Swan Graben in the north to the Kangaroo Trough in the south (Figs. 1, 16D). The depressions are probably rift-valleys. Magnetic lineations on the Argo Abyssal Plain, which trend almost east-west north of the Exmouth Plateau (Heirtzler & others, 1978) range in age from 148 to 153 m.y. (Fig. 1), and suggest that that margin formed by a combination of rifting and transform faulting in the Callovian. This dating is also supported by the existence of Oxfordian sediments immediately above oceanic basement at DSDP Site 261 (Veevers, Heirtzler & others, 1974). Any hypothetical landmass (or part of Tethys), which lay north of the Exmouth Plateau before breakup, has long since disappeared, probably by subduction in the northern Indian Ocean, together with the Jurassic spreading centre and the oceanic crust created north of it. Magnetic lineations, seismic character, and hyaloclastite samples recovered from the Joey Rise northwest of the Exmouth Plateau (Cook & others, 1978; Heirtzler & others, 1978) suggest that the Rise is a Late Jurassic volcanic epilith. This epilith might be explained by massive basaltic extrusions in a weakened lithosphere, at the boundary of two low-angle divergent spreading systems.

During the Late Jurassic and Early Cretaceous up to 5000 m of restricted marine sediments, especially claystones, were laid down in the Barrow-Dampier rift-valley (Powell, 1976). In the Canning Basin Upper Jurassic sediments are generally absent, but a thick Lower Cretaceous claystone sequence (nearly 1000 m in East Mermaid No. 1) was laid down on the continental shelf. During Late Jurassic to Neocomian times, a 2000-m thick delta built northward onto the Exmouth Plateau (Fig. 16D), and into the Barrow Sub-basin (Barrow Formation); relatively thin pro-delta muds accumulated north of the delta front. On the northern Exmouth Plateau variable thicknesses of Upper Jurassic and Lower Cretaceous rocks have been preserved.

During the Late Jurassic, sedimentation kept pace with subsidence; however, subsidence started to exceed sedimentation in the Early Cretaceous. The marked angular unconformity on the northern horsts (Figs. 9, 10, 11) apparently formed by erosion in a coastal plain or shelf environment, after the deposition of the Neocomian sequence, but before the margin started to subside rapidly. Sedimentation rates reached a maximum of 70 m per million years in the Barrow-Dampier Sub-basin, but averaged only 20 m per million years on the Exmouth Plateau.

Magnetic anomalies in the Cuvier and Gascoyne Abyssal Plains (Fig. 1) range in age from 108 to 123 m.y., and suggest that the southwestern and north-western margins of the Exmouth Plateau formed at the same time (Fig. 16E), in the late Neocomian (120-125 m.y.: Larson & others, 1979). The southwestern margin formed as a transform fault (Cape Range Fracture Zone), whereas the northwestern margin is a rifted margin. The separation of Greater India from

these two margins drastically reduced the clastic supply to the plateau, and thereafter deltaic sedimentation ceased and subsidence rates exceeded sedimentation.

As Greater India moved away from the Exmouth Plateau and Carnarvon Terrace areas in the late Neocomian and Aptian, new oceanic crust formed the sea-floor below the Cuvier and Perth Abyssal Plains.

A major transgression started in the Carnarvon and Canning Basins, and on the Exmouth Plateau, in the late Neocomian or Aptian (Fig. 16E). It documents a global sea-level rise and/or subsidence of the rifted margin after breakup. Shallow-marine detrital deposition continued from then through into the Cenomanian, and seismic evidence suggests that similar muds were laid down on the Wallaby Plateau too. Clues to the nature of deposition in the Late Jurassic and Early Cretaceous juvenile ocean come from fine-grained sediments recovered from 3 *Sonne* stations. Shallow-marine micaceous shale and siltstone, containing spores and marine dinoflagellates of latest Jurassic or earliest Cretaceous age, were deposited on the southern Exmouth Plateau. Silty quartzose claystones were laid down in a shallow-marine environment in the Swan Canyon area of the Exmouth Plateau. They may well be equivalents of the Gearle Siltstone (Winning Group) of the Carnarvon Basin.

#### *Volcanic origin of Wallaby Plateau (late Early Cretaceous)*

Before the *Sonne* cruise the Wallaby Plateau was regarded as a continental fragment by some authors (e.g., Symonds & Cameron, 1977), but as an epilith, an abnormally thick buildup of spreading ocean floor, by others (Veevers & Cotterill, 1978). The seismic interpretation of Symonds & Cameron (1977) suggested that about 300 m of pelagic carbonates and 200 m of mid Cretaceous shale unconformably overlies 3000 m or more of gently dipping layered strata. Symonds & Cameron (1977) suggested that the sequence beneath the main unconformity (D) consists of pre-drift sedimentary strata, whereas Veevers & Cotterill (1978) postulated that the stratified sequence beneath the main unconformity consists of layered volcanic and volcanogenic rocks.

The dipping sequence can be traced on seismic profiles from the center of the plateau to near the southern and eastern margins. Most probably the rocks recovered from Area J (Fig. 12) come from this sequence. In Area K (Fig. 13) it is difficult to trace the dipping sequence right to the plateau slope, because of marginal normal faulting. It is, however, likely that the rocks recovered from the area do represent the layered sequence. Although the seismic records allow a possible alternative interpretation — that we sampled a marginal intrusion, or extrusive sequence — the thickness (more than 1000 m) and nature of the rocks recovered does not support such an interpretation.

At Area I, on the southern margin of the Argo Abyssal Plain, altered differentiated alkali basalt (?hawaiite) and volcanoclastic breccia were recovered from Station 155, from what the seismic records indicate is oceanic crust like that of the Cuvier Abyssal Plain. At Area J, on the eastern margin of the Wallaby Plateau, only volcanoclastic sandstone and pebbly sandstone were recovered from 4 stations. At Area K, on the southern margin of the plateau, volcanic breccia, tuff, volcanoclastic claystone, and tholeiitic basalt, were dredged at three stations. We recovered no fossiliferous sediments from below the main unconformity.



We also sampled the Sonne Ridge, which projects into the Cuvier Abyssal Plain from the eastern margin of the Wallaby Plateau (Area H, Fig. 1). At two stations the sequence beneath the unconformity D consists of basalt, volcanoclastic sandstone and volcanic breccia, and vitric tuff.

Since Sonne Ridge appears to be a morphological and structural extension of the Wallaby Plateau epilith (Larson & others, 1979; Johnson & others, in press), we assume that the age of the plateau is similar to that of Cuvier Abyssal Plain (118-125 m.y.). The only datable, but weathered, tholeiitic basalt came from the southern margin of the Wallaby Plateau (Station 170) and gave a minimum K/Ar age of early Late Cretaceous (ca. 90 m.y.). This fits moderately well with the postulated age of the spreading, derived from magnetic anomalies, and we tentatively assume that all the dredged volcanic and volcanoclastic rocks from the Wallaby Plateau and Sonne Ridge are of late Neocomian to younger Early Cretaceous age.

The volcanoclastic sandstones and pebbly sandstones of the Wallaby Plateau were probably reworked from a large subaerial volcanic plateau, and deposited along the margins as volcanoclastic debris flows or turbidites, similar to the 5-20 m thick Miocene volcanoclastic debris flows derived from Fuerteventura and encountered south of Gran Canaria in DSDP Site 397 (Schmincke & von Rad, 1979). There the debris flows mark the relatively short period of extremely voluminous production of volcanics during the submarine and subaerial shield phase of the volcanic island. On the Wallaby Plateau the amygdaloidal basalt fragments attest to original shallow-water or subaerial extrusion. The volcanoclastic sediments were probably mainly eroded by wave action, and would have been deposited either as sediment wedges building the volcanic island shelf outward, or as deep marine deposits on the proto-abyssal plains.

In summary, the evidence suggests that the dipping layered material below the D unconformity on much of the plateau is of volcanic origin, supporting the idea that it is an epilith (Fig. 16). Hence, we envisage that the Wallaby Plateau had a similar origin to Iceland, with cessation of volcanism and subsidence below sea level after the oceanic ridge jumped to its new position further west. Whether continental crust lies below the layered volcanic material could be tested only by deep drilling in the centre of the plateau. The north-western part of the Exmouth Plateau is probably another such Early Cretaceous volcanic buildup (Fig. 16E), although it might be of comparable age to the Late Jurassic Joey Rise.

#### *Mature ocean stage (Late Cretaceous and Cainozoic)*

From Santonian times onward carbonate sedimentation predominated, in a mature ocean with thermohaline circulation of oceanic waters (Veevers & Johnstone, 1974). The Exmouth and Wallaby Plateaus sank 2000-3000 m, as did the adjacent abyssal plains, with most of the sinking in the latest Cretaceous and early Tertiary. Current action, probably related to global climatic changes and low stands of sea level, hampered the buildup of pelagic carbonates on both plateaus (Exmouth Plateau about 800 m, Wallaby Plateau 300 m) and gave rise to marked unconformities in the Paleocene and Oligocene.

The onset of the mature ocean phase on the Exmouth Plateau is documented by pelagic sediments recovered from its northern and western margins: an

Aptian radiolarian nanno chalk from the Swan Canyon area, perhaps an equivalent of the Windalia Radiolarite of the Carnarvon Basin, and a late Albian foraminiferal nanno chalk from Area E. Another possible pelagic sediment is the recrystallised ferruginous quartz chert from the western extension of the Carnarvon Terrace (Area L), containing circular bodies which are reminiscent of radiolarian ghosts.

Deposition of eupelagic foraminiferal or nannoplankton oozes, laid down in bathyal water depths (E facies), characterised Cainozoic sedimentation on the Exmouth and Wallaby Plateaus. However, a late Miocene-early Pliocene hemipelagic chalk may have been laid down on the outer shelf, because it contains about 5 percent of well-sorted sand-sized quartz. Perhaps, during the late Miocene period of low sea level, terrestrial sand was carried northward from the inner shelf into the Swan Canyon. Alternatively, the sand may have been derived from Middle Jurassic sandstones (A3 facies) exposed in the canyon walls.

During the Late Cretaceous and Cainozoic the Exmouth Plateau sank 2000-3000 m, and sedimentation did not keep pace; the amount of sediment laid down averages 800 m, representing a sedimentation rate of less than 10 m per million years (only a third of rates on the Northwest Shelf). The Wallaby Plateau sank about 3000 m in this period, and is covered by an average of 300 m of Late Cretaceous and Cainozoic sediment; this represents a pelagic sedimentation rate of less than 5 m per million years.

The northern margin of the plateau appears to have been affected by Late Cretaceous normal faulting which, for example, gave the half-graben south of the Wombat Plateau (Fig. 10, the Montebello Canyon) its final form. Gentle warping of the Exmouth Plateau may have been synchronous with the late Miocene folding of the Cape Range and Rough Range anticlines of the Exmouth Gulf area.

## References

- COOK, P. J., VEEVERS, J. J., HEIRTZLER, J. R., & CAMERON, P. J., 1978—The sediments of the Argo Abyssal Plain and adjacent areas, northeast Indian Ocean. *BMR Journal of Australian Geology & Geophysics*, **3**, 113-124.
- EVANS, P. R., 1966—Mesozoic stratigraphic palynology in Australia. *Australian Oil and Gas Journal*, **12**, 58-63.
- EXON, N. F., & WILLCOX, J. B., 1978—Geology and petroleum potential of Exmouth Plateau area off Western Australia. *American Association of Petroleum Geologists Bulletin*, **62**, 40-72.
- EXON, N. F., & WILLCOX, J. B., in press—The Exmouth Plateau: stratigraphy, structure and petroleum potential. *Bureau of Mineral Resources, Australia, Bulletin* **199**.
- FABER, E., & STAHL, W., in prep.—Origin of gases adsorbed in near-surface sediments, identified by carbon isotopes. *American Association of Petroleum Geologists Bulletin*.
- FALVEY, D. A., & VEEVERS, J. J., 1974—Physiography of the Exmouth and Scott Plateaus, Western Australia, and adjacent northeast Wharton Basin. *Marine Geology*, **17**, 21-59.
- FILATOFF, J., 1975—Jurassic palynology of the Perth Basin, Western Australia. *Palaeontographica*, B, **154**, 1-113.
- FRANKS, L. A., EXON, N. F., & GRANATH, J. W., 1977—Preliminary studies on the Cape Leeuwin manganese nodule deposit off Western Australia. *BMR Journal of Australian Geology & Geophysics*, **2**, 66-9.
- HAIG, D., 1979—Early Jurassic foraminifera from the western highlands of Papua New Guinea. *Neues Jahrbuch für Geologie und Paläontologie* 1979, 208-15.

- HEIRTZLER, J. R., CAMERON, P. J., COOK, P. J., POWELL, T., ROESER, H. A., SUKARDI, S., & VEEVERS, J. J., 1978—The Argo Abyssal Plain. *Earth and Planetary Science Letters*, **41**, 21-31.
- HINZ, K., BEIERSDORF, H., EXON, N. F., ROESER, H. A., STAGG, H. M. J., & VON STACKELBERG, U., 1978—Geoscientific investigations from the Scott Plateau off northwest Australia to the Java Trench. *BMR Journal of Australian Geology & Geophysics*, **3**, 319-40.
- JOHNSON, B. D., POWELL, C. M., & VEEVERS, J. J., in press—Early spreading history of the Indian Ocean between India and Australia. *Earth and Planetary Science Letters*.
- LARSON, R. L., MUTTER, J. C., DIEBOLD, J. B., CARPENTER, G. B., & SYMONDS, P., 1979—Cuvier Basin: a product of ocean crust formation by Early Cretaceous rifting off Western Australia. *Earth and Planetary Science Letters*, **45**, 105-14.
- MARKL, R. G., 1974—Evidence for the breakup of eastern Gondwanaland by the Early Cretaceous. *Nature*, **251**, 196-200.
- NOAKES, L. C., & JONES, H. A., 1976—Mineral resources offshore; in Knight, C. L., (Editor), *ECONOMIC GEOLOGY OF AUSTRALIA AND PAPUA NEW GUINEA: 1. METALS. Australasian Institute of Mining and Metallurgy, Melbourne*, 1093-104.
- NØRVANG, A., 1957—The foraminifera of the Lias series in Jutland, Denmark. *Meddelelser Dansk Geologisk Forening*, **13**(5), 1-135.
- POWELL, D. E., 1976—The geological evolution of the continental margin off northwest Australia. *APEA Journal*, **16**, 13-23.
- QUILTY, P. G., 1980—Tertiary Foraminifera and stratigraphy, northern Exmouth Plateau, Western Australia. *BMR Journal of Australian Geology & Geophysics*, **5**, 141-9.
- RIECH, V., & VON RAD, U., 1979—Silica diagenesis in the Atlantic Ocean: diagenetic potential and transformations. In Talwini, M., & others (Editors), *Deep Drilling Results in the Atlantic Ocean: Continental Margins and Paleoenvironment*, M. Ewing Series 3, *American Geophysical Union*, 315-40.
- SCHMINCKE, H. -U., & VON RAD, U., 1979—Neogene evolution of Canary Island volcanism inferred from ash layers and volcanoclastic sandstones of DSDP Site 397. *Initial Reports of the Deep Sea Drilling Project*, Volume **47**(1), U.S. Government Printing Office, Washington, 703-25.
- STAGG, H. M. J., 1978—The geology and evolution of the Scott Plateau. *APEA Journal*, **18**(1), 34-43.
- SYMONDS, P. A., & CAMERON, P. J., 1977—The structure and stratigraphy of the Carnarvon Terrace and Wallaby Plateau. *APEA Journal*, **17**(1), 30-41.
- TEICHERT, C., 1939—The Mesozoic transgressions in Western Australia. *Australian Journal of Science*, **2**, 84-86.
- VAN DER LINGEN, G. J., 1973—The Lord Howe Rise rhyolites. *Initial Reports of the Deep Sea Drilling Project*, Volume **21**. U.S. Government Printing Office, Washington, 523-39.
- VEEVERS, J. J., & COTTERILL, D., 1978—Western margin of Australia: evolution of a rifted arch system. *Geological Society of America Bulletin*, **89**, 337-55.
- VEEVERS, J. J., HEIRTZLER, J. R., & others, 1974—*Initial Reports of the Deep Sea Drilling Projects*, Volume **27**, U.S. Government Printing Office, Washington.
- VEEVERS, J. J., & JOHNSTONE, M. H., 1974—Comparative stratigraphy and structure of the Western Australian margin and the adjacent deep ocean floor. *Initial Reports of the Deep Sea Drilling Project*, Volume **27**, U.S. Government Printing Office, Washington, 571-85.
- VEEVERS, J. J., & POWELL, C. M., 1979—Sedimentary wedge progradation from a transform-faulted continental rim: southern Exmouth Plateau, Western Australia. *American Association of Petroleum Geologists Bulletin*, **63**, 2088-96.
- VON STACKELBERG, U., 1978—A polygenetic manganese nodule from the Scott Plateau off northwest Australia. *BMR Journal of Australian Geology & Geophysics*, **3**, 349-51.
- WRIGHT, A. J., & WHEATLEY, T. J., 1979—Trapping mechanisms and the hydrocarbon potential of the Exmouth Plateau, Western Australia. *APEA Journal*, **19**(1), 19-29.
- ZOBEL, B., 1960—Die Foraminiferen des Lias  $\gamma$  in Nordwestdeutschland. *Unpublished Ph.D. thesis, University of Tübingen*.

## Appendix — Petrology and organic geochemistry of Middle Jurassic coal and coaly mudstone

J. Koch & H. Wehner

The investigated sample of *Jurassic coal* (SO8-34 KD/4), consists of two clearly different layers: a 3-cm layer of bright coal, and a 2.5-cm layer of dull laminated coal. Some fractures and fissures have thin iron oxide infillings.

Microscopic examination shows that the bright coal consists of three vitrinitised wood fragments (probably *Gymnosperm* wood), separated by two fine-grained detrital clarite layers less than 100  $\mu\text{m}$  thick. The dull coal is predominantly laminated trimaceritic groundmass, which apart from vitrinite contains much liptinite (spores, algae, liptodetrinite and even fluorinite), and much inertinite, particularly in detrital form and as macrinite. Part of the vitrinite fluoresces weakly brown under ultraviolet light, the spores fluoresce dark yellow, and the algae fluoresce more-or-less light yellow. Vitrinite layers, up to 2 mm thick, are intercalated with the groundmass. Furthermore, fusinite and semifusinite lenses and thin layers are present. Weathering cracks on the margins of some of the semifusinite and macrinite fragments suggest reworking.

Noteworthy are relatively frequent inclusions of liptinite (fluorinite), which fluoresce intensely green and whose size varies from 1  $\mu\text{m}$  to over 200  $\mu\text{m}$  (in vitrinite). The groundmass contains some clay. The rare pyrite is very fine grained. Nevertheless the sulphur content of the total coal is fairly high at 2.06 percent (dry basis; Table 4).

The reflectance (oil immersion; 546 nm) of the bright coal vitrinite is 0.36 percent, and of the laminated coal vitrinite is 0.39 percent. Hence the coalification has reached the boundary between lignite and subbituminous coal. The volatile and carbon contents, as well as the calorific value, suggest lignite (Table 4). The relatively high extractibility with dichloromethane of 1.49 percent (Table 4) reflects the abundance of liptinite.

By analogy with recent peat facies, this Jurassic coal may have been a peaty mud with rhizomes of herbaceous plants, through which grew woody roots (thick vitrinite layers).

From the dark *coaly mudstone* (SO8-36KD/5), weakly gelified xylite fragments with visible woody structure were separated and investigated. They also probably represent *gymnosperm* wood. The high ash and sulphur contents (Table 4) are related to the abundance of disseminated pyrite. Pyrite is, in part, concentrated parallel to the growth rings, and has wea-

thered to iron oxides along fissures. Because of this the vitrinite reflectance of only 0.27 percent is irrelevant to maturity.

More representative of maturity are the reflectivities of 0.34 percent  $R_o$  from the few vitrinite inclusions in the silty mudstones. The main organic components are inertinite fragments, which are sometimes weathered. The liptinite macerals are dominantly spores and detritus with brownish yellow fluorescence; there are also some thick-walled cuticles and small algae. The organolithic facies thus fits the coal type, as is confirmed by the geochemical analyses. The pyrite is predominantly altered to iron oxide, as shown by the colour of the sediment.

	Coal (SO8-34 KD/4)	Xylite (SO8-36 KD/5)	Enclosing Sediments
Water (%)	9,8	10,4	
Ash, air dried (%)	9,7	18,3	
Ash, dry (%)	10,7	20,4	
Volatile matter, air dried (%)	48,9	42,7	
Volatile matter, dry (%)	54,2	47,7	
Volatile matter, dry & ash-free (%)	54,8	53,7	
Sulphur, air dried (%)	1,86	4,33	
Sulphur, dry (%)	2,06	4,84	
Gross calorific value:			
air dried (kJ/kg)	22940	18550	
dry (kJ/kg)	25440	20700	
Net calorific value, air dried (kJ/kg)	21590	17430	
C (%)	59,9	49,4	2,9
H (%)	5,1	4,0	
N (%)	1,2	1,0	
O (%)	23,2	20,7	
S + ash (%)	10,5	24,9	
Extract (%)	1,49	0,15	
Saturated hydrocarbons (ppm)	871		
Aromatic hydrocarbons (ppm)	3084		
Resins (ppm)	3486		
Asphaltene (ppm)	3607		
H/C	1,02	0,97	
O/C	0,29	0,31	
Amount of pyrolyzable organic matter (mg C/gC)		2	14

Table 4. Petrology and organic geochemistry of Middle Jurassic coal/coaly mudstone.

# Tertiary Foraminiferida and stratigraphy, northern Exmouth Plateau, Western Australia

P. G. Quilty<sup>1</sup>

The foraminiferid faunas of 14 samples of Tertiary nanno foram chalks of Late Paleocene to Early Pliocene age are documented. They are the first described from the Exmouth Plateau. The *Globorotalia fohsi* lineage is documented for the first time from northwestern Australia. '*Bulava*' *indica* Boltovskoy, originally described from the Indian Ocean, is part of a planktic species belonging to *Protentella* or *Hastigerinella*. Coiling ratio changes from several species of *Globorotalia* suggest cooling in the Middle Miocene.

## Introduction

Several samples recovered by the R.V. *Sonne* in January 1979 (von Stackelberg & others, 1980) have yielded useful faunas of Cainozoic planktic foraminiferids, the first described from the Exmouth Plateau.

The location of the new samples is shown on Figure 1 and the locality details and ages are given in Table 1. The fourteen samples studied are of two types. Those labelled KD are dredge samples; KL are from piston cores. Many other cores and dredges yielded Quaternary, Cretaceous and Jurassic foraminiferids and these will be reported separately.

One sample, 76KL, yielded a minute sample, too small for confident foraminiferid studies and is not described here. Shafik (per. comm.) recovered Middle Miocene calcareous nannoplankton, but the few foraminiferids seen (probably contaminants) were Quaternary.

Ages are expressed using the abbreviated nomenclature of Blow (1969) and Berggren (1972).

Specimens illustrated are housed in the Commonwealth Palaeontological Collection (CPC) at the Bureau of Mineral Resources, Canberra.

## Sample results

Table 2 is a summary of the results of studies of foraminiferids from Tertiary sediments collected by R.V. *Sonne*. The ages allocated are from species listed on

Tables 4 and 5. In most instances, the age is based on the occurrence of zone species, but for 46KD this is not true. That sample contains few diagnostic forms and the age is derived from the overlapping ranges of less diagnostic forms.

Two sections, 64KL and 78KL, deserve more detailed discussion because of the mixing of faunas or the effects of dissolution of calcite.

## 64KL

This core is 408 cm long, plus 10-20 cm for the core catcher. The core is calcareous, and contains evidence of several different Cainozoic ages. The normal pale pink oxidised surface zone gives way to very pale green deeper reduced material at 320 cm. Samples from 300 cm to the surface contain Quaternary faunas characterised by *Globorotalia truncatulinoides*. The other samples studied are all of mixed faunas and will be discussed separately. Faunas recognised indicate ages of Pliocene (N18), Middle Miocene (N12-13), Early Miocene (N8-9), Oligocene (N2-3), Middle Eocene (P13-14) and an older age, either Late Paleocene or Early Eocene (approximately P5-6). The results are summarised on Figure 2.

346-349 cm. The fauna has elements of at least four ages: Quaternary elements (*G. truncatulinoides*, and probably *Sphaeroidinella dehiscens dehiscens*, *Globorotalia unguolata* and *G. dutertrei*) are rare and probably represent contamination from the core margin, of

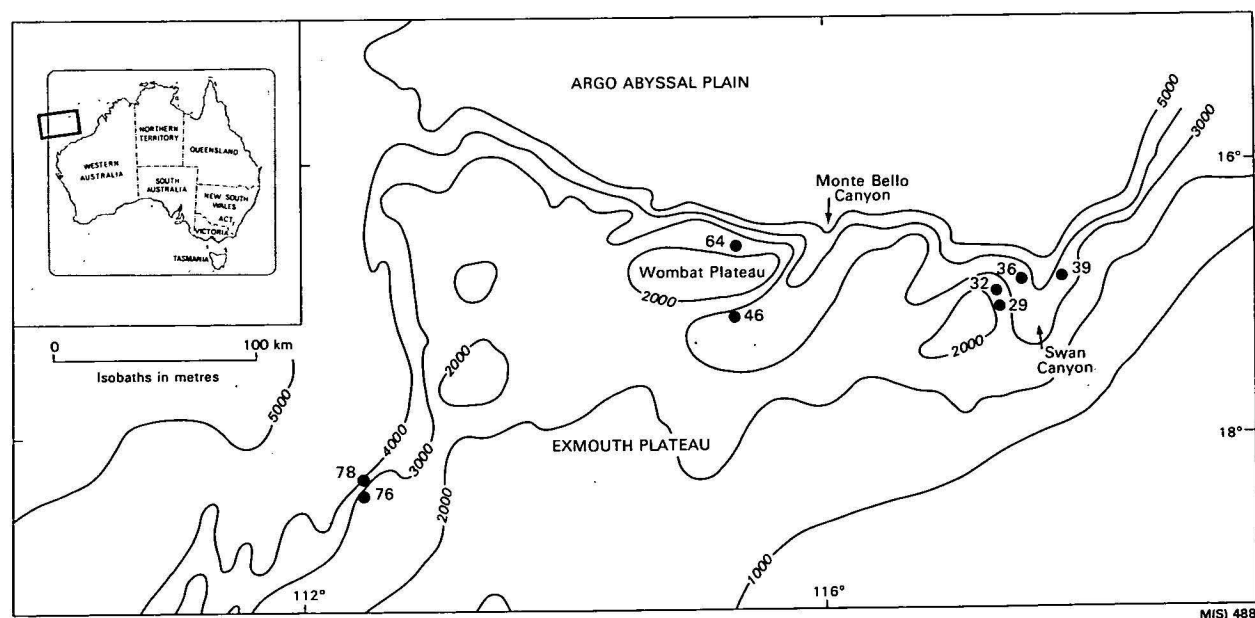


Figure 1. Locality map.

Sample No.	Type	Depth(m)	Latitude	Longitude	Age
29	KD	2530-2315	16°59.5'S*	117°21.8'E*	E. Pliocene
32	KD	3050-2420	16°55.2'S	117°20.8'E*	M. Miocene
36	KD	4250-3780	16°50.2'S	117°32.6'E*	E. Pliocene
39	KD	3950-3600	16°50.3'S*	117°50.7'E*	M. Miocene
46	KD	3140-2710	17°6.7'S*	115°19'E	L. Pliocene?
64	KL	2600	16°36.2'S	115°14.0'E	L. Paleocene-Quaternary
76	KL	3100	18°26.0'S	112°25.8'E	M. Miocene
78	KL	3855	18°19.5'S	112°26.0'E	E. Miocene

\*Mean position on dredged profile

Table 1. Locality details and sample ages.

Sample Number & Type	Lithology	Preservation of foraminiferids	Dissolution	Mixing	Age
29KD	White foram-nanno chalk	Good	None	None	Pliocene N19
32KD	White foram-nanno chalk	Good	None	None	M. Miocene N12/13
36KD a-e	White foram-nanno chalk with up to 15% quartz sand	Some fragmentation	Minor	None	Pliocene N19
39KD	Yellowish foram-nanno ooze	Good	None	None	M. Miocene N12
46KD	White foram-nanno ooze	Good	None	None	Miocene/Pliocene N17/18
64KL 0-320 cm	Pink foram-nanno ooze	Good	None	None	Quaternary N22/23
346-349 cm	Pale green foram-nanno ooze	Good	None	Extreme	Pliocene, N18* and older
361-420 cm	Pale green foram-nanno ooze	Good	None	Extreme	Late Oligocene, N2 and older*
78KL surface	Pink foram sand	Good	Minor	None	Quaternary N23
300 cm-base of core	Stiff brown ooze and clay	Very poor	Very marked	None?	E. Miocene N5/6

\*for explanation, see text

Table 2. Summary of results.

young material squeezed along the core edge during entry of the sediment into the core barrel. Remaining faunas can be related to at least three ages.

*Globigerinoides sicanus* (N8-9) is the only species that shows the presence of an Early Miocene fauna. Many other forms (*G. quadrilobatus* s.l., *Globoquadrina* spp., *Globigerinita* spp.) could also be expected in younger faunas.

*Globorotalia fohsi lobata* and *Globigerina druryi* are Middle Miocene (N12/13) elements and make up about 15% of the fauna. Preservation is excellent. Most other species in the fauna could be expected in faunas of N12/13 age.

The N18 age is not dependent on such diagnostic short-ranged species as the Early and Middle Miocene ages are, but is based on overlapping ranges of many species, including *Globigerina nepenthes*, *Globoquadrina altispira globosa*, *G. dehiscens dehiscens*, *Globorotalia tumida flexuosa*, *Sphaeroidinellopsis seminulina seminulina*, *Pulleniatina obliquiloculata praecursor* and *Globorotaloides variabilis*. In consequence, the N18 date may not represent deposition during N18 alone, but may be based on mixing of faunas of several Late Miocene and younger zones.

361-365 cm. The sample contains a mixed fauna, but there seem to be three ages represented, all older than in the sample above. The youngest (Oligocene, undifferentiated N2/3) is based on the presence of many Oligocene forms (*Globigerina sellii*, *G. tripartita*, *G. venezuelana*) and the characteristic form *G. angulissuturalis*. Many other forms such as *Chiloguembelina cubensis*, *Globigerina officinalis*, *G. angustium-bilicata*, *Globorotaloides suteri* could be expected in rocks of this age and one or both of the older ages. A feature of this sample is that the residue was very small showing that coccoliths are the dominant sediment particles.

Middle Eocene elements include *Hantkenina alabamensis*, *Globorotalia bullbrooki*, *Globigerinatheka mexicana*, *Globigerina eocaena-corpulenta*, *G. senni* and *Catapsydrax echinatus* of zones P13 and P14.

The oldest fauna consists of *Chiloguembelina midwayensis midwayensis*, *Truncorotaloides pseudotipilensis* and *Globorotalia rex*, the latter common and the former rare. No other elements of this older fauna are present. It is not clear exactly which zones are represented, but in the absence of diagnostic and, in Western Australia common, elements of P4, an age of P5 is



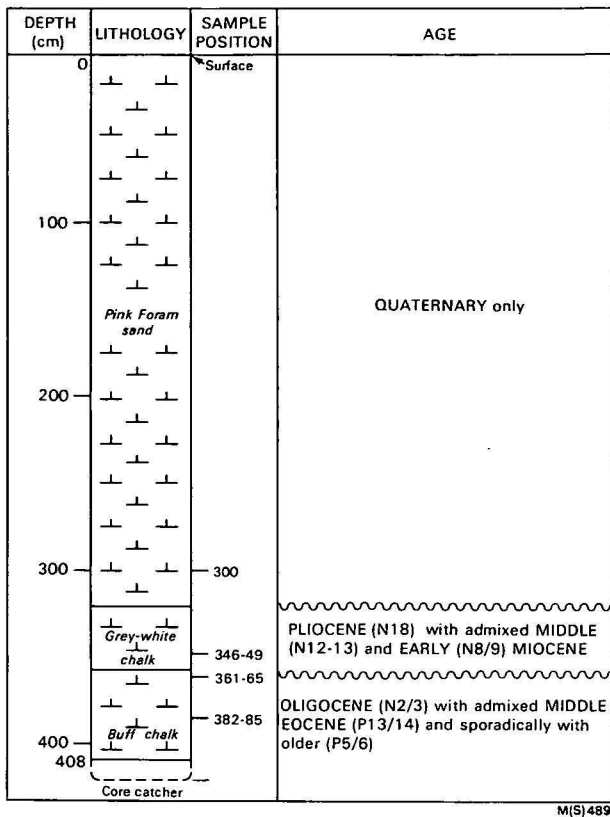


Figure 2. Summary, 64KL.

likely. The unusual feature of this element is the lack of normally expected accompanying species.

**382-385 cm.** This sample contains a less diverse fauna than that of 361-365 cm, and lacks the oldest element. Otherwise both N2/3 and P13/14 are recognisable. *Globigerina gortanii* and *Globorotalia opima nana* are elements not seen above and both are consistent with Oligocene (particularly N2) age.

**408 cm - base of core.** As with the sample at 361-365 cm, three ages are discernible and the late Oligocene species are dominant. Species not seen above include *Cassigerinella chipolensis*, *Pseudogloboquadrina primitiva* and *Globigerinatheka kugleri*.

**Core catcher, 10-20 cm below last sample.** Three ages (N2/3, P13/14 and P5/6) are again represented. *Globorotalia cerroazulensis cocoaensis* was not seen above.

Thus three lithologically similar but discrete units are present — Quaternary, Pliocene (with other Neogene

faunas), and Late Oligocene (with older admixed Palaeogene faunas).

The units are thin, and there is no mixing of material from unit to unit. Mixing probably does not reflect *in situ* bioturbation, but rather suggests that the Palaeogene and Miocene/Pliocene units slumped to their present position independently, being mixed on the way. The accumulation of Quaternary sediments was not subject to the same slumping.

There appears to be no significant size sorting during slumping, suggesting that in each unit, all material made its way to the depocentre. The poor sorting also denies the possibility that the sediments were eroded elsewhere by submarine currents and carried to their present position.

The slumping hypothesis requires that the Palaeogene and Miocene/Pliocene units were emplaced by the same process but at different times; the sources would be areas in which sediments of only the ages represented had accumulated.

It is also noteworthy that the ages represented correspond quite closely with periods that Quilty (1977, 1980) has regarded as periods of high sea level; thus his related Cycles 1, 2A, 3A, 3B and 4 of sedimentation all are represented (Fig. 6). Cycle 2B (Late

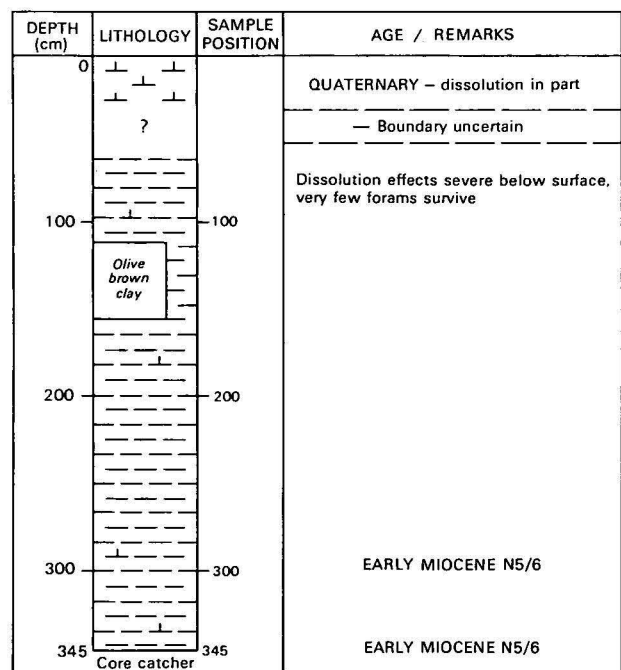


Figure 3. Summary, 78KL.

<i>Species</i>	<i>Age</i>		<i>No. of specimens</i>	<i>%S</i>	<i>%D</i>	<i>Sample</i>	<i>Temperature</i>
praemiocenica	Late Miocene	N17/18	25	96	4	46KD	Cool
mayeri	Mid. Miocene	N12/13	16	82	18	32KD	Cool
fohsi lobata	Mid. Miocene	N12/13	43	32	68	64KL	Warm
						346 cm	
scitula	Mid. Miocene	N12/13	13	31	69	64KL	Warm
						346 cm	
bullbrooki	Mid. Eocene	P13/14	27	29	71	64KL	Warm
						361 cm	
lensiformis	E. Eocene	P5/6	31	32	68	64KL	Warm
						361 cm	

Table 3. *Globorotalia* coiling ratio data.

SONNE CRUISE 8A															
CORE No.	29KD	36KD	46KD	32 KD		39KD	78 KL		64 KL						
				1	8		300	345	300	346	361	382	408	CC	
SPECIES	AGE	N 19	N 19	N 17/18	N 12	N 12/13	N 12	N 5/6	N 5/6	N 22/23	NEO	PALAEOGENE			
Globigerina bulloides		r													
G. dutertrei		r								c	f				
G. nepenthes - decoraperta		a													
G. subcretacea		f													
Globigerinoides conglobatus		r								f					
Goides quadrilobatus immaturus		c	c	a		c	c			f	c				
Goides q quadrilobatus		f			p		c			f					
Goides q trilobus		r	r	c		c	f			f	c				
Goides ruber		f		f			f			f	f				
Globigerinita glutinata		c				f			f	r	f				
Gita. incrusta		f		f		f	f	c		f	f				
Gita. uvula		r					r				f				
Globoquadrina dehiscens s.l.		c			p	f	c				r				
Gq. altispira globosa		r	r	f							r				
Globorotalia anfracta		r													
Glt. cultrata		f	r						* f	c					
Glt. humerosa		r	r												
Glt. inflata		r							* f	f	f				
Glt. tosaensis		r													
Glt. tumida tumida		r	r					* r	* f	c	r				
Glt. sp.		r													
Sphaeroidinella dehiscens s.s.		r								r	r				
Sphaeroidinellopsis seminulina		f	a	f		f					f				
S'opsis. sem. kochi		f	r	r											
Orbulina universa		f	c	c	p	c	f			r	f				
Borbulina bilobata		r								r					
Pulleniatina praecursor		r									r				
Pull. obliquiloculata s.s.		r							* f	f					
Candeina nitida praenitida		r													
Globigerina nepenthes			f	r		r					f				
G. vuezuelana			f	c	c				f		r	f	r	r	f
G. sp. indet			r				r	f	f				r	r	c
Globigerinoides mitra			r												
Goides quadrilobatus sacculifer			c	f		c	r			f	r				
Globoquadrina altispira altispira			c	c	a	c	c				f				
Globorotalia menardii			c	f		r									
Glt. obesa			r	r		? f	f				f				
Globorotaloides cf. suteri			f												
Gltoides. hexagona variabilis			r	r							r				
Globigerina druryi				f		f	f				f				
Globigerinoides extremus				c						f	c				
Globorotalia cf. unguolata				r											
Glt. praemiocena				c											
Candeina nitida nitida				f							r				
Hastigerina siphonifera				f							r				
Protentella ("Bulava") indica				r			r								
Globorotalia fohsi fohsi					p	f	r								
Glt. fohsi peripheroronda					p										
Glt. mayeri					p	c									
Globigerinoides subquadratus						r									
Globoquadrina s.p.						f									
Globigerina foliata						r		r							
G. bulloides - praebulloides							f	f	a		c				
Globigerinita s.p.							r								
Globorotalia praemenardii							c								
Glt. fohsi peripheroacuta							f								
Glt. siakensis							r								

## EXPLANATION

64 KL = location

300 = cm below sea floor  
in core sample

CC = core catcher sample

r = &lt; 1 %

f = 1 - 5 %

c = 5-20 %

a = &gt; 20 %

G. - Globigerina

Goides - Globigerinoides

Gita. - Globigerinita

Gq. - Globoquadrina

Glt. - Globorotalia

S'opsis - Sphaeroidinellopsis

Pull. - Pulleniatina

Gltoides - Globorotaloides

Cat. - Catapsydrax

SONNE CRUISE 8A														
CORE No.	29KD	36KD	46KD	32 KD		39KD	78 KL		64 KL					
				1	8		300	345	300	346	361	382	408	CC
SPECIES \ AGE	N 19	N 19	N <sup>17</sup> / <sub>18</sub>	N 12	N <sup>12</sup> / <sub>13</sub>	N 12	N <sup>5</sup> / <sub>6</sub>	N <sup>5</sup> / <sub>6</sub>	N <sup>22</sup> / <sub>23</sub>	NEO	PALAEOGENE			
<i>Globigerinoides diminutus</i>							c							
<i>Globigerinita ambitacrena</i>							r		r					
<i>Catapsydrax dissimilis dissimilis</i>							f							
<i>Cat. d. ciproensis</i>							r				r			
<i>Cat. unicavus unicavus</i>							a	a						
<i>Chiloguembelina cubensis</i>								f			r			
<i>Globigerina calida</i>									r					
<i>G. falconensis</i>									c					
<i>G. quinqueloba</i>									f					
<i>G. rubescens</i>									c					
<i>Globigerinoides bollii</i>									f					
<i>Goides gomitulus</i>									c					
<i>Globorotalia scitula scitula</i>									f	f				
<i>Glt. truncatulinoides s.s.</i>									f	r				
<i>Glt. tumida flexuosa</i>									r	r				
<i>Hastigerina pelagica</i>									r					
<i>Globigerina decoraperta</i>										f				
<i>Globigerinoides obliquus</i>										c				
<i>Goides. sicanus</i>										r				
<i>Globorotalia fohsi lobata</i>										c				
<i>Glt. miozea cibaoensis</i>										r				
<i>Glt. tosaensis</i>										r				
<i>Glt. unguolata</i>										r				
<i>Globigerina ampliapertura</i>											f	r	r	
<i>G. angulisuturalis</i>											f	f	r	f
<i>G. angustiumbilicata</i>											f	f	c	f
<i>G. corpulenta</i>											c	c	a	c
<i>G. eocaena</i>											f	c		c
<i>G. cf. higginsii</i>											r			
<i>G. linaperta</i>											r			
<i>G. pentacamerata</i>											r			
<i>G. praebulloides - ouachitaensis</i>											a	a	a	a
<i>G. sellii</i>											f	f	f	
<i>G. senni</i>											r			
<i>G. tripartita</i>											c	f	c	f
<i>Catapsydrax echinatus</i>											r			r
<i>Globigerinatheka mexicana</i>											f			
<i>Globorotalia bullbrookii</i>											c	r		f
<i>Glt. rex</i>											c			f
<i>Globorotaloides suteri</i>											f	f	f	c
<i>Truncorotaloides pseudotopilensis</i>											f			
<i>Hantkenina alabamensis</i>											f	r		
<i>Pseudohastigerina micra</i>											r		r	f
<i>Chiloguembelina midwayensis</i>											r			
<i>Globigerina ? angiporoides</i>												r		r
<i>G. gortanii</i>												r	r	
<i>Globorotalia opima nana</i>												c	c	
<i>Globigerina frontosa</i>													r	r
<i>Globigerinatheka kugleri</i>													r	f
<i>Globorotalia aequa</i>													r	
<i>Glt. opima opima</i>													f	
<i>Cassigerinella chipolensis</i>													r	
<i>Pseudogloboquadrina primitiva</i>													r	f
<i>Globigerina tapuriensis</i>														r
<i>Catapsydrax howei</i>														r
<i>Globorotalia cerroazulensis cocoaensis</i>														r

Tables 4, 5. Distribution of Foraminiferida in Sonne Tertiary samples.

Eocene) is not, but recent evidence suggests that 2A may have been more extensive in its effects than 2B.

The evidence is taken to indicate that during periods of low sea level, little sediment accumulated on the Exmouth Plateau, either because it was exposed or, more probably, because current activity over the Plateau prevented the sedimentation of planktic particles; the cross-sectional area of water current over the Plateau would be much less during low sea level — thus currents would need to be faster to transport the same volume of water.

### 78KL

This core is 3.45 m long and was sampled at 100 cm intervals to 300 cm, and at the core catcher. Samples below the surface are markedly affected by dissolution; the only samples to yield foraminiferids were from the surface, 300 cm and the core catcher. The lithology of the core is shown in Figure 3.

The surface is Quaternary with rare, sinistral *Globorotalia truncatulinoides* and abundant *G. menardii*. The effects of dissolution are evident on *Globorotalia*, but the fauna is essentially complete.

The sample from 300 cm is contaminated with Quaternary elements. If these are ignored, the fauna consists of *Catapsydrax unicavus unicavus*, *G. dissimilis dissimilis* and *G. d. ciperoensis*. Small *Globigerinoides* is present, but it is not clear whether it is *in situ* or a contaminant; if it is *in situ*, the age is Early Miocene (N5/6), if a contaminant, the age cannot be defined more precisely from the foraminifera than mid Oligocene-Early Miocene.

The core catcher sample represents a core depth of about 3.5 m. It also contains Quaternary species and is affected by dissolution. *In situ* elements include *Catapsydrax unicavus unicavus*, *Globigerina venezuelana* and a small, unidentified *Globigerinoides*. Also recovered was a single specimen of *Chiloguembelina cubensis*. It is regarded as a contaminant of uncertain origin.

### Climatic information from *Globorotalia* coiling ratios

Study of coiling ratios of *Globorotalia* can give an insight into climatic change (Bandy, 1964; Bolli, 1971); there are now signature curves for various species in many parts of the world. Sinistral coiling generally represents cooler climates and dextral warmer climates. The study of coiling ratios is however, in its infancy in Australia — only Quilty (1974) and Rögl (1974) have investigated this feature close to the continent.

None of the Exmouth Plateau samples is part of a major continuous sequence, the ideal for coiling ratio studies. Nevertheless, a few species are abundant enough for useful figures to be plotted. The main species are shown in Table 2. Species with less than 10 specimens in any sample are not plotted here, but were counted.

When all *Globorotalia* are counted and combined, it is found that the Late Miocene samples and one Middle Miocene sample are about 85 percent sinistrally coiled, suggesting cool conditions; two Middle Miocene samples are about 70 percent dextrally coiled, suggesting warm conditions. A Late Palaeocene-Early Eocene, and a Middle Eocene sample are about 70 percent dextrally coiled, also suggesting warm conditions. A fall of temperature in the Middle Miocene is indicated, which agrees with worldwide data, e.g. Shackleton & Kennett, 1975.

### Systematic palaeontology

Order FORAMINIFERIDA Eichwald, 1830

Family GLOBOROTALIIDAE Cushman, 1927

Genus *Globorotalia* Cushman, 1927

Type species. *Pulvinulina menardii* var. *tumida* 1877

*Globorotalia praemiocenica* Lamb & Beard, 1972,

Figure 5 C. D

*Globorotalia praemiocenica* Lamb & Beard, 1972, p. 55, pl. 17, figs. 1-3, 6.

Remarks. Stainforth & others (1973) refer to Late Miocene dextral forebears of *G. praemiocenica*, but suggest a Middle Pliocene to Early Pleistocene age for the species. They also commented on the existence of very similar forms in the Late Miocene of the Pacific region. The occurrence in 46KD suggests that *G. praemiocenica* did exist as early as Late Miocene.

Family HANTKENINIDAE Cushman, 1927

Genus *Protentella* Lipps, 1964

Type species. *Protentella prolixa* Lipps, 1964

*Protentella indica* (Boltovskoy), 1978

Figure 5 I-L

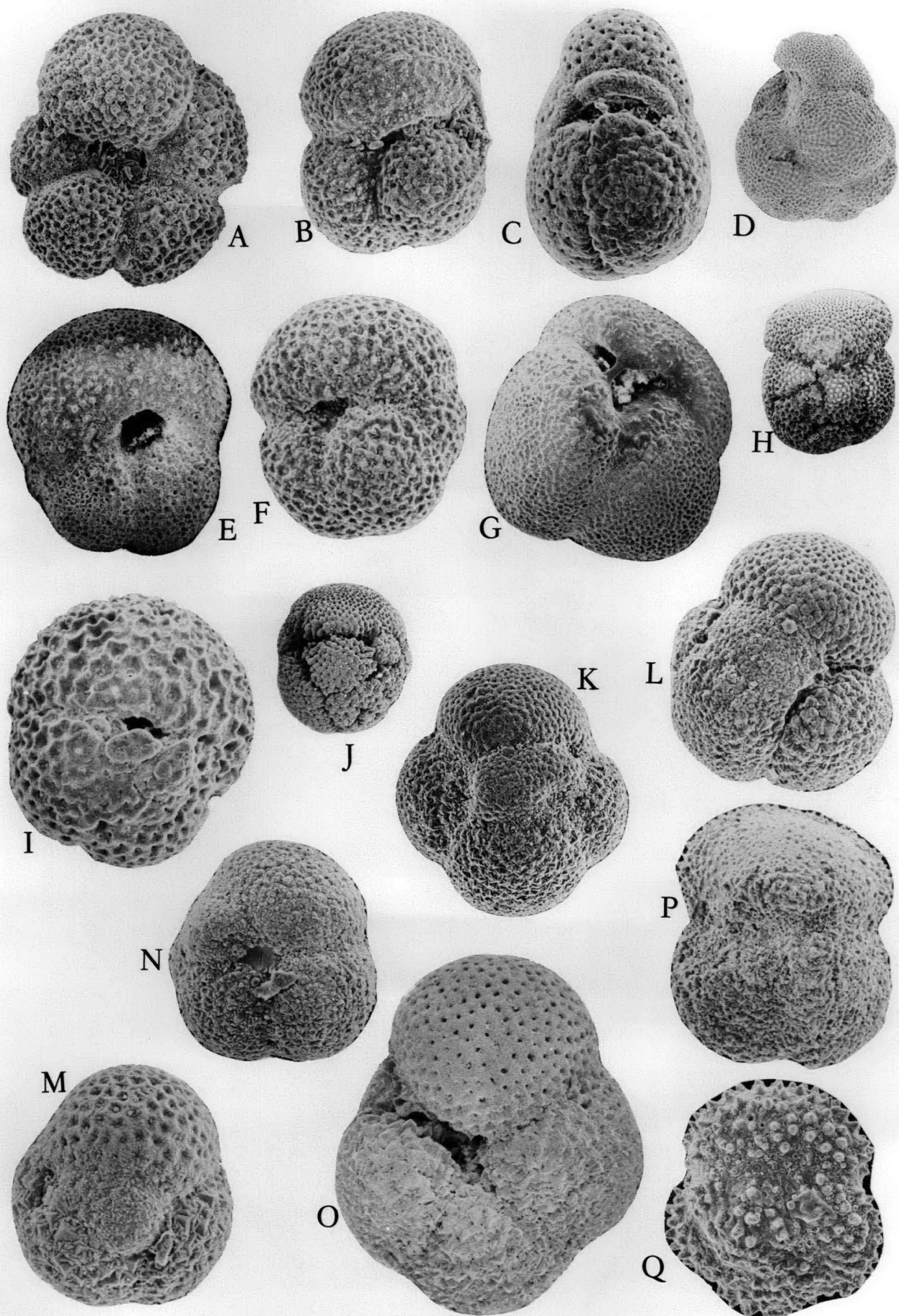
*Bulava indica* Boltovskoy, 1978, p. 301, pl. 1, figs. 1-23.

Remarks. Boltovskoy (1976, 1978) described '*Bulava*' *indica* as a benthic form from Deep Sea Drilling Project Leg 26 samples from the Indian Ocean, but recognised (1978) that it may be the broken clavate chamber of a planktic species akin to '*Clavigerinella*' *nazcaensis* (see Quilty, 1976). In addition to the discrete clavate chambers a single broken source of such chambers was recovered and is figured. It differs from '*C*' *nazcaensis* in being smaller and in having well marked large spine bases on the distal end of the clavate chambers. These show the triradiate spine bases. '*C*' *nazcaensis* is trochospiral whereas *P. indica* is not. A better generic name probably is *Protentella*, although the degree of elongation of the chambers is much greater than would seem to be suggested by the generic diagnosis.

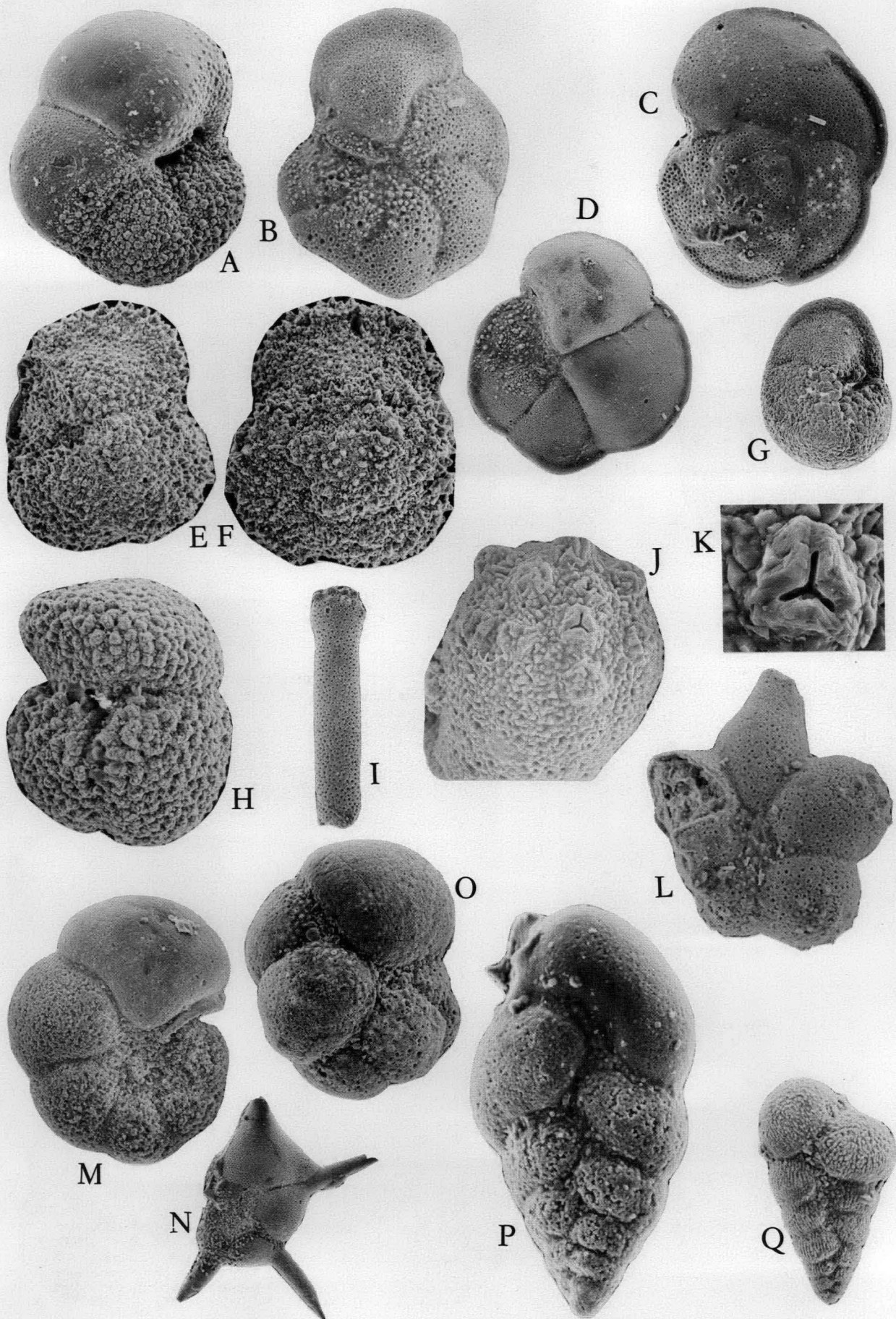
Figure 4.

A — *Globigerina angulisuturalis* Bolli CPC19940; 64KL, 361-365 cm, X 220. B — *G. linaperta* Finlay. CPC19941; 64KL, 361-365 cm; X120. Specimen lost. C — *G. nepenthes* Todd. CPC19942; 36KD, 3C; X180. D — *G. gortanii* Borsetti. CPC19943; 64KL, 382-385 cm; X65. E — *G. selli* Borsetti. CPC19944; 64KL, 361-365 cm; X80. F — *G. tapuriensis* Blow & Banner. CPC19945; 64KL, core catcher; X150. G — *G. tripartita* Koch. CPC19946; 64KL, 361-365 cm; X95. H — *Globigerinoides conglobatus* (Brady), CPC19947; 64KL, 300 cm; X55. I — *G. sicanus* de Stefani. CPC19948; 64KL, 346-349 cm; X185. J — *Globigerinatheka mexicana* (Cushman). CPC19949; 64KL, 361-365 cm, X50. K — *Catapsydrax dissimilis ciperoensis* Blow & Banner. CPC 19950; 78KL, 300 cm; X90. L — *C. dissimilis dissimilis* (Cushman & Bermudez). CPC19951; 78KL, 300 cm; X110. M — *C. unicavus unicavus* Bolli, Loeblich & Tappan. CPC19952; 78KL, 300 cm; X150. N — *Globorotaloides suteri* Bolli. CPC19953; 64KL, 361-365 cm; X145. O — *Globorotalia acostaensis* Blow. CPC19954; 39KD; X190. P — *G. aequa* Cushman & Renz. CPC19955; 64KL, 408 cm; X145. Q — *G. bullbrookii* Bolli. CPC19956; 64KL, 361-365 cm; X220.









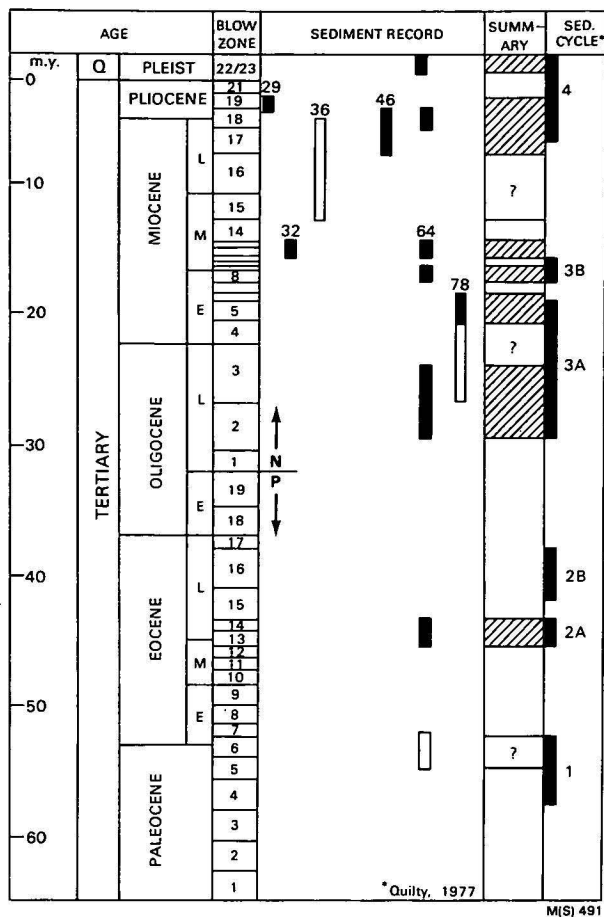


Figure 6. Relationship of samples examined to time scales and sedimentary cycles.

### References

- BANDY, O. L., 1964—Cenozoic planktonic foraminiferal zonation. *Micropaleontology*, **10**, 1-17.
- BERGGREN, W. A., 1972—A Cenozoic time scale — some implications for regional geology and palaeobiogeography. *Lethaia*, **5**, 265-88.
- BLOW, W. H., 1969—Late Middle Eocene to Recent planktonic foraminiferal biostratigraphy. *Proceedings of the First International Conference on planktonic Microfossils*, Geneva, **1**, 199-422.
- BOLLI, H. M., 1971—The direction of coiling in planktonic foraminifera. In Funnell, B. M. and Riedel, W. R. (Editors). *THE MICROPALAEONTOLOGY OF OCEANS*, 639-40. Cambridge University Press, Cambridge.
- BOLTOVSKOY, E., 1976—'Bulava indica' a new foraminiferal guide fossil from the Indian Ocean, *Revue Espanola Micropaleontol*, **8**, 301-3.
- BOLTOVSKOY, E., 1978—Late Cenozoic benthonic foraminifera of the Ninetyeast Ridge (Indian Ocean). *Marine Geology*, **26**, 139-75.
- EXON, N. F., & WILCOX, J. B. 1978—The geology and petroleum potential of the Exmouth Plateau area off Western Australia. *American Association of Petroleum Geologists Bulletin*, **62**, 40-72.
- LAMB, J. L., & BEARD, J. H., 1972—Late Neogene planktonic foraminifers in the Caribbean Gulf of Mexico, and Italian stratotypes. *University of Kansas Paleontological Contributions*, Article 57.
- QUILTY, P. G., 1974—Tertiary stratigraphy of Western Australia. *Journal of the Geological Society of Australia*, **21**, 301-18.
- QUILTY, P. G., 1976—Planktonic foraminifera DSDP Leg 34 — Nazca Plate. In Yeats, R. S., Hart, S. R., & others, *Initial Reports of the Deep Sea Drilling Project*, **34**, 629-703. US Government Printing Office, Washington.
- QUILTY, P. G., 1977—Cenozoic sedimentation cycles in Western Australia. *Geology*, **5**, 336-40.
- QUILTY, P. G., 1980—Sedimentation cycles in the Cretaceous and Cenozoic of Western Australia. *Tectonophysics*, **63**, 349-66.
- RÖGL, F., 1974—The evolution of the *Globorotalia truncatulinoides* and *Globorotalia crassaformis* group in the Pliocene and Pleistocene of the Timor Trough, DSDP Leg 27, site 262. In Veevers, J. J., Heirtzler, J. R., & others, *Initial Reports of the Deep Sea Drilling Project*, **27**, 743-67. US Government Printing Office, Washington.
- STAINFORTH, R. M., LAMB, J. L., LUTERBACHER, H., BEARD, J. H., & JEFFORDS, R. M., 1975—Cenozoic planktonic foraminiferal zonation and characteristics of index forms. *University of Kansas Paleontological Contributions*, Article 62.
- VAN ANDEL, Tj. H., 1975—Mesozoic/Cenozoic calcite compensation depth and the global distribution of calcareous sediments. *Earth and Planetary Science Letters*, **26**, 187-94.
- VON STACKELBERG, U., EXON, N. F., VON RAD, U., QUILTY, P. G., SHAFIK, S., BEIERSDORF, H., SEIBERTZ, E., & VEEVERS, J. J., 1980—Geology of the Exmouth and Walaby Plateaus off northwest Australia: sampling of seismic sequences. *BMR Journal of Australian Geology & Geophysics*, **5**, 113-140.

Figure 5.

A — *Globorotalia cerroazulensis cocoaensis* Cushman. CPC19957; 64KL, core catcher; X125. B — *G. johsi peripheroacuta* Blow & Banner. CPC19958; 39KD, X160. C, D — *G. praemiocenica* Lamb & Beard. CPC19959; 39KD: C.X130.D.X90. E, F — *G. rex* Martin. CPC19960; 64KL, 361-365 cm; X125. G — *G. tumida* (Brady). CPC19961; 64KL, 300 cm; X50. H — *Truncorotaloides pseudotopilensis* (Subbotina). CPC19962, 64KL, 361-365 cm; X160. I-L — *Protentella indica* (Boltovskoy). I. disjunct chamber. CPC19963; 39KD; X80. J, K CPC19964; 36KD, 3C; J. X300; K. X900. Note triradiate spine base. L. specimen from which disjunct chambers break. CPC19965; 36KD, 3C; X200. M — *Pseudohastigerina micra* (Cole). CPC19966; 64KL, 361-365 cm, X220. N — *Hantkenina alabamensis* Cushman. CPC19967; 64 KL, 361-365 cm; X55. O — *Cassigerinella chipolensis* (Cushman & Ponton) CPC19968, 64KL, 408 cm; X240. P — *Chiloguembelina midwayensis midwayensis* (Cushman) CPC19969; 64 KL, 361-365 cm; X250. Q — *C. cubensis* (Palmer). CPC19970; 64KL, 361-365 cm; X160.

# Middle Ordovician conodonts from the Pittman Formation, Canberra, ACT

Robert S. Nicoll

A small conodont fauna consisting of *Pygodus serrus* (Hadding) and *Periodon aculeatus aculeatus* Hadding has been recovered from the middle part of the Pittman Formation on Black Mountain, ACT. A Middle Ordovician (Llanvirnian) age (*Pygodus serrus* conodont Zone) has been ascribed to the fauna, which is representative of the North Atlantic conodont faunal province.

## Introduction

Early geological mapping of the Canberra City district by Öpik (1958, p. 15) recorded the presence of conodonts in the Middle Ordovician Pittman Formation. The present note describes this fauna, correlates it with established conodont zonations and discusses provincial affinities. The fauna studied includes the original collection of Öpik, which was blackened by fire in 1954, and new material (See Table 1).

Öpik (1958) referred to the presence of conodonts in sandstone, shale, and chert from two different horizons within the Pittman Formation, but only one locality was accurately located in the text. All the conodonts examined came from a 13 cm (5 inch) shale band (bed 14) in the lower part of Öpik's measured section of the Pittman Formation located in the bed of Etheridge Creek (Figs. 1, 2).

## The Fauna

The conodonts are mostly preserved as moulds in the silty shale, but also as limonite replacements and in a few cases as the original apatite. Weathered specimens are surrounded by a brown halo. Specimens were obtained by splitting the shale and examining the resulting surfaces microscopically. As with all conodont

faunas with this type of preservation, good three-dimensional specimens are rare; thus discrimination of morphologic features is reduced and the recognition of individual elements of the P (Pa, Pb) and S (Sa, Sb, Sc, Sd) types (notation by Sweet & Schönlaub, 1975) may be difficult or impossible.

The conodont fauna is very restricted: only two multielement species, a few unidentified cone elements, and an unassignable S type element. The two multielement taxa recognised are *Pygodus serrus* (Hadding) and *Periodon aculeatus aculeatus* Hadding.

*Pygodus serrus* contains only two element types (Bergström, 1971), Pb (ambalodontiform) and Pa (amorphognathodontiform). The Pa element is easily distinguished from its counterpart in *P. anserinus* by having only three denticle rows on the oral surface. The specimens from this study all exhibit only three denticle rows. The Pb element is easily distinguished from the *Periodon* apparatus, but the available specimens could not be distinguished from the Pb element of *Pygodus anserinus* because the angular relationship of the processes is not easily observed.

*Periodon aculeatus aculeatus* Hadding is a well-established multielement taxon (Bergström & Sweet, 1966). Most authors recognise only six element types, but Dzik (1976) suggests that *P. aculeatus zgierzensis* has seven. Owing to the type of preservation, only the three major element types (P, S and M) can be differentiated in the present material. The P and S elements are similar to those previously illustrated from *Periodon*, and appear to be most closely related to skeletal elements of *P. aculeatus aculeatus*. The M element (falcodontiform = oistodontiform) is identical to the M element of *P. aculeatus aculeatus*, especially in the development of the minor denticles on the anterior margin.

The remaining elements in the collection, mostly cones and S-type ramiform? elements, are too poorly preserved to assign to either form or multielement taxa. Two cone elements are illustrated as documentation (Fig. 3—M, N).

## Age

The conodont fauna recovered is of Middle Ordovician (middle to late Llanvirnian) age based on recognition of *Pygodus serrus*, the principal zonal indicator of the *Pygodus serrus* conodont Zone in the Balto-Scandic area (Bergström, 1971, 1973b; Löfgren, 1978). The *Pygodus serrus* Zone has been subdivided into a number of subzones based on the evolution of *Eoplacognathus* Hamar, but that genus has not been recovered from the Pittman Formation. *Periodon aculeatus aculeatus* Hadding ranges from latest Arenigian to latest Llandeilian (Löfgren, 1978), which helps confirm the age.

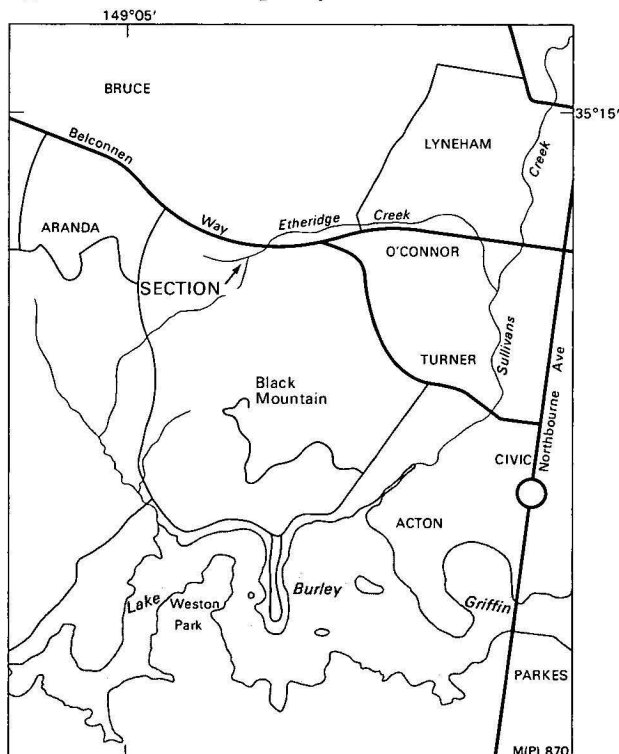


Figure 1. Locality map, showing location of measured section.



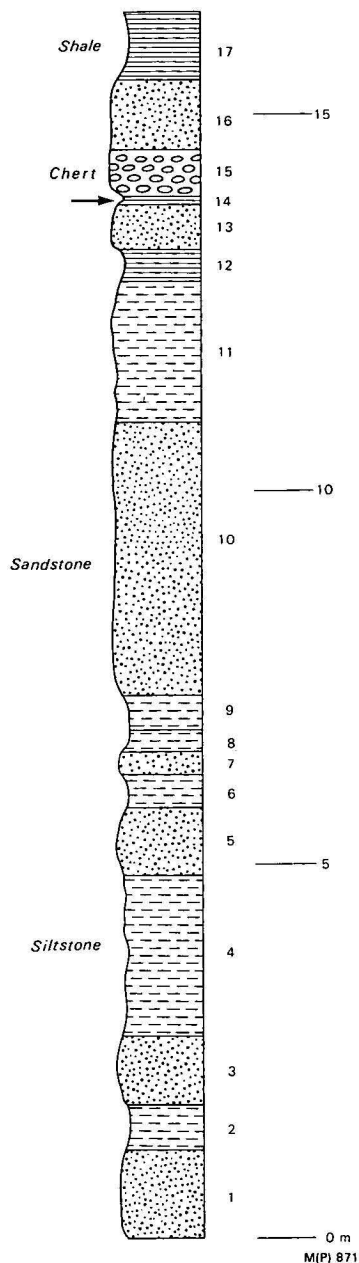


Figure 2. Lower part of Öpik's measured section of the Pittman Formation located in the bed of Etheridge Creek (Canberra 1:100 000 topographic map grid, ref. 906957).

Bed numbers refer to lithologic units described in Öpik (1958, Table 1). The arrow indicates the position of the shale bed containing the conodonts.

Öpik (1958), from a study of the graptolites, considered the Pittman Formation to range in age from early Middle Ordovician to early Late Ordovician (Gisbornian). He considered the section along Etheridge Creek to be representative of the middle part of the formation, corresponding to the upper half of the Middle Ordovician. The conodonts indicate that at least the lower part of the Etheridge Creek section is slightly older than envisaged by Öpik, and corresponds to the early Middle Ordovician.

### Provinciality

Ordovician conodont faunas have generally been divided into two major faunal provinces: a North American Midcontinent fauna and a North Atlantic fauna (Sweet & others, 1959; Bergström, 1973; Barnes

& Fahraeus, 1975). The restricted conodont fauna recovered in this study is representative of the North Atlantic (European) conodont province (Bergström, 1971).

There are conflicting interpretations of the causes of the provincialism observed in the Midcontinent and North Atlantic conodont faunas. Bergström and Sweet (Bergström, 1973a; Sweet & Bergström, 1974) ascribe the cause of the provincialism primarily to climate and latitude. Barnes and Fahraeus (Barnes & others, 1973; Barnes & Fahraeus, 1975) think that hypersalinity and water depth may also be important factors. As a generalisation the Midcontinent fauna is thought to represent an equatorial, warm water, possibly hypersaline, inner-shelf environment; and the North Atlantic fauna to represent adaptation for temperate to cold water of normal salinity which may be restricted to the continental margins and slopes. *Periodon* is cited by Barnes & others (1973) as coming from sediments deposited on the outer shelf and slope of continental margins.

The only conodont faunas that may be of similar age to the Pittman fauna in Australia and New Zealand are those described by Cawood (1976), and Wright (1968). Both these faunas have a North Atlantic aspect. The fauna illustrated by Cawood (1976) from northern New South Wales, contains *Periodon aculeatus*, and the fauna discussed by Wright (1968) from New Zealand also contains *P. aculeatus* and other taxa.

Australian and New Zealand conodont faunas of Early and Late Ordovician age have aspects of both Midcontinent and North Atlantic faunal provinces. The three lower Middle Ordovician localities discussed above all have a North Atlantic faunal aspect, while a slightly younger (Llandeilian-Caradocian) fauna from the Sofala Volcanics (Pickett, 1978) has a Midcontinent aspect. A more intensive investigation of Ordovician conodont faunas will be required before the relationship between Midcontinent and North Atlantic faunal provinces can be closely delineated in Australia and New Zealand.

### Acknowledgements

The author thanks Drs K. A. W. Crook (Australian National University) and D. L. Strusz for their assistance in relocating Dr A. A. Öpik's measured section of the Pittman Formation on Black Mountain. The manuscript was critically read by Dr D. L. Strusz, and reviewed by Dr B. J. Cooper. Arthur T. Wilson and Ken Heighway assisted with the plate preparation and photography.

### Specimen details

	figured	unfigured
<i>Periodon aculeatus aculeatus</i> (Hadding)		
M elements	CPC 19809	CPC 19810-12
S elements	CPC 19817-20	CPC 19821-25
P elements	CPC 19813-14	CPC 19815-16
<i>Pygodus serrus</i> (Hadding)		
Pa elements	CPC 19826-28	CPC 19829-31
Pb elements	CPC 19832-33	CPC 19834
genus et species indet.		
cone elements	CPC 19835-36	CPC 19837-39

Table 1. List of figured and unfigured specimens deposited in the Commonwealth Palaeontological Collection (CPC), housed in the Bureau of Mineral Resources, Canberra, Australia. Additional material, partly identified, is deposited in the BMR as part of the A. A. Öpik Canberra Collection under the Öpik locality number 230, and includes both original material collected by Öpik and recollected material.

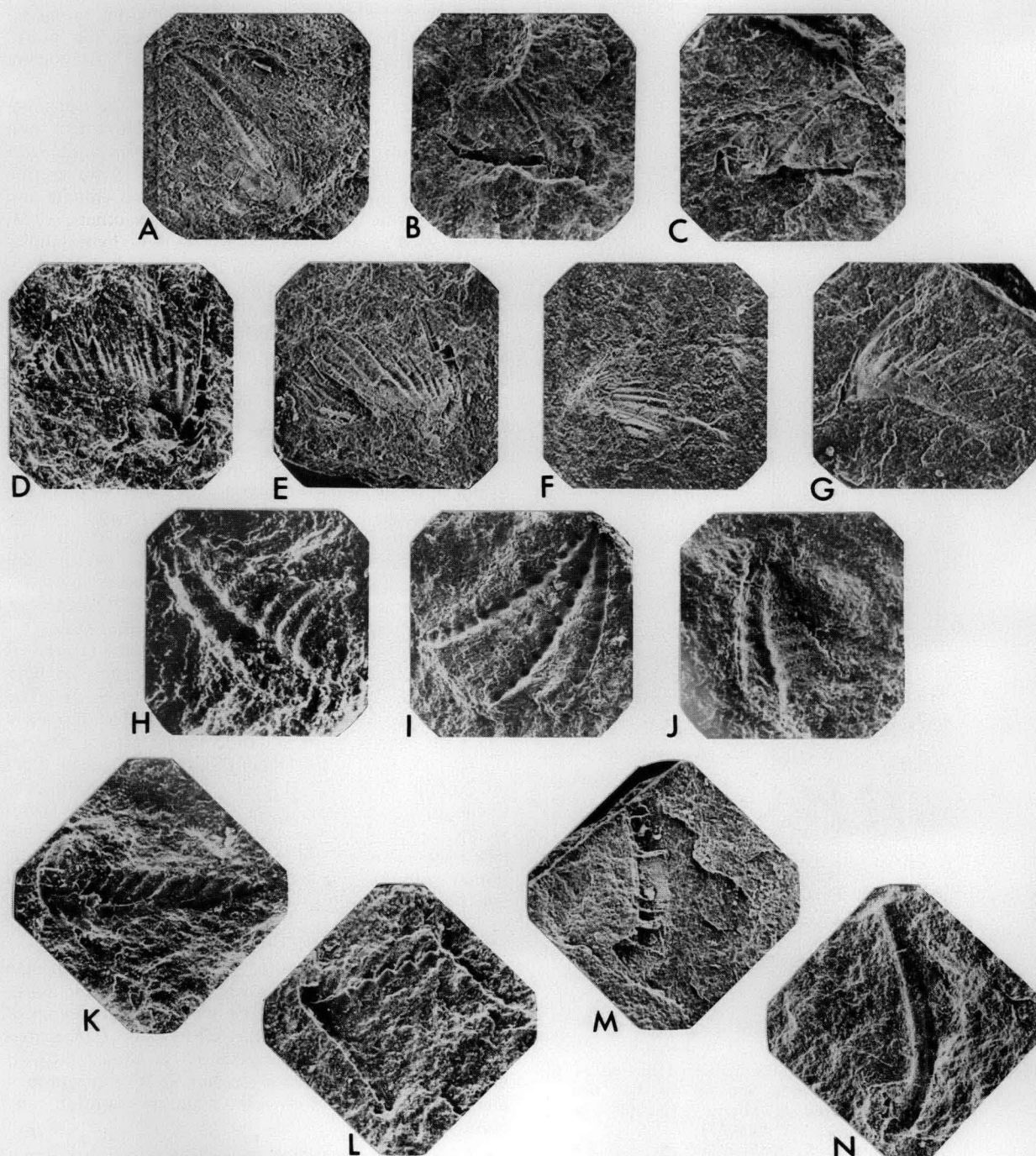


Figure 3.

A-G *Periodon aculeatus aculeatus* Hadding — A: M element, CPC19809, X30; B: P element, CPC19813, X30; C: P element, CPC19814, X30; D: S element, CPC19817, X50; E: S element, CPC19818, X30; F: S element, CPC19819, X40; G: S element, CPC19820, X40. H-L *Pygodus serrus* (Hadding) — H: Pa element, CPC19826, X90; I: Pa element, CPC19827, X40; J: Pa element, CPC19828, X40; K: Pb element, CPC19832, X50; L: Pb element, CPC19833, X60. M, N genus et species indet. — M: cone element, CPC19835, X20; N: cone element, CPC19836, X30.

### References

- BARNES, C. R., & FAHRAEUS, L. E., 1975—Provinces, communities, and the proposed nekto-benthic habit of Ordovician conodontophorids. *Lethaia*, **8**, 133-49.
- BARNES, C. R., REXROAD, C. B., & MILLER, J. F., 1973—Lower Paleozoic Conodont Provincialism; in Sweet, W. C. & Bergström, S. M. (Editors), Symposium on Conodont Biostratigraphy. *Geological Society of America, Memoir* **127**, 157-190.
- BERGSTRÖM, S. M., 1971—Conodont Biostratigraphy of the Middle and Upper Ordovician of Europe and Eastern North America; in Sweet, W. C. & Bergström, A. M. (Editors), Symposium on Conodont Biostratigraphy. *Geological Society of America, Memoir* **127**, 83-162.
- BERGSTRÖM, S. M., 1973a—Ordovician Conodonts; in Hallam, A. (Editor), *Atlas of Palaeobiogeography*. Elsevier, London, 47-58.
- BERGSTRÖM, S. M., 1973b—Correlation of the late Lasmagian Stage (Middle Ordovician) with the graptolite succession. *Geologiska Föreningen i Stockholm Förhandlingar*, **95**, 9-18.
- BERGSTRÖM, S. M., & SWEET, W. C., 1966—Conodonts from the Lexington Limestone (Middle Ordovician) of Kentucky. *Bulletins of American Palaeontology*, **50**, 271-424.



- CAWOOD, P. A., 1976—Cambro-Ordovician Strata, Northern New South Wales. *Search*, 7, 317-8.
- DZIK, J., 1976—Remarks on the Evolution of Ordovician Conodonts. *Acta Palaeontologica Polonica*, 21, 395-455.
- LÖFGREN, A., 1978—Arenigian and Llanvirnian conodonts from Jämtland, northern Sweden. *Fossils and Strata*, 13.
- ÖPIK, A. A., 1958—The Geology of the Canberra City District. *Bureau of Mineral Resources, Australia, Bulletin* 32.
- PICKETT, J., 1978—Further Evidence for the Age of the Sofala Volcanics. *Quarterly Notes, Geological Survey of New South Wales*, 31, 1-4.
- SWEET, W. C., & BERGSTRÖM, S. M., 1974—Provincialism Exhibited by Ordovician Conodont Faunas; in Ross, C. A. (Editor), *Paleogeographic Provinces and Provinciality. Society of Economic Paleontologists & Mineralogists, Special Publication* 21, 189-202.
- SWEET, W. C., & SCHÖNLAUB, H. P., 1975—Conodonts of the Genus *Oulodus* Branson & Mehl, 1933. *Geologica et Palaeontologica*, 9, 41-59.
- SWEET, W. C., TURCO, C. A., WARNER, E., & WILKIE, L. C., 1959—The American Upper Ordovician Standard. I. Eden conodonts from the Cincinnati region of Ohio and Kentucky. *Journal of Paleontology*, 33, 1029-68.
- WRIGHT, A. J., 1968—Ordovician Conodonts from New Zealand. *Nature*, 218, 664-5.

*BMR Journal of Australian Geology & Geophysics*, 5, 1980, 153-156

## The 1961 Robertson earthquake — more evidence for compressive stress in southeast Australia

D. Denham

A new focal mechanism for the 1961 Robertson earthquake provides further evidence of contemporary thrust faulting in southeast Australia. When this is combined with the earlier work of Cleary & Doyle (1962) on the locations of the earthquake and its aftershocks, it seems that the earthquake was associated with a high angle ( $\sim 80^\circ$ ) thrust fault, about 10 km wide and in the depth range 7 to 20 km, caused by northeast-southwest compression.

This fault model is similar to that found by Mills & Fitch (1977) for the 1973 Picton earthquake, which also took place beneath the southern Sydney Basin. However, *in situ* stress measurements and earthquake data from immediately to the west in the Lachlan Fold Belt, suggest a different stress regime dominated by north-south compression. Thus, although the crust in southeast Australia is being compressed, the directions of maximum stress appear to change from region to region.

### Introduction

In the last twenty years, two moderate-sized earthquakes have occurred beneath the southern part of the Sydney Basin. These were the 1961 Robertson and the 1973 Picton earthquakes. Both had Richter magnitudes of about 5.5 (Drake, 1974) and caused minor damage in the epicentral regions.

Fitch (1976) and Mills & Fitch (1977) studied the mechanism of the Picton earthquake in detail. They found that the distribution of aftershocks and the body-wave and surface-wave radiation patterns were consistent with the earthquake being associated with a steeply dipping thrust fault having a lateral extent of about 8 km and a depth range from 8 to 24 km. A plot of the body-wave solution is shown in Figure 1 and the appropriate parameters for both solutions are listed in Table 1. Mills & Fitch (1977) concluded that this 'mid-crustal earthquake . . . provides unambiguous evidence of contemporary thrust faulting in south-eastern Australia'.

The 1961 Robertson earthquake (see Table 1 for earthquake parameters) has been studied by Cleary & Doyle (1962), Cleary (1963), and Doyle & others (1968). The aftershocks formed an approximately linear pattern extending NW-SE for 10 km and covering a depth range of 7 to 19 km (see Fig. 2). If the aftershock sequence defines the fault plane then a vertical or nearly vertical fault would be inferred.

Cleary (1963) made several attempts to determine a focal mechanism from the directions of the first motions on local seismograph stations. He obtained two solutions for the main earthquake and two for the aftershock sequence, each of which fitted the first motions at the local stations. The solution he preferred for the main earthquake ' . . . represents a high-angle reverse fault striking about  $30^\circ$  and dipping about  $60^\circ$  WNW, with motion up and southwest on the west side'.

This solution has never been very satisfactory, firstly because it infers a fault plane almost perpendicular to the aftershock sequence — a difficult situation to accept — and secondly, the solution was poorly controlled by the first motion observations.

I have therefore attempted to determine a better solution using improved travel-times and more stations, so that the earthquake mechanism could be compared to that of the 1973 Picton earthquake and also to the *in situ* stress measurements that have recently been carried out in the nearby Lachlan Fold Belt (Denham & others, 1979).

### The analysis

First motions from 25 seismic stations are displayed on a stereographic equal-area Schmidt projection of the lower half of the focal sphere in Figure 3. Apart from the usual problems of determining which way the trace first moves on the seismogram when the seismic energy

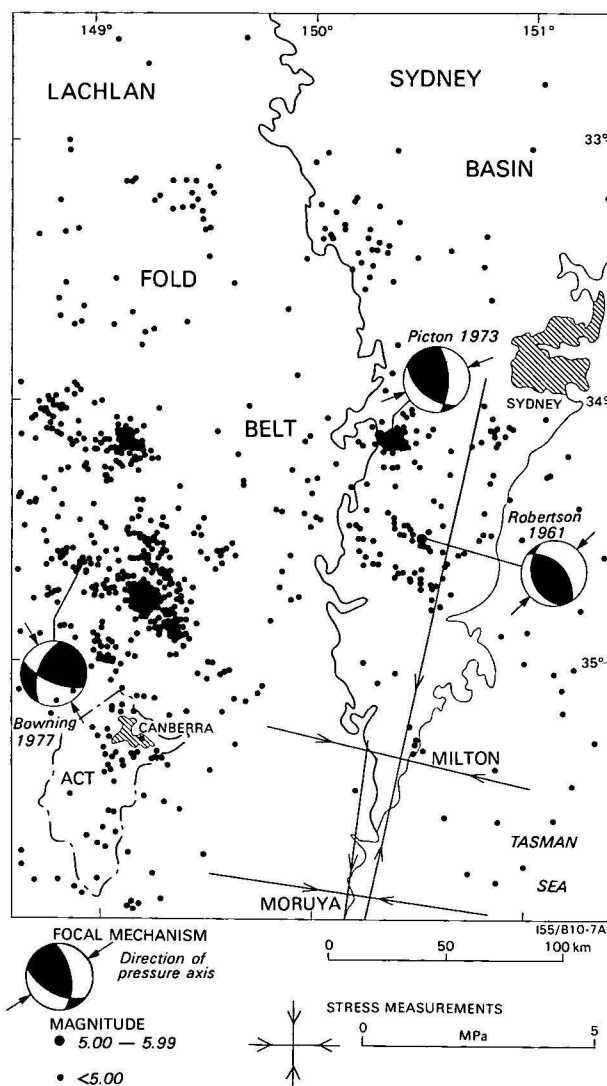


**Figure 1.** Distribution of earthquakes from 1900 to 1977 located by five or more seismic stations; earthquake focal mechanisms — lower focal hemisphere displayed, black represents an upward ground motion, the arrows show the azimuths of compression and *in situ* stress measurements made at depths less than 10 m, the arrows show the directions and magnitudes of the principal horizontal stresses.

is weak, there are two other major problems associated with this earthquake. The first is to determine the correct polarity of the seismographs in May 1961 and the second is to determine accurately the angles of incidence of the P-waves at the focus for near stations.

To solve the first problem ten large deep earthquakes, from Fiji, Indonesia, Japan, the Philippines, Papua New Guinea and the Kuriles, that occurred from 2-22 May 1961, were selected as calibration events. These were necessary to determine the correct polarity of DAR, MAW, SBA & SPA, and they also provided a valuable check on the eastern Australian stations. First motions for LEM, and SHL were not determined from the seismographs but were obtained from International Seismological Survey's bulletin (ISS, 1967).

The second problem, of calculating the angles of incidence of the P-waves, was solved by using recently determined travel-times from explosion seismology studies (Finlayson & others, 1979) for near stations

(<200 km). There is still some uncertainty in the angles obtained because of inhomogeneity in the crust, but the results appear to be consistent. For stations more than 200 km from the epicentre the 1968 Seismological Tables for P phases (Herrin & others, 1968; Nuttli, 1969) were used. These tables agree well with the observed travel-times in eastern Australia (see Finlayson & others, 1979).

Using only the first motions plotted in Figure 3 it is not possible to determine a well-constrained focal mechanism; there is one steeply dipping nodal plane between DAR and MAT, and an orthogonal plane with a very shallow dip. However, the azimuth of the steeply dipping plane is poorly controlled because of the paucity of stations east of the epicentre — none of the New Zealand stations recorded the earthquake well enough for a first motion to be determined.

I therefore assumed that the aftershocks determined the azimuth of the steeply dipping plane. The justification for this is based on many recent studies that have found that the aftershock pattern defines the fault plane (see for example Stewart & Denham, 1974).

A least-squares fit of the epicentres of the first seven earthquakes in the sequence, listed in Cleary & Doyle (1962) and plotted in Figure 2, gives an azimuth for the trend of  $130 \pm 9^\circ$ . This fits the first motion data and has been adopted as the azimuth of the nodal plane. If all the 24 earthquakes listed by Cleary (1963) are used (these took place over a five-month as opposed to a 24-hour period for the seven examined above) a similar azimuth of  $125 \pm 3^\circ$  is obtained — but this does not fit the JNL, CAN and WER first motions. The faulting therefore consists of mainly high-angle thrusting with a very small component of left-lateral strike-slip movement; Table 1 lists the adopted parameters for the focal mechanism.

## Conclusions

The evidence presented implies that the 1961 Robertson earthquake was associated with high-angle thrust faulting and that the mechanism was very similar to the 1973 Picton earthquake (see Table 1). Cleary (1967) inferred high-angle thrust faulting in the Gunning region some 50 km north of Canberra; Everingham & Smith (1979) showed that the 1977 Bowring earthquake was associated with compressive stresses, and Denham & others (1979) showed that the near-

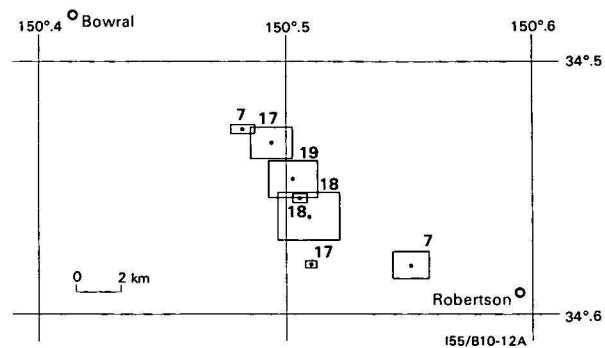


**Figure 2.** Plot (from Cleary & Doyle, 1962) showing the spatial distribution of the Robertson earthquake and the first six aftershocks.

All these earthquakes took place within a 24-hour period. The numbers refer to the depth of the earthquakes in kilometres, and the length of the sides of the rectangles represent the standard errors of the epicentral parameters.

Location and date	Lat°S	Long°S	depth km	Magnitude Richter scale	Poles of nodal planes		Axis of compression		Axis of tension		Null axis	
					trend	plunge	trend	plunge	trend	plunge	trend	plunge
A Robertson 21 May 1961	34.55	150.50	19	5.6	074	78	046	34	212	55	312	07
					220	10						
B Picton 29 March 1973	34.17	150.32	21	5.5	B265	36	064	06	323	65	157	24
					040	44						
					C266	12	073	25	287	54	172	11
					039	67						
D Bowning 4 July 1977	34.66	148.89	20	4.8	107	20	151	10	059	20	263	68
					015	08						

A, Solution from this paper; B, Fitch (1976), using body waves; C, Mills & Fitch (1977), using surface waves; D, Everingham & Smith (1979).

Table 1. Earthquake focal mechanisms for southeast Australian earthquakes.

surface *in situ* stress measurements also indicate that the region is being compressed. However, the directions of maximum principal stress are not consistent over the whole region. The Bowning earthquake and the *in situ* measurements suggest a NNW-SSE stress in that part of the Lachlan Fold Belt, whereas the Robertson and Picton earthquakes give a northeast-southwest direction for the maximum stress. Therefore, the crust beneath the Sydney Basin may be controlled by a different stress regime to that in the Lachlan Fold Belt.

One of the problems of using earthquake focal mechanisms is that in areas where there are zones of weakness associated with existing faults, the stress axes determined from earthquake focal mechanisms tend to be dominated by the geometry of the faults and may not coincide with the regional crustal stress (McKenzie, 1969). Within the Lachlan Fold Belt most of the major faults trend north-south, but beneath the Sydney Basin, where both the Robertson and Picton earthquakes took place, the main trends are not known, so the full significance of the differences in the axes of compression cannot be evaluated properly.

The only firm conclusion that can be drawn is that the crust in both the Lachlan Fold Belt and beneath the Sydney Basin is currently being compressed.

### Acknowledgements

I thank I. B. Everingham for useful discussion throughout this study, I. D. Ripper and K. McCue for valuable comments, and I. Hartig who drew the figures.

### References

CLEARY, J. R., 1963—Near earthquake studies in south-eastern Australia. *Ph.D. thesis, Australian National University, Canberra* (unpublished).  
 CLEARY, J. R., 1967—The seismicity of the Gunning and surrounding areas, 1957-1961. *Journal of the Geological Society of Australia*, **14**, 23-30.  
 CLEARY, J. R., & DOYLE, H. A., 1962—Application of a seismograph network and electronic computer in near earthquake studies. *Bulletin of the Seismological Society of America*, **52**, 673-82.  
 DENHAM, D., ALEXANDER, L. G., & WOROTNICKI, G., 1979—Stresses in the Australian crust: evidence from earthquakes and *in situ* stress measurements. *BMR Journal of Australian Geology & Geophysics*, **4**, 289-95.  
 DOYLE, H. A., CLEARY, J. R., & GRAY, N. M., 1968—The seismicity of the Sydney Basin. *Journal of the Geological Society of Australia*, **15**, 175-81.  
 DRAKE, L. A., 1974—The seismicity of New South Wales. *Journal & Proceedings of the Royal Society of New South Wales*, **107**, 35-40.  
 EVERINGHAM, I. B., & SMITH, R. S., 1979—Implications of fault-plane solutions for Australian earthquakes of 4 July 1977, 6 May 1978, and 25 November 1978. *BMR Journal of Australian Geology & Geophysics*, **4**, 297-301.

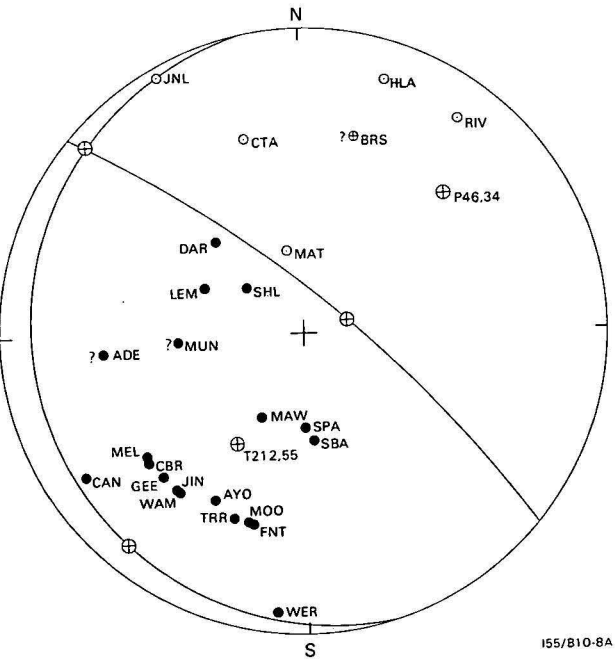


Figure 3. Focal mechanism solution of the May 1961 Robertson earthquake. Data are displayed on an equal-area Schmidt projection of the lower focal hemisphere. Solid circles and open circles represent upward and downward first motions respectively. Where the first motions are not certain a question mark has been added. The arrivals at AVO and WER have been transferred from the upper to the lower focal hemisphere. P and T stand for the axes of maximum and minimum pressure respectively. Azimuth and plunge (in that order) are given for both axes. The poles of the nodal planes and the null axes are also shown; the Table lists these parameters in detail.

- FINLAYSON, D. M., PRODEHL, C., & COLLINS, C. D. N., 1979—Explosion seismic profiles, and their implications for crustal evolution, in southeastern Australia. *BMR Journal of Australian Geology & Geophysics*, **4**, 243-52.
- FITCH, T. J., 1976—The Picton earthquake of March 9, 1973: a seismic view of the source. In Denham, D. (Editor), *Seismicity and earthquake risk in Eastern Australia. Bureau of Mineral Resources, Australia, Bulletin 164*.
- HERRIN, & others, 1968—1968 Seismological tables for P phases. *Bulletin of the Seismological Society of America*, **58**, 1193-228.
- ISS, 1967—International Seismological Summary, 1961, April, May, June, Kew observatory, UK.
- McKENZIE, D. P., 1969—The relation between fault plane solutions for earthquakes and the directions of the principal stresses. *Bulletin of the Seismological Society of America*, **59**, 591-601.
- MILLS, J. M., & FITCH, T. J., 1977—Thrust faulting and crust-upper mantle structure in East Australia. *Geophysical Journal of the Royal Astronomical Society*, **48**, 351-84.
- NUTTLI, O. W., 1969—Tables of angles of incidence of P waves at focus, calculated from 1968 P tables. *Earthquake Notes*, **40**, 21-5.
- STEWART, I. C. F., & DENHAM, D., 1974—Simpson Desert earthquake. Central Australia, August 1972. *Geophysical Journal of the Royal Astronomical Society*, **39**, 335-51.

*BMR Journal of Australian Geology & Geophysics*, **5**, 1980, 156-158

## An inexpensive and efficient double-tube, hand-coring device

M. H. Tratt & R. V. Burne

**A double-tube coring device able to retain sampled core, to recover sandy sediments, and to be easily extracted, has been designed. It consists of two PVC pipes with an intervening air space. The inner tube takes the main stress of coring, the outer tube acts as a sleeve to provide an environment of minimum friction for withdrawal. The corer is fitted with an anvil, and driven into the sediment by hammer blows. Sensitive variation of hammering force when cutting the core enables excellent recovery, with little or no compaction, of a range of sediment types.**

### Introduction

Sedimentological studies of shallow-water and sub-aerial environments commonly involve the use of simple hand-coring devices such as those described by Hanna (1954) and Ginsburg & Lloyd (1956). Bouma (1969), in reviewing these coring methods, has described two of their limitations, namely the difficulty of coring sand, and the loss of sample during pullout. Our experience with these devices has pointed to another limitation: long cores are very difficult to extract because of suction. To recover complete long cores it is often necessary to dig them out, a lengthy and environmentally disturbing operation.

We have developed a double-tube coring device that eliminates these problems; it can be handled easily by one operator. Previous double-tube systems have employed an outer metal core barrel — for strength in coring, and an inner plastic liner — removed after extraction of the core for ease of extrusion (Hanna, 1954). In our system the inner tube takes the main stress of the coring, with the outer tube acting as a sleeve to provide an environment of minimum friction for the removal of the inner tube. We employ a finger core catcher, made of 0.010" gauge phosphor-bronze, to ensure complete recovery of the core. This material is sufficiently flexible to prevent any serious disturbance of the core. The current cost of materials is  $\pm$  \$A6 for a corer of 1 metre length.

### Design

The apparatus consists of two PVC tubes, one inside the other, with an intervening air space 1 mm in width.

The inner core tube is of 50 mm hard PVC (class 12 pressure pipe). The outer casing tube is made of 65 mm SWV (soil, waste, vent) pipe, which is softer than the pressure pipe (Fig. 1a).

The core tube extends 100 mm above the casing tube at the driving end. At the cutting end both tubes are level, and chamfered at the same angle (approximately 60°) to provide a cutting edge. The chamfer is formed with a wood rasp. When the chamfer is finished, the inner coring tube (the harder tube) forms the leading edge, and is able to handle most material to be cored.

A finger core catcher is fashioned from .010 phosphor-bronze shim (Fig. 1b); it is held inside the core tube with 3 mm aluminium rivets, about 5 mm from the cutting edge (Fig. 1c). A 2.5 mm lip is turned on the leading edge of the core catcher so that, when the rivets are drawn up, the core catcher fits snugly in the tube and presents no obstruction to entry of the cored material. The core catcher is fitted before chamfering the cutting edge.

75 mm below the top edge of the casing tube a 10-mm clearance hole is drilled through both tubes, and a bolt of suitable length is inserted and nipped up, finger tight. Finally a 12 mm-clearance hole is drilled through the core tube 50 mm from the end.

### Coring methods

With the tubes assembled and held upright, a mild-steel anvil (Fig. 1d) is placed in the core tube and struck with a four-pound club hammer. When the tubes have been driven into the sediment to the required depth, the 10-mm bolt is removed and a 12 mm-dia-

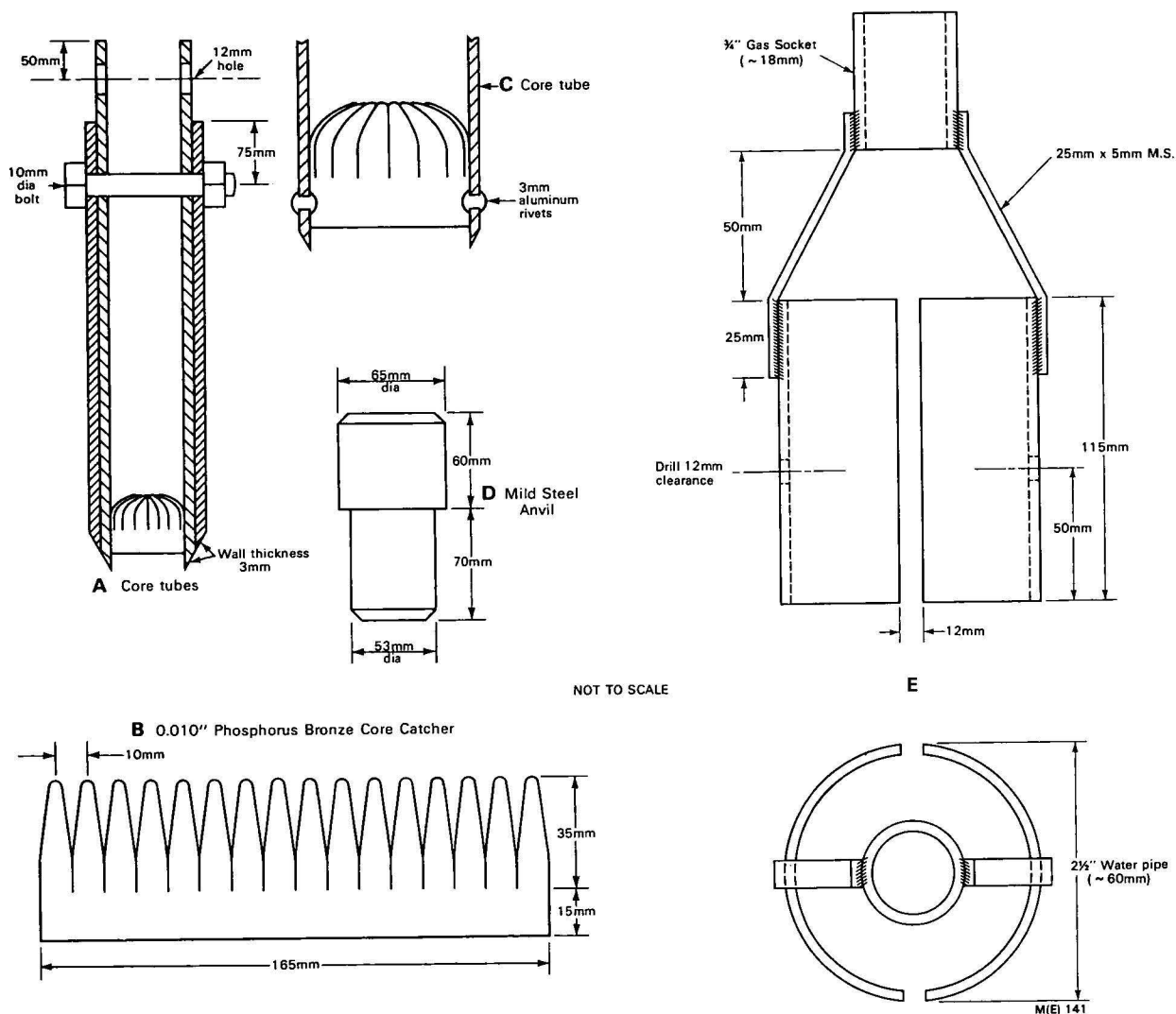


Figure 1. Plan drawings for coring device.

A: Complete, assembled corer, B: Template for cutting core catcher, C: Detail of inner core tube showing location of core catcher, D: Anvil for driving corer, E: Attachment for use with extension tubes for under water coring.

meter steel bar is inserted in the upper hole in the core tube. The inner core tube can then be easily lifted from the casing. The casing tube may be left in the ground to act as a piezometer, or it too may be readily removed.

The difference in diameters of the tubes is a critical feature of this system. If the difference between the inside diameter of the casing tube and the outside diameter of the inner, coring tube is too great the material cored is driven up between the walls of the tubes, making the withdrawal of the core tube very difficult; whereas, if the gap between the tubes is too small (a sliding fit), and water penetrates between them from the cored sequence, a vacuum is formed, and withdrawal again becomes very difficult. After some experimentation a satisfactory gap was discovered to be 1 mm which, happily, can be provided by two sizes of readily available PVC plumber's pipe.

The coring system can be used from a small boat, using an adaptor clamp (Fig. 1e), extension tubes (2 1/2" (218 mm) water pipe), and driving end with a 'T' handle. The adaptor is clamped to the core tube using the 12-mm bar hole, and a 12 mm bolt. It is however necessary that the boat be held stable with three anchors. The extension tubes are added to the clamp via

sockets until the core tube is resting on the bottom, with the 'T' handle above the gunwale. The device is then driven into the sediment as previously described. When the desired depth is reached, a short dive is necessary to remove the 10 mm bolt and withdraw the core tube.

### Coring technique and results

Proper coring technique is essential for good core recovery. The hammer blows should be medium and rapid rather than heavy and spasmodic. Even when little resistance to core penetration is felt the tendency to employ rapid forceful penetration should be avoided. We have noted that, in using large vibro-coring systems offshore in coring seagrass-fibre-bearing, unconsolidated sediments, the sudden release of the full corer weight results in the core clogging, despite the vibration, and the core tube is pushed down as a solid probe into the sediments. Although penetration is good, core recovery is minimal. However, by releasing the weight of the corer gradually, but vibrating vigorously, the fibrous sediments are cut cleanly by the corer and excellent core recovery results. Similarly, with the system described here, sensitive variation of hammering force in response to changes in resistance as the core is cut,



has resulted in excellent recovery of a range of sediment types with little or no compaction. One limitation of this method is that the length of core is dependent on the necessity to get above the end of the core to hammer it in. Cores up to 3 metres long have been successfully recovered.

Figure 2 illustrates a core, prepared and peeled in the manner of Burne & Tratt (1979), showing an undisturbed succession of gravel, partially lithified carbonate sand, poorly sorted sands with sea-grass roots and fibres, and, at the base, calcrete nodules.

### References

- BOUMA, A. H., 1969—METHODS FOR THE STUDY OF SEDIMENTARY STRUCTURES. *Wiley-Interscience, New York*.
- BURNE, R. V., & TRATT, M. H., 1979—Epoxy relief sediment-peel and latex-replication techniques used in the study of Spencer Gulf sediments. *BMR Journal of Australian Geology & Geophysics*, **4**, 395-8.
- HANNA, M. A., 1954—A simple coring tube for soft sediment. *Journal of Sedimentary Petrology*, **24**, 263-9.
- GINSBURG, R. W., & LLOYD, R. M., 1956—A manual piston coring device for use in shallow water. *Journal of Sedimentary Petrology*, **26**, 64-6.

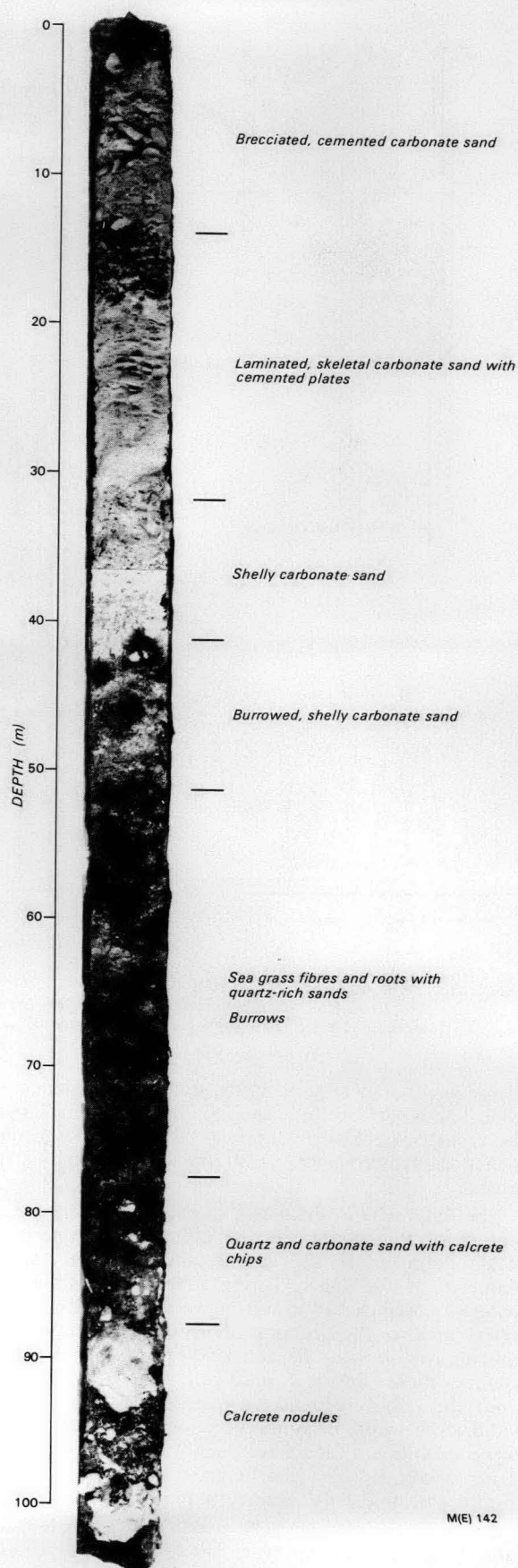


Figure 2. Example of a core recovered from the supratidal plain (station 09-3/4) at Fisherman Bay, Spencer Gulf. The top of this cored section lies beneath 50 cm of lithified carbonate.

## Palaeontological evidence for the Early Cambrian age of the Bukalara Sandstone, McArthur Basin, NT

M. D. Muir

The Bukalara sandstone overlies the Proterozoic rocks of the McArthur Basin, Northern Territory. Trace fossils are present in it at 5 localities on the Mount Young 1:250 000 Sheet: they include *Skolithos*, a probable *Charniodiscus* Ford 1958, and possibly the Annelid *Dickinsonia* Glaessner 1966. The trace fossils support the tentative Early Cambrian age suggested earlier for the Bukalara Sandstone.

The Bukalara Sandstone unconformably overlies the Proterozoic rocks of the McArthur Basin, Northern Territory. It crops out widely, and forms the Bukalara Plateau, which covers a large area to the east of the McArthur Mine (see the Bauhinia Downs 1:250 000 Geological Sheet). No fossils have been found in this area (Smith, 1964), but in the Hodgson Downs 1:250 000 Geological Sheet area, a possible Cambrian age for the formation was suggested by Dunn (1963), because sandstone dykes from the Bukalara Sandstone have been observed projecting into the overlying Lower Cambrian Nutwood Downs Volcanics.

In 1979 several new localities on the Mount Young 1:250 000 Geological Sheet area were visited. Some had been previously mapped as Warramanna Sandstone, a formation name that has subsequently been discarded (Plumb & Brown, 1973). Plumb & Brown equated the Warramanna Sandstone with the Tatoola Sandstone of the McArthur Group, but exposures mapped as Warramanna Sandstone include sandstones from the Master-ton Formation of the Tawallah Group, the Tatoola Sandstone, the Bukalara Sandstone, and some of Early Cretaceous age.

Trace fossils are present in five localities in the Mount Young 1:250 000 Geological Sheet area to the east of the Tawallah and Yiyintyi Ranges and north of Batten Creek (Tawallah Range Sheet 6066 1:100 000 topographic map at 9375.5585, 8785.7665, and 8785.7680; and on Mount Young Sheet 6067 1:100 000 topographic map at 9230.0110 and 9220.0070). Vertical tubes, about 8 mm in diameter, very similar to *Skolithos* in appearance, were observed at two localities, and in this and two other localities, fairly long (up to 70 cm), sub-cylindrical, meandering burrows up to 1.5 cm in diameter occur on large, scoop-shaped cross-beds. These are interpreted as feeding burrows. No back-fill (spreite) structures have been observed, but this may be because of the coarse grain-size and poorly cemented nature of the matrix. In two of these localities paired tracks are present on the same slabs as the feeding burrows. Each mark is about 1.5 cm long and each individual is separated from the other in the pair by about 0.5 cm, at their nearest point. The pairs overlap by less than 2 mm. These tracks also meander over the surface of cross-bedding planes.

At one locality, a small arcuate impression, 1 cm wide and 4 cm long, is present on the underside of a bedding-plane overhang. The impression has striations on a millimetre scale at right angles to its length. Preservation was poor, mainly because of the coarse grain-size of the matrix. However, the impression bears some resemblance to the Annelid *Dickinsonia* Glaessner

1966. *Skolithos* and paired tracks are associated with this impression.

At the fifth locality, concentric impressions bear a striking resemblance to *Charniodiscus* Ford 1958. These range from 2-5 cm in diameter and occur on a single bedding plane. Feeding burrows and *Skolithos* occur at this locality, too.

The *Skolithos* indicates an earliest Cambrian age for the base of the Bukalara Sandstone. *Charniodiscus* is latest Precambrian to earliest Cambrian. The feeding burrows and paired tracks could also occur in rocks of this age. All of the fossils occur within 20 m of the base of the formation, which reaches a maximum thickness of just over 300 m in the Abner Range 80 km to the south of the fossiliferous localities. The stratigraphically equivalent Riversdale Formation and Mount Birnie Beds of the Georgina Basin are diachronous and transgress from Lower Cambrian into Middle Cambrian (Cook & Shergold, 1978). The Mount Birnie Beds contain a number of trace fossils, none of which are considered to be diagnostic (Carter & Öpik, 1963), but they are overlain unconformably by the Middle Cambrian fossiliferous Thornton Limestone. The Riversdale Formation is unfossiliferous. *Skolithos* from the Buckingham Bay Sandstone is now regarded as being of Early or Middle Cambrian age (Plumb & others, 1976). The Buckingham Bay Sandstone has been correlated on regional stratigraphy with the Bukalara Sandstone.

The palaeontological evidence presented here supports the tentative Early Cambrian age (Dunn, 1963; Smith, 1964) of the Bukalara Sandstone.

### References

- CARTER, E. K., & ÖPIK, A. A., 1963—Duchess, Qld., 4-mile Geological Series Sheet. *Bureau of Mineral Resources, Australia — Explanatory Notes F/54-6*.
- COOK, P. J., & SHERGOLD, J. H. (Editors) 1979—Proterozoic-Cambrian Phosphorites. PROCEEDINGS 1ST INTERNATIONAL FIELD WORKSHOP AND SEMINAR ON PROTEROZOIC-CAMBRIAN PHOSPHORITES. *Canberra Publishing & Printing Co*.
- DUNN, P. R., 1963—Hodgson Downs, N. T., 1:250 000 Geological Series, *Bureau of Mineral Resources, Australia — Explanatory Notes SD53-14*.
- FORD, T. D., 1958—Pre-Cambrian Fossils from Charnwood Forest. *Proceedings of the Yorkshire Geological Society*, 31, 211-17.
- GLAESSNER, M. F., 1966—The Late Precambrian fossils from Ediacara, South Australia. *Palaeontology*, 9, 599-628.

- PLUMB, K. A., & BROWN, M. C., 1973—Revised correlations and stratigraphic nomenclature in the Proterozoic carbonate complex of the McArthur Group, Northern Territory. *Bureau of Mineral Resources, Australia — Bulletin* 139, 103-15.
- PLUMB, K. A., & PAINE, A. G. L., 1963—Mount Young, N.T., 1:250 000 Geological Series. *Bureau of Mineral Resources, Australia — Explanatory Notes* SE53-15.

- PLUMB, K. A., SHERGOLD, J. H., & STEFANSKI, M. Z., 1976—Significance of Middle Cambrian Trilobites from Elcho Island, Northern Territory. *BMR Journal of Australian Geology & Geophysics*, 1, 51-5.

- SMITH, J. W., 1964—Bauhinia Downs, N.T., 1:250 000 Geological Series. *Bureau of Mineral Resources, Australia — Explanatory Notes* SE53-3.

*BMR Journal of Australian Geology & Geophysics*, 5, 1980, 160-163

## A potential dolostone reservoir in the Georgina Basin: the Lower Ordovician Kelly Creek Formation

*B. M. Radke & P. Duff*

The extensive dolostone unit of the Lower Ordovician Kelly Creek Formation in the Toko Syncline, Georgina Basin, has significant potential as a hydrocarbon reservoir with variable porosity and permeability characteristics. The porous dolostone is 107 metres thick. Measured porosities of 19 core plugs from this section average 11 per cent, average horizontal permeability (gas) was 234 md, and vertical permeability (gas) 28 md. Permeability is more variable vertically, being generally low but with random higher values. Porosity is dominantly intercrystalline in mottled and stratified distribution, with associated vug, channel, fracture and breccia types; the porosity developed late in diagenesis, during and after pervasive dolomitisation of the sequence. The dolostone interdigitates with overlying thin calcareous dolomitic sandstone beds which have higher porosity (19%) and permeability ( $K_{aH}$  270 md,  $K_{aV}$  54 md). Traces of liquid hydrocarbons in the dolostone and previously reported gas flows from the overlying sandstone in AOD Ethabuka No. 1 indicate significant potential for these porous units as a reservoir in suitable structural traps.

### Introduction

The Georgina Basin has, overall, been regarded as having low potential for hydrocarbon accumulations because of the thin sequence and apparent fresh-water flushing in near-surface aquifers, even though traces of oil and bitumen have been found in previous drilling (Smith, 1972). The greatest potential in the basin is in the Toko Syncline (Fig. 1) in which the Cambrian-Ordovician sequence thickens to the southeast where it is covered by the Eromanga Basin. Anticlinal structures have been seismically defined at depth in the syncline, adjacent to the overthrust western margin (Alliance Oil Development, 1975; Harrison, 1979). On the Ethabuka Structure, a moderate gas flow (estimated at 7080 m<sup>3</sup>/day from open hole) was produced from a Lower Ordovician sandstone in AOD Ethabuka No. 1 (Alliance Oil Development, 1975), and bitumens were reported at and below the same interval in GSQ Mount Whelan 2 (Green & Balfe, 1980). The Geological Survey of Queensland drilled GSQ Mount Whelan 1 and 2 on the eastern limb of the Toko Syncline, to provide stratigraphic control for a concurrent BMR seismic survey across the syncline. This drilling enabled appraisal of hydrocarbon potential of the sequence from core examination. Harrison (1979, Table 1) considered likely caprocks to be the Nora and Mithaka Formations, and potential reservoirs to include the Georgina Limestone, Ninmaroo and Kelly Creek Formations. The Kelly Creek Formation has the greatest potential because of the gas flow from its upper sandstone unit, and a thicker porous dolostone immediately beneath.

Carbonates, as reservoirs, tend to have more varied and unpredictable petrophysical properties than sandstones (Landes, 1946); consequently our study was aimed at evaluation of the porous dolostone unit of the Kelly Creek Formation and Ninmaroo carbonates,

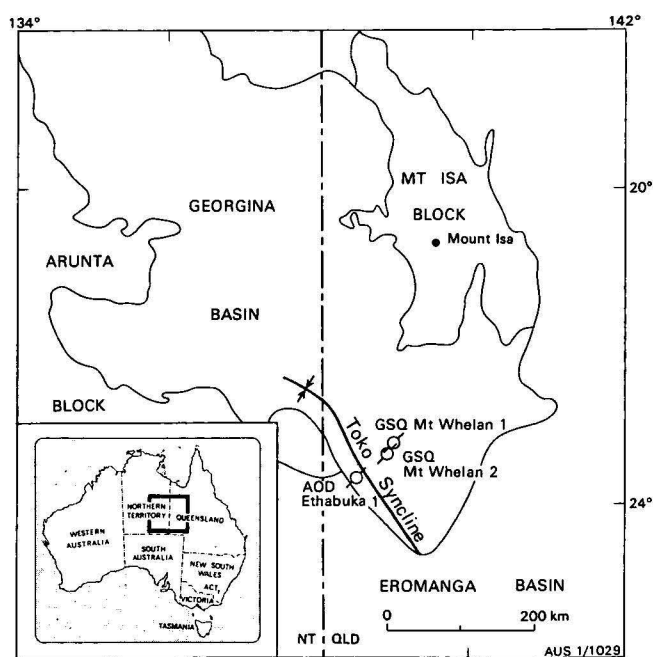


Figure 1. Regional setting of the Toko Syncline.

	Rock type	Depth metres	Sample length cms	Apparent grain density	Effective porosity % B.V.	Permeability (gas) horizontal		md vertical	Inter particle	Porosity type					Porosity distribution
						position A	position B			Moldic	Inter- crystal	Vug	Channel	Breccia fracture	
Kelly Creek Formation	POROUS, DOLOMITIC SANDSTONE	450.74	13	2.84	19.3	241	306	54	X	XXX					Uniform
		473.94	14	2.81	12.7	12	7	1.8			XXXX				Mottled, following bioturbation; stylolite confined.
		476.44	19	2.82	9.8	77	92	0.4			XXXX	X			Mottled, following bioturbation and sulphate fabric; stylolite confined.
		485.40	9	2.84	5.6	43	<	0.2				XXXX			Stratiform along bedding.
		492.78	12	2.84	5.8	4.4	18	<			XX	XXX			Localised patches.
		494.88	21	2.80	13.7	156	186	19			XXXX	X			Interconnected mottling.
		501.35	17	2.80	1.05	<	<	<				XXXX			Scattered ?fenestrae.
	POROUS, CALCAREOUS DOLOSTONE	505.69	9	2.89	11.5	24	23	1.9			XXXX	X			Mottled (30% rock).
		508.32	15	2.86	13.9	111	346	12			XXXX	X			Mottled (bitumen stained).
		515.05	13	2.83	10.5	308	4.3	0.8			XX		XX		Mottled; stylolite confined.
		517.33	17	2.79	13.1	73	93	2.0			XXXX	X			Mottled; stylolite confined.
		530.07	13	2.81	16.5	287	387	17			XXXX	X	X		Follows bedding and in matrix of a conglomerate.
		541.23	25	2.80	6.4	144	245	0.1			XX	X	XX		Stratified.
		552.16	14	2.85	17.0	556	791	336			XXXX	X	X		Pervasive.
		553.73	15	2.87	11.4	428	390	72			XX		XXX		Cement-occluded in patches.
		563.66	8	2.81	17.0	351	320	18			XXXX				Mottled, variable with bedding.
		571.53	11	2.85	11.2	298	198	<			XX	XX			Bands occluded by anhydrite; bitumen staining; sphalerite.
		573.30	28	2.81	10.8	215	208	0.4			XXXX	X			Follows lamination.
		577.17	19	2.79	15.0	159	142	3.1			XX	X	X		Mottled, variable with bedding.
		580.72	4	2.79	6.3	1160	521	43			XX			XXX	Random intercrystal patches.
Ninmaroo Formation	POROUS, DOLOMITIC CALCAREOUS SANDSTONE	709.16	14	2.82	24.3	271	314	144	XXXX	X					Pervasive.

Comments. 1. X — 0-25%; XX — 25-50%; XXX — 50-75%; XXXX — 75-100%; < — less than 0.1. 2. Common range of Apparent Grain Densities (Core Laboratories, pers. comm.): limestone 2.68-2.76; dolostone 2.78-2.82 (2.86-2.93—Deer & others, 1962); limestone/dolostone 2.72-2.80; sandstone 2.65. 3. Core diameter 48 mm. 4. Whole core analysis procedure of Bynum & Koepf (1957), American Petroleum Institute (1960). 5. Horizontal permeabilities of orthogonal directions, A & B. 6.  $\frac{K_{brine}}{K_{gas}}$  was 38% for  $K_{gas}$  144 md; 17% for  $K_{gas}$  72 md.

Table 1. Porosity and gas permeability characteristics, GSQ Mount Whelan No. 2.



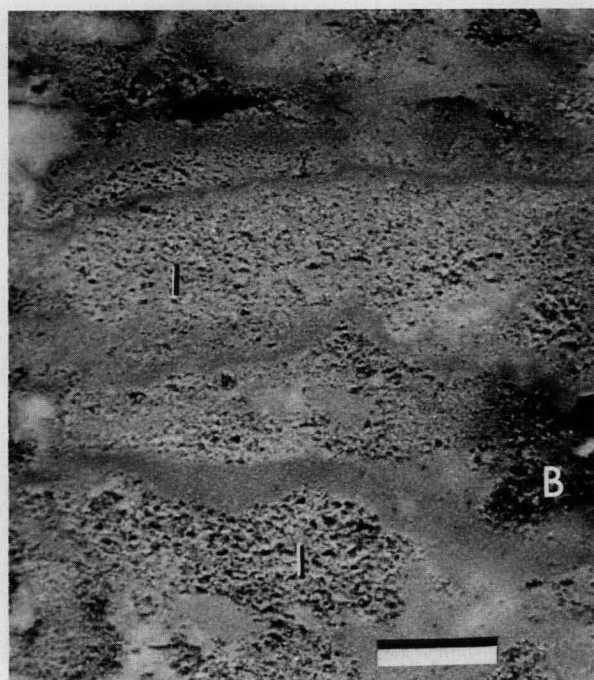


**Figure 2.** Intercrystalline porosity (I) comprising small and large mesopores in the dolostone, confined by thin, less permeable laminae. Embayed area of porosity is bitumen-stained (B).  $\phi$ 16.5%,  $K_{aH}$  337 md,  $K_{aV}$  17 md. Bar scale 1 cm. Core slab from GSQ Mount Whelan No. 2, 530.07 m.

based on whole-core petrophysical analysis of material from GSQ Mount Whelan 2.

This note outlines the petrophysical and petrographic characteristics of the Kelly Creek dolostone unit. For a lithological comparison, characteristics are given for two porous sandstones that are in close proximity to the dolostone. Ninmaroo carbonates were characteristically much lower in porosity and consequently are not included.

The Kelly Creek dolostone unit is apparently continuous throughout the Toko Syncline, and has been mapped from the west around to the eastern limb as the Withillindarmna Dolostone Member (Druce, pers. comm.). The unit was intersected over 107 m in GSQ Mount Whelan 2 (Green & Balfe, 1980), and 103 m in AOD Ethabuka No. 1 (Alliance Oil Development, 1975), overlying limestone or calcareous sandy dolostone and interdigitating upwards into a calcareous dolomitic sandstone.

In this note, porosity terminology follows that of Choquette & Pray (1970).

### Petrophysical and petrographic characteristics

#### Dolostone

Average petrophysical values (19 whole core plugs) for the interval of dolostone from 473.94 to 580.72 m (Table 1) are:

- Effective porosity ( $\phi$ ) 11%
- Horizontal permeability ( $K_{aH}$ ) 234.4 md
- Vertical permeability ( $K_{aV}$ ) 27.8 md

Porosity is dominantly intercrystalline throughout the unit, with lesser vug, channel, fracture and breccia types. In the reduction or absence of intercrystalline porosity and permeability from 501.35 to 485.40 m, vug

porosity is dominant. Channel and fracture porosity occur only in the lower part of the unit below 508 m.

Intercrystalline porosity is in small and large mesopores (Fig. 2) which were solution-enlarged prior to subsequent reduction by further growth of dolomite rhombs. This porosity occurs in an idiopathic dolostone host and where well developed, is pervasive and uniform in distribution, obliterating primary structures. More commonly intercrystalline porosity is not pervasive, but has a mottled distribution selectively following bioturbation or sulphate-crystal pseudomorphs, or is laminated and stratified where it selectively follows specific lithologies. Vugs are an extension of intercrystalline porosity where leaching has enlarged the pores to large meso or megapore size (Fig. 3). Where vugs have stratified distribution and have coalesced, channel porosity developed. Fracture and breccia porosity have limited random distribution, usually cutting across impermeable beds and interconnecting other porosity types.

Permeability data indicate good horizontal permeability which generally increases towards the bottom of the unit, but a lower and more variable vertical component. Stratification from alternating permeable-impermeable beds or laminae causes this. Localised vertical impermeability is controlled by these bedding variations, and by stylolites lined with insolubles and bitumen residues. These stylolites are probably discontinuous laterally over several metres. Where porosity is in irregular or embayed patches, bitumen plugging and probable oil staining is common. This bitumen may have been emplaced as a residual product during hydrocarbon migration through the zone.

#### Dolomitic sandstone

Porous dolomitic sandstone was sampled from two horizons, one from the upper unit of the Kelly Creek Sandstone above the dolostone (450.74 m), the other

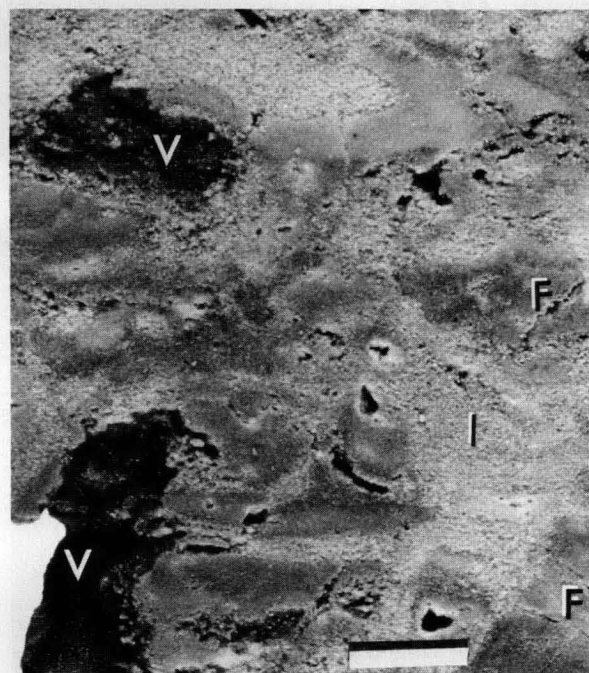


**Figure 3.** Vug (V), intercrystalline (I), and fracture (F) porosity in the dolostone.  $\phi$ 15%,  $K_{aH}$  151 md,  $K_{aV}$  3.1 md. Bar scale 1 cm. Core slab from GSQ Mount Whelan No. 2, 577.17 m.



below (709.16 m) at the top of the Ninmaroo Formation. These sandstones have high porosities (19-20%) and permeabilities (both horizontal,  $K_{aH}$  241-314 md, and vertical  $K_{aV}$  54-144 md). Porosity in this rock type results from a combination of primary interparticle and secondary moldic components. Moldic porosity has apparently formed after carbonate particles in the sandstone have been leached out. Interparticle pores are partially reduced by carbonate cements.

### Porosity history

Porosity in the dolostones is entirely secondary and developed during and after dolomitisation of the host limestones. While dolomite precipitated as replacement euhedral rhombs, interstitial and host carbonate was being leached more readily, producing intercrystalline porosity. Further enlargement of these pores by both dissolution and collapse has produced vugs and channels. Counteracting this solution-enhancement process has been later reduction and even occlusion of porosity by precipitation of cements—mostly calcite and saddle dolomite, with some anhydrite and traces of pyrite and low-iron sphalerite. This mineral suite is epigenetic, generally related to hydrocarbon migration (Dunsmore, 1973; Radke & Mathis, in press) or post-dating it. Evidence for this is the lack of hydrocarbon staining on these later cements which have precipitated from fluids migrating through the permeable zones. It is most likely that, where traps developed after the first dolomitisation phase, accumulation of hydrocarbons has reduced water saturation in the porosity, thus preventing subsequent occlusion of porosity by these later cements.

### Discussion

Hydrocarbon reservoirs in carbonates, where porosity has resulted from dolomitisation, have previously been unknown in Australia although they are common in North America. Examples of such reservoirs are the Clear Creek field, Williston Basin (Stout, 1964); Trenton field, Ohio and Indiana; Adams and Deep River fields in Michigan (Landes, 1946); and 'Midale' carbonates, southeastern Saskatchewan (Robinson, 1966). A common characteristic of such fields is the unpredictability of porous pay zones (Landes, 1946). However, average porosities of such carbonate petroleum reservoirs is between 5 and 15 percent (Choquette & Pray, 1970).

The Kelly Creek dolostone is comparable to these reservoirs in having an average porosity of 11 percent, variability in porosity distribution, and consequently permeability variations. This variability is on the mesoscopic scale (whole core), but over larger areas may still be effective because of randomly distributed fracture and breccia porosity which is penetrative, inter-connecting porous patches that would be otherwise isolated by impermeable beds or stylolites.

Interdigitation of permeable dolomitic sandstones above is an ideal relationship where the sandstone acts as an extensive stratiform conduit that could localise hydrocarbons from the thicker dolostone below. The gas flow in AOD Ethabuka No. 1 was from this sandstone, called Coolibah Formation by Alliance Oil Development (1975). Apart from poor cut and bitumen traces, no oil was recorded from the dolostone

in this well and no electric logs were run to this level because of drilling problems. Core from the dolostone in GSQ Mount Whelan 2 has considerable surface hydrocarbon staining and residual hydrocarbons were extracted, indicating an 'oil' saturation of 0.7 percent two years after drilling. This oil comprises 28 percent saturated, 15 percent aromatic and 57 percent polar compounds, had a density of 0.9485 gm.cc<sup>-1</sup>, and a pristane/phytane ratio of 2.5, which is comparable to other hydrocarbons extracted from the sequence in GSQ Mount Whelan 1 and 2 (K. Jackson, pers. comm.).

In conclusion, our data indicate that the dolostone unit of the Kelly Creek Formation has significant porosity and permeability. Recurring evidence of hydrocarbons in the unit implies its potential as a carbonate reservoir in a suitable structural setting.

### Acknowledgements

Whole core material was loaned by the Mines Department, Queensland. Thanks are extended to P. Green for his patient assistance in sampling and K. Heighway for the preparation of the core. B. McKay supported the study and arranged development of the equipment and modifications necessary for the analyses which were conducted in the BMR Petroleum Technology Laboratory.

### References

- ALLIANCE OIL DEVELOPMENT N.L., 1975—Well completion report; Alliance Ethabuka No. 1 well. (Unpublished company report).
- AMERICAN PETROLEUM INSTITUTE, 1960—*API Recommended practice for core-analysis procedure*. API RP40, Dallas, Texas.
- BYNUM, R. S., Jr., & KOEPF, E. H., 1957—Whole-core analysis methods and interpretation of data from carbonate reservoirs. *Journal of Petroleum Technology*, **9**, 11-16.
- CHOQUETTE, P. W., & PRAY, L. C., 1970—Geologic nomenclature and classification of porosity in sedimentary carbonates. *American Association of Petroleum Geologists Bulletin* **54**, 207-50.
- DEER, W. A., HOWIE, R. A., & ZUSSMAN, J., 1962—*ROCK-FORMING MINERALS, 5, NON-SILICATES*. John Wiley, New York.
- DUNSMORE, H. E., 1973—Diagenetic processes of lead-zinc emplacement in carbonates. *Transactions of Institute of Mining and Metallurgy*, **82**, B168-73.
- GREEN, P. M., & BALFE, P. E., 1980—Stratigraphic drilling report GSQ Mount Whelan 1 and 2. *Queensland Government Mining Journal*, **81**, 162-78.
- HARRISON, P. L., 1979—Recent seismic studies upgrade the petroleum prospects of the Toko Syncline. *APEA Journal*, **19**, 30-45.
- LANDES, K. K., 1946—Porosity through dolomitisation. *American Association of Petroleum Geologists Bulletin*, **30**, 305-18.
- RADKE, B. M., & MATHIS, R. L., in press—On the formation and occurrence of saddle dolomite. *Journal of Sedimentary Petrology*.
- ROBINSON, R. B., 1966—Classification of reservoir rocks by surface texture. *American Association of Petroleum Geologists Bulletin*, **50**, 547-59.
- SMITH, K. G., 1972—Stratigraphy of the Georgina Basin. *Bureau of Mineral Resources, Australia, Bulletin* **111**.
- STOUT, J. L., 1964—Pore geometry as related to carbonate stratigraphic traps. *American Association of Petroleum Geologists Bulletin* **48**, 329-37.

# THE BUREAU OF MINERAL RESOURCES, GEOLOGY AND GEOPHYSICS

## Publications issued in 1979

All publications listed below can be obtained from

Publication Sales,  
Bureau of Mineral Resources,  
P.O. Box 378,  
Canberra City,  
ACT 2601, Australia



### BULLETINS

172. Middle Cambrian agnostids: systematics and biostratigraphy, by A. A. Öpik (\$19.50).
184. The Dromornithidae—a family of large extinct ground birds endemic to Australia, by P. V. Rich (\$16.75).
185. Carboniferous, Permian, and Triassic conchostracans of Australia—three new studies, by P. Tasch & P. J. Jones (\$5.00).
190. Conodonts from the Fairfield Group, Canning Basin, Western Australia, by R. S. Nicoll & E. C. Druce (\$10.50).
195. Marine geology of the continental shelf off south-east Australia by P. J. Davies (\$12.75).
200. The geology of the Fairfield Group, Canning Basin, WA, by E. C. Druce & B. M. Radke (\$6.00).

### REPORTS

184. An analysis of strong-motion accelerograms from Yonki, PNG, 1967-1972, by D. Denham (Microform MF10—\$0.50).
186. Acquisition, processing and interpretation of airborne gamma-ray spectrometry data, by P. G. Wilkes (Microform MF73—\$1.00).
191. Officer Basin seismic, gravity, magnetic, and radiometric survey, Western Australia, 1972, by P. L. Harrison & I. Zadoroznyj (Microform MF69—\$2.00).
193. Stratigraphic tables, Papua New Guinea, by S. K. Skwarko (Microform MF61—\$1.50).
200. Isotopic ages of rocks from the Georgetown/Mount Garnet/Herberton area, by L. P. Black (Microform MF28—\$1.00).
201. The Great Australian Bight: a regional interpretation of gravity, magnetic, and seismic data from the Continental Margin Survey, by J. B. Willcox (Microform MF25—\$1.00).
203. Mount Turner geophysical survey, Georgetown area, Queensland, 1976, by J. A. Major (Microform MF93—\$0.50).
204. Catalogue of airborne magnetic and radiometric surveys up to December 1977, by W. J. Gerula (Microform MF78 plus maps—\$8.75).
205. Combined ground geophysical survey—Alligator Rivers area, Northern Territory, 1975, by B. R. Spies (Microform MF29—\$0.50).
206. Ground geophysical surveys, Mary River area, NT, 1973, by I. G. Hone & J. A. Major (Microform MF30—\$0.50).
207. Australian gravity network adjustment, 1975, by H. McCracken (Microform MF68—\$1.00).
209. Late Cainozoic volcanoes of north-central New Britain and the Witu Islands, PNG, by R. W. Johnson & B. W. Chappell (Microform MF76—\$0.50).
211. Annotated bibliography of the Georgina Basin, NT and Qld, by E. C. Druce & J. H. Shergold (Microform MF77—\$0.50).
212. Geological Branch summary of activities, 1978 (Microform MF81—\$2.00).
213. Geophysical Branch summary of activities, 1978 (Microform MF97—\$1.50).
215. Preliminary report on the Cadoux earthquake, Western Australia, 2 June 1979, by P. J. Gregson & E. P. Paull (Microform MF100 plus 14 postcards—\$2.00).
217. Abstracts of 8th BMR Symposium, Canberra, 1-2 May 1979 (Microform MF105—\$0.50).

### YEARBOOK

BMR 78. Report and articles on BMR activities in 1978 (\$2.75).

### BMR JOURNAL OF AUSTRALIAN GEOLOGY & GEOPHYSICS

Vol. 4, Nos. 1, 2, 3, 4 (\$3.00 each, \$10.00 p.a.).

### BMR EARTH SCIENCE ATLAS OF AUSTRALIA

Plate tectonics, Major structural elements, Bouguer gravity anomalies, Free-air gravity anomalies. (Maps with commentaries \$3.00 each; Atlas cover \$5.00 plus postage.)

### PUBLICATIONS ON THE MINERAL & PETROLEUM INDUSTRIES

Australian Mineral Industry Annual Review 1977 (\$18.00).

Australian Mineral Industry Quarterly, Vol. 31, Nos. 3, 4; Vol. 32, Nos. 1, 2 (\$2.00 each).

Preprints from Australian Mineral Industry Annual Review 1978 (Tin, Aluminium—\$1.50 each).

Australian molybdenum deposits, compiled by N. D. Knight (Mineral Resources Report 9—\$2.50).

The Petroleum Newsletter, Nos. 74, 75, 76, 77 (free).

Petroleum exploration and development titles map and key, 1 January 1979 (\$3.00).

### 1:250 000 GEOLOGICAL MAPS & EXPLANATORY NOTES

Green Swamp Well, Lander River Tennant Creek (Northern Territory); Mornington-Cape Van Diemen (Queensland); Morris, Percival, Plumridge, Ranton, Ryan, Sahara, Tabletop, Ural, Wilson (Western Australia); Port Moresby-Kalo-Aroa (Papua New Guinea) (\$3.00 each).

### PRELIMINARY GEOLOGICAL MAPS

1:100 000—Adam (Special), Aileron, Fergusson Range, Howship, Oenpelli (Northern Territory); Cloncurry, Duchess, Malbon (Queensland).

1:250 000—Broome, Joanna Springs, Lagrange, McLarty Hills, Mandora, Munro, Patterson Range, Port Hedland/Bedout Island (Western Australia).

1:500 000—Ngalia Basin (Northern Territory).

1:1 000 000—Wiso Basin (Northern Territory).

(Preliminary maps are \$1.00 each.)

### SPECIAL MAPS ON THE PINE CREEK GEOSYNCLINE

1:500 000 geology, gravity, magnetic, radiometric.

### STREAM SEDIMENT GEOCHEMISTRY MAPS

Seigal 1:100 000 Sheet area, Northern Territory, 6 maps—U-Cu-Sn, Ni-Cu-Zn, Pb-As-Zn, U-As-Bi, U-Ce-Th, W-Be-Nb.

Hedleys Creek 1:100 000 Sheet area, Queensland, 5 maps—U-As-Bi, Pb-As-Zn, Ni-Cu-Zn, U-Cu-Sn, U-Ce-Th.

(Stream sediment geochemistry maps are \$1.50 each.)

### GEOPHYSICAL MAPS

1:5 000 000 gravity map of Melanesia (\$2.00).

1:250 000 total magnetic intensity—Alcoota (Northern Territory); Cloncurry, Westmoreland (Queensland) (\$1.00 each).

## CONTENTS

	Page
B. R. Spies TEM model studies of the Elura deposit, Cobar, New South Wales .....	77
H. A. Jones and G. R. Holdgate Shallow structure and Late Cainozoic geological history of western Bass Strait and the west Tasmanian Shelf .....	87
E. M. Truswell Permo-Carboniferous palynology of Gondwanaland: progress and problems in the decade to 1980 .....	95
U. von Stackelberg, N. F. Exon, U. von Rad, P. G. Quilty, S. Shafik, H. Beiersdorf, E. Seibertz, and J. J. Veevers Geology of the Exmouth and Wallaby plateaus off northwest Australia: sampling of seismic sequences .....	113

## Notes

P. G. Quilty Tertiary Foraminiferida and stratigraphy, northern Exmouth Plateau, Western Australia .....	141
R. S. Nicoll Middle Ordovician conodonts from the Pittman Formation, Canberra, ACT .....	150
D. Denham The 1961 Robertson earthquake — more evidence for compressive stress in southeast Australia .....	153
M. H. Tratt and R. V. Burne An inexpensive and efficient double-tube, hard-coring device .....	156
M. D. Muir Palaeontological evidence for the Early Cambrian age of the Bukalara Sandstone, McArthur Basin, Northern Territory .....	159
B. M. Radke and P. Duff A potential dolostone reservoir in the Georgina Basin: the Lower Ordovician Kelly Creek Formation .....	160